

**Impacts of airborne volcanic ash on
the surface ocean biogeochemistry and
marine ecosystems**



Dissertation

**zur Erlangung des Doktorgrades
der Mathematisch-Naturwissenschaftlichen Fakultät
der Christian-Albrechts-Universität zu Kiel**

vorgelegt von

Nazlı Olgun

Kiel 2012

Referent: Prof. Dr. Martin Frank

Koreferent: Prof. Dr. Douglas Wallace

Tag der mündlichen Prüfung: 16 Dezember 2011

Zum Druck genehmigt: 02 Februar 2012

Prof. Dr. rer. nat. Lutz Kipp

Der Dekan

ERKLÄRUNG

Hiermit erkläre ich, dass ich die vorliegende Arbeit selbständig und ohne unerlaubte Hilfe angefertigt habe. Es wurden keine anderen Hilfsmittel außer den angegebenen Quellen benutzt. Diese Arbeit wurde weder ganz noch zum Teil einer anderen Stelle im Rahmen eines Prüfungsverfahrens vorgelegt. Ferner habe ich noch keinen Promotionsversuch an dieser oder einer anderen Hochschule unternommen.

Nazlı Olgun

ACKNOWLEDGEMENTS

Firstly and foremost I thank my advisor Dr. Svend Duggen. It has been an honor for me to be his first PhD student and as he says the best one he ever had!.. This dissertation would not have been possible without his guidance and support. Above all, his amazing enthusiasm will always motivate me in my carrier and in my life.

I gratefully acknowledge the funding sources that provide me the chance to work on this fascinating research topic. This dissertation arose from my years of research in the interdisciplinary research project NOVUM (Nutrients originating volcanoes and their affects in the euphotic zone of the marine ecosystems) at IFM-GEOMAR. I thank to NOVUM-contributors Dr. Svend Duggen (project leader), Dr. Peter Croot, Dr. Heiner Dietze, Prof. Dr. Kaj Hoernle and Prof. Dr. Douglas Wallace.

I thank Research Unit Palaeoceanography at IFM-GEOMAR for the financial support during the last stage of my PhD. I further thank project SFB-574 at IFM-GEOMAR (Volatiles and Fluids in Subduction Zones) for the support for financing the publication of the manuscripts, and I thank to Dr. Armin Freundt and Erna Lange for their efforts in these processes.

I am particularly grateful to Prof. Dr. Martin Frank for his time and support during the production of my dissertation. I further thank him for his efforts for the funding he arose by the Research Unit Palaeoceanography at IFM-GEOMAR.

I am indebt to Dr. Peter Croot for his analytical support and his contribution. My study would not exist without his impressive knowledge in seawater chemistry. I further gratefully acknowledge Dr. Steffen Kutterolf for his support with his outstanding experience in volcanology, which I benefited much for the volcanic ash flux estimates.

Many thanks go to my cooperation colleagues in Sicily, in INGV-Catania and in University of Palermo. I especially thank to Dr. Salvatore Giammanco for the fascinating field trip to Etna volcano (with a tiny but a 4 x 4 Fiat-Panda). It was one the most exciting times of my life when I first saw an erupting volcano. I further thank to Dr. Daniele Andronico for the nice ash sample set and his input in the Etna study. I also thank to Prof. Dr. Paolo Censi for his collaborations. Special thanks go to Dr. Loredana Randazzo for her scientific collaboration, her friendship and our joyful days in Palermo.

Individual acknowledgement goes to Claudia Teschner for her successful investigations in her master study in the NOVUM-Project. I further thank her for creating a pleasant atmosphere during our POSEIDON cruise in the Atlantic Ocean and her great friendship.

I would like to express my deepest gratitude to the collaborating scientists who inspired and supervised me. Many thanks go in particular to Dr. Linn Hoffmann, who was always willing to help and give her best suggestions. I very much appreciated her amazing input with the biological experiments. I acknowledge Dr. Baerbel Langmann and Prof. Dr. Matthias Hort for their encouraging and inspiring discussions, and great interest in my research. I also thank Dr. Pierre Delmelle for his constructive critics and his input in the revision of the manuscript.

In regards to laboratory work, I thank Dr. Dieter-Garbe Schönberg and Ulrike Westernstöer for their guidance during the production of ICP-MS data. I want to thank Frank Malien for the photometric analyses. Further thanks go to Mario Thöener for his support in developing these nice electron microprobe data.

I gratefully acknowledge the co-authors Prof. Dr. Niels Oskarsson, Dr. Claus Siebe, Dr. Andreas Auer, Dr. Ulrike Schacht, Dr. Christopfer Waythomas and Dr. Heiner Dietze for their helpful suggestions that helped to improve the quality of manuscripts. It was a pleasure to collaborate you.

And foremost I want to thank my encouraging family and friends. I dedicate this study to Tahsin Olgun, my father whom I always keep his memories. I thank my mother Suna Olgun for all her support and encourage and my beloved sister Dilek Olgun Erdikmen who raised me with love and is an excellent example of a successful women scientist. I thank my sweetheart nephew Yagmur Olgun for being such a wonderful child and a good friend, making me smile even in those days with a lot of stress. I thank to my best friend Sena Ünal for her support and motivation through the good times and the bad. And most of all I thank my beloved boyfriend Erdem Kıyak for his infinite patience and encourage especially during the last stage of my PhD. Thank you all...

LIST OF CHAPTERS

This thesis comprises the following publications and manuscripts:

Chapter I:

“The role of airborne volcanic ash for the surface ocean biogeochemical iron-cycle:
A review.”

Published in Biogeosciences, 2010.

Contribution:

The concept of this review paper was derived by S. Duggen and me based the discussions held at the EUR-OCEANS Workshop “Iron biogeochemistry across marine systems at changing times” in Gothenburg, 14-16 May 2008. The publication was written by S. Duggen, I contributed by writing two chapters, summarizing the literature data and helped in the revision process.

Chapter II:

“Surface ocean iron fertilization: The role of airborne volcanic ash from subduction zone and hotspot volcanoes and related iron-fluxes into the Pacific Ocean.”

Published in Global Biogeochemical Cycles, 2011.

Contribution:

Laboratory experiments were performed and analyzed by me. The manuscript was written by me. S. Duggen was involved in major concept of the manuscript and the data interpretation. P. Croot assisted me in planning of voltammetric experiments and was involved in revision of the manuscript. Acid digestion of the bulk samples was done by me, the ICP-AES and ICP-MS measurements were performed by D. Garbe-Schönberg. P. Delmelle, H. Dietze, U. Schacht, N. Óskarsson, C. Siebe and A. Auer provided scientific advice.

Chapter III:

“Geochemical evidence of oceanic iron-fertilization by the Kasatochi 2008 volcanic eruption and evaluation of the potential impacts on sockeye salmon population”.

Submitted to Marine Ecology Progress Series.

Contribution:

Laboratory experiments were performed and analyzed by me. The manuscript was written by me. S. Duggen, B. Langmann, M. Hort, C. F. Waythomas, L. Hoffmann and P. Croot provided scientific advice.

Chapter IV:

“Possible impacts of volcanic ash emissions of Mount Etna on the oligotrophic Mediterranean Sea: Results from the nutrient-release experiments in seawater.”

Submitted to Marine Chemistry.

Contribution:

Laboratory experiments were performed and analyzed by me. The manuscript was written by me. S. Duggen assisted with the major concept of the manuscript. D. Andronico provided the ash samples. P. Croot, D. Andronico, S. Giammanco, P. Censi, and L. Randazzo provided scientific advice.

Chapter V:

“Influence of trace metal release from volcanic ash on growth of *Thalassiosira pseudonana* and *Emiliana huxleyi*.”

Submitted to Marine Chemistry.

Contribution:

L. Hoffmann conducted the experiments and wrote the manuscript. I conducted the voltametric experiments for pre-analysis of the ash samples for sample selection, and involved in the data interpretation and revision of the manuscript. E. Breitbarth, M. Hasselhöf and S. Å. Wängberg assisted in the biological experiments. M. V. Ardelan performed the ICP-MS analyses. S. Duggen was involved in the major concept of the manuscript and provided scientific advice.

In addition I have co-supervised Claudia Teschner during her Masters thesis (Diplomarbeit) in the project NOVUM (Nutrients Originating in Volcanoes and their effect on the eUphotic zone of the Marine ecosystem).

Teschner, C. (2009): “Pumice from Central American Arc volcanoes: Release of iron and silica on contact with seawater and implications for the diatom growth in the Eastern Equatorial Pacific Ocean.”

I have also contributed to the following publications and cruise reports during my PhD:

Olgun, N., Botz R., Schmidt, M. (2010): “Holocene marine carbonates in the northern Red Sea, heat affected foraminiferal alteration in the Shaban Deep”. VDM Verlag Dr. Müller e.K., Saarbrücken, Germany, ISSN: 9783639277760.

Botz, R., Schmidt, M., Kus, J., Ostertag-Henning, C., Ehrhardt, A., **Olgun, N.**, Garbe-Schönberg, D., Scholten, J. (2011): “Carbonate recrystallisation and organic matter maturation in heat-affected sediments from the Shaban Deep, Red Sea.” *Chemical Geology* 280, 126-123

Duggen, S., **Olgun, N.**, Teschner, C., Schmidt, A., Meissl, S. (2009) Cruise Report: Vulkanismus in Karibik-Kanaren-Korridor (ViKKi), *IFM-GEOMAR REPORTS*, doi: 10.3289/ifm-geomar_rep_28_2009, 74 pp.

Duggen, S., **Olgun, N.**, Teschner, C., Schmidt, A., Meissl, S., Gehrman, R., Schröder, P. (2009) Cruise Report: Mid-Atlantic-Researcher Ridge Volcanism (MARRVi), *IFM-GEOMAR REPORTS*, doi: 10.3289/ifm-geomar_rep_29_2009, 80 pp.

TABLE OF CONTENTS

SUMMARY	1
ZUFAMMENFASSUNG	3
INTRODUCTION	7
State of the art.....	9
Nutrient limitation in the surface ocean	10
The atmosphere: A major nutrient source in the surface ocean	12
What is volcanic ash ?	13
Distribution of subaerial volcanoes in the world	15
Volcanic processes that modify the surface composition of volcanic ash particles.....	16
Birth of a new interdisciplinary research field: Oceanic fertilization by volcanic ash.....	19
Aims and outline of the thesis	25
Sampling and analytical methods.....	28
References	34
CHAPTER I:	
The role of volcanic ash for the surface ocean biogeochemical iron-cycle: A review	43
CHAPTER II:	
Surface ocean iron fertilization: The role of airborne volcanic ash from subduction zone and hot spot volcanoes and related iron fluxes in the Pacific Ocean.....	63
Supplementary Chapter II	81
CHAPTER III:	
Geochemical evidence of oceanic iron fertilization by the Kasatochi 2008 eruption and evaluation of the possible impacts on the sockeye salmon population.....	93
CHAPTER IV:	
Possible impacts of volcanic ash emissions of Mount Etna on the oligotrophic Mediterranean Sea: Results from the nutrient-release experiments in seawater	113
CHAPTER V:	
Influence of trace metal release from volcanic ash on growth of <i>Thalassiosira pseudonana</i> and <i>Emiliana huxleyi</i>	165
CONCLUSIONS AND FUTURE PERSPECTIVES	187

SUMMARY

The availability of nutrients in the surface ocean affects the marine primary productivity (MPP), and the atmosphere represents an important source of nutrients to the euphotic zone of the in the global ocean. Volcanic eruptions, can through atmospheric transport, deposit volcanic ash into the ocean and partial dissolution of ash particles in seawater can provide biologically relevant elements for the ocean. Despite the high input of volcanic ash into the ocean, the role of volcanic eruptions in the surface ocean biogeochemistry was largely overlooked.

The primary goal of this study is to evaluate the possible impact of explosive volcanic eruptions on the surface ocean nutrient and its influence on MPP in different oceanic regions (in high- and low-nutrient, low production areas), and influence on the oceanic food-web. By using new clean-laboratory-based geochemical nutrient release data from volcanic ash, and estimates of the marine flux of volcanic ash over long-term periods and/or during single major eruptions, the study provides a new constraints on the importance of volcanic ash deposition for marine nutrient-cycles compared to other major sources such as desert dust. It is also indicated that increased phytoplankton abundance in the surface ocean in large-scale ash fall-out regions can impact the marine food-web (e.g., the increased abundance of zooplankton and salmon fish). Shifts in the phytoplankton community upon addition of volcanic ash can influence the export of biogenic material into the deep ocean, and may eventually affect the carbon cycle.

The first paper reviews the role of volcanic ash for the biogeochemical iron-cycle. It provides a summary of iron solubility of volcanic ash in seawater and freshwater. Also discussed are the important parameters that may affect the iron-solubility from volcanic ash (e.g., solution pH, grain size). The study illuminates unanswered important questions within this new research field and provides recommendations for future studies.

The second paper examines the relative importance of volcanic ash on the high-nutrient, low-chlorophyll (HNLC) regions with a focus on the Pacific Ocean. Fe-release of a large number of volcanic ash samples from subduction zone volcanoes from the *Pacific Ring of Fire* and also hot spot volcanoes were determined in clean-laboratories. By using marine drill core data, the millennial-scale volcanic ash flux into the Pacific

Ocean is estimated. The significance of ash- and related iron-fluxes is evaluated by comparing with the flux from mineral dust into the Pacific Ocean. The study shows that volcanic ash is an important but hitherto underestimated atmospheric iron-source for the Pacific surface ocean biogeochemical iron-cycle.

Satellite data demonstrated that the 2008 Kasatochi eruption caused a massive phytoplankton bloom occurring in the ashfall region in the northeast Pacific (Langmann et al. 2010). The third manuscript focuses on the impact the 2008 Kasatochi eruption may have had on the marine food-web. The study provides geochemical evidence that the iron-release from Kasatochi volcanic ash was sufficient to iron-fertilize the iron-limited northeast Pacific. Moreover, it evaluates whether the Kasatochi eruption through Fe-fertilization and increased phytoplankton growth and zooplankton abundance was ultimately responsible for significantly enhancing the marine survival of sockeye salmon and the unexpected salmon flood in the Fraser River in 2010.

The fourth manuscript investigates the impacts of Etna volcanic ash fall-out on the Mediterranean surface ocean, a low-nutrient, low-chlorophyll (LNLC) region. I did nutrient leaching experiments in seawater with thirteen ash samples from Mount Etna. Moreover, I estimated the volcanic ash flux in the Mediterranean Sea (4 November 2002 eruption, as a case study) as a function of distance from the volcano in order to evaluate the impact of a major Etna eruption. The study highlights the importance of phosphate, iron and fixed nitrogen (e.g., nitrate) supply by the Etna volcanic ash fall potentially impacting the MPP in the oligotrophic Mediterranean Sea. The biogeochemical impact of ash fall from Etna volcano can cover distances as far as 400 km downwind from the volcano.

The last manuscript focuses on the fertilizing and/or toxic effects of the volcanic ash on different phytoplankton species in laboratory experiments. The diatom species *Thalassiosira pseudonana* generally showed higher growth rates in seawater fertilized with volcanic ash, whereas coccolithophoride species *Emiliana huxleyi* showed either no or negative response. The study indicates that volcanic ash fall-out can cause changes in the phytoplankton community structure, leading to diatom domination in the ash fall-out regions.

ZUSAMMENFASSUNG

Die Verfügbarkeit von Nährstoffen im Oberflächenozean beeinflusst die marine Primärproduktion (MPP). Die Atmosphäre stellt eine wichtige Nährstoff-Quelle für die euphotische Zone dar. Vulkanausbrüche können durch atmosphärischen Transport Vulkanasche in den Oberflächenozean eintragen, wobei die partielle Auflösung von Vulkanaschepartikeln in Berührung mit Meerwasser biologisch relevante Elemente freisetzen können. Trotz des bekanntermaßen hohen Eintrags von Vulkanasche war die Bedeutung von vulkanischen Eruptionen für die Biogeochemie des Oberflächenozeans bislang weitgehend übersehen worden.

Das primäre Ziel der vorliegenden Dissertation ist es, den möglichen Impact explosiver Vulkanausbrüche auf das Nährstoffbudget des Oberflächenozeans sowie den Einfluss auf die MPP in unterschiedlichen Ozeanregionen (in sowohl Hoch- als auch Niedrignährstoffgebieten mit niedriger MPP) zu evaluieren. Weiterhin sollte der mögliche Einfluss auf das marine Nahrungsnetz mit in die Betrachtungen einbezogen werden. Dies wurde erreicht durch die Generierung neuer Daten zur Freisetzung von Nährstoffen von Vulkanaschen in Reinraumlaboratorien, Abschätzungen zum Fluss vulkanischer Asche in den regionalen und globalen Ozean sowohl im Zusammenhang mit einzelnen größeren Ausbrüchen als auch über geologische Zeiträume für Ozeanbecken. Die Untersuchungen führen hierdurch und durch den Vergleich mit Wüstenstaub als andere wichtige Nährstoffquelle zu neuen Einsichten und einem besseren Verständnis der Bedeutung von Vulkanasche für marine Nährstoffkreisläufe. Es gibt Hinweise, dass Vulkanausbrüche durch die Anregung der MPP innerhalb großskalierter Aschefallregionen sogar Einfluss auf das marine Nahrungsnetz nehmen können (z.B. der Erhöhung der Häufigkeit von Zooplankton und Lachs). Weiterhin kann der Eintrag vulkanischer Asche in den Oberflächenozean zu Änderungen der Phytoplanktonvergesellschaftung innerhalb der Aschefallregion führen, was über den Einfluss auf den Export von biogenem Material in den tiefen Ozean den Kohlenstoffkreislauf berühren kann.

Die erste Studie liefert eine Übersicht über die Rolle von Vulkanasche für den biogeochemischen Eisenkreislauf. Sie fasst die Erkenntnisse zum Eisen-Freisetzungverhalten von Vulkanasche in Meer- und Süßwasser zusammen und

diskutiert den Einfluss unterschiedlicher Parameter wie pH-Wert und Korngröße der Aschepartikel. Die Studie beleuchtet ungeklärte wichtige Fragen in einem neuen Forschungsgebiet und bietet Empfehlungen für zukünftige Studien.

Die zweite Studie untersucht die relative Bedeutung von Vulkanasche in Hochnährstoff-, Niedrig-Produktivitätsgebieten (HNLC) mit Fokus auf dem Pazifischen Ozean. Es wurde die Eisenfreisetzung einer größeren Zahl vulkanischer Ascheproben von Subduktionszonenvulkanen des Pazifischen Feuerrings und einiger Ascheproben von Hotspot-Vulkanen in Reinraumlaboratorien gemessen. Weiterhin wurde basierend auf marinen Bohrdaten der millenische Eintrag von Vulkanasche in den Pazifischen Ozean abgeschätzt. Die Bedeutung des Eintrags von Vulkanasche und der daran geknüpften Freisetzung des Nährstoffs Eisen für den Pazifischen Ozean wurde durch den Vergleich mit dem Fe-Eintrag durch Wüstenstaub abgeleitet. Die Studie verdeutlicht, dass Vulkanasche eine wichtige und hinsichtlich ihrer Bedeutung bislang unterschätzte atmosphärische Fe-Quelle für den Pazifischen Ozean und den biogeochemischen Eisen-Kreislauf des Oberflächenozeans darstellt.

Satellitendaten belegen eine massive Erhöhung des Phytoplankton-Wachstums im Aschefallgebiet der 2008 Kasatochi Eruption (Langmann et al. 2010). Die dritte Studie dieser Dissertation konzentriert sich auf den möglichen Einfluss des Ausbruchs auf das marine Nahrungsnetz der Region. Die Studie liefert geochemische Daten dafür, dass das Ausmass der Fe-Freisetzung der Vulkanasche des 2008 Kasatochi-Ausbruchs für eine Fe-Düngung des Fe-limitierten nordöstlichen Pazifik ausreichte. Die Untersuchung evaluiert außerdem, ob die Kasatochi-Eruption über eine Fe-Düngung, der Stimulierung des Phytoplanktonwachstums und über eine Erhöhung der Zooplanktonhäufigkeit zu der unerwarteten massiven Zunahme von Lachs im Fraser River im Jahr 2010 geführt haben kann.

Die vierte Studie untersucht den Einfluss von Vulkanaschenfall des Ätna Vulkans auf den mediterranen Oberflächenozean, einer Niedrig-Nährstoff, Niedrig-Chlorophyll Region. Ich analysierte die Freisetzung von Makro-Nährstoffen und Spurenmetallen verschiedener Vulkanascheproben des Ätna in Berührung mit Meerwasser. Der Eintrag von Vulkanasche ins Mittelmeer (im Zusammenhang mit einem Ausbruch vom 4. November 2002 als Fallstudie) wurde als Funktion des Abstands vom Vulkan

abgeschätzt, um den möglichen marin-biogeochemischen Einfluss eines größeren Ausbruchs des Ätna in unterschiedlichen Abständen vom Vulkan einzugrenzen. Die Studie konzentriert sich auf die Bedeutung von aus Vulkanasche freigesetztem Phosphat, Eisen und fixiertem Stickstoff (z.B. Nitrat) und den möglichen Einfluss auf die MPP des oligotrophen Mittelmeers. Hieraus geht hervor, dass der Vulkan in bis zu 400 km Entfernung Einfluss auf biogeochemische Kreisläufe nehmen kann.

Die letzte Studie untersucht die düngenden bzw. toxischen Effekte von Vulkanasche auf unterschiedliche Phytoplankton-Spezies im Zusammenhang mit Laborexperimenten. Die Diatomee *Thalassiosira pseudonana* zeigt erhöhte Wachstumsraten in mit Vulkanaschen gedüngtem Meerwasser, während die Coccolithophoride *Emiliana huxleyi* entweder keine oder eine negative Reaktion zeigt. Die Studie weist darauf hin, dass Vulkanaschenfall im Meer zu einer Begünstigung von Diatomeen und somit zu einer Veränderung der Phytoplanktonvergesellschaftung führen kann.

INTRODUCTION

INTRODUCTION

State of the art

Volcanic eruptions can eject vast amounts of volcanic ash that can be transported far into remote parts of the ocean (Fig. 1). Upon deposition, volcanic ash can release nutrients into the seawater and therefore may affect the marine primary production (MPP), phytoplankton community structure, and can eventually (directly or indirectly) impact the higher trophic levels in the oceanic food-web (e.g., zooplankton, fish). The atmosphere is considered as a major route by which macro-nutrients and trace metals reach the surface ocean (Duce et al., 1991; Guerzoni et al., 1999; Jickells, 1995). The importance of volcanic ash on the biogeochemistry of the surface ocean, however, has attracted only limited attention compared to the much better investigated effects of desert dust.

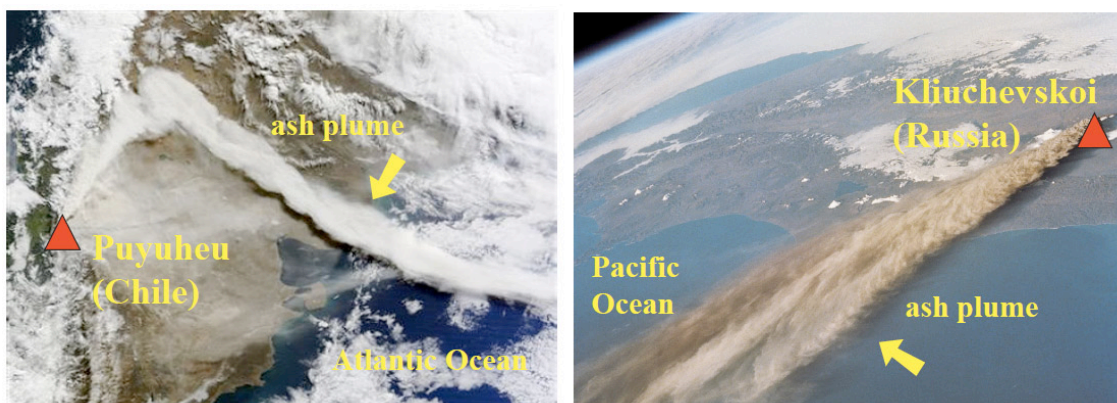


Figure 1: Satellite images illustrating volcanic ash plumes transported in the ocean. Left panel shows the Puyehue (Chile) eruption on 6 June 2011, the white ash plume across Argentina and transported toward the Atlantic Ocean (MODIS, NASA). Right panel shows the eruption of Kliuchevskoi volcano (Russia) on 30 September 1994, the brown ash plume spreading out across in the northwest Pacific Ocean (captured by ISS, NASA).

Nutrient limitation in the surface ocean

The marine primary production (MPP) contributes to about half the Earth's net primary production (Field et al., 1998). Enhancement of MPP can strongly impact the marine ecosystems and also may affect the global climate through drawdown of atmospheric carbon dioxide. In addition, oceanic fertilization may increase the production of dimethyl sulfide (DMS), which in turn impacts the formation of clouds and can exert a climate cooling affect by influencing the global albedo (Lohmann and Feichter, 2005; Turner et al., 2004).

The availability of nutrients in the sunlit part of the oceans is essential for the key metabolic processes of the phytoplankton. Nitrate and phosphate are involved in the nutritional processes and are incorporated into the soft-tissue of the plankton, while silica is used in building the silicate skeletons of the diatoms (Chester, 2000). Essential trace metals, such as iron, are involved in the metallo-enzymes that are crucial in the photosynthetic and respiratory processes, chlorophyll synthesis and bacterial fixation of atmospheric nitrogen (Morel et al., 2003; Sunda, 2001). In the present text, “nutrients” refer to all the essential elements, while “macro-nutrients” refer to nitrate, phosphate and silica, and “micro-nutrients” refer to the trace-metals.

Vertical distribution of nutrients in the water column is typically depleted in the surface due to utilization by the phytoplankton, and enriched in deep-water following remineralization of the sinking detritus. Upwelling process can bring nutrient-rich deep-waters to the surface ocean, and increase the MPP in the regions such as the western Africa, the western USA, the Peru and the southeast Asia (Chester, 2000) (Fig. 2). Horizontal distribution of nutrients in the surface ocean is characterized by higher levels in the coastal regions and the upwelling areas.

In terms of chlorophyll-a and the macro-nutrient concentrations, ocean regions can be divided into three major classes; a) the high-nutrient, high-chlorophyll regions (e.g., coastal zones), b) the high-nutrient, low-chlorophyll regions, and c) the low-nutrient, low-chlorophyll regions (Fig. 2). If concentrations of a particular (or more) nutrient(s) in the surface ocean are lower than the demand of the phytoplankton, these oceanic regions become under-productive (low-chlorophyll regions). The biological

impact of atmospheric supply of nutrients (e.g., via volcanic ash or desert dust) is expected to be higher in the low-chlorophyll regions.

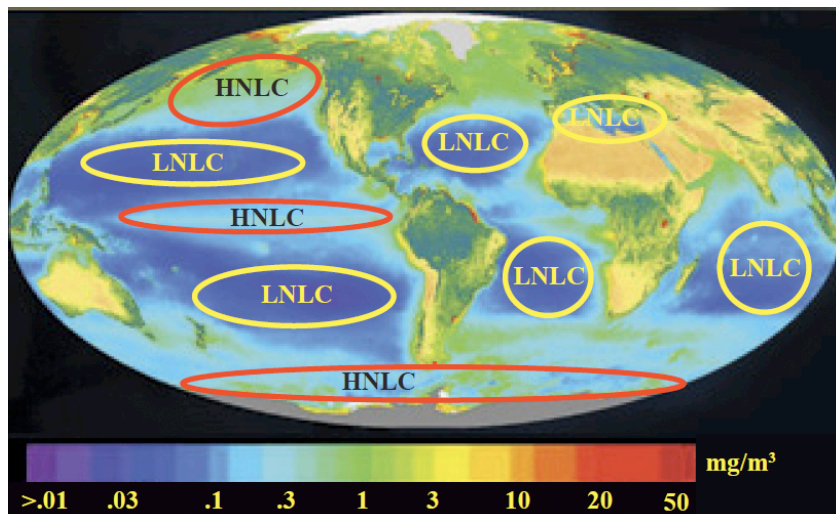


Figure 2: Marine primary production in the global ocean. NASA Sea-viewing Wide Field-of-view Sensor (SeaWiFS) image showing the chlorophyll-a concentrations. Arbitrary locations of the high-nutrient, low chlorophyll (HNLC) (red circles), and the low-nutrient, low-chlorophyll (LNLC) ocean regions (yellow circles) are drawn based on the comparisons of the chlorophyll-a concentrations and the macro-nutrient levels in the surface ocean.

High-nutrient, low-chlorophyll (HNLC) regions have excess nitrate (5-30 $\mu\text{mol/l}$), and variable silica (< 5 $\mu\text{mol/l}$ in the low silica regions, and > 60 $\mu\text{mol/l}$ in the high silica regions) but very low amounts of iron (<0.2 $\mu\text{mol/l}$) (Boyd et al., 2004; Coale et al., 2004; Parekh et al., 2005). HNLC regions cover about 40% of the global ocean and located mainly in the subarctic Pacific, the eastern equatorial Pacific and the Southern Ocean (Fig. 2) (Watson, 2001). HNLC regions are biologically active regimes with intermediate but lower than expected primary production. Iron-deficiency is considered to limit the MPP in the HNLC regions and the iron-hypothesis has been confirmed by a range of iron-enrichment laboratory and field studies (e.g., (Behrenfeld et al., 1996; Boyd et al., 2004; Coale et al., 2004; Martin and Fitzwater, 1988)).

Low-nutrient and low-chlorophyll (LNLC) regions offer very low amounts of macro-nutrients in the surface waters (nitrate < 50 nmol/l, phosphate < 20 nmol/l, silica < 700 nmol/l) (Bonnet et al., 2005; Bruland and Lohan, 2003; Dugdale and Wilkerson, 1992; Sarthou and Jeandel, 2001). LNLC regions account for about half of the global ocean, and are located mainly in the subtropical ocean gyres (little continental input) and can be found in the regions with limited deep water mixing such as the Mediterranean Sea (Fig. 2). Although nitrate has been traditionally known as the major nutrient, phosphate can also be considered as the ultimate limiting nutrient in the LNLC regions (Thyrrell, 1999).

The atmosphere: A major nutrient source in the surface ocean

The major external source of nutrients in the remote ocean is known to be atmospheric deposition of wind-transported mineral dust (eroded crustal material) (Jickells et al., 2005). Mineral dust, also referred as desert dust or aerosol dust, is derived from arid and semi arid regions of the world (e.g., Sahara) and mainly deposited in the Equatorial Atlantic and North East Pacific Ocean (Fig. 3) (Jickells et al., 2005). Mineral dust is deposited into ocean by dry deposition and wet (by rain) deposition {Jickells, 2001 #1280}.

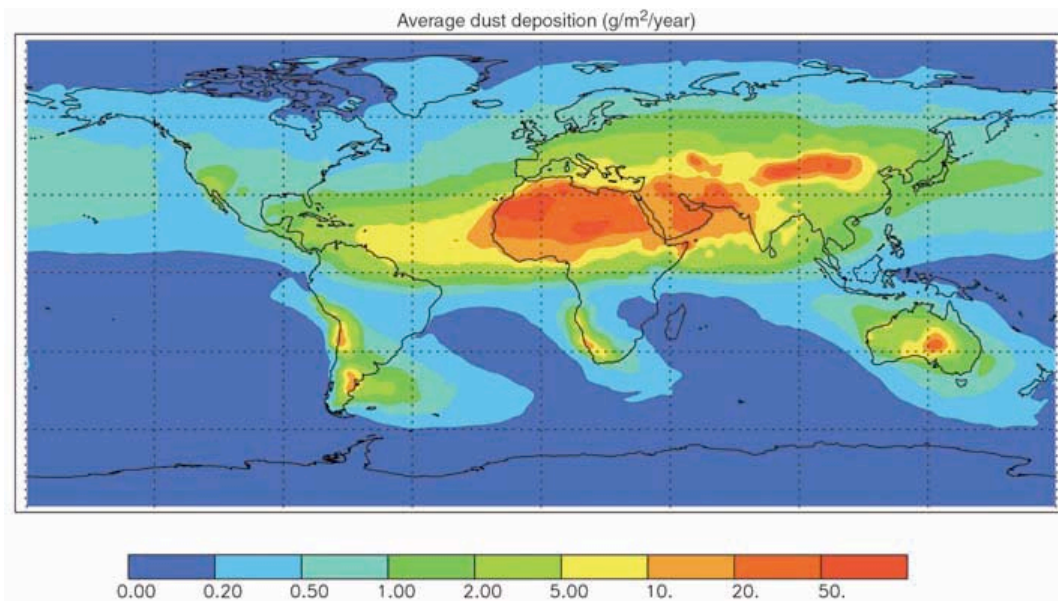


Figure 3: Mineral dust deposition in the world oceans based on (Jickells et al., 2005).

In terms of nutrient input, the dominating deposition mode is uncertain. Some studies suggest that about 70% of the atmospheric particles are removed through dry deposition {Jickells, 2001 #1280}, on the hand some studies suggested up to 95% of the removal is through wet deposition {Jickells, 2005 #1760}. The processes in the atmosphere (e.g., cloud cycling) and in the ocean (e.g., organic complexation) can be extremely important for the solubility of nutrients released from the atmospheric particles (Baker and Croot, 2010). For example, based on the small-scale experimental data, the fraction of iron that is soluble in the aerosol dust ranges more than an order of magnitude (0.001-80%) (Baker and Croot, 2010; Mahowald et al., 2009). Other atmospheric nutrient inputs to the surface ocean considered so far are the extraterrestrial dust (Johnson, 2001), and anthropogenic aerosols such as combustion products of biomass burning (Guieu et al., 2005; Luo et al., 2008). In contact with surface ocean, volcanic ash particles can also rapidly release both macro-nutrients and trace metals that can be bio-available for the MPP, but the relative significance of volcanic ash remains poorly understood.

What is volcanic ash?

Volcanic ash is a size class referring to fragmented fine-grained particles of submicron to less than two millimetres that are produced during volcanic eruptions (Fig. 4). Volcanic ash is generated by fragmentation of magma within the volcanic conduit during eruptions (e.g., bubble burst due to gas expansion, water interaction, or rupture of magma) (Dingwell, 1996). Tephra is the general term for fragmented volcanic material that includes ash particles (submicron to <2 mm), lapilli (2 mm - 64 mm), and bombs and blocks (> 64 mm) (Fisher and Schmincke, 1984; Schmincke, 2004). Since the term is a size classification, it does not provide information about the chemical composition or a particular volcanic process from which the ash is formed. The focus of this study is the airborne volcanic ash that is produced during subaerial volcanic eruptions and which can reach the surface ocean through atmospheric transport (Fig. 6).

Chemical composition of volcanic ash can range from silicic (relatively lower MgO and FeO and higher SiO₂) to mafic (relatively higher MgO and FeO and lower SiO₂ contents). Volcanic ash can be in colours ranging from white, brown, grey or black (e.g.,

Fig. 1), reflecting the magma composition, where silicic ash has lighter colours compared to mafic ash. In terms of nutrient supply into the oceans, silicic ash can play a more important role as it is found more widespread in the ocean sediments due to higher explosivity of subduction zone volcanoes. Aeolian fractionation can also affect the chemical composition of the ash deposits since denser minerals tend to settle first compared to silicate glass (e.g., olivine, clinopyroxene) (Larsson, 1937; Middleton et al., 2003).

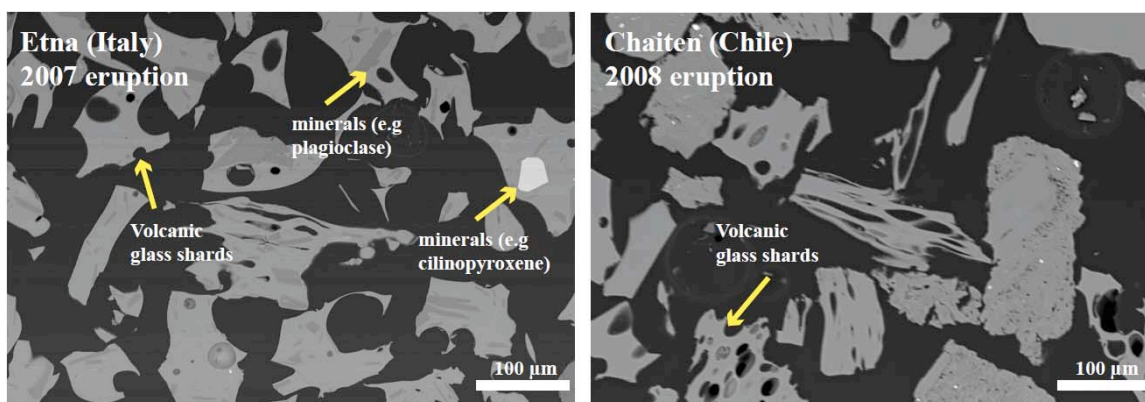


Figure 4: Electron microprobe image of volcanic ash from (left) Etna eruption on 23 November 2007, and (right) Chaiten eruption on 3 May 2008. Ash samples consist of volcanic glass shards indicated as the angular irregular particles (resembling puzzle-pieces), and minerals (e.g., plagioclase, clinopyroxene).

Volcanic ash particles are typically composed of vitric fragments (volcanic glass, pumice), pyrogenic crystalline minerals (inherited from magma), and lithic particles eroded from the conduit (pieces of pre-existing rocks of any origin) (Fig. 4). Silicate glass (or glass shard) is the chilled and fragmented magma, and typically is the dominating component of a volcanic ash sample (Fisher and Schmincke, 1984). All solid particles found in the volcanic ash plumes interact with the volcanic gases/acids forming a thin layer of water-soluble salt coatings on the ash surface (Óskarsson, 1980) (Fig 7). Glass shards are typically angular, irregular fragments with extraordinarily large surface-to-volume ratio (Fig. 4). Pyrogenic minerals mainly include silicates, such as amphibole, biotite, feldspar, olivine, pyroxene and quartz. Minerals are more abundant in the grain size of about 63 µm - 2 mm and are generally absent below 10 µm, whereas glass shards

can be much smaller like aerosols (Fisher and Schmincke, 1984). Total (bulk) nutrient content of volcanic ash can vary by the proportions and composition of these individual fragments (Delmelle et al., 2007; Fisher and Schmincke, 1984; Óskarsson, 1981).

Distribution of subaerial volcanoes in the world

Volcanoes are widespread around the world and found in all climate regions from polar Alaska to tropical Indonesia (Fig. 5). Most of the subaerial volcanoes are concentrated along the subduction zones (convergent plate boundaries) where oceanic plates dive under the continental plates (Fig. 7) (Simkin and Siebert, 2000). For example, a chain of numerous active and explosive volcanoes encircles the Pacific Ocean, so called *the Pacific Ring of Fire* (Fig. 5). Hot spots are the volcanic regions that are thought to be fed by an underlying mantle plume, such as the Hawaii hot spot region (Hall, 1987; Simkin and Siebert, 2000).

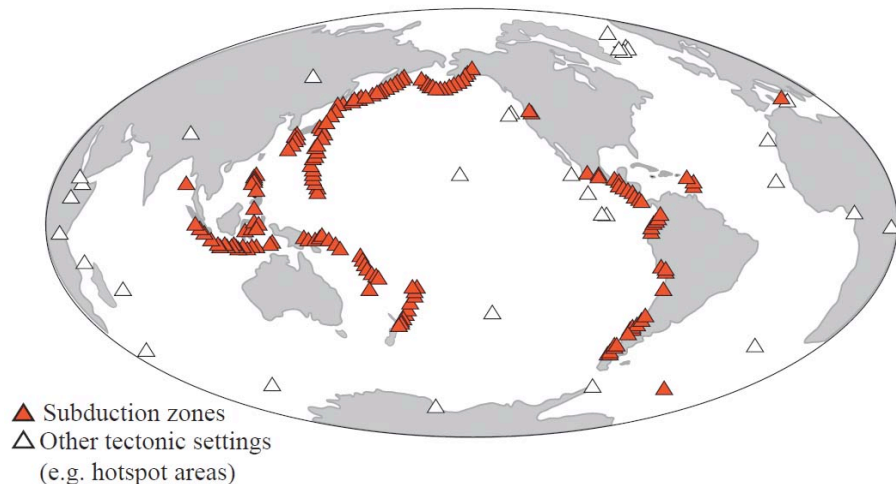


Fig 5: Distribution of subaerial volcanoes in subduction zones (red triangles) and other tectonic settings such as hot spots (white triangles) based on (Simkin and Siebert, 1994).

The exact number of volcanoes that have erupted during the whole life span of the Earth is not precisely known. During the past 10,000 years, there are about 1,500 volcanoes on land that have been active (Simkin and Siebert, 2000). The number of submarine volcanoes is thought to be even larger than the number of subaerial volcanoes. At present, there are about 550 volcanoes that have had known eruptions during the recorded history (Simkin and Siebert, 2000). About 50-70 volcanoes erupt every year, with at least one large eruption each year (e.g., Puyehue (Chile) and Grimsvötin (Iceland)

in 2011, Table 1). An average of about 20 volcanoes erupt at any given time. The frequency of volcanic eruptions can range from daily/weekly to a few years to hundred thousand years, based on the scale of the eruptions. Table 1 summarizes the frequency of eruptions based on the eruption magnitude described as “Volcanic Explosivity Index” (VEI) that ranges from 0 to 8. Small-scale eruptions occur more frequent compared to large-scale eruptions (Table 1).

Table 1: The type and frequency of volcanic activity based on Volcanic Explosivity Index (VEI) (Newhall and Self, 1982; Simkin and Siebert, 1994).

VEI	Plume height (km)	Eruptive volume (km ³)	Eruption type	Frequency	Example
0	0.1	10 ⁻⁶	Hawaiian	Continuous	Kilauea
1	0.1-1	10 ⁻⁵	Hawaiian/Strombolian	Months	Stromboli
2	1-5	10 ⁻³	Strombolian/Vulcanian	Months/year	Galeras
3	3-15	10 ⁻²	Vulcanian	Year/few years	Puyehue (2011)
4	10-25	10 ⁻¹	Vulcanian/Plinian	Year/few years	Eyjafjallaökull (2010)
5	> 25	1	Plinian	5-10 years	Pinatubo (1991)
6	> 25	10	Plinian/Ultra-Plinian	1,000 years	Krakatoa (1883)
7	> 25	100	Ultra-Plinian	10,000 years	Tambora (1815)
8	> 25	1,000	Ultra-Plinian	100,000 years	Toba (74 ka)

Volcanic processes that modify the surface composition of the volcanic ash particles

During an eruption, the surface composition of the ash particles is modified by various reactions involved in different temperature dependent zones in the ash plume (Óskarsson, 1980; Rose, 1977) (Fig. 6). In terms of surface composition and nutrient solubility, freshly erupted volcanic ash is different from fossil ash. Fossil volcanic ash that has been deposited on land for a few years to a few thousands of years becomes an aeolian dust, and not reflect the same surface chemistry of freshly erupted ash. Fresh (pristine) volcanic ash particles have water-soluble metal-bearing salt coatings and can through volcanic eruptions be transported directly into the surface ocean and can rapidly release soluble and bio-available nutrients (Duggen et al., 2007; Frogner et al., 2001; Jones and Gislason, 2008).

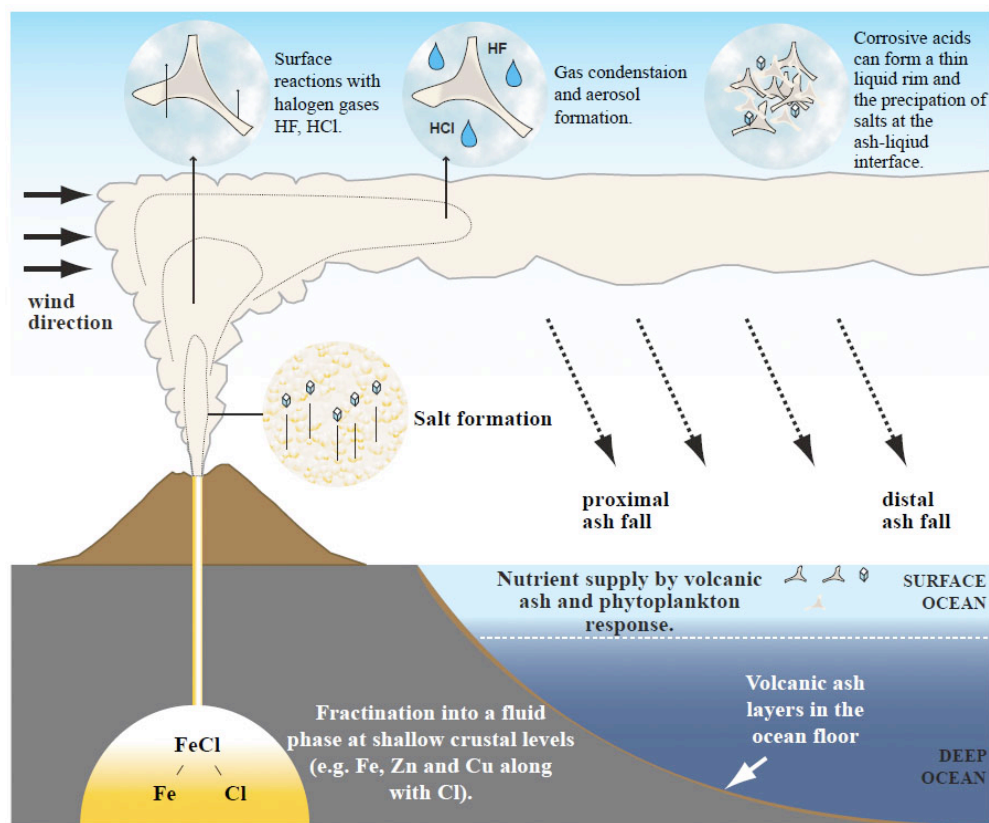


Figure 7: Volcanic processes occurring in the ash plume that can affect the surface composition of the volcanic ash particles. The temperature dependent zones are based on Óskarsson (1980).

Volcanic aerosols contain metal salts and acids which are adsorbed on the to the surface of volcanic ash particles, forming deliquescent metal salt encrustations, and crystalline salts (Óskarsson, 1980; Óskarsson, 1981). Acid magmatic gases such as HF, HCl and SO_2 are the major anion donors of these highly soluble compounds adhering to ash particles (Fig. 6) (Naughton et al., 1976; Óskarsson, 1981; Thordarson and Self, 1996).

The metal salts are commonly found as fluorides, chlorides and sulfates (Naughton et al., 1976; Óskarsson, 1981; Thordarson and Self, 1996) and formed at magmatic temperatures ($\sim 1300^\circ\text{C}$) from the degassed volatiles (e.g., ammonium iron (III) chloride hydrate ($2\text{NH}_4\text{Cl}\cdot\text{FeCl}_3\cdot\text{H}_2\text{O}$) (Fig. 6) (Óskarsson, 1980). Aerosol salts later interact with the ash and are adsorbed to the ash particle surface (Smith et al., 1983).

Upon further cooling ($<700^{\circ}\text{C}$), possibly within the first minutes of the eruption, halogen gases HF and HCl directly interact with the solidified silicate material by surface adsorption (Óskarsson, 1980). Condensation of acids and formation of acid aerosols takes place at lower temperatures. Sulphuric acid and halogen acids condensate at temperatures below 338°C and 120°C , respectively (Óskarsson, 1980). Acids leach the ash surface and forms a thin film (of nanometre scale) enriched in silica, aluminium and iron (the glass forming elements) (Delmelle et al., 2007). The in-plume reactions (Fig. 6) can remove loosely bound cations (such as iron) in the silicate glass structure and transforms the surface into more soluble halide and sulphate salts (Fig. 6) (Delmelle et al., 2007; Frogner et al., 2001), and in turn, affect the solubility of nutrients released from volcanic ash.

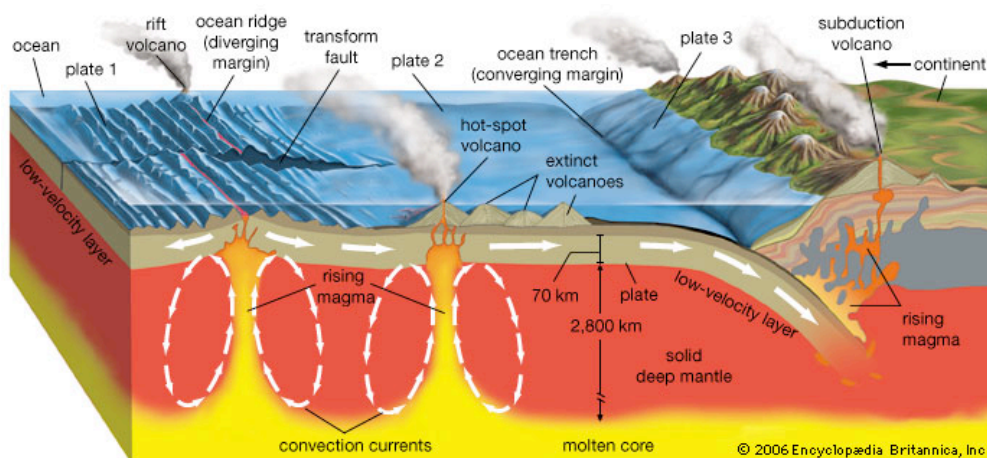


Figure 7: Volcanic environments at the plate boundaries and at the hot spot regions (<http://www.britannica.com/EBchecked/topic/632078/volcanism>).

Magma source and volcanic gases can, therefore, play an essential role in the content of bio-relevant elements in the surface of the volcanic ash particles, particularly the soluble salt coatings. It has been suggested that the HCl/HF volcanic gas ratio affects the metal composition of the salt coatings (Óskarsson, 1980). For example, iron, zinc and copper are found to be enriched in the salts that are created in volcanic environments with high HCl/HF gas ratios (Óskarsson, 1980). Due to recycling of chlorine-rich seawater in convergent plate margins (Fig. 7) (Anderson, 1975; Óskarsson, 1980; Symonds et al.,

1988), subduction zone volcanoes generally have higher HCl/HF gas ratios compared to hot spot volcanoes (Oppenheimer, 2004; Sigurdsson et al., 2000), and therefore likely to produce ash that has higher iron contents in the soluble salt coatings. Explosive volcanoes with larger eruption columns can provide longer volcanic gas and ash interaction, and therefore may favour the soluble salt formation on the ash surface (Witham et al., 2005).

Dispersal of volcanic ash depends on the scale of the eruption (e.g., Hawaiian or Plinian, Table 1), the wind strength and direction, and the grain-size distribution of the ash particles (Fig. 6). Ash particles fall out of an ash plume according to their settling velocities (denser settles first). Grain size-distribution of the ash deposits, therefore, decreases with increasing distance from the volcanic source (Walker, 1971). Very fine ash particles can be agglutinated, and deposited together with larger particles, therefore, the ash deposits are rarely well-sorted (Wiesner et al., 1995). Fragments with low air-fall velocities compared to wind strength may circle the globe before settling to ground (e.g., Pinatubo 1991 eruption) (Wiesner et al., 1995).

Birth of a new interdisciplinary research field: Oceanic fertilization by volcanic eruptions

The majority of previous studies on volcanic ash had focused on the effects on the soil fertility (Ugolini and Dahlgren, 2002) or the fertilizing/toxic effects on fresh waters (Witham et al., 2005). Oceanic fertilization by explosive volcanic eruptions is a new but rapidly growing research field showing a remarkable increase in the number of publications over the last years (Fig. 8). In the frame of the interdisciplinary research project NOVUM-1 (Nutrients originating volcanoes and their effects in the euphotic zone of the marine ecosystems. Part 1: volcanic ash) funded by IFM-GEOMAR, I have contributed to six publications related to this new research field, five of which are presented in this dissertation (Chapter I to V). Figure 8 summarizes the publications focusing on the oceanic biogeochemical impacts of volcanic eruptions. Although, the present dissertation focuses on volcanic ash ejected from subaerial eruptions, I did not exclude the few publications focusing on other volcanic products (aerosols, gases and pumice rafts) and a submarine eruption (Fig. 8).

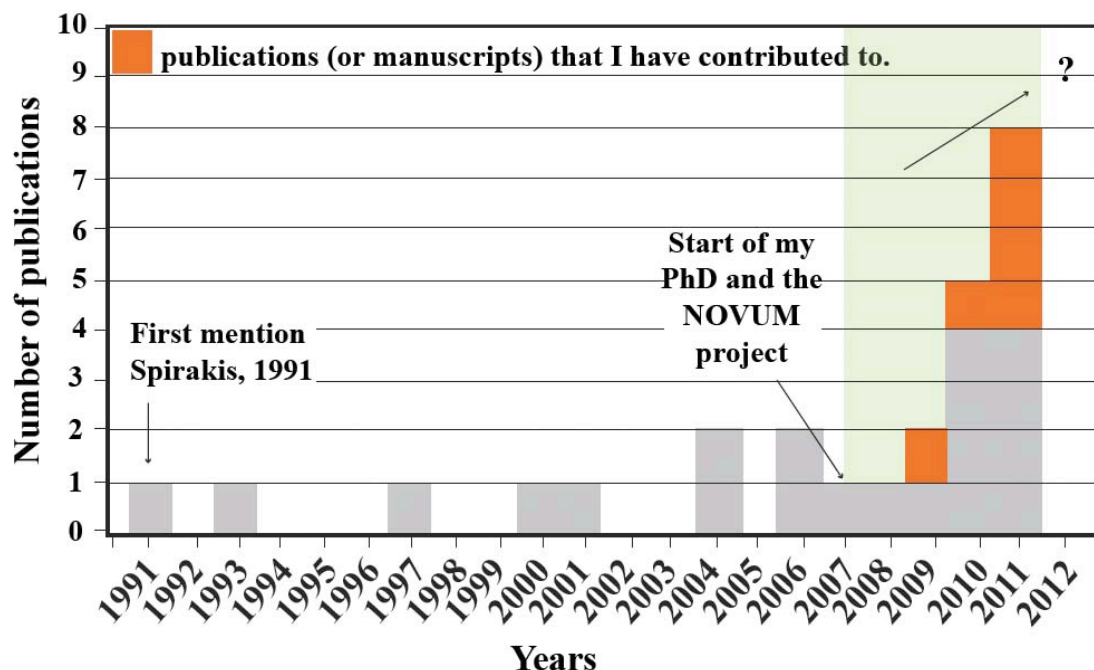


Figure 8: Graph showing the increasing scientific interest on the marine biogeochemical impacts of volcanic eruptions. The publications are referred in the main text and contain scientific papers, communication letters, a master thesis and recent manuscripts (excludes poster abstracts). The studies that I have contributed to are; Duggen et al. (2010); Hoffmann et al. (submitted to Marine Chemistry); Olgun et al. (submitted to Marine Chemistry); Olgun et al. (2011); Olgun et al. (submitted to Marine Ecology Progress Series); Teschner (2009).

The communication letter by (Spirakis, 1991) was the first publication mentioning the potential oceanic iron-fertilization by volcanic ash. In June 1991, Pinatubo volcano in Philippines created a large-scale volcanic eruption and ejected vast amounts of ash and aerosols in the atmosphere that traveled around the globe. Just after the large Pinatubo eruption, an unexpected CO_2 drawdown occurred in the Northern Hemisphere, which has been speculated to be linked to iron-fertilization of Southern Ocean by the Pinatubo ash (Sarmiento, 1993). Hemispheric O_2/N_2 gradient were found to be consistent with additional O_2 pulse from Southern Hemisphere oceans during austral summer 1991-92 (Keeling et al., 1996).

In a subsequent paper, Watson (1997) discussed the possible long-term affects of oceanic fertilization by Pinatubo volcanic ash, which was based on the changes in the

rain ratio of inorganic to organic carbon by the diatom blooms (Watson, 1997). However, due to lack of satellite images in the year of Pinatubo eruption, it remained speculative whether the carbon anomaly was triggered by a CO₂ uptake by the oceans or the land biota (Jones and Cox, 2001).

Based on the four marine drill cores collected along the Atlantic Ocean (on a north-south transect), Bains et al. (2000) suggested that oceanic fertilization by volcanic ash fallouts or increased inputs from the continents may have caused an increased export primary productivity in the Paleocene/Eocene (thermal maximum) boundary (about 55 Myr ago). The authors argued that increased biological carbon pump into the oceans may have effectively reduced atmospheric greenhouse gases, cooling the Earth and returning the climate back to late Paleocene conditions (Bains et al., 2000).

Frogner et al. (2001) was the first experimental study examined the release of nutrients (phosphate, silica, iron and manganese, by means of flow-through experiments) in seawater from a volcanic ash sample from the Icelandic Hekla eruption in 1991. The study also suggested that the adsorbed metal-salts on the ash particles would dissolve much faster than volcanic glass pointing out the importance of the surface reactions in the eruptive plume (Frogner et al., 2001).

In the following years, studies focusing on the ice-cores from Antarctica and Greenland evidenced strong correlations between the volcanism and the climate, potentially due to oceanic fertilization by volcanic eruptions (Bay et al., 2004; Bay et al., 2006). However, no firm conclusions could be drawn from the findings whether the climate affected the volcanism (e.g., ice-sheet unloading) or volcanism affected the climate (via ocean fertilization) (Bay et al., 2004; Bay et al., 2006).

Frogner Kockum (2006) investigated the aluminum and fluoride related to volcanic aerosols and discussed the possible consequences on the phytoplankton in fresh waters and the seawater. The results of the geochemical experiments and the modeling data (by PHREEQC geochemical model) suggested that high pH buffering capacity of seawater will reduce the toxic effects of aliminoflouride complexes in marine environments (Frogner Kockum, 2006).

The first satellite evidence showing enhanced MPP related to a volcanic eruption was the study by Uematsu et al. (2004). Based on the SeaWiFS data, the authors showed

the enhanced chlorophyll-a concentrations in the surface ocean after the eruption of Miyake-Jima (Japan) in 2001 in the south of Kuroshio Island (Uematsu et al., 2004). A likely reason of the enhanced chlorophyll-a concentrations in this nutrient-deficient ocean region has been suggested to be high emissions of ammonia gas (NH_3) from the Miyake-Jima volcano (Uematsu et al., 2004).

Duggen et al. (2007) conducted the first voltametric experiments with volcanic ash and also the first ash-fertilization bio-incubation experiments providing direct evidence that marine diatom species *Chaetoceros dictyota* can utilize iron released from volcanic ash (Fig. 9). The comprehensive study showed that an array of nutrients (fixed-nitrogen, phosphate, silica, iron, zinc and copper) rapidly (on minute-scale) mobilized from volcanic ash (Duggen et al., 2007). The study also provided evidence by satellite data pointing increased chlorophyll-a (captured by SeaWiFS) during the July 2003 eruption of Soufrière Hills volcano in Lesser Antilles (Duggen et al., 2007).

Another geochemical study by Jones and Gislason (2008) focused on the nutrient release from six volcanic ash samples, by means of flow-through experiments. The authors suggested a potential pH decrease in the ash fallout regions (Jones and Gislason, 2008). Although there has been no evidence from field measurements confirming the pH-drop in seawater, malformation of aragonite pteropod shells found in the marine sediments has been linked to a pH decrease during recent eruptions Soufrière Hills Volcano (Montserrat) (Wall-Palmer et al., 2011).

Gabrielli et al. (2008) examined Greenland ice by using sixty snow pits and found anomalous methane sulfonic acid peaks associated with early biological productivity in late winter 1991 in the North Atlantic Ocean possibly due to oceanic (phosphate-)fertilization by the Hekla (Iceland) 1991 eruption (Gabrielli et al., 2008). The study also provided evidence for Pinatubo (Philippines) 1991 fallout as far as Greenland (Gabrielli et al., 2008).

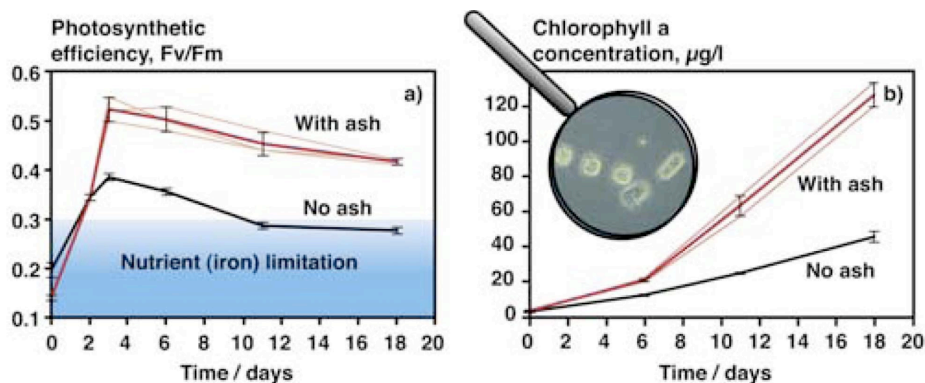


Figure 9: Increase in the photosynthetic efficiency and chlorophyll-a concentrations in the volcanic ash fertilized natural seawaters, based on the bio-incubation experiments with diatom species *Chaetoceros dichchaeta* by Duggen et al. (2007).

Cather et al. (2009) proposed that large ignimbrite eruptions might have produced climate forcing through oceanic iron fertilization by silicic volcanic ash and expanded the primary production that leads to a drop in CO₂ from the atmosphere (Cather et al., 2009). The study correlates the ignimbrite fluxes (back to early Eocene, about 50 Myr) with the oxygen and carbon isotopic anomalies compiled from benthic foraminifera from more than forty Deep Sea Drilling Project and Ocean Drilling Programme sites (Cather et al., 2009). Atmospheric CO₂ anomalies between 1958-1995 at Mauna Loa Observatory (Hawaii) also showed remarkable CO₂ drawdown followed by two large eruptions (Agung 1963 and Pinatubo 1991) (Cather et al., 2009).

In another paper in the same year, Jicha et al. (2009) found strong relation between the deep-sea oxygen isotopes and the peak periods of arc volcanism, and the authors suggested that voluminous circum-Pacific volcanism during the late Eocene may caused fertilization of the Pacific Ocean and cooled the climate in Eocene/Oligocene boundary (about 34 Myr ago) (Jicha et al., 2009).

The experimental study by Teschner (2009), in the frame of NOVUM-project, focused on pumice, another volcanic product that is highly porous and can float in the surface ocean long-distances. Based on the experimental data, the study suggested that the release of iron and silica from pumice can fertilize the eastern equatorial Pacific Ocean, a major HNLC region (Teschner, 2009).

A submarine volcanic eruption in August 2006 by the Home Reef volcano in Tonga in southwest Pacific ejected pumice material that reached the surface ocean resulting a greenish-blue discoloration in the surface water (Mantas et al., 2011; Teschner, 2009). Investigation of the satellite data (MODIS) indicated enhanced chlorophyll-a concentrations in the pumice raft region (Mantas et al., 2011). Based on the visual interpretations, the bloom detected in southwest Pacific was dominated by the nitrogen-fixing cyanobacteria *Trichodesmium sp.*, which is known to positively respond to the external input of iron (Mantas et al., 2011).

The 7-8 August 2008 eruption of the Kasatochi volcano in Aleutian Islands located in the north Pacific has been suggested to fertilize the iron-limited northeast Pacific Ocean and created a massive diatom bloom evidenced by the satellite data (MODIS) (Hamme et al., 2010; Langmann et al., 2010a; Langmann et al., 2010b). The Kasatochi eruption provided the first satellite evidence of ash fertilization in an iron-limited region.

In the study by Lin et al. (2011), the authors diagnosed a bloom-like patch a week after the Anatahan 2003 eruption in the Mariana Islands located in the LNLC north west Pacific Ocean oligotrophic gyre. In addition, nutrient release (nitrate, phosphate and iron) experiments with ash sample from Anatahan eruption (in Milli-Q water), confirmed the likelihood of oceanic fertilization by the Anatahan ash fallout (Lin et al., 2011).

The role of airborne volcanic ash for the surface ocean biogeochemical iron cycle has been reviewed in Duggen et al. (2010) (presented in Chapter I). More recently, another review paper has focused on volcanic and atmospheric controls on the iron solubility of volcanic ash particles (Ayris and Delmelle, in press). Synopsis of the publications and manuscripts that I have contributed is given in the following section “Aims and outline of the thesis”.

Aims and outline of the thesis

The major goal of this thesis is to evaluate the possible impacts of volcanic ash deposition on the surface ocean biogeochemistry and the MPP. I focused primarily on the nutrient release behavior of volcanic ash in the seawater. In order to better understand the relative importance of volcanic ash for the surface ocean, another necessary aspect was the quantification of the volcanic ash deposition into the oceans. Therefore, we estimated the offshore volcanic ash flux over large ocean basins or during single large eruptions, and evaluated the nutrient input from volcanic ash in comparison with that from mineral dust, in terms of not only the chemical behavior but also the particle fluxes into the ocean.

Iron is a key nutrient, which affects the MPP in various ocean areas including HNLC and LNLC regions. The first three chapters of the thesis focus on iron input from volcanic ash. The first paper (Chapter I) reviews the chemical behavior of volcanic ash in terms of iron release in freshwater and in seawater (Duggen et al., 2010). The paper also summarizes the experimental literature data and discusses the major discrepancies related to the experimental set-ups (e.g., solution pH, ash-to-seawater ratio, particle size effect). The review paper provides milestones and key future research questions in order to develop a better understanding of volcanic iron and surface ocean interactions.

The second paper (Chapter II) focuses on the Pacific Ocean, the largest ocean body that covers about 70% of the major HNLC regions (Fig. 10). The Pacific Ocean at the same time hosts various active and explosive volcanoes (the *Pacific Ring Fire*, Fig. 10) and exposed frequently to volcanic ash deposition (Olgun et al., 2011). The paper provides a nearly global range of Fe-release from volcanic ash in seawater. Furthermore, volcanic ash flux into the Pacific Ocean is estimated (based on the marine drill core data), and the results are compared with the mineral dust and associated iron deposition. Spatial distribution of volcanic ash and mineral dust deposition are discussed with a particular focus on the iron-limited regions.

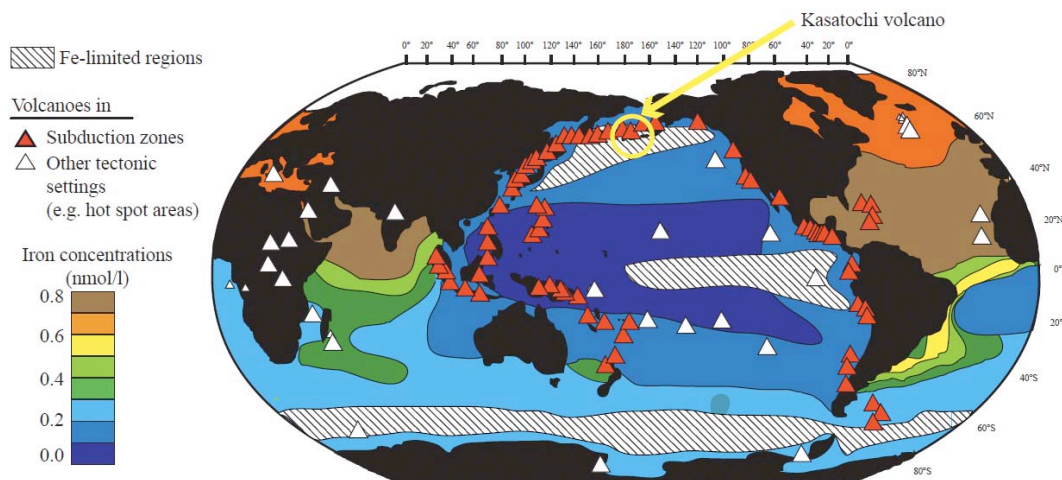


Figure 10: Iron-limited ocean regions and distribution of active volcanoes based on (Olgun et al., 2011). Average surface ocean iron concentrations are based on (Parekh et al., 2005). Distribution of volcanoes are based on (Sigurdsson et al., 2000).

The third manuscript (Chapter III) focuses on a specific eruption the Kasatochi August 2008 in the Aleutian Islands that deposited volcanic ash into the iron-limited northeastern Pacific Ocean (Fig. 10) (Olgun et al., submitted to Marine Ecology Progress Series). The Kasatochi eruption has been suggested to create a massive diatom bloom in the northeastern Pacific Ocean evidenced by the satellite data (Hamme et al., 2010; Langmann et al., 2010b). The manuscript examines the iron-input from the Kasatochi ash fallout and provides geochemical evidence for the iron-fertilization by the Kasatochi eruption. The manuscript further evaluates the possible marine ecological impacts of the Kasatochi eruption on the higher trophic levels in the marine food-web, including the sockeye salmon population in the Fraser River in Canada.

The fourth manuscript (Chapter IV) concentrates on the Mount Etna, one of the most active volcanoes in the world, which is located in the low-nutrient, low-chlorophyll Mediterranean Sea (Fig. 11) (Olgun et al., to be submitted). The manuscript examines the release of nutrients; fixed-nitrogen, phosphate, silica, and iron, zinc, copper from Etna ash, with a particular focus on the phosphate since MPP in the Mediterranean Sea is limited largely by the availability of dissolved phosphorous. The manuscript also provides ash flux estimates as function of distance from the volcano during an explosive Etna eruption (4-5 November 2002 eruption). Ash and related nutrient flux during an

Etna eruption is discussed in comparison with the mineral dust flux during dust storm events in the Mediterranean.

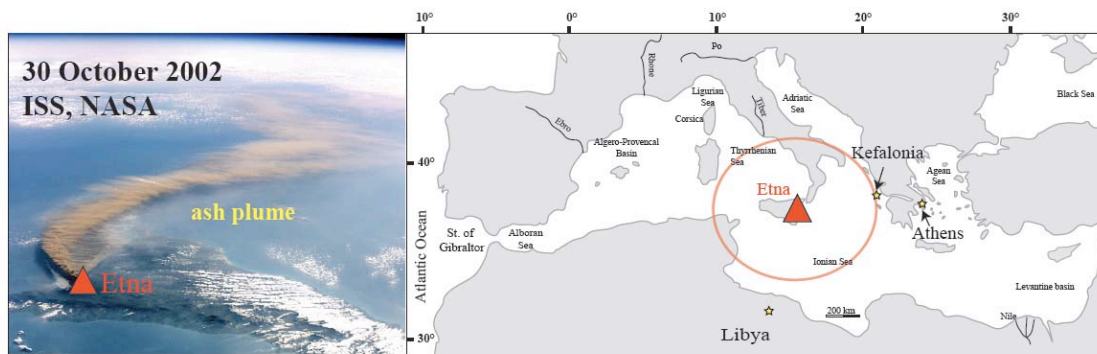


Figure 11: (Left) An ash plume ejected from Mount Etna (Sicily, Italy) on 30 October 2002. The ash plume was transported as far as Libya (ISS, NASA). (Right) Map of the Mediterranean Sea showing the region that is likely to be affected during explosive volcanic eruptions of Mount Etna (Olgun et al., submitted to Marine Chemistry).

The fifth manuscript (Chapter V) shows the results of bio-incubation experiments with volcanic ash conducted by Dr. Linn Hoffmann. The aim of the manuscript is to understand how phytoplankton responds to different types volcanic ash with a focus not only on the fertilizing but also the potential toxic effects of volcanic ash on the phytoplankton growth. The species dependence is tested by two different phytoplankton; a diatom species *Thalassiosira pseudonana*, and a coccolithophoride species *Emiliania huxleyi*. The results of the biological experiments are discussed in relation with the trace-metal release from volcanic ash samples and copper ligand production of phytoplankton when grown in the ash fertilized seawater.

Sampling and analytical methods

Sampling

Volcanic ash samples used in this study are dry (pristine) samples that are collected soon after the eruptions. I have analyzed fifty eight pristine volcanic ash samples that stem from sixteen different volcanoes distributed world-wide, including the chain of active volcanoes around the Pacific Ocean (the *Pacific Ring Fire*) and hot spot volcanic regions such as Hawaii and Iceland (Fig. 12).

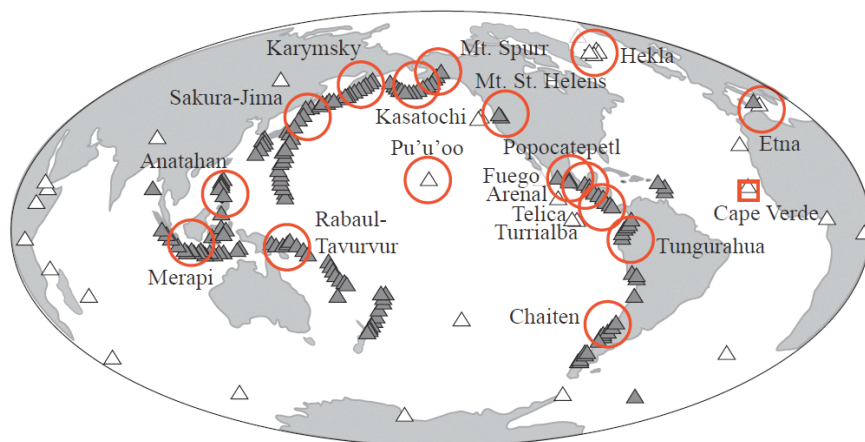


Fig 12: Location of the samples used in this study. Red circles indicate locations of the volcanic ash samples. Volcanoes located in the subduction zones are indicated as gray triangles, and other tectonic regions (e.g., hot spots) as white triangles. The dust sample collected on Cape Verde Island is indicated as a red rectangle.

The composition of the volcanic ash samples ranges widely from basaltic (with silica <50 wt.%) to rhyolitic (silica > 50 %). Ash deposits that lay several months to hundreds of years (fossil ash) are less relevant for this study since they are exposed to weathering and the most soluble compounds (e.g., the metal-salts) on the ash surface are likely to be leached by rain. Aside from the fossil ash, which is readily available, the freshly- and dry-collected ash is less accessible. The ash sample set is therefore a valuable compilation and was provided by scientific collaborations with several universities and institutes all around the world such as Japan, Russia, Europa, USA (see Supplementary Chapter II).

Most of the ash samples were collected during the field studies shortly after the eruptions (i.e. couple of hours to 1-2 days). To avoid the contamination from the ground or mixing with the older deposits, these samples were picked from the upper layer of the ash deposits. Some of the samples were collected from the plastic plates provided for ash sampling nearby the volcano or within the university campuses (e.g., Sakura-Jima, Japan). Only one sample, the Kasatochi volcanic ash sample used in Chapter III, was collected from a fishing boat, which entered the heavy volcanic ashfall region in northeast Pacific around 13 km distant from the volcano. The sampling sites vary from a few kilometers to more than a hundred kilometers from the volcanic source. The samples were stored in plastic bags, and any contact with metal-bearing material was avoided (e.g., metal-sieves).

In addition to volcanic ash samples, a dust sample was used for comparison of the nutrient from volcanic ash and mineral dust. The mineral dust sample was provided by Dr. Maija Heller (IFM-GEOMAR). The dust sample was collected from the loess deposits in Calhua (Fig. 12) located in the northwestern part of the Cape Verdean island of Sao Vicente (16.9°N, 24.9°W) on July 2007. The loess deposits are composed of aerosols transported from arid regions in North African deserts (e.g., Mali, Niger, Chad and southern Algeria), which are transported by the west African trade winds. The dust sample was sieved through 100 µm plastic filters and stored in plastic bags. Based on the elemental analyses (Heller and Croot, 2011) the dust sample consists of silt from the Sahara desert.

Analytical Methods

Trace metal release measurements by stripping voltammetry

Seawater release of iron, zinc and copper were determined by electrochemical analyses by means of stripping voltammetry based on (Croot and Johansson, 2000; Duggen et al., 2007), under clean laboratory conditions with a hanging mercury drop electrode, a Metrohm VA757 at IFM-GEOMAR (Fig. 13). Voltametric method allows determination of specific ionic species of concentrations as low as 10^{-12} mol/l (Croot and Johansson, 2000). Iron-release measurements were done by Cathodic Stripping Voltammetry (CSV), while zinc and copper measurements were done by Anodic

Stripping Voltammetry (ASV).

The measurements were conducted *in situ* in seawater by mixing defined quantities of sample (~50 mg) and natural seawater (~20 ml) following the method previously applied by (Duggen et al., 2007) for the trace-metal release from volcanic ash. The ash samples were unsieved representing the dissolution of a natural sample. The mass (mg) to solute (ml) ratio is 1:400 mimics the deposition of centimeter-to decimeter-scale ash layers in the ocean, which are frequently found in the marine sediments (Straub and Schmincke, 1998).



Figure 13: The author doing voltammetric trace-metal measurements in the clean laboratory at the west-shore campus of IFM-GEOMAR.

The seawater used for the experiments was retrieved during the Meteor cruise M68-3 in the Eastern Equatorial Atlantic, filtered with 0.2 μm membranes immediately after collection and stored in an acid-cleaned polyethylene carboy. Other containers used during the experiment were made of cleaned quartz glass or polytetrafluoroethylene. The pH of the natural seawater is buffered at pH 8 by adding 200 μl of 1 M EPPS pH-buffer (4-(2-hydroxyethyl)piperazine-1-propanesulfonic acid) to 20 ml seawater. The solution-pH chosen for the experiments mimic the dissolution of trace-metals under seawater conditions through dry deposition process, which is considered the globally dominant deposition process for atmospheric dust particles (Jickells and Spokes, 2001).

Labile Fe measurements were performed by using an established CSV-method using a competing ligand (Croot and Johansson, 2000). Dissolved Fe in oxic seawater precipitates quickly through oxidation of more soluble Fe (II) to poorly soluble Fe (III) (Millero and Sotolongo, 1989). Prior to measurements, a competing ligand TAC (2-(2-Thiazolylazo)-p-cresol) was added to seawater to avoid adsorption of the released Fe (Boyd et al., 2000). 20 ml of Atlantic seawater were mixed with 20 μ l of 10 nM TAC ligand and 200 μ l of 1M EPPS. The release of Fe from the Cape Verde dust sample was determined in the same way to allow direct comparison with the volcanic ash data.

The samples are added into seawater in a polyethylene voltametric cell-cup. Prior to the mixing of volcanic ash and the seawater, the background concentrations of the seawater were measured by three blank measurements. After addition of the samples into the seawater (t_0), the concentrations were measured every few minutes (t_n) during the 60 minutes contact with seawater, to test the rapid impact of a volcanic ash fall in seawater. Background concentrations were subtracted from the concentrations after the sample addition. Trace-metal release after sample addition were later converted into release in nanomoles per gram of ash (nmol/g). The sensitivity of analyses was referred from repeat measurements.

Macro-nutrient release from volcanic ash by Agitation experiments

The release of NO_3^- , NH_4^+ , NO_2^- , PO_4^{3-} and SiO_2 were examined by means of leaching experiments. One gram of unsieved ash sample was mixed with 50 ml low-nutrient seawater (nutrient $<1 \mu\text{mol/l}$) from Ocean Scientific International. The solution is prepared in 60 ml Nalgene polypropylene (PP) plastic bottles, and shaken gently for about twenty minutes. After agitation times of one hour and twenty hours (for selected samples), the particulate material was separated from the seawater by filtering through a 5 μm mesh PTFE filter (Sartorius). Macro-nutrient concentrations in the seawater were measured by standard routine photometry at IFM-GEOMAR. Measurements with the dust sample followed by the same methodology used for volcanic ash for direct comparison. The measured concentrations of dissolved macro-nutrients (in $\mu\text{M/L}$) were converted to nanomoles per gram of ash and dust (nmol/g ash, nmol/ g dust).

Analyses of volcanic glass composition by means of electron microprobe

The major elemental compositions of the glass shards (or the matrix glass) of volcanic ash samples were determined by electron microprobe analysis by a JEOL-JXA-8200, at IFM-GEOMAR (Fig. 14). For the measurements, a ~10 mg sub-sample of volcanic ash sample was sieved to 32-125 μm size using de-ionized (DI) water. The ash particles were mounted on a tray with resin, polished and analyzed with a beam current of 6 nA and a beam size of 5 μm . Element compositions were calibrated by the standards with different glass compositions, i.e. LIPARI for basaltic samples, VGA99 for andesitic samples and RHYO for rhyolitic samples. Average glass composition of a sample were inferred from ~25 individual measurement points on the ash particles. The chemical composition of the glass (or the matrix) were tested by Energy Dispersive X-ray (EDX) analyses.



Figure 14: Picture of the electron microprobe used for volcanic glass composition determination at the east-shore campus of IFM-GEOMAR.

Bulk composition analyses of volcanic ash and Cape Verdean loess by means of inductively coupled plasma spectrometry

Bulk (total) element-contents of the volcanic ash samples and the dust sample were determined by inductively coupled plasma spectrometry at the Institute of Geosciences at the University of Kiel. Approximately 100 mg of volcanic ash and the loess sample(s) were weighed into perfluoralkoxy (PFA) vials and digested using a multi-

step table-top procedure with hydrofluoric acid, aqua regia, and perchloric acid. Fe-content (in wt.%) was determined by inductively coupled plasma-optical emission spectrometry (ICP-OES) using a Spectro Ciros SOP instrument. SiO₂ content of the Saharan loess sample was referred from the lithium tetraborate fusion analyses (digestion with 0.5 % tartaric acid and 4% nitric acid) in ITS Testing Services (UK). Concentrations were measured by ICP-OES analyses. Zn, Cu, Pb and Cd contents (in ppm) of the digest solutions were performed by ICP-mass spectrometry (ICP-MS) using an Agilent 7500cs instrument. Analytical quality routines involved the preparation and analysis of procedural blanks, sample duplicates, and international certified reference materials BHVO-2, JR-1, BR measured as unknowns. Analytical error as estimated from replicate measurements was better than 2 % RSD for Zn, Cu, Pb and Cd and below 1 % RSD for Fe. Details of analytical procedures can be found in (Garbe-Schönberg, 1993).

References

- Anderson, A.T., 1975. Some basaltic and andesitic gases. *Reviews of Geophysics and Space Physics*, 13: 37-55.
- Ayris, P. and Delmelle, P., in press. Volcanic and atmospheric controls on ash iron solubility: A review. *Physics and Chemistry of the Earth*.
- Bains, S., Norris, R.D., Corfield, R.M. and Faul, K.L., 2000. Termination of global warmth at the Palaeocene/Eocene boundary through productivity feedback. *Nature*, 407: 171-174.
- Baker, A. and Croot, P., 2010. Atmospheric and marine controls on aerosol iron solubility in seawater. *Marine Chemistry*, 120: 4-13.
- Bay, R.C., Bramall, N. and Price, P.B., 2004. Bipolar correlation of volcanism with millennial climate change. *Proceedings of the National Academy of Sciences of the United States of America*, 101: 6341–6345.
- Bay, R.C. et al., 2006. Globally synchronous ice core volcanic tracers and abrupt cooling during the last glacial period. *Journal of Geophysical Research*, 111.
- Behrenfeld, M.J., Bale, A.J., Kolber, Z.S., Aiken, J. and Falkowski, P.G., 1996. Confirmation of iron limitation of phytoplankton photosynthesis in the equatorial Pacific Ocean. *Nature*, 383: 508-511.
- Bonnet, S., Guie, C., Chiaverini, J., Ras, J. and Stock, A., 2005. Effect of atmospheric nutrients on the autotrophic communities in a low Nutrient, low chlorophyll system. *Limnology and Oceanography*, 50: 1810-1819.
- Boyd, P.W. et al., 2004. The decline and fate of an iron-induced subarctic phytoplankton bloom. *Nature*, 428: 549.
- Boyd, P.W. et al., 2000. A mesoscale phytoplankton bloom in the polar Southern Ocean stimulated by iron fertilization. *Nature*, 407: 695-702.
- Bruland, K.W. and Lohan, M.C., 2003. Controls of trace metals in seawater. In: H. Elderfield (Editor), *The Oceans and Marine Geochemistry. Treatise on Geochemistry*. Elsevier Pergamon, Amsterdam-Boston-Heidelberg-London-New

- York-Oxford-Paris-San Diego-San Francisco-Singapore-Sydney-Tokyo, pp. 23-47.
- Cather, S.M., Dunbar, N.W., McDowell, F.W., McIntosh, W.C. and Scholle, P.A., 2009. Climate forcing by iron fertilization from repeated ignimbrite eruptions: The icehouse–silicic large igneous province (SLIP) hypothesis. *Geosphere* 5: 315-324.
- Chester, R., 2000. *Marine Geochemistry*. Blackwell Science, Oxford - London - Edinburgh - Malden - Carlton - Paris, 506 pp.
- Coale, K.H. et al., 2004. Southern Ocean iron enrichment experiment: Carbon cycling in high- and low-Si waters. *Science*, 304: 408-414.
- Croot, P. and Johansson, M., 2000. Determination of iron speciation by cathodic stripping voltammetry in seawater using the competing ligand 2-(2-Thiazolylazo)-*p*-creosol (TAC). *Electroanalysis*, 12(8): 565-576.
- Delmelle, P., Lambert, M., Dufrene, Y., Gerin, P. and Oskarsson, N., 2007. Gas/aerosol–ash interaction in volcanic plumes: New insights from surface analyses of fine ash particles. *Earth and Planetary Science Letters*, 259: 159-170.
- Dingwell, D.B., 1996. Volcanic dilemma: flow or blow? *Science*, 273: 1054–1055.
- Duce, R.A., Liss, P.S. and Merrill, J.T., 1991. The atmospheric input of trace species to the world ocean. *Global Biogeochemical Cycles*, 5: 193-259.
- Dugdale, R.C. and Wilkerson, F.P., 1992. Nutrient limitation of new production. In: P.G. Falkowski and A.D. Woodhead (Editors), *Primary Productivity and Biogeochemical Cycles in the Sea*. Plenum Press, New York, pp. 107-122.
- Duggen, S., Croot, P., Schacht, U. and Hoffmann, L., 2007. Subduction zone volcanic ash can fertilize the surface ocean and stimulate phytoplankton growth: Evidence from biogeochemical experiments and satellite data. *Geophysical Research Letters*, 34.
- Duggen, S. et al., 2010. The role of airborne volcanic ash for the surface ocean biogeochemical iron-cycle: a review. *Biogeosciences*, 7(Iron biogeochemistry across marine systems at changing times).
- Field, C.B., Behrenfeld, M.J., Randerson, J.T. and Falkowski, P., 1998. Primary production of the biosphere: Integrating terrestrial and oceanic components. *Science*, 281: 237–240.

- Fisher, R.V. and Schmincke, H.-U., 1984. *Pyroclastic Rocks*. Springer-Verlag, Berlin-Heidelberg-New York-Tokyo, 472 pp.
- Frogner Kockum, P.C., 2006. A diverse ecosystem response to volcanic aerosols. *Chemical Geology*, 231: 57-66.
- Frogner, P., Gislason, S.R. and Óskarsson, N., 2001. Fertilizing potential of volcanic ash in ocean surface water. *Geology*, 29: 487–490.
- Gabrielli, P. et al., 2008. Siderophile metal fallout to Greenland from the 1991 winter eruption of Hekla (Iceland) and during the global atmospheric perturbation of Pinatubo. *Chemical Geology*, 255: 78–86.
- Garbe-Schönberg, C.D., 1993. Simultaneous determination of thirty-seven trace elements in twenty-eight international rock standards by ICP-MS. *Geostandard Newsletters*, 17(1): 81-97.
- Guerzoni, S. et al., 1999. The role of atmospheric deposition in the biogeochemistry of the Mediterranean Sea. *Progress in Oceanography*, 44: 147–190.
- Guieu, C., Bonnet, S. and Wagener, T., 2005. Biomass burning as a source of dissolved iron to the open ocean? *Geophysical Research Letters*, 32.
- Hall, A., 1987. Volcanism. In: A. Hall (Editor), *Igneous Petrology*. John Wiley & Sons, New York, pp. 24-65.
- Hamme, R.C. et al., 2010. Volcanic ash fuels anomalous plankton bloom in subarctic northeast Pacific. *Geophysical Research Letters*, 37.
- Heller, M.I. and Croot, P.L., 2011. Superoxide decay as a probe for speciation changes during dust dissolution in Tropical Atlantic surface waters near Cape Verde. *Marine Chemistry*, 126(1-4): 37-55.
- Hoffmann, L. et al., submitted to *Marine Chemistry*. Influence of volcanic ash and pumice on phytoplankton growth and Cu ligand production of *Thalassiosira pseudonana* and *Emiliana huxleyi*.
- Jicha, B.R., Scholl, D.W. and Rea, D.K., 2009. Circum-Pacific arc flare-ups and global cooling near the Eocene-Oligocene boundary. *Geology*, 37: 303–306.
- Jickells, T.D., 1995. Atmospheric inputs of metals and nutrients to the oceans: their magnitude and effects. *Marine Chemistry*, 48: 199-214.

- Jickells, T.D., An, Z.S. and Andersen, K.K., 2005. Global iron connections between desert dust, ocean biogeochemistry, and climate. *Science*, 308: 67-71.
- Jickells, T.M. and Spokes, L.J., 2001. Atmospheric iron inputs to the oceans. In: D.R. Turner and K. Hunter (Editors), *Biogeochemistry of Iron in Seawater*. Wiley, Chichester, UK, pp. 85-121.
- Johnson, K.S., 2001. Iron supply and demand in the upper ocean: Is extraterrestrial dust a significant source of bioavailable iron? *Global Biogeochemical Cycles*, 15: 61-63.
- Jones, C.D. and Cox, P.M., 2001. Modeling the volcanic signal in the atmospheric CO₂ record. *Global Biogeochemical Cycles*, 15: 453-465.
- Jones, M.T. and Gislason, S.R., 2008. Rapid releases of metal salts and nutrients following the deposition of volcanic ash into aqueous environments. *Geochimica et Cosmochimica Acta*, 72: 3661–3680.
- Keeling, R.F., Piper, S.C. and Heimann, M., 1996. Global and hemispheric CO₂ sinks deduced from changes in atmospheric O₂ concentration. *Nature*, 381: 218-221.
- Laeßle, A. et al., 2003. Deep dissolved iron profiles in the eastern North Atlantic in relation to water masses. *Geophysical Research Letters*, 30.
- Langmann, B., Zakšek, K. and Hort, M., 2010a. Atmospheric distribution and removal of volcanic ash after the eruption of Kasatochi volcano: A regional model study. *Journal of Geophysical Research*, 115.
- Langmann, B., Zakšek, K., Hort, M. and Duggen, S., 2010b. Volcanic ash as fertiliser for the surface ocean. *Atmospheric Chemistry and Physics*, 10: 3891–3899.
- Larsson, W., 1937. Vulkanische Asche vom Ausbruch des chilenischen Vulkans Quizapu (1932) in Argentinien gesammelt. Eine Studie über vulkanische Differentiation. *Geological Institute of Upsala, Bulletin of Fisheries Research Board of Canada*, 26: 27-52.
- Lin, I.I. et al., 2011. Fertilization potential of volcanic dust in the low-nutrient low-chlorophyll western North Pacific subtropical gyre: Satellite evidence and laboratory study. *Global Biogeochemical Cycles*, 25.
- Lohmann, U. and Feichter, J., 2005. Global indirect aerosol effects: a review. *Atmospheric Chemistry and Physics*, 5: 715-737.

- Luo, C. et al., 2008. Combustion iron distribution and deposition. *Global Biogeochemical Cycles*, 22.
- Mahowald, N. et al., 2009. Atmospheric Iron Deposition: Global Distribution, Variability, and Human Perturbations. *Annual Review of Marine Science*, 1: 245-278.
- Mantas, V., Pereira, A.J.S.C. and Morais, P.V., 2011. Plumes of discolored water of volcanic origin and possible implications for algal communities. The case of the Home Reef eruption of 2006 (Tonga, Southwest Pacific Ocean). *Remote Sensing of Environment*, 115: 1341-1352.
- Martin, J.H. and Fitzwater, S.E., 1988. Iron deficiency limits phytoplankton growth in the north-east Pacific subarctic. *Nature*, 331: 341-343.
- Middleton, G.V., Church, M.J. and Coniglio, M., 2003. *Encyclopedia of Sediments and Sedimentary Rocks*. Springer, Boston.
- Millero, F.J. and Sotolongo, S., 1989. The oxidation of Fe(II) with H₂O₂ in seawater. *Geochim. Cosmochim. Acta*, 53: 1867.
- Morel, F.M.M., Milligan, A.J. and Saito, M.A., 2003. Marine bioinorganic chemistry: The role of trace metals in the oceanic cycles of major nutrients. In: H. Elderfield (Editor), *Treatise on Geochemistry*. Elsevier, Oxford, pp. 113-143.
- Naughton, J.J., Greenberg, V.A. and Googuel, R., 1976. Incrustations and fumarolic condensates at Kilauea Volcano, Hawaii: Field, drill-hole, and laboratory observations. *Journal of Volcanology and Geothermal Research*, 1: 149–165.
- Newhall, C.G. and Self, S., 1982. The volcanic explosivity index (VEI): an estimate of explosive magnitude for historical volcanism. *Journal of Geophysical Research (Oceans & Atmospheres)*, 87: 1231-1238.
- Olgun, N. et al., submitted to *Marine Chemistry*. Possible impacts of volcanic ash emissions of Mount Etna on the oligotrophic Mediterranean Sea: Results from the nutrient-release experiments in seawater.
- Olgun, N. et al., 2011. Surface ocean iron fertilization: The role of airborne volcanic ash from subduction zone and hotspot volcanoes and related iron-fluxes into the Pacific Ocean. *Global Biogeochemical Cycles*, 25.

- Olgun, N. et al., submitted to Marine Ecology Progress Series. Geochemical evidence for oceanic iron fertilization from the Kasatochi 2008 volcanic eruption and evaluation of the potential impacts on sockeye salmon population. .
- Oppenheimer, C., 2004. Volcanic degassing. In: R.L. Rudnick (Editor), *The Crust. Treatise on Geochemistry*. Elsevier Pergamon, Amsterdam-Boston-Heidelberg-London-New York-Oxford-Paris-San Diego-San Francisco-Singapore-Sydney-Tokyo, pp. 123-166.
- Óskarsson, N., 1980. The interaction between volcanic gases and tephra: Flourine adhering to tephra of the 1970 Hekla eruption. *Journal of Volcanology and Geothermal Research*, 8: 251-266.
- Óskarsson, N., 1981. The chemistry of Icelandic lava incrustations and the latest stages of degassing. *Journal of Volcanology and Geothermal Research*, 10: 93-111.
- Parekh, P., Follows, M.J. and Boyle, E.A., 2005. Decoupling of iron and phosphate in the global ocean. *Global Biogeochemical Cycles*, 19(GB2020): 1-16.
- Rose, W.I., 1977. Scavenging of volcanic aerosol by ash: atmospheric and volcanologic implications. *Geology* 5: 621-624.
- Sarmiento, J.L., 1993. Atmospheric CO₂ stalled. *Nature*, 365: 697-698.
- Sarthou, G. and Jeandel, C., 2001. Seasonal variations of iron concentrations in the Ligurian Sea and iron budget in the Western Mediterranean Sea. *Marine Chemistry*, 74: 115–129.
- Schindler, D.W., 1977. Evolution of phosphorus limitation in lakes. *Science*, 195: 260-262.
- Schmincke, H.-U., 2004. *Volcanism*. Springer-Verlag, Berlin Heidelberg New York, 324 pp.
- Sigurdsson, H., Houghton, B., McNutt, S.R., Rymer, H. and Stix, J. (Editors), 2000. *Encyclopedia of Volcanoes*. Academic Press, San Diego CA.
- Simkin, T. and Siebert, L., 1994. *Volcanoes of the World*. Geoscience Press in association with the Smithsonian Institution Global Volcanism Program, Tucson AZ.

- Simkin, T. and Siebert, L., 2000. Earth's volcanoes and eruptions: An overview. In: H. Sigurdsson (Editor), *Encyclopedia of Volcanoes*. Academic Press, San Diego CA, pp. 249-261.
- Smith, D.B., Zielinski, R.A., Taylor, H.E. and Sawyer, M.B., 1983. Leaching characteristics of ash from the May 18, 1980, eruption of Mount St. Helens volcano, Washington. *Bulletin of Volcanology*, 46: 103–123.
- Spirakis, C.S., 1991. Iron fertilization with volcanic ash Eos, *Transactions of the American Geophysical Union*, 72(47).
- Straub, S.M. and Schmincke, H.-U., 1998. Evaluating the tephra input into Pacific Ocean sediments: distribution in space and time. *Geologische Rundschau*, 87: 461-476.
- Sunda, W.G., 2001. Bioavailability and bioaccumulation of iron in the sea. In: K.A. Hunter (Editor), *The biogeochemistry of iron in seawater*. John Wiley and Sons, Chichester, pp. 41-84.
- Symonds, R.B., Rose, W.I. and Reed, M.H., 1988. Contribution of Cl- and F-bearing gases to the atmosphere by volcanoes. *Nature*, 334: 415-418.
- Teschner, C., 2009. Pumice from Central American Arc volcanoes: Release of iron and silica on contact with seawater and implications for the diatom growth in the Eastern Equatorial Pacific Ocean, University of Kiel, Kiel.
- Thordarson, T. and Self, S., 1996. Sulfur, chlorine, and fluorine degassing and atmospheric loading by the Roza eruption, Columbia River Basalt Group. *Journal of Volcanology and Geothermal Research*, 74: 49–74.
- Thyrrell, T., 1999. The relative influences of nitrogen and phosphorus on oceanic primary production. *Nature*, 400: 525-531.
- Turner, S.M., Harvey, M.J., Law, C.S., Nightingale, P.D. and Liss, P.S., 2004. Iron-induced changes in oceanic sulfur biogeochemistry. *Geophysical Research Letters*, 31: L14307.
- Uematsu, M. et al., 2004. Enhancement of primary productivity in the western North Pacific caused by the eruption of the Miyake-jima volcano. *Geophysical Research Letters*, 31(L06106): 1-4.
- Ugolini, F.C. and Dahlgren, R.A., 2002. Soil development in volcanic ash. *Global Environmental Research*, 6: 69-81.

- Walker, G.P.L., 1971. Grain-size characteristics of pyroclastic deposits. *Journal of Geology*, 79: 696-714.
- Wall-Palmer, D. et al., 2011. Explosive volcanism as a cause for mass mortality of pteropods. *Marine Geology*, 282: 231-239.
- Watson, A.J., 1997. Volcanic Fe, CO₂, ocean productivity and climate. *Nature*, 385: 587-588.
- Watson, A.J., 2001. Iron limitation in the oceans. In: D.R. Turner and K.A. Hunter (Editors), *The Biogeochemistry of Iron in Seawater*. UIPAC Series in Analytical and Physical Chemistry and Environmental Systems, West Sussex, pp. 9-39.
- Wiesner, M.G., Wang, Y. and Zheng, L., 1995. Fallout of volcanic ash to the deep South China Sea induced by the 1991 eruption of Mount Pinatubo (Philippines). *Geology*, 23(10): 885-888.
- Witham, C.S., Oppenheimer, C. and Horwell, C.J., 2005. Volcanic ash-leachates: a review and recommendations for sampling methods. *Journal of Volcanology and Geothermal Research*, 141: 299-326.

Chapter I

**The role of airborne volcanic ash for the surface ocean
biogeochemical iron-cycle: A review.**

The role of airborne volcanic ash for the surface ocean biogeochemical iron-cycle: a review

S. Duggen^{1,2}, N. Olgun^{1,3}, P. Croot³, L. Hoffmann^{4,5}, H. Dietze³, P. Delmelle⁶, and C. Teschner^{1,7}

¹IFM-GEOMAR, Leibniz-Institute of Marine Sciences, Division Dynamics of the Ocean Floor, Wischhofstrasse 1–3, 24148 Kiel, Germany

²A. P. Møller Skolen, Upper Secondary School and Sixth Form College of the Danish National Minority in Germany, Fjordalle 1, 24837 Schleswig, Germany

³IFM-GEOMAR, Leibniz-Institute of Marine Sciences, Division Marine Biogeochemistry, Düsternbrooker Weg 20, 24105 Kiel, Germany

⁴Department of Plant and Environmental Sciences, Göteborg University, Carl Skottsberg Gata 22 B, 40530 Gothenburg, Sweden

⁵Department of Chemistry, University of Otago, P.O. Box 56, Dunedin 9054, New Zealand

⁶Environment Department, University of York, Heslington YO10 5DD, York, UK

⁷IFM-GEOMAR, Leibniz-Institute of Marine Sciences, Division Ocean Circulation and Climate Dynamics, Wischhofstrasse 1–3, 24148 Kiel, Germany

Received: 29 May 2009 – Published in Biogeosciences Discuss.: 1 July 2009

Revised: 14 February 2010 – Accepted: 17 February 2010 – Published: 3 March 2010

Abstract. Iron is a key micronutrient for phytoplankton growth in the surface ocean. Yet the significance of volcanism for the marine biogeochemical iron-cycle is poorly constrained. Recent studies, however, suggest that offshore deposition of airborne ash from volcanic eruptions is a way to inject significant amounts of bio-available iron into the surface ocean. Volcanic ash may be transported up to several tens of kilometers high into the atmosphere during large-scale eruptions and fine ash may stay aloft for days to weeks, thereby reaching even the remotest and most iron-starved oceanic regions. Scientific ocean drilling demonstrates that volcanic ash layers and dispersed ash particles are frequently found in marine sediments and that therefore volcanic ash deposition and iron-injection into the oceans took place throughout much of the Earth's history. Natural evidence and the data now available from geochemical and biological experiments and satellite techniques suggest that volcanic ash is a so far underestimated source for iron in the surface ocean, possibly of similar importance as aeolian dust. Here we summarise the development of and the knowledge in this fairly young research field. The paper

covers a wide range of chemical and biological issues and we make recommendations for future directions in these areas. The review paper may thus be helpful to improve our understanding of the role of volcanic ash for the marine biogeochemical iron-cycle, marine primary productivity and the ocean-atmosphere exchange of CO₂ and other gases relevant for climate in the Earth's history.

1 Introduction

1.1 Purpose and structure of the review paper

It is widely recognised that soils formed on volcanic materials are highly fertile (Schmincke, 2004). This is due to the relative ease with which a range of macro- and micronutrients are released from the silicate glass and minerals upon weathering. In contrast, the fertilising potential of tephra for the marine environment is not well understood. There is, however, evidence from ocean sediment cores that large amounts of volcanic ash (tephra with size less than 2 mm) produced during explosive events can enter the marine environment. Volcanic ash plumes can travel considerable distance before the ash is being deposited onto the surface of open oceanic regions (Fig. 1). Whilst the process



Correspondence to: S. Duggen
(svend.duggen@skoleforeningen.de)



Fig. 1. NASA satellite images of eruptions of the volcanoes Chaiten in Southern Chile in 2008 and Etna on Sicily in 2002. The pictures illustrate seaward transport and offshore deposition of volcanic ash (eastward in the Atlantic sector of the Southern Ocean for Chaiten and southward into the Central Mediterranean Sea for Etna volcano). Depending on composition the colour of the volcanic ash visible from space ranges from white (e.g. Chaiten) to brown (e.g. Etna).

is somewhat similar to mineral dust deposition, only a few recent studies have attempted to describe the effect that ash addition may have on the ocean nutrient budget, marine primary productivity (MPP), biological carbon pump and climate (Olgun et al., 2010; Duggen et al., 2007; Jones and Gislason, 2008; Frogner et al., 2001; Langmann et al., 2010). Laboratory and field investigations suggest that, through the addition of key micronutrients such as Fe, volcanic ash deposition over the ocean may repeatedly have been responsible or at least involved in climate forcing mechanisms throughout the Earth's history (Jicha et al., 2009; Cather et al., 2009; Bay et al., 2004, 2006; Bains et al., 2000).

The purpose of this review is to critically summarise our current knowledge on surface ocean fertilisation in relation to volcanic ash input. We briefly outline this young research field from a historic perspective, thereby showing how ideas and complexity developed. Milestones and problems in improving our understanding of this subject are highlighted and we try to draw the reader's attention to key future research questions. The first sections provide a general introduction to the field and are followed by a more in-depth discussion on various physico-chemical and biological aspects linked to volcanic ash-ocean surface interaction. We hope that this contribution will provide the ground for developing future interdisciplinary research activities involving both the Earth and Ocean science communities.

1.2 Giving birth to a new interdisciplinary research focus – overview from a historical perspective

More than 70 years ago, Gran (1931) and Harvey (1937) suggested that the lack of Fe in surface oceanic areas receiving little continental inputs is a limiting factor to phytoplankton growth and thus marine primary productivity (MPP) (Gran, 1931; Harvey, 1937). It is only in the late 80s that ship-based

experiments in the subarctic North Pacific ocean confirmed this idea (Martin and Fitzwater, 1988). Since then, the role of artificial and natural Fe sources or inputs in influencing the surface ocean nutrient budget, MPP, biological carbon pump and atmosphere-ocean exchange in oceanic regions has been a very active research area, involving a range of laboratory, mesocosm and field studies (Blain et al., 2007; Martin et al., 1990; Boyd et al., 2000, 2004; Cooper et al., 1996; Coale et al., 1996, 2004; Behrenfeld et al., 1996).

Although Fe concentrations are very low (<1 nM) in vast areas of the surface ocean (De Baar and De Jong, 2001) (Fig. 2), the effect of Fe-fertilisation on MPP varies across regions. Artificial and natural inputs of Fe are particularly relevant for biogeochemical cycles in high-nutrient low-chlorophyll (HNLC) oceanic areas, which have plenty of macro-nutrients, such as nitrate and phosphate but are Fe-limited. In these areas, the addition of minor amounts of Fe to surface waters can trigger large phytoplankton blooms and MPP increase. In other parts of the ocean, where the levels of both macro- and micro-nutrients (e.g. Fe) are relatively low (Low-Nutrient Low-Chlorophyll (LNLC) or oligotrophic areas such as the subtropical ocean gyres), additional Fe alone is unlikely to have the same immediate biological effects as in HNLC areas. In open oceanic regions with relatively low fixed nitrogen concentrations (e.g. nitrate), however, Fe can control rates of nitrogen fixation (partly in connection with phosphate) (Mills et al., 2004; Morel et al., 2004).

Spirakis (1991) was the first author who envisaged the potential for volcanic ash to influence the marine biogeochemical Fe-cycle. In his abstract, Spirakis hypothesised that volcanic ash can deliver bio-available Fe to the ocean in the same way as mineral dust does, and that increases in MPP following ash deposition should be detectable by monitoring the ocean colour from space (Spirakis, 1991). Mt. Pinatubo volcano, Philippines, erupted about at the same time, and Sarmiento suggested that the observed relative drawdown of atmospheric CO_2 in the Northern Hemisphere following this eruption was the result of increased MPP fertilisation due to Fe-fertilisation of the Southern Ocean by Pinatubo ash (Sarmiento, 1993). Unfortunately, satellite-derived ocean colour images were not available at that time to verify this idea. In a subsequent paper, Watson suggested that the atmospheric oxygen pulse detected in the Southern Hemisphere ocean following the 1991 eruption of Mt. Pinatubo (Keeling et al., 1996) was a consequence of ash addition to the Fe-limited Southern Ocean, a major HNLC area (Watson, 1997). Cather et al. (2009) show, using a plot of the development of atmospheric CO_2 in the period of 1958–1997, that two of the four largest eruptions in this period (Agung in 1963 and Pinatubo in 1991) were followed by a pronounced atmospheric CO_2 -drawdown. Watson (1997) emphasised that large-scale Fe-fertilisation by volcanic ash may also have longer term effects, on the order of thousands of years, through changes in the inorganic to organic carbon rain ratio associated with a diatom phytoplankton bloom. In

order to link oceanic Fe-addition to C-cycles, Watson used the C:Fe ratio of diatom phytoplankton observed in iron-limited areas, which is on the order of 10^5 . This large number stresses that even relatively small amounts of iron added to the surface ocean may have a strong impact on the MPP and C-cycles. Bains et al. (2000) and Jicha et al. (2009) took the ash fertilisation hypothesis further by suggesting that intense volcanism in the past contributed to the termination of global warmth at the Paleocene/Eocene boundary and global cooling at the Eocene/Oligocene boundary. This implies that surface ocean Fe-fertilisation by volcanic ash might be among the essential processes shaping the Earth's climate history. More recently, Bay et al. (2004) and Bay et al. (2006) provided statistical evidence from ice core data for a causal connection between volcanism and millennial climate change. Unclear, however, is whether volcanism caused climate change (e.g. through increased Fe supply to large surface ocean areas) or, vice versa, climate change rapidly influenced volcanic activity (e.g. through sea level change causing changing pressure conditions in magma chambers of coastal volcanoes).

It had long been known that leaching of fresh ash (ash which has not been exposed to rain water) with near-neutral pH water results in the mobilisation of soluble salts present on the ash surface (Witham et al., 2005). The first experimental test, however, specifically dedicated to assessing the seawater solubility of Fe and other macro- and micro-nutrients in volcanic ash was carried out only recently (Frogner et al., 2000, 2001). Using ash from the 1991 eruption of Hekla, Iceland, these authors demonstrated that an array of macro- and micro-nutrients relevant to phytoplankton, including P, Si, Fe, and various trace metals were readily released upon exposure of the ash material to seawater. Importantly, most of the nutrient release occurred within ~ 45 min of contact time implying that a significant fraction is released in the sun-lit surface ocean where algae can thrive on it. These results added more credence to the suggestion that volcanic ash can fertilise the ocean, and hence influence MPP in certain oceanic areas. A more comprehensive study on the potential role of volcanic ash in influencing the surface ocean biogeochemical iron-cycle was presented by Duggen et al. (2007). The results of time-dependent solubility experiments with Antarctic seawater and five ash samples from three subduction zone volcanoes (Arenal in Costa Rica; Mt. Spurr in Alaska and Sakura-jima in Japan) demonstrated a rapid (minute-scale) release of iron along with several other nutrients. The ash materials studied were from subduction zone-related volcanoes (SZV), which are more likely to generate large and far-reaching ash eruptive plumes than volcanoes from hot-spot zones. Bulk (i.e. unsieved) ash was used in all experiments, and an iron-complexing organic ligand was added to the Antarctic seawater, mimicking the presence of siderophores in natural surface ocean water. Duggen et al.'s data showed that significant amounts of iron (on the order of several tenths to hundred nmol per gram of ash) can be released from the ash at

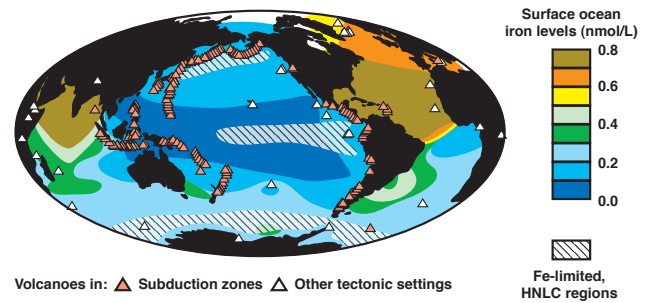


Fig. 2. World map showing surface ocean iron-concentrations, locations of iron-limited (HNLC) regions and subaerially active volcanoes in subduction zones and other tectonic settings. Data sources are: Surface ocean iron-concentrations (Parekh et al., 2005), location of volcanoes (Sigurdsson et al., 2000).

time-scales matching those required for the ash particles to sink through the sunlit part of the surface ocean where phytoplankton thrives (the euphotic zone) (Fig. 3). The source of this soluble and rapidly delivered iron is believed to be the sulphate and halide salts deposited onto the surface of ash particles. These probably occur as thin (< 10 nm) coatings on the ash and are formed during interaction of the ash and gas materials within the volcanic eruption plume (Delmelle et al., 2007) (Fig. 4).

Another geochemical study examined the release of biologically relevant elements, including iron, upon exposure of volcanic ash to seawater and ultra-pure water (Jones and Gislason, 2008) by means of flow-through experiments. The ash samples (sieved to 45–125 μm size) used in this study were mainly from subduction zone volcanoes (Galeras in Columbia; Lascar in Chile; Soufrière Hills on Montserrat; Mt. St. Helens in the USA; Sakura-jima in Japan; Santiaguito in Guatemala) but one was from the Iceland hotspot (Hekla volcano). The study confirms that airborne volcanic ash releases significant amounts of iron on contact with water. Interestingly, Jones and Gislason (2008) also measured a large but transient reduction in pH (up to ~ 4 pH units) of the water immediately after contact with the ash, although this did not occur with all samples. As discussed in details below this effect of the ash on pH bears important implications for the oceanic iron-cycling. First, despite the pH-buffering capability of the surface ocean, a temporary drop in pH can potentially occur in marine ash fall-out areas with high ash-loadings, e.g. in the vicinity of a volcano, thereby affecting surface ocean iron solubility (direct pH effect). Second, an increase in the acidity of fog and cloud water in contact with airborne ash may promote iron leaching from the silicate glass and mineral components of the ash material. The amount of iron added to the ocean surface through volcanic ash may thus vary depending on the predominant deposition process (wet or dry) (Fig. 3).

More recently, Olgun et al. (2010) presented an extended set of data demonstrating the release of soluble iron from

airborne volcanic ash. Data for geochemical experiments with forty pristine ash samples from fourteen subduction zone and two hotspot volcanoes confirm that ash from volcanoes in different tectonic settings release significant amount of iron on contact with seawater. The study also includes aeolian dust samples and suggests that, for dry deposition, the iron release behaviour of the two atmospheric sources is comparable (35–340 nmol Fe/g ash and 20–200 nmol/g dust during the first hour of contact with seawater). The role of wet deposition (involving the interaction with fog or cloud water prior to deposition into the surface ocean) for the soluble iron-release from volcanic ash and aeolian dust, however, remains to be investigated. As outlined in the discussion below the Fe-release behaviour of volcanic ash is likely to be higher for wet compared to dry deposition.

In their experiments, Duggen et al. (2007) also measured the biological response of phytoplankton to ash in contact with seawater. The bio-incubation tests were performed under iron-limited conditions with an Antarctic diatom species (*Chaetoceros dichaeta*), typically found in phytoplankton assemblages in the iron-limited (HNLC) Southern Ocean. Two key biological parameters, namely chlorophyll *a* (Chl-*a*) concentration (as a proxy of biomass) and the photosynthetic efficiency (as a measure of the efficiency with which algae use sunlight for photosynthesis) were monitored during 18 days. Both the Chl-*a* and photosynthetic efficiency were significantly higher when the diatoms grew in the ash-fertilised seawater. For the first time, this study demonstrated that ash-derived iron can boost phytoplankton growth in iron-limited oceanic areas. However, Duggen et al. (2007) stressed that volcanic ash in contact with seawater also releases metals such as copper and zinc that may be toxic to phytoplankton. Assessment of the relative importance of these elements in mitigating the positive effect of volcanic iron requires further investigations. Recent unpublished works conducted with different phytoplankton species, representative of other oceanic regions, also reveal that the biological response to volcanic ash addition differs with the species considered (L. Hoffmann, personal communication, 2008).

Scientists interested in the potential for volcanic ash to act as fertiliser for oceanic phytoplankton growth are also searching for natural evidence. Since 1997, satellite-borne detectors such as MODIS (Moderate-Resolution Imaging Spectroradiometer) and SeaWiFS (Sea-viewing Wide Field-of-View Sensor) have provided true colour images of the surfaces of the oceans on a daily basis. These data can be used to retrieve bio-optical parameters such as Chl-*a* (see summary of satellite techniques in Langmann et al., 2010). Using SeaWiFS images, Uematsu et al. (2004) argued that the plume produced by the powerful 2000 eruption of Miyakejima volcano, ~200 km offshore Japan, instigated a rise in surface ocean Chl-*a* levels in the oligotrophic area downwind of the source (Uematsu et al., 2004). However, in this case, the inferred increase in MPP was primarily linked to inputs of ammonium-sulphate aerosols present in the volcanic

cloud. By combining MODIS and SeaWiFS data, Duggen et al. (2007) noticed that the large (ca. 160 km×140 km) greenish-blue discolouration repeatedly observed in the oligotrophic water in the vicinity of the active Soufrière Hills volcano, Montserrat (Lesser Antilles) was associated with significant increases in Chl-*a* levels. This was tentatively attributed to increased phytoplankton growth due to frequent ash addition. However, mineral dust both airborne or suspended in surface ocean water may also affect the satellite-derived image colour, and this may be misinterpreted for an increase in Chl-*a*, or may add a pseudo-Chl signal to a true Chl-signal. Further, it is unclear whether the alleged phytoplankton bloom near Montserrat was due to iron release following ash input, deposition of N-rich salt aerosols, or both. Noticeably, data from seawater samples collected during a cruise east of Sicily in the ash fall-out area of the large-scale 2001 eruption of Etna volcano (see Fig. 1) showed strongly increased concentrations of dissolved iron (up to several hundred nM) and other trace metals that are reported to be linked to enhanced Chl-*a* levels (Randazzo et al., 2009). In a more recent contribution, Langmann et al. (2010) provided new satellite-based evidence that volcanic ash fall-out can be a significant source of available iron in HNLC areas. These authors argue that the ash from the Kasatochi volcano in the Aleutian subduction zone caused a large-scale phytoplankton bloom in August 2008 in the northeast subarctic Pacific. The bloom started several days after the onset of ash deposition over the surface ocean. Convincingly, the area studied corresponds to that where biological experiments were conducted to demonstrate the so-called iron fertilisation hypothesis (Martin and Fitzwater, 1988).

Jones and Gislason (2008) drew attention to the problem posed by ageing of the ash, even when the sample is stored in dry conditions. Apparently, ash ageing leads to a decrease in the amounts of elements that can be mobilised from ash. New data determined on a large number of ash samples originating from subduction zone volcanoes seems to support this theory (Olgun et al., 2010). The decay appears to affect samples more than a few years old. Clearly, this issue will have to be taken into consideration for future flux estimates of iron to the surface ocean, both on a regional, short-term scale (e.g. during single major eruptions) or on a basin-wide long-term scale (e.g. for an oceanic basin over geological timescales).

Estimates of the flux of iron from volcanic ash to the surface ocean are necessary to improve our understanding of the role of volcanic ash for the oceanic iron-cycle. Based on iron-release data, Duggen et al. (2007) calculated that the deposition of 1 mm of subduction zone-related ash over the ocean may raise the surface ocean iron concentrations by a few nM. Such input would be enough to cause significant MPP response in an iron-limited (HNLC) oceanic area, as >2 nM Fe-increase were shown in mesoscale iron-enrichment experiments to be sufficient to stimulate a massive phytoplankton bloom (Wells, 2003). Further, deep oceanic sediments, including those in iron-limited HNLC

areas, contain ash layers with thickness on the mm-, dm- and even up to the meter-scale (Straub and Schmincke, 1998). Thus, heavy volcanic ash fall may swamp the surface of the ocean with iron, at least within the ash fall-out area. In such case, iron fertilisation may extend outside the ash fall-out area, as oceanic currents can transport iron-fertilised surface ocean waters far away from the site of iron-injection. However, it remains unclear how much of the iron added by a single major eruption remains in solution and in a bio-available form. As discussed in more detail below, this strongly depends on iron speciation and on the presence of iron-complexing organic ligands.

Olgun et al. (2010) provided estimates of the flux of iron linked to the dry deposition of volcanic ash into the surface ocean. In their study the authors consider two endmember-scenarios: 1) the effect within the ash-fall out area of a single major volcanic eruption and 2) the flux of iron from subduction and hotspot volcanic ash into the entire Pacific surface ocean over geological time-scales. The study demonstrates that a single major eruption can have a significant impact on the surface coastal and open ocean iron budget and may be able to raise iron-concentrations by up to several tenths or hundreds of nM. The basin-wide flux estimate suggests that the flux of iron from volcanic ash into the Pacific surface ocean is within the same order of magnitude as the flux of iron from aeolian dust. The study also compares deposition patterns of the two atmospheric iron sources into the Pacific surface ocean and stresses that their relative importance in a given area of the Pacific depends strongly on the short- to long-term temporal and spatial distribution patterns. It thus appears that volcanic ash is a major and hitherto underestimated component in the millennial-scale atmospheric input of iron to the surface ocean. This holds particularly for the Pacific Ocean that covers about half of the Earth's surface, hosts about 70% of the iron-limited, HNLC oceanic areas and is surrounded by a ring of explosive subaerial volcanoes (the so-called Pacific Ring of Fire).

Finally, it is worth noting that input of volcanic ash carrying soluble iron may also be mediated through the melting of ice that received ash fall. A recent piston core study of sediments in the Atlantic sector of the Southern Ocean suggests that ash which fell on sea ice was subsequently transported more than 1000 km away from the site of deposition (Nielsen et al., 2007). If the ash deposited in sea ice has maintained its full potential to release soluble and bio-available iron, natural iron addition during ice melting may occur in the open ocean far away from the ash fall-out area of the volcano.

2 What is volcanic ash?

Freshly erupted volcanic ash (pristine or juvenile ash) is different from “fossil ash” and aeolian dust. The surfaces of pristine ash particles were argued to host soluble salts that may contain iron and were formed through gas-particle in-

teraction in the plume of volcanic eruptions (see Delmelle et al., 2007; Duggen et al., 2007; Jones and Gislason, 2008; Frogner et al., 2001 for discussion) (Fig. 4). Fossil volcanic ash, on the other hand, is ash that has been deposited on land and was subject to hydrological and soil processing, which effectively removed any soluble salts attached to the surface of ash particles. Fossil ash particles may be remobilised by wind and become a component of the aeolian mineral dust load but in general, the readily soluble salts adsorbed onto pristine ash are washed away during exposure to meteoric water. Therefore, fossil ash does not exhibit the same behaviour as pristine ash when exposed to water.

Volcanic ash is produced by a variety of volcanic processes such as bubble burst due to gas expansion in the magma, magma rupture at high shear rates, abrasion from friction and collision (e.g. during an explosive eruption), magma-water interaction at crustal depth and crystal disintegration, and can be emitted by both subaerial and submarine volcanic eruptions. A general term for fragmented volcanic material is “tephra”, the classification of which is based on the grain size, distinguishing three main types: 1) ash (particles below 2 mm down to the micrometer-scale), 2) lapilli (2–64 mm), and 3) bombs and blocks (>64 mm) (Schmincke, 2004; Fisher and Schmincke, 1984). Here we focus on the significance of airborne volcanic ash that may reach the surface ocean through atmospheric transport following explosive subaerial eruptions.

The atmospheric dispersal of airborne volcanic ash is governed by the type and magnitude of the volcanic eruption (e.g. Strombolian, Hawaiian, Plinian etc.), wind direction and size and density of the ash particles (Fig. 3). Sedimentation of airborne ash particles from the volcanic eruption plume depends on settling velocity, which in turn, depends on density and particle diameter. In general, maximum particle size and grain size distribution decreases with distance from the volcanic source (Walker and Croasdale, 1972). However, sorting is rarely perfect since fine particles commonly aggregate (e.g. through electrostatic forces and under the effect of moisture) and are deposited together with larger particles. The median diameter of ash particles in deep oceanic sediments usually varies between 125 to 63 μm and smaller (Pedersen and Surlyk, 1977). Volcanic fine ash with a particle size smaller than 15 μm can have a lifetime of days to weeks in the stratosphere (Niemeier et al., 2009).

The chemical composition of airborne volcanic ash ranges from mafic (relatively high MgO and FeO but low SiO₂ contents) to silicic (relatively low MgO and FeO but higher SiO₂). The bulk composition of volcanic ash is defined by the proportions and compositions of individual vitric fragments (glass shards, pumice), pyrogenic minerals, lithic particles (pieces of pre-existing rocks) and salt coatings (Fisher and Schmincke, 1984; Óskarsson, 1981; Delmelle et al., 2007). Glass shards usually dominate explosive magmatic eruptions; this material represents quenched magma fragments and has angular and irregular shapes (Fig. 4) (Fisher

and Schmincke, 1984). The FeO content of volcanic glass particles found in ash may range from below 1% in felsic to well above 10 wt. % in mafic compositions (Schmincke, 2004). Pyrogenic minerals are crystals precipitated in the magma prior to the eruption and consist mainly of silicate and oxide minerals such as amphibole, biotite, feldspar, olivine, pyroxene, quartz and Fe-Ti-oxides, depending on the chemistry of the magma. Minerals are more abundant in the grain size range ~ 2 mm to $63 \mu\text{m}$ and are generally absent below $10 \mu\text{m}$, whereas glass shards can be micrometric in size. Lithic particles include pieces of old volcanic rocks and/or the subvolcanic basement rock; the latter being of any crustal origin (Fisher and Schmincke, 1984). Silicic ash is more widespread than its mafic counterpart. This is due to (i) a generally greater explosivity of SiO_2 -rich, high-viscosity magmas, although there are records of large-scale explosive basaltic eruptions (Schmincke, 2004), and (ii) because SiO_2 -poor components such as ferromagnesian minerals (e.g. olivine, clinopyroxene) have higher densities than the coexisting, SiO_2 -rich glass and will tend to settle faster than the glass shards (aeolian fractionation) (Larsson, 1937; Middleton et al., 2003).

3 Processes that transfer volcanic iron into soluble and bio-available form

There are two principal mechanisms by which iron in volcanic ash can be mobilised into soluble forms upon contact with seawater and thus, become bio-available in the surface ocean (Fig. 3): (i) dissolution of iron-containing salt coatings found on the surface of ash particles in the volcanic plume, and (ii) (partial) dissolution of the silicate glass and silicate and non-silicate mineral components of the ash (e.g. glass shards, crystalline igneous and non-igneous minerals, secondary minerals formed through hydrothermal processes prior to the eruption). Moreover, there are two principal ways by which soluble iron can be mobilised from volcanic ash and then be injected into the surface ocean: 1) by direct mobilisation from relatively dry ash that is deposited into seawater (dry deposition), or 2) by mobilisation from ash through interaction with cloud water prior to entering the surface ocean as rain (wet deposition) (Fig. 3).

The formation of iron-containing soluble salts on the surface of volcanic ash relates to the interaction between the gas, aerosol and ash materials within the eruption plume (Delmelle et al., 2007; Rose, 1977; Óskarsson, 1980). In contrast to some other metals, iron in magma has a low volatility (lithophilic element). This is supported by volcanic gas measurements that indicate little iron enrichment, if any, in the gaseous and particulate phases emitted during magma degassing processes and volcanic eruptions (Symonds et al., 1987). Thus, the presence of readily soluble iron on the surface of volcanic ash is more likely due to partial dissolution of the ash through reactions with the acidic gases (i.e., mainly

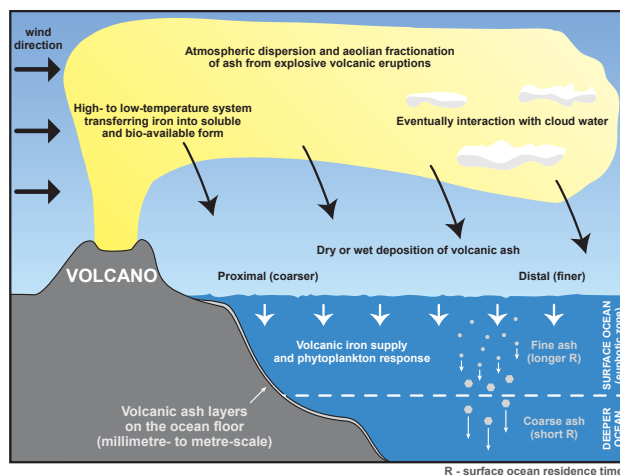


Fig. 3. Sketch displaying the possible effects of major volcanic eruptions on the marine environment, with focus on the surface ocean.

SO_2 , HCl, HF) and aerosols (i.e., H_2SO_4) of the plume, followed by precipitation at the ash-liquid interface. Extremely thin sulphate and halide deposits (< 10 nm) on the surface of ash are formed by this process (Delmelle et al., 2007). These materials may contain iron salts such as FeCl_2 , FeCl_3 , FeF_2 , FeF_3 , $\text{FeSO}_4 \cdot 7\text{H}_2\text{O}$ but more complex compounds also may exist on the ash surface. The salt coatings have been made visible recently by microscopic methods (Fig. 4e,f) (Delmelle et al., 2007) and are easily dissolved upon contact of the ash with seawater or cloud water.

Silicate and non-silicate ash particles may also be able to mobilise iron into water. Iron concentrations can range from well below 1 wt. % to well above 10 wt. % (FeO) in these particles (and much higher for Fe-oxides), depending on their composition. Therefore, even partial dissolution of these particles with seawater or cloud water may transfer significant amounts of iron into solution. Volcanic glass for example, which is a main component of volcanic ash, is metastable and may therefore readily react with water. The rate of silicate glass dissolution in the aqueous phase can be reasonably described in terms of pH and aluminium dependencies, although the presence of fluoride in the system can dramatically increase glass dissolution rates (Wolff-Boenisch et al., 2004a, b; Flaathen et al., 2008). Since glass dissolution is a relatively slow process in seawater, the fast release of iron observed in geochemical experiments with seawater is best explained by dissolution of iron-bearing salts occurring on the ash surface (Olgun et al., 2010, 2010; Jones and Gislason, 2008; Duggen et al., 2007). Very little, however, is known about the mobilisation of iron from volcanic ash that interacts with cloud water. A brief discussion of the possible significance of wet deposition for the mobilisation of iron from volcanic ash is presented below in Sect. 4.1.5.

4 Chemical behaviour of volcanic ash upon contact with water

Constraints on the iron-mobilisation behaviour of volcanic ash mostly are from leaching experiments, where ash is shaken in an aqueous solution and the leachate is analysed for its anionic and cationic contents. In order to evaluate the full potential of ash for releasing soluble compounds upon contact with seawater, it is necessary to use pristine ash, i.e. ash that has not been leached by rain or melting snow. Unfortunately, such ash material is relatively rare since many eruptions occur in humid regions of the world, or in remote places. Since the release of iron and other elements in fossil ash (ash washed by rain) is controlled by glass dissolution rate, this material is not suitable in studies examining the transfer of nutrients in the euphotic zone, where the ash spends a relatively short period of time (minutes through hours to days, depending on particle size). The only available report providing chemical measurements of the surface water following an ash deposition event was conducted in the Mediterranean Sea when Mt. Etna volcano erupted in 2001. Randazzo et al. (2009) detected a large increase in dissolved iron concentration (up to ca. 650 nM) down to 300 m depth. Given the difficulty posed by ash sampling, laboratory leaching studies that use pristine ash materials constitute a valuable source of information for assessing the potential fertilising effect of ash upon entry into the surface ocean.

Leaching experiments with pristine volcanic ash and deionised and/or slightly acidic/alkaline water have been performed for decades (see review by Witham et al., 2005). Ash leaching experiments are traditionally carried out with the aim to determine the contribution of magmatic volatile scavenging by ash or to assess environmental effects on the terrestrial environment and the potential hazards to human health and livestock. The environmental problems arising from ash fall-out on land or into fresh water systems are mainly associated with the release of fluoride and other toxic elements or compounds (Witham et al., 2005; Frogner Kockum, 2006) and references therein). Iron has gained limited attention in such experiments, and only in the past decade that its release by volcanic ash in contact with seawater has been investigated in details (see Table 1 for an overview).

4.1 The iron-release behaviour of volcanic ash

As outlined in Table 1, so far three different laboratory approaches have been used to determine the release of iron from volcanic ash in seawater or ultrapure water: 1) agitation experiments, 2) flow-through reactor experiments and 3) experiments with iron concentrations determined in situ in an aqueous solution. In agitation experiments, a given amount of ash is shaken with a known volume of water. In flow-through reactor experiments, water is slowly pumped through a batch of ash. In both cases the resulting solution is separated from the ash by filtration and analysed for iron and

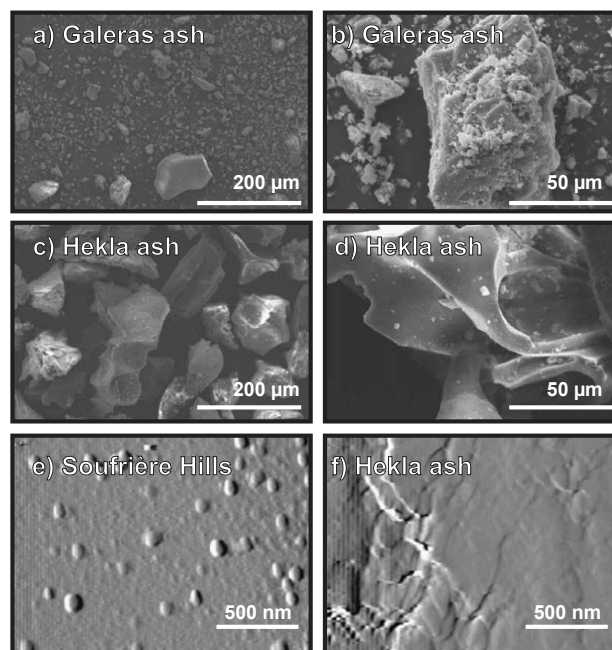


Fig. 4. Examples of volcanic ash and its physical properties such as grain size distribution, shape and surface topography of the particles. The ash displayed at different magnifications is from the 2005 eruption of Galeras volcano in Columbia (**a, b**) and 2000 eruption of Hekla volcano in Iceland (**c, d**). Panels e and f show AFM images showing nodules and smooth terraces forming soluble salt coatings at the surface of ash particles from eruptions of Soufrière Hills volcano 1999 (Montserrat) (**e**) and Hekla volcano 1970 (**f**). Data sources are: scanning electron microscope (SEM) images (Jones and Gislason, 2008), atomic force microscope (AFM) images (Delmelle et al., 2007).

other elements (e.g. by ICP-AES). In in situ experiments, a given amount of ash is added to a known volume of water and the change in dissolved Fe-concentration in the mixture is measured as a function of time (e.g. by electrochemical stripping voltammetry). The amount of ash required for the different experimental setups ranges from several grams (agitation and flow-through experiments) down to several tens of micrograms (in situ measurements).

Studies on the (sea)water solubility of iron in ash have used different volcanic ash samples but also different experimental protocols: 1) ash samples from different volcanoes in distinct tectonic settings (e.g. subduction zones and hotspots), 2) sieved or non-sieved (bulk) ash samples, 3) variable ash-to-seawater ratios, 4) different contact times between the ash and aqueous solvent, 5) a variation of the type of the solvent (natural or artificial seawater, ultrapure water, acidified or alkaline water), and 6) absence/presence of organic ligands.

A key result from these minute- to day-scale experiments is that iron is always released from pristine volcanic ash in amounts that may alter the surface ocean iron-budget

Table 1. Overview of the iron-release behaviour of pristine (unhydrated or dry) volcanic ash from geochemical (leaching) experiments in the literature.

Reference	Method	Duration of the experiment	Number and type of ash sample(s)	Particle size fraction	Ash/solute ratio (g/ml)	Solute	Fe-release (nmol Fe/g ash)
(Fruchter et al., 1980)	Agitation	1 h (10 min. stirring followed by resting)	9 samples from 1 SZ volcano (Mt. St. Helens, 1980)	unsieved	1:10 (quantities not mentioned, only the ratio!)	Distilled water	0.9-315.2
(Taylor and Lichte, 1980)	Agitation	4 h in column	4 samples from 1 SZ volcano (Mt. St Helens 1980)	unsieved	1:0.58 (172 g ash and 100 ml solvent)	Deionised water	0.2-0.4
(Nehring and Johnston, 1981)	Agitation	1 h stirring	4 samples from 1 SZ volcano (Mt. St Helens 1980)	unsieved	1: 2.5 (20 g ash, 50 ml solvent)	Triply distilled water	0.2-13.9
(McKnight et al., 1981)	Flow-through columns	9h,12h,14h in columns followed by elution	2 samples from 1 SZ volcano (Mt. St Helens 1980)	unsieved	1: 1.25 1: 0.87 (15-20 g ash, 50-70 ml solvent)	WC medium	< 0.2
(Smith et al., 1982)	Agitation	1 h shaking followed by resting overnight	30 samples from 3 SZ volcanoes (Fuego 1974, 13 samples; Fuego 1973, 5 samples; Pacaya 1974, 7 samples; Santiaguita 1967, 1 sample; Santiaguita 1976, 1975, 4 samples)	850-106 μ m and 106 μ m after crushing	1:4 (5 g ash, 20 ml solvent)	Distilled-deionized water HCl solution (pH: 3.5-4.0) 0.05 M sodium carbonate and bicarbonate (pH = 9.9)	2.0-401.1 0.7-458.4 12.9-71.6
(Smith et al., 1983)	Agitation	1 h agitation followed by resting overnight (1 week for the carbonate solution)	19 samples from 1 SZ volcano (Mt. St. Helens, 1980)	unsieved	1:4 (5 g ash, 20 ml solvent)	Distilled-deionized water HCl solution (pH: 3.5-4.0) 0.05 M sodium carbonate and bicarbonate (pH:9.9)	<0.1-8.6 <0.1-93.1 5.6-34.4
(Cimino and Toscano, 1998)	Agitation	24 h	Fresh lava ash (Mt. Etna, 1996)	0.1-0.3 mm	1:10 1:33 1:500 1:1,000 (1, 2, 30, 100 g ash, 1 L solvent)	Doubly distilled water	< 0.1-268.6

Table 1. Continued.

Reference	Method	Duration of the experiment	Number and type of ash sample(s)	Particle size fraction	Ash/solute ratio (g/ml)	Solute	Fe-release (nmol Fe/g ash)
(Christenson, 2000)	Agitation	15 min. agitation followed by resting overnight	22 samples from 1 SZ volcano (Mt. Ruapehu 1995, 1996)	unsieved	1:10 (10 g ash, 100 g water)	Distilled-deionised water, then heated to 60°C	17.9 - 1,504
(de Hoog et al., 2001)	Agitation	4 h	8 samples from 1 SZ volcano (Galunggung, 1982)	unsieved	1:80 (0.5 g ash, 40 ml solvent)	DI water 1M HNO ₃	1,000 - 23,000 200,000 - 1,500,000
(Frogner et al., 2001)	Flow-through reactor	Solute sampled every ca. 45 min. Total duration 8 h.	1 sample from 1 HS volcano (Hekla, 2000)	45-74 µm	1:8 (5 g ash, 40 ml solvent)	Artificial seawater North Atlantic seawater	39,000 within 45 min. 37,000 within 45 min.
(Duggen et al., 2007)	In situ by stripping voltammetry	Up to 1 h with measurements every several minutes. One experiment with 15 h	5 samples from 3 SZ volcanoes (Sakura-Jima 1986, 1987, 1999 3 samples; Mt. Spurr 1991, 1 sample; Arenal 1993, 1 sample) Arenal 1 sample	unsieved	1:400 (50 mg ash, 20 ml seawater)	Antarctic seawater	18.4 - 72.4 after 1 h 135.4 after 15h
(Jones and Gislason, 2008)	Flow-through reactor	Solute sampled every ca. 45 min. Total duration 8 h (DI water) or 24 h (seawater)	3 samples from 3 SZ volcanoes and 1 sample from 1 HS volcano (Galeras 2005, 1 sample; Montserrat 2003, 1 sample; Santiaguito 1998, 1 sample; Hekla 2000, 1 sample)	45-125 µm	1:8 (5 g ash, 40 ml solvent)	De-ionized (DI) water Atlantic seawater Southern Ocean seawater	10-120 (for SZVA) 10,900 (for HSVA) 20-100 (for SZVA) 7,100 for HSVA 10 - 40 (for SZVA)
(Olgun et al., 2010)	In situ by stripping voltammetry	Up to 1 h with measurements every several minutes.	40 samples from 14 SZ volcanoes and 4 samples from 2 HS volcanoes (* see below for details)	unsieved	1:400 (50 mg ash, 20 ml seawater)	Atlantic seawater	8,900 (for HSVA) 42-336 (for SZVA) 35-107 (for HSVA)

* Sakura-Jima volcano 1986, 1987, 1999, 2007, 2009, 5 samples; Arenal 1992, 1993, 2003, 2004, 4 samples; Mt. Spurr 1992 1 sample; Turrialba 1864, 1 sample; Rabaul-Tavurvur 2002, 2008, 3 samples; Popocatepetl 1998, 2000, 2001, 2003, 8 samples; Karymsky 2005, 10 samples; Chaiten 2008, 2 samples; Anatahan 2003, 1 sample; Merapi 2006, 1 sample; Mt. St. Helens 1980, 1 sample; Fuego 1974, 1 sample; Telica 2000, 1 sample; Tungurahua 2000, 1 sample; Hekla 1947, 1970, 1980, 3 samples; Pu'u'Ō'o 2005, 1 sample.

(Table 1). Many more ash samples from volcanoes in subduction zones rather than other tectonic settings have so far been analysed. The reason obviously is that most subaerially active volcanoes are found in subduction zones (Sigurdsson et al., 2000) (Fig. 3) and therefore more pristine ash sample material is available from subduction zone volcanoes than volcanoes in other settings (e.g. hotspots). The iron-release data available indicate that subduction zone volcanic ash (SZVA) in general mobilises between 100–400 nmol Fe per gram during dry deposition, apparently largely independent of the experimental setup (but not the solvent) used. The few iron-release data available for experiments with seawater and hotspot volcanic ash (HSVA) samples shows much larger scatter, ranging from around 35–107 nmol Fe/g ash (in situ experiments determined by stripping voltammetry) to between 7100–39 000 nmol Fe/g ash (in flow-through reactor experiments followed by ICP-AES analysis) (Table 1). Of note, ash material tends to release significantly more iron upon contact with acidified water than with seawater (e.g. up to 1 500 000 nmol Fe/g Galunggung ash in contact with 1M HNO₃, Table 1). These data suggest a higher potential for iron mobilisation when the ash is deposited via processes involving fog or cloud water rather than dry deposition into the surface ocean.

4.1.1 Decay of soluble salt coatings? – Implications for flux estimates

Jones and Gislason (2008) recently raised concerns regarding the stability of soluble salt coatings on ash particle surfaces. Using the same experimental set up as Frogner et al. (2001), they re-analysed the 2000 Hekla ash in 2007 and found substantially less iron release (ca. 7–9 μ mole Fe/g ash) compared to the value reported earlier (ca. 36 μ mole Fe/g ash). The ash used by Frogner et al. was sieved to 44–74 μ m, whereas Jones and Gislason used the 45–125 μ m size fraction. The change, however, between these two experiments are considered to be greater than the change in relative surface area (M. Jones, personal communication, 2009), supporting the hypothesis that soluble salt coatings may be prone to decay on the year-scale.

Further insights into the decay of soluble salt coatings on ash particles come from experiments with a larger number of subduction zone volcanic ash samples (Olgun et al., 2010). In general, older samples tend to release iron by a factor of up to ten less than younger samples. For example, five samples from Sakura-jima volcano, collected since the mid-80s, show a linear decrease of Fe-release with increasing age. The Sakura-jima ash samples suggest that the Fe-mobilisation potential (and thus probably element-mobilisation potential in general) of an ash sample from a subduction zone volcano may be reduced to about 50% after 10 years of storage and to about 10% after ca. 20–25 years (Olgun et al., 2010).

In summary, ageing of the ash needs to be considered carefully as it may affect estimates of the flux of ash-derived iron into the marine environment. Further experiments and investigations will be useful to improve our understanding of the reason for and the significance of ash sample decay.

4.1.2 Significance of the ash-to-seawater ratio – proximal versus distal ash fall-out

The ash-to-seawater ratio may influence the amount of iron released from ash to surface ocean water. As observed for mineral dust deposition, large particle loadings may act as a sink rather than a source for iron (e.g. Baker and Croot, 2010). Olgun et al. (2010) therefore pointed out that high ash loadings may not necessarily lead to higher Fe-release. As shown in Table 1, geochemical experiments examining the release of iron in (sea)water have been performed with different ash-to-water ratios. These range from about 1:0.5 to 1:1000, corresponding from very high to very low ash load. No correlation between Fe-release behaviour and ash-to-seawater ratio can be inferred based on existing data (Table 1). The reason for a lack of a correlation, however, may be sought in the use of different experimental setups and the data available does thus neither support nor exclude the possibility of scavenging of soluble Fe from the surface ocean during high particle loadings. As the effect would have important bearings on the link between volcanic ash fall-out and surface ocean iron-cycle, systematic studies will be necessary to address this issue in detail.

Since the ash flux to the ocean varies spatially and temporally depending on volcanological and meteorological factors, no simple recommendation can be provided regarding the ash-to-water ratio to be used in iron solubility determinations. Variables which influence ash deposition fluxes offshore are: 1) the magnitude of the volcanic eruption, which includes the erupted ash volume and the altitude to which the ash is injected into the atmosphere (can be up to 30–50 km), 2) the ash emission rate at the source, 3) the wind speed and direction, in combination with the density and grain size spectrum of the ash particles, which determine how far the particles travel before being deposited in the surface ocean, and 4) the distance of a given surface ocean region from the volcanic source (proximal or distal) (Fig. 3).

In general, the offshore ash load (or flux) in a given oceanic area is high if the volcanic mass flux is high (high volume erupted over a short period of time) during low wind speed conditions and the oceanic area is located close to the volcano (e.g. a proximal coastal oceanic area). The ash load in a given location would be low the smaller the scale of the eruption and the slower the rate of ash release, the stronger the winds and the further the oceanic area is located away from the volcanic source (e.g. a distal open oceanic area). For example, the thickness of the ash layer deposited by the 1991 eruption of Mt. Pinatubo, Philippines, in the coastal region was about 10–20 cm (Wiesner et al., 2004), which (with

a density of ca. 2.5 g/cm^3 and a porosity of ca. 30 %) corresponds to an ash load of about 2500 to 5000 g/dm^2 . Assuming a 50 m mixed layer depth, i.e. if equilibrated with a well-mixed 50 m water column, this ash load is equivalent to an ash-to-water ratio of about 1:200 to 1:100. However, the ash input in coastal areas near active volcanoes can be much larger, on the order of one meter or more (e.g. the Toba super-eruption ca. 75 ka ago, Oppenheimer, 2002). Evidence for the thickness of ash layers in the open ocean comes from scientific ocean drilling, where it has been observed that volcanic ash layers, even hundreds and thousands of kilometers away from the coast can have thickness on the millimeter-, centimeter- and decimeter-scale, occasionally even up to the meter-scale (Rea et al., 1995; Kutterolf et al., 2008). Millimeter- and meter-thick ash layers yield an ash load of ca. 25 g/dm^2 and $25\,000 \text{ g/dm}^2$, respectively, which is equivalent to an ash-to-seawater ratio of 1:20 000 and 1:20, assuming settling of the ash through a well-mixed 50-meter water column. Low ash-to-seawater ratios are expected for the deposition of the very fine ash fraction that has a relatively long residence time in the atmosphere. The amount of iron that can be released from this material, however, may be comparatively higher due to its larger surface area to volume ratio. Most of the 1991 Pinatubo volcanic ash was deposited in the South China Sea (Wiesner et al., 2004) so that the hypothesized iron-fertilisation effect of the Southern Ocean with Pinatubo ash (Sarmiento, 1993; Watson, 1997) may have been associated with such very fine ash, that had longer residence times in the atmosphere and therefore was able to reach the Southern Ocean (F. Prata, personal communication, 2008).

Several authors have argued that their experiments were designed to mimic the settling of ash through the surface ocean (Olgun et al., 2010; Frogner et al., 2001; Jones and Gislason, 2008; Duggen et al., 2007). As described above, the actual ash-to-seawater ratio can vary by several orders of magnitude. The ash-to-seawater ratio of 1:8 used by Frogner et al. (2001) and Jones and Gislason (2008) in their flow-through experiments corresponds to a very high ash load representative of voluminous and rare volcanic eruptions that may deposit up to one meter of ash in the ocean. The 1:400 ash-to-seawater ratio in Duggen et al.'s (2007) and Olgun et al.'s (2010) in situ experiments is closer to ash loads associated with centimeter-scale ash layers. Such deposits are frequently encountered in open ocean sediments (e.g. Rea et al., 1995). Experiments at very low ash-to-seawater ratios (e.g. below <1:500) that would be associated with ash layer thickness on the millimeter-scale have rarely been performed (Table 1). One may extrapolate the results of geochemical experiments to lower (or higher) ash-to-seawater ratios. However, this approach is probably not valid, in particular for measurements carried out at high ash-to-seawater ratios as for example effects such as re-adsorption of Fe to the surface of the ash particles and solubility limitations (e.g. due to pH-dependent Fe-solubility and the presence/absence of

organic ligands) may introduce large errors to extrapolation. Therefore, the ash-to-(sea)water ratio chosen in a particular geochemical experiment should be representative of natural conditions. This is, of course, problematic as for both dry and wet ash deposition the ash-to-water ratio may be highly variable.

Direct in situ measurements in nature, linking the increase of surface ocean iron concentrations within a volcanic ash fall-out area to ash-to-seawater ratio have not yet been performed. Unfortunately, such studies within the marine ash fall-out area of a volcanic eruption are difficult to plan and not easy to perform but they would be very useful to validate the outcome of laboratory experiments.

4.1.3 Sieving or not sieving? – Relevance for proximal and distal ash fall-out

Due to aeolian fractionation of ash particles of variable size and density, deposits near the volcanic source are generally coarser (e.g. in coastal areas) than distal ones (e.g. in open ocean areas). Of note, the ratio of surface area to volume increases with decreasing grain size (Fig. 4), in particular for particle diameters below 200–300 μm (assuming that particles are spherical) (Witham et al., 2005). Assuming that the amount of salt coating and the solubility of a solid substance in general is a function of the surface area implies that the release of soluble components increases (on a per volume basis) with decreasing particle size. This is supported by leaching studies of pristine ash from Mt. Hudson (Chile) and Hekla (Iceland) volcanoes showing that the release of soluble components such as Cl, F, Ca and Na strongly increases with smaller grain size fraction below 100–200 μm (Óskarsson, 1980; Rubin et al., 1994). Thus, fine ash particles below about 100 μm may have the potential to release significantly more Fe than coarser particles; partly because fine ash may carry more Fe-bearing soluble salts on their surface per mass unit but also because the solubility of a solid substance in general is size-dependent, which should also be valid for the silicate glass and silicate and non-silicate mineral components of the ash.

Systematic measurements of the iron-release as a function of grain size, especially distinguishing that of fine (<100–200 μm) from coarser ash, have as yet not been performed. Such measurements, however, would be very useful to examine the impact of dry and wet deposition of volcanic ash for the marine biogeochemical iron-cycle, as a function of (i) the distance from the volcanic source (coastal or near-coastal areas versus remote open ocean areas) and (ii) ash particle residence times in the surface ocean and cloud water.

4.1.4 Influence of pH

Initial low pH was observed in both artificial and natural seawater used in flow through disequilibrium experiments with relatively high volcanic ash loads (ca. 1:8) (Jones and

Gislason, 2008; Frogner et al., 2001). The pH-decrease in the seawater ranged from 0.1–1.5 pH units for ash samples from subduction zone volcanoes (Galeras, Montserrat, Santiaguito) and up to 5 pH units for those from hotspot volcanoes (Hekla ash) and was strongest within the first ca. three hours of the experiments. De Hoog et al. (2001) exposed pristine ash for four hours in ultrapure (de-ionised) water and in 1 M HNO₃. The amount of iron released increased by roughly two orders of magnitude in the acidic solvent (Table 1), indicating a strong influence of pH on iron solubility in ash. Experiments conducted with four SZVA samples using ultrapure water and seawater did not produce large differences in the iron released from the ash samples (Jones and Gislason, 2008). The experiment, however, in which an ash sample released more iron in de-ionised water also showed the lowest pH values for the solution (3.5–4.0 for the Hekla ash sample), consistent with the aforementioned that pH may have a strong effect on the amount of Fe released from ash.

An explanation as to why pH impacts on the iron-release behaviour probably lies in the composition and mineralogy of the different Fe pools associated with the ash. Salts found on the surface of ash particles are halogenides, sulphates and oxides (Óskarsson, 1981). While some iron-bearing salts (e.g. halogenides and sulphates) are readily dissolved by de-ionised and slightly alkaline seawater, other compounds (e.g. oxides) may require acidic conditions to dissolve more swiftly (Smith et al., 1982).

In addition to the rapid dissolution of the soluble salt coatings, additional iron may be released through (partial) volcanic glass dissolution. The rate of glass dissolution, however, is strongly dependent on pH: relatively slow for seawater pH of ca. 8 and faster for an acidic pH <7, especially if fluorine and sulphate anions are present (Gislason and Oelkers, 2003; Flaathen et al., 2008; Wolff-Boenisch et al., 2004a). A transient pH decrease of surface seawater following ash addition could therefore potentially lead to enhanced glass dissolution. However, due to the pH-buffering capacity of seawater, a decrease in local pH is unlikely to play a role in the surface ocean for low ash-to-seawater ratios (e.g. generally in an open ocean scenario) but may become significant in areas with high ash-to-seawater ratios (e.g. in coastal areas in the vicinity of the volcanic source and even in the open ocean for very large-scale eruptions).

4.1.5 Wet and dry deposition

There are two principal mechanisms by which volcanic ash may influence the marine biogeochemical iron-cycle: 1) via offshore deposition of ash and subsequent dissolution of soluble salt coatings in direct contact with seawater (dry deposition) and 2) through dissolution of soluble salts and eventually partly of silicate and non-silicate ash particles (e.g. glass) in contact with fog or cloud water, which very likely occurs at lower pH, followed by offshore rain fall (wet deposition). Various aspects of the dry deposition process were outlined

above but the mechanism of wet deposition merits further consideration.

The role of wet deposition of volcanic ash for the ocean surface iron-cycle is poorly constrained. Some predictions, however, can be made from what is known about glass dissolution rates and the solubility of iron: volcanic ash typically reacts moderately to strongly acidic in contact with non-pH-buffered fresh water (Óskarsson, 1980; Jones and Gislason, 2008) but glass dissolution rates increase dramatically with decreasing pH at acidic conditions (Gislason and Oelkers, 2003). Moreover, at acidic pH, the presence of fluoride and probably sulphate significantly further increases glass dissolution rate (Wolff-Boenisch et al., 2004a; Flaathen et al., 2008). Fluoride and sulphate are both contained in the soluble salt coatings associated with volcanic ash (Delmelle et al., 2007). HF and SO₂ gases are typically released during volcanic eruptions (Oppenheimer, 2004) and may find their way into the water droplets of clouds crossing the volcanic plume. Such low-pH cloud water may interact with fine ash particles that can have relatively long residence times in the atmosphere, which could result in elevated cloud water iron-levels downwind volcanic eruptions. Moreover, iron solubility strongly increases below pH 4 under oxidizing conditions (Kraemer, 2004). Volcanic particulate matter may also act as cloud condensation nuclei and fine ash particles with coatings of hygroscopic salts are particularly suitable to initiate the formation of water drops from atmospheric vapour (Textor et al., 2006) and references therein). Together, wet deposition of volcanic ash into the surface ocean may well be an important process for the marine biogeochemical iron-cycle.

Cloud water samples collected on Hawaii placed some constraints on iron concentrations in cloud water: The measured iron concentrations were highly variable, ranging from <6 nM to 6420 nM, with a median of 32 nM (Benitez-Nelson et al., 2003). The source of this iron enrichment was attributed to volcanic activity, such as scavenging of volcanic gases while clouds pass over a degassing/erupting volcano (e.g. active Pu'u'Ō'o) or through the formation of large aerosol clouds when lava flows enter the sea. Aerosol clouds formed due to the interaction of hot (ca. 1100–1200 °C) lava with seawater (a process producing large amounts of volcanic glass shards) were shown to have extraordinarily high concentrations of iron (ca. 250 μM) (Sansone et al., 2002), which is two to three orders of magnitude more than the iron levels in the Hawaiian cloud water samples. In these cases the elevated iron levels in the fog or cloud water are unlikely to be associated with airborne volcanic ash. It is noteworthy, however, that cloud water does not have a pH-buffer like seawater and that Hawaiian cloud water had acidic pH values between 2.6 and 5 (Benitez-Nelson et al., 2003). Interestingly, the cloud water samples with the highest Fe concentrations also had the lowest pH of around 2.7.

Further geochemical experiments with ultrapure water and volcanic ash as well as direct measurements of Fe-levels in cloud water that interacted with a volcanic ash plume can

help to improve our understanding of the possible significance of wet deposition of volcanic ash for the marine biogeochemical iron-cycle.

4.1.6 Significance of Fe-complexing organic ligands

As detailed by Baker and Croot (2010) the solubility and thus, maximum concentration of iron in seawater is closely linked to the presence of organic ligands. Organic molecules in surface ocean water are produced directly in response to iron limitation by phytoplankton and bacteria and by the decomposition of biomass and subsequent release of iron-containing proteins and enzymes (Baker and Croot, 2010). Some of these molecules are organic chelators with a low molecular weight and a very high and specific affinity for Fe^{3+} (siderophores). More than 99% of the iron in surface ocean waters is complexed by such organic ligands that exist at sub-nanomolar levels usually in slight excess of the dissolved iron (Bruland and Lohan, 2004 and references therein). The presence and content of organic ligands can therefore strongly affect the solubility and biogeochemical cycling of iron from volcanic sources in the surface ocean.

In geochemical experiments with volcanic ash and natural seawater it is common practice to filter the water through a $0.2\ \mu\text{m}$ filter and to expose it to UV-light prior to use in order to remove/destroy organic molecules and biota. Seawater samples treated this way do not contain natural marine organic ligands. The seawater used for the flow-through experiments with volcanic ash was free of marine organic ligands (Frogner et al., 2001; Jones and Gislason, 2008). For in situ iron measurements in seawater by means of stripping voltammetry, an electrochemically active organic ligand (e.g. TAC) was added (Duggen et al., 2007; Croot and Johansson, 2000; Olgun et al., 2010). In some of these experiments, the seawater was treated with UV-light (Duggen et al., 2007), whereas more recently it was not (Olgun et al., 2010), because the TAC-ligand used is stronger than natural siderophores and binds most of the water soluble iron. Addition of an organic ligand to a solution may also prevent loss of oxidised iron to container walls and re-precipitation to ash particle surfaces during the experiment and therefore, tend to give more representative analytical results.

A recent study suggests that the amount of iron that can be released from aeolian dust to seawater is strongly linked to the presence and content of natural organic ligands (Mendez et al., 2010). Thus, organic ligands probably control the amount of iron that can be kept in solution when volcanic ash fall-out swamps a surface oceanic area with bio-available iron. We are still far from a comprehensive understanding of this control, a fact highlighted in a leaching study with Mt. St. Helens volcanic ash (Taylor and Lichte, 1980), which suggests that volcanic ash may inject organic ligands to experimental solutes and surface ocean water: the authors analysed the organic compounds by oxidation of the leachate followed by infrared CO_2 -measurement of the released gas

and found considerable amounts of organic substances in leachates of several ash samples. They argued that organic carbon on the surface of ash particles is associated with atmospheric condensation of organic compounds. These may originate from entrainment of burnt vegetation in volcanic eruption plumes. Low molecular weight organic compounds can also be found in volcanic gases (Capaccioni and Mangani, 2001 and references therein). They may originate from carbon-containing host rocks, sediments and soils that interacted with the ascending hot magma. Other authors speculate that volcanic ash injection may cause lysis (decomposition) of phytoplankton in the surface ocean, leading to an enhancement of iron-complexing ligands in seawater (Randazzo et al., 2009). Clearly, the role played by iron-complexing organic ligands, especially those directly or indirectly associated with volcanic ash injection, requires further studies as these compounds are known to determine the availability of iron inputs for oceanic biogeochemical processes.

5 Biological response to volcanic ash fall-out in surface waters

5.1 Biological effects in fresh water systems

Biological events in lakes and rivers within ash fall-out areas of volcanic eruptions may provide constraints on the possible effects in the surface ocean. Eicher and Rounsefell (1957) observed a strong decrease in the abundance of young salmon in the four years after the eruption of Katmai volcano in 1912 in Alaska. This was followed by a rapid recovery of the salmon stock. The recovery indicates very favourable growth conditions, which could for example result from a fertilising effect of the ash on diatom growth and thus, an increased zooplankton standing stock as a food source for the salmon (Eicher and Rounsefell, 1957). In a bioassay study variable amounts of pristine volcanic ash from the 1980 Mt. St. Helens eruption were added to containers with Columbia River water and juvenile salmon (Newcomb and Flagg, 1983). The results show that initial salmon mortality was due to mechanical gill damage caused by particulate matter rather than the soluble material coating the ash. The drop in pH of the moderately hard Columbia River water was relatively minor (from 7.8 down to 7.6), well above the threshold detrimental to salmonids (pH=5.5).

Several authors indicated that the eruptions of Alaid and Besymjanny volcanoes had a significant influence on phytoplankton growth in lakes affected by the ash (Kurenkov, 1966; Felitsyn and Kirianov, 2002; Lepskaya, 1993). Kurenkov (1966) describes a strong increase of diatom biomass in 1956 in the lake Asabatchye following ash addition during the great eruption of Mount Besymjanny volcano. The concentration of diatom remained above normal values 9 years after the eruption. Possibly as a result of increased diatom abundance, the copepod *Cyclops scutifer* also

increased in winter 1960 and was 10 to 48 times higher in the period of 1960–1964 than in the 10 years before the eruption (Kurenkov, 1966). Interestingly, Kurenkov (1966) already mentioned that the unusual development of the algae may have been stimulated by increased iron availability from the volcanic ash. Increases in the population of golden algae and diatoms were also observed in several lakes in the ash fall-out area of the May 1980 eruption of Mount St. Helens volcano (Smith and White, 1985). However, it was also shown that Mt. St. Helens ash leachates caused toxic effects on blue-green algae (McKnight et al., 1971, 1981).

In summary, these studies suggest that the initial toxic effects of volcanic ash on phytoplankton are subsequently over-compensated by a multi-annual increase of biomass. Grazing zooplankton and fish seem to benefit from moderate volcanic ash fall-out.

5.2 Biological effects in the surface ocean in the Earth's history

A recent study showed that forests on western Pacific ocean islands benefit from large-scale volcanic ash fall-out (Rolett and Diamond, 2004). If plants on ocean islands do, why should phytoplankton between these islands, where the ash is deposited as well, not benefit too? Key questions in this context are if both toxic and fertilising effects in the marine environment are analogous to those identified in lakes, which species are affected and if marine iron-fertilisation with volcanic ash is only of regional or even global relevance for C-cycles and climate throughout much of the Earth's history?

Iron-limitation and iron-fertilisation are likely to have played an important role for the marine primary productivity at least for a few millions of years but relatively little is known about how long back in the Earth's history surface ocean iron-limitation existed. Hence the role of volcanic ash in shaping the marine biogeochemical iron- and carbon-cycle in the past is highly uncertain. There are indications on how oceanic iron-fertilisation with volcanic ash might be connected to events of marine primary productivity feedback, among these are: 1) a termination of global warmth at the Paleocene/Eocene boundary, revealed from scientific drill core material (Bains et al., 2000), 2) global cooling at the Eocene/Oligocene boundary argued to be linked to episodes of increased volcanic output in several Pacific subduction zones as inferred from age data of volcanic eruptions (Jicha et al., 2009), 3) the development of the Cenozoic icehouse in the middle Eocene to middle Miocene partly caused by a prolonged period of great silicic subduction zone volcanic eruptions in North America (Cather et al., 2009), 4) the association of diatomites and volcanic ash layers in the Tertiary Danish Mo-clay formation (Duggen et al., 2007), 5) a significant increase of the relative abundance of the marine diatom *Thalassiosira oestrupii* after the deposition of a ca. 10 cm ash layer ca. 450 ka ago, found in a drill core from the Southern Ocean (Kunz-Pirring et al., 2002; Duggen et al., 2007) and

6) a correlation between volcanism and millennial climate change inferred from ice core data (Bay et al., 2004).

For the recent surface ocean, the effect of volcanic ash on the marine trace metal budget and marine phytoplankton growth is not well understood either. Geochemical experiments demonstrate an (iron-)fertilising potential of volcanic ash in several oceanic regions (Olgun et al., 2010; Jones and Gislason, 2008; Frogner et al., 2001; Duggen et al., 2007). Laboratory experiments show that marine diatoms such as *Chaetoceros dichaeta* are able to use iron from volcanic ash and that they grow faster in water that has been in short-term contact with volcanic ash (ca. 20 min) compared to untreated water (Duggen et al., 2007). Recent studies indicate that the diatom *Thalassiosira pseudonana* shows higher growth rates in waters that have been in contact with volcanic ash, while the same material has no, or a strong negative effect on growth of the coccolithophoride *Emiliania huxleyi* (L. Hoffmann, unpublished data). Iron inputs through volcanic eruptions have been discussed as a possible factor controlling phytoplankton seasonality in the subarctic Pacific (Banse and English, 1999).

An anomalous oxygen pulse emanating from the Southern Hemisphere in the years following the 1991 Pinatubo eruption has been linked to an ash fertilisation effect (Keeling et al., 1996; Watson, 1997; Sarmiento, 1993). It was proposed that the oxygen pulse was linked to an atmospheric CO₂-drawdown in the same years and also causally related to an iron-fertilisation event triggered by the deposition of Pinatubo ash in the iron-limited Southern Ocean (Sarmiento, 1993; Watson, 1997). It was recently shown that a pronounced atmospheric CO₂-drawdown also followed the major eruption of Agung volcano in 1963 (Cather et al., 2009). However, the exact causes for the post-Agung and post-Pinatubo CO₂-drawdown has not yet been fully elucidated. A relative atmospheric CO₂-reduction may also be explained by an increase in net primary production (NPP) of the terrestrial biomass, although several studies indicate a decrease in terrestrial NPP of up to eight years after the Pinatubo eruption, possibly due to a decrease in mean summer temperatures and a shortening of the growing season (Lucht et al., 2002; Nemani et al., 2003; Awaya et al., 2004; Krakauer and Randerson, 2003).

Near Soufrière Hills volcano on Montserrat, the phytoplankton bloom detected in the oligotrophic oceanic water by satellite images in mid-July 2003 (e.g. Duggen et al., 2007) may be due to fertilisation with fixed nitrogen (e.g. ammonia or nitrate) rather than iron from volcanic ash. The type of phytoplankton species responsible for this bloom has not yet been identified. The Soufrière Hills volcano has been active since 1995, and in the past years the phenomenon of a seawater discolouration has been visible several times in MODIS satellite images (e.g. Duggen et al., 2007). In the near future valuable biogeochemical data may be obtained from water samples of surface oceanic areas that are located within an ash fall-out area and which show a contemporaneous

discolouration. Recently, satellite data provided the first evidence for volcanic ash fall-out causing a large-scale phytoplankton bloom in an iron-limited oceanic area: a significant MPP increase was observed for the subarctic NW Pacific following the August 2008 eruption of Kasatochi volcano in the Aleutian subduction zone (Langmann et al., 2010). Such satellite techniques have only been available for about a decade and can be expected to provide more important information about the role of volcanic ash fall-out for the MPP.

Today, the overall effects of volcanic eruptions on marine ecosystems are not yet comprehensively understood. It is very likely that volcanic ash fall-out impacts in different ways in distinct oceanic regions and that different phytoplankton species behave in various and differing ways through their specific nutrient demands and tolerance levels for toxic trace metals. More detailed research in this context is needed to improve our understanding of the complex relationships between geology and biology and their implications for the development of climate and life on our planet. However, at this stage investigations and data suggest that the impact of volcanic activity on oceanic biota and associated carbon-cycles has been underestimated.

Acknowledgements. The authors are grateful to the other participants of the “Iron biogeochemistry across marine systems at changing times” workshop, held 14–16 May 2008 in Gothenburg, Sweden, for constructive and fruitful discussions and inspiring conversations. The constructive comments and suggestions of the reviewers (Morgan Jones and Paul Frogner-Kockum) are gratefully acknowledged. The multi-disciplinary research group NOVUM “Nutrients Originating in Volcanoes and their effects on the eUphotic zone of the Marine ecosystem” was established with financial support from IFM-GEOMAR. SD was also supported by the German Science Foundation (DFG) (projects Ho 1833/16-1 and 18-1). Aspects of this work have also been supported by DFG-projects CR145/7-1 and CR145/9-1, awarded to PC. LH was funded by the German Academic Exchange Service (DAAD) and the DFG (HO 4217/1-1). HD was supported by the DFG through the SFB 754 at Kiel University. PD’s contribution to this project was supported by a Vice-Chancellor’s Anniversary Lectureship, University of York.

Edited by: D. Turner

References

- Awaya, Y., Kodani, E., Tanaka, K., Liu, J., Zhuang, D., and Meng, Y.: Estimation of the global net primary productivity using NOAA images and meteorological data: changes between 1988 and 1993, *Int. J. Remote Sens.*, 25, 1597–1613, 2004.
- Bains, S., Norris, R. D., Corfield, R. M., and Faul, K. L.: Termination of global warmth at the Palaeocene/Eocene boundary through productivity feedback, *Nature*, 407, 171–174, 2000.
- Baker, A. R. and Croot, P. L.: Atmospheric and marine controls on aerosol iron solubility in seawater, *Mar. Chem.*, doi:10.1016/j.marchem.2008.09.003, in press, 2010.
- Banse, K. and English, D. C.: Comparing phytoplankton seasonality in the eastern and western subarctic Pacific and the western Bering sea, *Prog. Oceanogr.*, 43, 235–288, 1999.
- Bay, R. C., Bramall, N., and Price, P. B.: Bipolar correlation of volcanism with millennial climate change, *Proceedings of the National Academy of Science of the United States of America*, 101, 6341–6345, 2004.
- Bay, R. C., Bramall, N. E., Price, P. B., Clow, G. D., Hawley, R. L., Udisti, R., and Castellano, E.: Globally synchronous ice core volcanic tracers and abrupt cooling during the last glacial period, *J. Geophys. Res.*, 111, D11108, doi:10.1029/2005JD006306, 2006.
- Behrenfeld, M. J., Bale, A. J., Kolber, Z. S., Aiken, J., and Falkowski, P. G.: Confirmation of iron limitation of phytoplankton photosynthesis in the equatorial Pacific Ocean, *Nature*, 383, 508–511, 1996.
- Benítez-Nelson, C. R., Vink, S. M., Carrillo, J. H., and Huebert, B. J.: Volcanically influenced iron and aluminium cloud water deposition to Hawaii, *Atmos. Environ.*, 37, 535–544, 2003.
- Blain, S., Quéguiner, B., Armand, L., Belviso, S., Bombled, B., Bopp, L., Bowie, A., Brunet, C., Brussaard, C., Carlotti, F., Christaki, U., Corbière, A., Durand, I., Ebersbach, F., Fuda, J.-L., Garcia, N., Gerringa, L., Griffiths, B., Guigue, C., Guillemin, C., Jaquet, S., Jeandel, C., Laan, P., Lefèvre, D., Monaco, C. L., Malits, A., Mosseri, J., Obernosterer, I., Park, Y.-H., Picheral, M., Pondaven, P., Remenyi, T., Sandroni, V., Sarthou, G., Savoye, N., Scouarnec, L., Souhaut, M., Thuiller, D., Timmermans, K., Trull, T., Uitz, J., van Beel, P., Veldhuis, M., Vincent, D., Viollier, E., Vong, L., and Wagener, T.: Effect of natural iron fertilization on carbon sequestration on the Southern Ocean, *Nature*, 446, 1070–1074, 2007.
- Boyd, P. W., Watson, A. J., Law, C. S., Abraham, E. R., Trull, T., Murdoch, R., Bakker, D. C. E., Bowie, A. R., Buesseler, K. O., Chang, H., Charette, M., Croot, P., Downing, K., Frew, R., Gall, M., Hadfield, M., Hall, J., Harvey, M., Jameson, G., LaRoche, J., Liddicoat, M. I., Ling, R., Maldonado, M. T., McKay, R. M., Nodder, S., Pickmere, S., Pridmore, R., Rintoul, S., Safi, K., Sutton, P., Strzepek, R., Tanneberger, K., Turner, S., Waite, A., and Zeldis, J.: A mesoscale phytoplankton bloom in the polar Southern Ocean stimulated by iron fertilization, *Nature*, 407, 695–702, 2000.
- Boyd, P. W., Law, C. S., Wong, C. S., Nojiri, Y., Tsuda, A., Levasseur, M., Takeda, S., Rivkin, R., Harrison, P. J., Strzepek, R., Gower, J., McKay, R. M., Abraham, E. R., Arychuk, M., Barwell-Clarke, J., Crawford, W., Crawford, D., Hale, M., Harada, K., Johnson, K., Kiyosawa, H., Kudo, I., Marchetti, A., Miller, W., Needoba, J., Nishioka, J., Ogawa, H., Page, J., Robert, M., Saito, H., Sastri, A., Sherry, N., Soutar, T., Sutherland, N., Taira, Y., Whitney, F., Wong, S.-K. E., and Yoshimura, T.: The decline and fate of an iron-induced subarctic phytoplankton bloom, *Nature*, 428, 549–553, 2004.
- Bruland, K. W. and Lohan, M. C.: Controls of trace metals in seawater, in: *The Oceans and Marine Geochemistry*, edited by: Elderfield, H., Treatise on Geochemistry, Elsevier Pergamon, Amsterdam-Boston-Heidelberg-London-New York-Oxford-Paris-San Diego-San Francisco-Singapore-Sydney-Tokyo, 23–47, 2004.
- Capaccioni, B. and Mangani, F.: Monitoring of active but quiescent volcanoes using light hydrocarbon distribution in volcanic gases:

- the results of 4 years of discontinuous monitoring in the Campi Flegrei (Italy), *Earth Planet. Sci. Lett.*, 188, 543–555, 2001.
- Cather, S. M., Dunbar, N. W., McDowell, F. W., McIntosh, W. C., and Scholle, P. A.: Climate forcing by iron fertilization from repeated ignimbrite eruptions: The icehouse-silicic large igneous province (SLIP) hypothesis, *Geosphere*, 5, 315–324, 2009.
- Christenson, B. W.: Geochemistry of fluids associated with the 1995–1996 eruption of Mt. Ruapehu, New Zealand: signatures and processes in the magmatic-hydrothermal system, *J. Volcanol. Geoth. Res.*, 97, 1–30, 2000.
- Cimino, G. and Toscano, G.: Dissolution of trace metals from lava ash: influence on the composition of rainwater in the Mount Etna volcanic area, *Environ. Pollut.*, 99, 389–393, 1998.
- Coale, K. H., Johnson, K. S., Fitzwater, S. E., Gordon, R. M., Tanner, S. J., Chavez, F. P., Ferioli, L., Sakamoto, C., Rogers, P., Millero, F., Steinberg, P., Nightingale, P., Cooper, D., Cochlan, W. P., Landry, M. R., Constantiniou, J., Rollwagen, G., Trassvina, A., and Kudela, R.: A massive phytoplankton bloom induced by an ecosystem-scale iron fertilization experiment in the equatorial Pacific Ocean, *Nature*, 383, 495–501, 1996.
- Coale, K. H., Johnson, K. S., Chavez, F. P., Buesseler, K. O., Barber, R. T., Brzezinski, M. A., Cochlan, W. P., Millero, F., Falkowski, P. G., Bauer, J. E., Wanninkhof, R. H., Kudela, R. M., Altabet, A. M., Hales, B. E., Takahashi, T., Landry, M. R., Bidigare, R. R., Wang, X., Chase, Z., Strutton, P. G., Friederich, G. E., Gorbunov, M. Y., Lance, V. P., Hiltling, A. K., Hiscock, W. T., Sullivan, K. F., Tanner, S. J., Gordon, R. M., Hunter, C. N., Elrod, V. A., Fitzwater, S. E., Jones, J. L., Tozzi, S., Koblizek, M., Roberts, A. E., Herndon, J., Brewster, J., Ladizinsky, N., Smith, G., Cooper, D., Timothy, D., Brown, S. L., Selph, K. E., Sheridan, C. C., Twining, B. S., and Johnson, Z. I.: Southern Ocean iron enrichment experiment: Carbon cycling in high- and low-Si waters, *Science*, 304, 408–414, 2004.
- Cooper, D. J., Watson, A. J., and Nightingale, P. D.: Large decrease in ocean-surface CO₂ fugacity in response to *in situ* iron fertilization, *Nature*, 383, 511–513, 1996.
- Croot, P. and Johansson, M.: Determination of iron speciation by cathodic stripping voltammetry in seawater using the competing ligand 2-(2-Thiazolylazo)-*p*-creosol (TAC), *Electroanalysis*, 12, 565–576, 2000.
- De Baar, J. W. O. and De Jong, J. T. M.: Distributions, Sources and Sinks of Iron in Seawater, in: *Biogeochemistry of iron in seawater*, edited by: Turner, D. R. and Hunter, K., Wiley, Chichester, 124–233, 2001.
- de Hoog, J. C. M., Koetsier, G. W., Bronto, S., Sriwana, T., and van Bergen, M. J.: Sulfur and chlorine degassing from primitive arc magmas: temporal changes during the 1982–1963 eruptions of Galunggung (West Java, Indonesia), *J. Volcanol. Geoth. Res.*, 108, 55–83, 2001.
- Delmelle, P., Lambert, M., Dufrene, Y., Gerin, P., and Óskarsson, N.: Gas/aerosol-ash interaction in volcanic plumes: New insights from surface analyses of fine ash particles, *Earth Planet. Sci. Lett.*, 259, 159–170, 2007.
- Duggen, S., Croot, P., Schacht, U., and Hoffmann, L.: Subduction zone volcanic ash can fertilize the surface ocean and stimulate phytoplankton growth: Evidence from biogeochemical experiments and satellite data, *Geophys. Res. Lett.*, 34(5), L01612, doi:10.1029/2006GL027522, 2007.
- Eicher, G. J. and Rounsefell, G. A.: Effects of lake fertilization by volcanic activity on abundance of salmon, *Limnol. Oceanogr.*, 2, 70–76, 1957.
- Felitsyn, S. B. and Kirianov, V. Y.: Mobility of phosphorous during weathering of volcanic ashes, *Lithol. Miner. Resour.*, 37, 275–278, 2002.
- Fisher, R. V. and Schmincke, H.-U.: *Pyroclastic Rocks*, Springer-Verlag, Berlin-Heidelberg-New York-Tokyo, 472 pp., 1984.
- Flaathen, T. K., Oelkers, E. H., and Gislason, S. R.: The effect of aqueous sulphate on basaltic glass dissolution rates, *Mineralogical Magazine*, 72, 39–41, 2008.
- Frogner Kockum, P. C.: A diverse ecosystem response to volcanic aerosols, *Chem. Geol.*, 231, 57–66, 2006.
- Frogner, P., Gislason, S. R., and Óskarsson, N.: Fertilization Potential of Volcanic Ash in Ocean Surface Waters, *Journal of Conference Abstracts (Goldschmidt Conference 2000, Oxford)*, 5, 415, 2000.
- Frogner, P., Gíslason, S. R., and Óskarsson, N.: Fertilizing potential of volcanic ash in ocean surface water, *Geology*, 29, 487–490, 2001.
- Fruchter, J. S., Robertson, D. E., Evans, J. C., Olsen, K. B., Lepel, E. A., Laul, J. C., Abel, K. H., Sanders, R. W., Jackson, P. O., Wogman, N. S., Perkins, R. W., van Tuyl, H. H., Beauchamp, R. H., Shade, J. W., Daniel, J. L., Erikson, R. L., Schmel, G. A., Lee, R. N., Robinson, A. V., Moss, O. R., Briant, J. K., and Cannon, W. C.: Mount St. Helens Ash from the 18 May 1980 Eruption: Chemical, Physical, Mineralogical, and Biological Properties, *Science*, 209, 1116–1125, 1980.
- Gislason, S. R. and Oelkers, E. H.: Mechanism, rates, and consequences of basaltic glass dissolution: II. An experimental study of the dissolution rates of basaltic glass as a function of pH and temperature, *Geochim. Cosmochim. Acta*, 67, 3817–3832, 2003.
- Gran, H. H.: On the conditions for the production of plankton in the sea, *Rapp. Proc. Verb. Cons. Int. Explor. Mer*, 75, 37–46, 1931.
- Harvey, H. W.: The supply of iron to diatoms, *Journal of the Marine Biology Association*, XXII, 205–219, 1937.
- Jicha, B. R., Scholl, D. W., and Rea, D. K.: Circum-Pacific arc flare-ups and global cooling near the Eocene-Oligocene boundary, *Geology*, 37, 303–306, doi:10.1130/G25392A.1, 2009.
- Jones, M. T. and Gislason, S. R.: Rapid releases of metal salts and nutrients following the deposition of volcanic ash into aqueous environments, *Geochim. Cosmochim. Acta*, 72, 3661–3680, 2008.
- Keeling, R. F., Piper, S. C., and Heimann, M.: Global and hemispheric CO₂ sinks deduced from changes in atmospheric O₂ concentration, *Nature*, 381, 218–221, 1996.
- Kraemer, S. M.: Iron oxide dissolution and solubility in the presence of siderophores, *Aquat. Sci.*, 66, 3–18, 2004.
- Krakauer, N. Y. and Randerson, J. T.: Do volcanic eruptions enhance or diminish net primary production? Evidence from tree rings, *Global Biogeochem. Cy.*, 17, 002003, doi:10.1029/2003GB002076, 2003.
- Kunz-Pirrung, M., Gersonde, R., and Hodell, D. A.: Mid-Brunhes century-scale diatom sea surface temperature and sea ice records from the Atlantic sector of the Southern Ocean (ODP Leg 177, sites 1093, 1094 and core PS2089-2), *Palaeogeogr. Palaeoclimatol.*, 182, 305–328, 2002.
- Kurenkov, I. I.: The influence of volcanic ashfall on biological processes in a lake, *Limnol. Oceanogr.*, 11, 426–429, 1966.
- Kutterolf, S., Freundt, A., and Pérez, W.: Pacific offshore record

- of plinian arc volcanism in Central America: 2. Tephra volumes and erupted masses, *Geochem. Geophys. Geosy.*, 9, 1–19, 2008.
- Langmann, B., Zakšek, K., Hort, M., and Duggen, S.: Volcanic ash as fertiliser for the surface ocean, *Atmos. Chem. Phys. Discuss.*, 10, 711–734, 2010, <http://www.atmos-chem-phys-discuss.net/10/711/2010/>.
- Larsson, W.: Vulkanische Asche vom Ausbruch des chilenischen Vulkans Quizapu (1932) in Argentinien gesammelt. Eine Studie über äolische Differentiation., Geological Institute of Uppsala Bulletin, 26, 27–52, 1937.
- Lepskaya, E. V.: Influence of Ash from the Alaid Volcano on Phytoplankton of Lake Kurile (Southern Kamchatka), in: *Issledovaniya biologii i dinamiki chislennosti promyslovyykh ryb Kamchatskogo shel'fa* (The Study of Biology and Dynamics of Commercial Fish Population on the Kamchatka Shelf), 2, Minvo Rybn, Khoz-va, Petropavlovsk-Kamchatskii, 21–24, 1993.
- Lucht, W., Prentice, I. C., Myneni, R. B., Sitch, S., Friedlingsstein, P., Cramer, W., Bousquet, P., Buermann, W., and Smith, B.: Climatic control of the high-latitude vegetation greening trend and Pinatubo effect, *Science*, 296, 1687–1689, 2002.
- Martin, J. H. and Fitzwater, S. E.: Iron deficiency limits phytoplankton growth in the north-east Pacific subarctic, *Nature*, 331, 341–343, 1988.
- Martin, J. H., Gordon, R. M., and Fitzwater, S. E.: Iron in Antarctic waters, *Nature*, 345, 156–158, 1990.
- McKnight, D. M., Feder, G. L., and Stiles, E. A.: Effects on a blue-green alga of leachates of ash from the May 18 eruption, in: *The 1980 Eruptions of Mount St. Helens*, edited by: Lipman, P. W. and Mullineaux, D. R., USGS Professional Paper, Washington, 733–741, 1971.
- McKnight, D. M., Feder, G. L., and Stiles, E. A.: Toxicity of volcanic-ash leachate to a blue-green alga: results of a preliminary bioassay experiment, *Environ. Sci. Technol.*, 15, 362–364, 1981.
- Mendez, J., Guieu, C., and Adkins, J.: Atmospheric input of manganese and iron to the ocean: Seawater dissolution experiments with Saharan and North American dusts, *Mar. Chem.*, in press, 2010.
- Middleton, G. V., Church, M. J., and Coniglio, M.: *Encyclopedia of Sediments and Sedimentary Rocks*, Springer, Boston, 2003.
- Mills, M. M., Ridame, C., Davey, M., La Roche, J., and Geider, R.: Iron and phosphorus co-limit nitrogen fixation in the eastern tropical North Atlantic, *Nature*, 429, 292–294, 2004.
- Morel, F. M. M., Milligan, A. J., and Saito, M. A.: Marine bioinorganic chemistry: The role of trace metals in the oceanic cycles of major nutrients, in: *The Oceans and Marine Geochemistry*, edited by: Elderfield, H., Treatise on Geochemistry, Elsevier Pergamon, Amsterdam-Boston-Heidelberg-London-New York-Oxford-Paris-San Diego-San Francisco-Singapore-Sydney-Tokyo, 113–143, 2004.
- Nehring, N. L. and Johnston, D. A.: Use of ash leachates to monitor gas emissions, in: *The 1980 Eruptions of Mount St. Helens*, edited by: Lipman, P. W., and Mullineaux, D. R., USGS Professional Paper, Washington, 251–254, 1981.
- Nemani, R. R., Keeling, C. D., Hashimoto, H., Jolly, W. M., Piper, S. C., Tucker, C. J., Myneni, R. B., and Running, S. W.: Climate-driven increases in global terrestrial net primary production from 1982–1999, *Science*, 300, 1560–1563, 2003.
- Newcomb, T. W. and Flagg, T. A.: Some Effects of Mt. St. Helens Volcanic Ash on Juvenile Samlon Smolts, *Mar. Fish. Rev.*, 45, 8–12, 1983.
- Nielsen, S. H. H., Hodell, D. A., Kamenov, G., Guilderson, T., and Perfit, M. R.: Origin and significance of ice-rafted detritus in the Atlantic sector of the Southern Ocean, *Geochem. Geophys. Geosy.*, 8, 1–23, 2007.
- Niemeier, U., Timmreck, C., Graf, H.-F., Kinne, S., Rast, S., and Self, S.: Initial fate of fine ash and sulfur from large volcanic eruptions, *Atmos. Chem. Phys.*, 9, 9043–9057, 2009, <http://www.atmos-chem-phys.net/9/9043/2009/>.
- Olgun, N., Duggen, S., Croot, P. L., Delmelle, P., Dietze, H., Schacht, U., Óskarsson, N., Siebe, C., and Auer, A.: Surface ocean iron fertilization: The role of airborne volcanic ash from subduction zone and hotspot volcanoes and related fluxes into the Pacific Ocean, *Global Biogeochem. Cy.*, in review, 2010.
- Oppenheimer, C.: Limited global change due to the largest known Quaternary eruption, Toba 74 kyr BP?, *Quaternary Sci. Rev.*, 21, 1593–1609, 2002.
- Oppenheimer, C.: Volcanic Degassing, in: *The Crust*, edited by: Rudnick, R. L., Treatise on Geochemistry, Elsevier Pergamon, Amsterdam-Boston-Heidelberg-London-New York-Oxford-Paris-San Diego-San Francisco-Singapore-Sydney-Tokyo, 123–166, 2004.
- Óskarsson, N.: The interaction between volcanic gases and tephra: Flourine adhering to tephra of the 1970 Hekla eruption, *J. Volcanol. Geoth. Res.*, 8, 251–266, 1980.
- Óskarsson, N.: The chemistry of Icelandic lava incrustations and the latest stages of degassing, *J. Volcanol. Geoth. Res.*, 10, 93–111, 1981.
- Parekh, P., Follows, M. J., and Boyle, E. A.: Decoupling of iron and phosphate in the global ocean, *Global Biogeochem. Cy.*, 19, 1–16, 2005.
- Pedersen, G. K., and Surlyk, F.: Dish structures in Eocene volcanic ash layers, Denmark, *Sedimentology*, 24, 581–590, 1977.
- Randazzo, L. A., Censi, P., Saiano, F., Zuddas, P., Aricò, P., and Mazzola, S.: Trace elements release from volcanic ash to seawater. Natural concentrations in Central Mediterranean Sea, European Geosciences Union Meeting, Vienna, 2009.
- Rea, D. K., Scholl, D. W., and Allan, J. F.: Proceedings of the Ocean Drilling Program 145, Scientific Results, 1995.
- Rolett, B. and Diamond, J.: Environmental predictors of pre-European deforestation on Pacific islands, *Nature*, 431, 443–446, 2004.
- Rose, W. I.: Scavenging of volcanic aerosol by ash: atmospheric and volcanologic implications, *Geology*, 5, 621–624, 1977.
- Rubin, C. H., Noji, E. K., Seligman, P. J., Holtz, J. L., Grande, J., and Vittani, F.: Evaluating a flourosis hazard after a volcanic eruption, *Arch. Environ. Health*, 49, 395–401, 1994.
- Sansone, F. J., Benitez-Nielson, C. R., DeCarlo, E. H., Resing, J. A., Vink, S. M., Heath, J. A., and Huebert, B. J.: Geochemistry of atmospheric aerosols generated from lava-seawater interactions, *Geophys. Res. Lett.*, 29, 1–4, 2002.
- Sarmiento, J. L.: Atmospheric CO₂ stalled, *Nature*, 365, 697–698, 1993.
- Schmincke, H.-U.: *Volcanism*, Springer-Verlag, Berlin Heidelberg New York, 324 pp., 2004.
- Sigurdsson, H., Houghton, B., McNutt, S. R., Rymer, H., and Stix, J.: *Encyclopedia of Volcanoes*, Academic Press, San Diego California, 2000.

- Smith, D. B., Zielinski, R. A., and Rose, W. I.: Leachability of uranium and other elements from freshly erupted volcanic ash, *J. Volcanol. Geoth. Res.*, 13, 1–30, 1982.
- Smith, D. B., Zielinski, R. A., Taylor, H. E., and Sawyer, M. B.: Leaching Characteristics of Ash from the May 18, 1980, Eruption of Mount St. Helens Volcano, Washington, *Bulletin of Volcanology*, 46, 103–124, 1983.
- Smith, M. A. and White, M.: Observations on lakes near Mount St. Helens: Phytoplankton, *J. Arch. Hydrobiol.*, 104, 345–363, 1985.
- Spirakis, C. S.: Iron fertilization with volcanic ash?, *Eos Trans. AGU*, 72(47), 525–526, 1991.
- Straub, S. M. and Schmincke, H.-U.: Evaluating the tephra input into Pacific Ocean sediments: distribution in space and time, *Geol. Rundsch.*, 87, 461–476, 1998.
- Symonds, R. B., Rose, W. I., Reed, M. H., Lichte, F. E., and Finnegan, D. L.: Volatilization, transport and sublimation of metallic and non-metallic elements in high temperature gases at Merapi Volcano, Indonesia, *Geochim. Cosmochim. Acta*, 51, 2083–2101, 1987.
- Taylor, H. E. and Lichte, F. E.: Chemical composition of Mount St. Helens volcanic ash, *Geophys. Res. Lett.*, 7, 949–952, 1980.
- Textor, C., Graf, H. F., Herzog, M., Oberhuber, J. M., Rose, W. I., and Ernst, G. G. J.: Volcanic particle aggregation in explosive eruption columns. Part I: Parameterization of the microphysics of hydrometeors and ash, *J. Volcanol. Geoth. Res.*, 150, 359–377, 2006.
- Uematsu, M., Toratani, M. M. K., Narita, Y., Senga, Y., and Kimoto, T.: Enhancement of primary productivity in the western North Pacific caused by the eruption of the Miyake-jima volcano, *Geophys. Res. Lett.*, 31, 1–4, 2004.
- Walker, G. P. L. and Croasdale, R.: Characteristics of some basaltic pyroclastics, *Bull. Volcanol.*, 35, 303–317, 1972.
- Watson, A. J.: Volcanic Fe, CO₂, ocean productivity and climate, *Nature*, 385, 587–588, 1997.
- Wells, M. L.: The level of iron enrichment required to initiate diatom blooms in HNLC waters, *Mar. Chem.*, 82, 101–114, 2003.
- Wiesner, M. G., Wetzel, A., Catane, S. G., Listanco, E. L., and Mirabueno, H. T.: Grain size, areal thickness distribution and controls on sedimentation of the 1991 Mount Pinatubo tephra layer in the South China Sea, *Bull. Volcanol.*, 66, 226–242, 2004.
- Witham, C. S., Oppenheimer, C., and Horwell, C. J.: Volcanic ash-leachates: a review and recommendations for sampling methods, *J. Volcanol. Geoth. Res.*, 141, 299–326, 2005.
- Wolff-Boenisch, D., Gislason, S. R., and Oelkers, E. H.: The effect of fluoride on the dissolution rates of natural glasses at pH 4 and 25 °C, *Geochim. Cosmochim. Acta*, 68, 4571–4582, 2004a.
- Wolff-Boenisch, D., Gislason, S. R., Oelkers, E. H., and Putnis, C. V.: The dissolution rates of natural glasses as a function of their composition at pH 4 and 10.6, and temperatures from 25 to 74 °C, *Geochim. Cosmochim. Acta*, 68, 4843–4858, 2004b.

Chapter II

**Surface ocean iron fertilization: The role of airborne
volcanic ash from subduction zone and hot spot
volcanoes and related iron-fluxes
into the Pacific Ocean.**

Surface ocean iron fertilization: The role of airborne volcanic ash from subduction zone and hot spot volcanoes and related iron fluxes into the Pacific Ocean

Nazlı Olgun,^{1,2} Svend Duggen,^{1,3} Peter Leslie Croot,^{2,4} Pierre Delmelle,⁵ Heiner Dietze,² Ulrike Schacht,⁶ Niels Óskarsson,⁷ Claus Siebe,⁸ Andreas Auer,⁹ and Dieter Garbe-Schönberg¹⁰

Received 15 December 2009; revised 15 March 2011; accepted 8 June 2011; published 1 October 2011.

[1] Surface ocean iron (Fe) fertilization can affect the marine primary productivity (MPP), thereby impacting on CO₂ exchanges at the atmosphere–ocean interface and eventually on climate. Mineral (aeolian or desert) dust is known to be a major atmospheric source for the surface ocean biogeochemical iron cycle, but the significance of volcanic ash is poorly constrained. We present the results of geochemical experiments aimed at determining the rapid release of Fe upon contact of pristine volcanic ash with seawater, mimicking their dry deposition into the surface ocean. Our data show that volcanic ash from both subduction zone and hot spot volcanoes ($n = 44$ samples) rapidly mobilized significant amounts of soluble Fe into seawater (35–340 nmol/g ash), with a suggested global mean of 200 ± 50 nmol Fe/g ash. These values are comparable to the range for desert dust in experiments at seawater pH (10–125 nmol Fe/g dust) presented in the literature (Guieu et al., 1996; Spokes et al., 1996). Combining our new Fe release data with the calculated ash flux from a selected major eruption into the ocean as a case study demonstrates that single volcanic eruptions have the potential to significantly increase the surface ocean Fe concentration within an ash fallout area. We also constrain the long-term (millennial-scale) airborne volcanic ash and mineral dust Fe flux into the Pacific Ocean by merging the Fe release data with geological flux estimates. These show that the input of volcanic ash into the Pacific Ocean ($128\text{--}221 \times 10^{15}$ g/ka) is within the same order of magnitude as the mineral dust input ($39\text{--}519 \times 10^{15}$ g/ka) (Mahowald et al., 2005). From the similarity in both Fe release and particle flux follows that the flux of soluble Fe related to the dry deposition of volcanic ash ($3\text{--}75 \times 10^9$ mol/ka) is comparable to that of mineral dust ($1\text{--}65 \times 10^9$ mol/ka). Our study therefore suggests that airborne volcanic ash is an important but hitherto underestimated atmospheric source for the Pacific surface ocean biogeochemical iron cycle.

Citation: Olgun, N., S. Duggen, P. L. Croot, P. Delmelle, H. Dietze, U. Schacht, N. Óskarsson, C. Siebe, A. Auer, and D. Garbe-Schönberg (2011), Surface ocean iron fertilization: The role of airborne volcanic ash from subduction zone and hot spot volcanoes and related iron fluxes into the Pacific Ocean, *Global Biogeochem. Cycles*, 25, GB4001, doi:10.1029/2009GB003761.

¹Dynamics of the Ocean Floor Division, Leibniz-Institute of Marine Sciences, IFM-GEOMAR, Kiel, Germany.

²Marine Biogeochemistry Division, Leibniz-Institute of Marine Sciences, IFM-GEOMAR, Kiel, Germany.

³A. P. Møller Skolen, Upper Secondary School and Sixth Form College of the Danish National Minority in Northern Germany, Schleswig, Germany.

⁴Plymouth Marine Laboratory, Plymouth, UK.

⁵Environment Department, University of York, York, UK.

⁶CO2CRC, Australian School of Petroleum, University of Adelaide, Adelaide, Australia.

⁷Institute of Earth Sciences, University of Iceland, Reykjavik, Iceland.

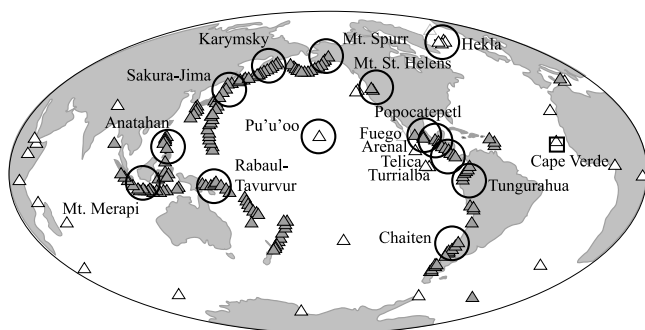
⁸Departamento de Vulcanología, Instituto de Geofísica, Universidad Nacional Autónoma de México, Coyoacan, Mexico.

⁹Department of Geology, University of Otago, Dunedin, New Zealand.

¹⁰Institute of Geosciences, University of Kiel, Kiel, Germany.

1. Introduction

[2] Iron (Fe) is a key micronutrient, essential for phytoplankton biochemical processes such as photosynthesis and nitrogen fixation [Morel and Price, 2003]. Marine primary production (MPP) is limited by Fe deficiency in High-Nutrient Low-Chlorophyll (HNLC) regions that cover about 40% of the oceans and are mainly located in the subarctic Pacific, the eastern equatorial Pacific, and the Southern Ocean [Watson, 2001]. Recent mesoscale Fe fertilization experiments have demonstrated that an increase in dissolved Fe concentration by a few nanomolars in Fe-limited oceanic regions can trigger large-scale diatom blooms [Behrenfeld et al., 1996; Boyd et al., 2000; Coale et al., 1996; Cooper et al., 1996; Martin and Fitzwater, 1988; Turner et al., 1996; Wells, 2003]. Moreover, addition of Fe to the surface ocean may enhance bacterial nitrogen fixation and contribute



Sample locations	Subaerial volcanoes in
○ Volcanic ash	▲ Subduction zones
□ Dust sample	△ Other tectonic settings (e.g. hotspot areas)

Figure 1. World map showing the provenance of pristine volcanic ash and dust samples used in this study. Also shown is the distribution of subaerially active volcanoes based on the work of *Sigurdsson et al.* [2000].

to N fertilization in open oceanic areas deficient in fixed nitrogen [Moore et al., 2009; Morel et al., 2003]. Changes in surface ocean Fe concentrations can therefore play an important role in the ocean-atmosphere exchange of the greenhouse gas CO₂ both through short-term and long-term effects [Langmann et al., 2010; Martin et al., 1994; Martin and Fitzwater, 1988; Martin et al., 1990, 1991; Watson et al., 1991]. Enhancement of the MPP through Fe fertilization may also produce additional biogenic dimethyl sulfide (DMS) and organic carbon (OC), which upon release into the atmosphere impact on the formation and distribution of clouds, and thus on atmospheric albedo [Lohmann and Feichter, 2005; Moore et al., 2009; O'Dowd et al., 2004; Turner et al., 2004].

[3] The concentration of Fe in vast areas of the surface ocean is very low [Boyd et al., 2007, 2000; Coale et al., 2004; De Baar and De Jong, 2001; Liu and Millero, 2002]. The marine deposition of atmospherically transported dusts from deserts or of anthropogenic and extraterrestrial origin has been recognized an important source of soluble (and bioavailable) Fe for the surface ocean [Jickells and Spokes, 2001; Johnson, 2001; Mahowald et al., 2009; Sedwick et al., 2007]. The role of airborne volcanic ash in supplying Fe to the oceans, however, was poorly constrained despite a suggestion almost 20 years ago that it may well be significant [Spirakis, 1991]. Recent studies demonstrate that volcanic ash fallout can significantly raise surface ocean Fe levels [Censi et al., 2010; Duggen et al., 2007, 2010; Frogner et al., 2001; Jones and Gislason, 2008] and has the potential to trigger large-scale phytoplankton blooms in Fe-limited (HNLC) oceanic regions [Hamme et al., 2010; Langmann et al., 2010] and eventually affect the marine food web [Hamme et al., 2010]. Moreover, several authors have argued that surface ocean Fe fertilization through major volcanic eruptions led to atmospheric CO₂ drawdowns in the younger part of the Earth's history [Bay et al., 2004; Cather et al., 2009; Delmelle et al., 2009; Langmann et al., 2010; Sarmiento, 1993; Watson, 1997]. For a recent review of the possible role of volcanic ash for the marine biogeochemical

Fe cycle the reader is referred to the work of *Duggen et al.* [2010].

[4] The Pacific Ocean is the largest of the ocean basins and covers about 70% of the Fe-limited oceanic regions. It is encircled by multitudinous active and explosive volcanoes (the Pacific Ring of Fire) and also hosts numerous hot spot volcanic ocean islands (Figure 1). In the Pacific region, at least 50–60 volcanoes are erupting each year and more than 1,300 erupted in the past 10,000 years (<http://www.volcano.si.edu/world/>). Major eruptions (e.g., Pinatubo 1991) are episodic events from an annual to centennial timescale point of view. Over much longer, geological timescales can the ash input into the Pacific Ocean, which is surrounded by thousands of volcanoes that were active in the Quaternary, be regarded a quasi-continuous process. The flux of volcanic ash into the Pacific Ocean is thus a key parameter in evaluating the significance of Fe flux linked to volcanic ash deposition but has not been constrained until this study.

[5] This paper aims at improving our understanding of the relative importance of volcanic ash as an atmospheric Fe source for the surface ocean. Specifically, our objectives are to (1) produce a robust data basis for the seawater Fe solubility (focusing on the dry deposition process) of pristine volcanic ash from different tectonic settings, (2) constrain the possible regional impact on the surface ocean Fe budget within the ash fallout area of major volcanic eruptions, and (3) improve our understanding of the significance of volcanic ash deposition for the Pacific surface ocean marine biogeochemical Fe cycle.

2. Samples and Methods

[6] The 44 pristine (unhydrated) volcanic ash and one dust sample(s) used in this study were collected from the ground due after deposition and stored dry in plastic bags. The volcanic ash samples were collected fresh shortly (i.e., a couple of hours to 1–2 days) after the eruption in order to prevent Fe-bearing soluble salt coatings to be washed away by rain. Contact with Fe-containing material was avoided (e.g., sieving with metal sieves). The provenance and age of the ash samples is described in more detail in Table S1 in the auxiliary material.¹

[7] The subduction zone volcanic ash (SZVA) samples stem from 14 different volcanoes in the Pacific Ring of Fire: Sakura-jima (5 samples), Tungurahua (1 sample), Arenal (4 samples), Fuego (1 sample), Turrialba (1 sample), Mt. St. Helens (1 sample), Karymsky (10 samples), Popocatepetl (8 samples), Anatahan (1 sample), Rabaul-Tavurvur (3 samples), Mt. Merapi (1 sample), Chaitén (2 samples), Telica (1 sample), and Mt. Spurr (1 sample). The hot spot volcanic ash (HSVA) samples were collected from 2 different volcanoes: Hekla (3 samples) and Pu'u'oo (1 sample). Locations of the volcanoes are shown in Figure 1, and a detailed description of the ash samples is provided in Table S1. The mineral dust sample was collected on July 2007 from loess deposits (aerosols transported from Sahara) in Calhua (Figure 1) located in the northwestern part of the Cape Verdian island Sao Vicente (16.9°N, 24.9°W). The sample was collected from ground, sieved through 100 μm plastic

¹Auxiliary materials are available in the HTML. doi:10.1029/2009GB003761.

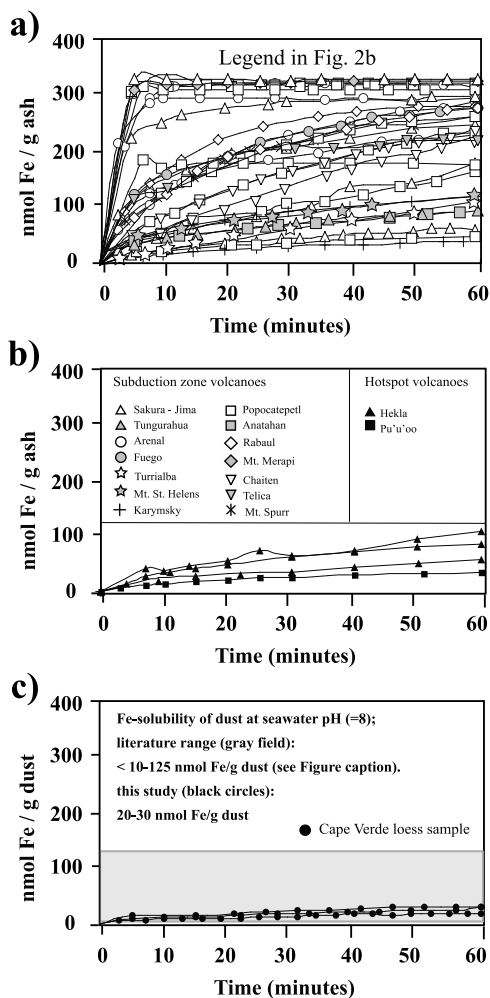


Figure 2. Fe release of (a) subduction zone volcanic ash (SZVA), (b) hot spot volcanic ash (HSVA), and (c) Cape Verde loess sample on contact with natural seawater (buffered at pH 8), determined in situ by means of Cathodic Stripping Voltammetry (CSV). Legend for volcanic ash samples is given in Figure 2b. Symbols indicate ash samples from same volcano collected from different eruptions or different collection distances (see also Table S1). Literature data for mineral dust Fe solubility based on the experiments at seawater pH (=8) including the Cape Verdian loess sample from this study fall within the range of <math>< 10</math> to 125 nmol/g dust (gray bar in Figure 2c, also shown in Table 4) (Guieu and Thomas [1996], Spokes and Jickells [1996], and this study). The literature data are recalculated from the fractional Fe solubilities ($\%Fe_S = 0.001\%–0.02\%$) to nmol Fe/g of dust , assuming that 3.5 wt.% of dust is Fe. The calculations are based on the following equation: $\text{Fe release in nmol/g dust} = (\%Fe_S \times \text{Fe wt.}\% \times 10^9) / (55.85 \text{ g Fe/mol})$.

filters and stored in plastic bags. Based on the elemental analyses [Heller and Croot, 2011], the dust sample is mainly composed of silt from Sahara (generally 80%–95% in the region; [Desboeufs et al., 1999]), which is possibly derived from different sources (Mali, Niger, Chad and southern Algeria) and transported by the West African trade wind.

[8] The Fe release experiments with unsieved pristine volcanic ash samples were performed in situ in natural

seawater buffered at seawater pH (=8) by using Cathodic Stripping Voltammetry (CSV, Metrohm VA 757) under clean laboratory conditions, using EPPS as pH buffer and organic ligands to avoid adsorption of the released Fe [Croot and Johansson, 2000; Duggen et al., 2007]. The seawater used for the experiments was retrieved during the Meteor cruise M68-3 in the eastern equatorial Atlantic, filtered with $0.2 \mu\text{m}$ membranes immediately after collection and stored in an acid-cleaned polyethylene carboy. Other containers used during the experiment were made of cleaned quartz glass or polytetrafluoroethylene. Dissolved Fe in oxic seawater precipitates quickly through oxidation of the soluble Fe (II) to less soluble Fe (III) [Millero and Sotolongo, 1989] and in order to keep Fe in solution, a thiazolyazo compound (TAC) was used as an Fe-binding ligand [Croot and Johansson, 2000]. Prior to the measurements, 20 ml of Atlantic seawater were mixed with $20 \mu\text{l}$ of 10 mM TAC ligand (2-(2-Thiazolyazo)-p-cresol) and 200 μl of 1M EPPS (4-(2-(hydroxyethyl) piperazine-1-propanesulfonic acid) solutions in a polyethylene cell cup. A known quantity of ash ($\sim 50 \text{ mg}$) was then added to the prepared seawater and measurements done every few minutes. The release of Fe from the Cape Verde dust sample was determined in the same way to allow direct comparison with the volcanic ash data. The experimental setup mimics the soluble Fe input from volcanic ash and mineral dust into seawater through dry deposition, which is considered the globally dominant deposition process for atmospheric particles [Jickells and Spokes, 2001].

[9] The major elemental compositions of glass shards and matrix glass of twenty SZVA and four HSVA samples were determined by electron microprobe analysis (EMPA, JEOL-JXA-8200). For the measurements, a $\sim 10 \text{ mg}$ subsample of pristine ash was sieved to $32–125 \mu\text{m}$ size using deionized (DI) water. The ash particles were mounted on a tray with resin, polished and analyzed with a beam current of 6 nA and a beam size of $5 \mu\text{m}$. Average glass compositions were inferred from ~ 25 individual measurements.

[10] The bulk Fe content of selected samples (twelve volcanic ash and one mineral dust sample) was analyzed by inductively coupled plasma-optical emission spectrometry (ICP-OES) with a Spectro Ciros SOP in the Geological Institute of Kiel University. Prior to ICP-OES analyses, 100 mg mill-homogenized dry subsamples were digested by a clean acid mixture of 1 ml HNO_3 , 3 ml HCl and 4 ml HF .

3. Results

[11] The in situ increase in dissolved Fe concentrations after addition of the ash/dust material into seawater was converted to Fe release in nanomoles per gram of ash or dust. As shown in Figure 2, between 35 to $340 \text{ nmol Fe/g ash}$ were released within the first 60 min of contact with seawater, with SZVA generally mobilizing more Fe ($40–340 \text{ nmol/g ash}$) than HSVA ($35–107 \text{ nmol/g ash}$; see Figures 2a and 2b). These results are in accordance with previous Fe dissolution experiments with SZVA and seawater ($10–100 \text{ nmol/g}$ [Duggen et al., 2007; Jones and Gislason, 2008]). Most of the ash samples displayed a similar pattern of Fe mobilization, with the highest rates occurring within the first 5–15 min. The Cape Verde mineral dust sample shows a similar Fe mobilization pattern, releasing about $20–30 \text{ nmol Fe/g}$

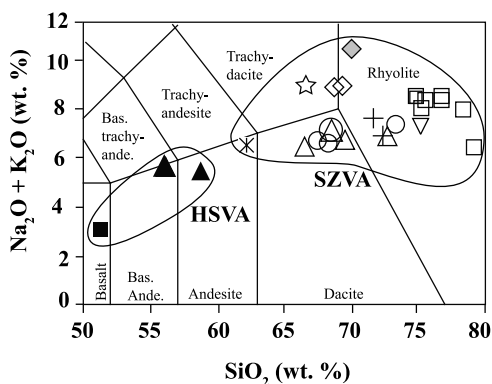


Figure 3. Total silica versus alkali diagram [Le Bas, 1984] used to classify volcanic ash samples based on the major element concentrations of glass shards, determined by electron microprobe.

dust (Figure 2c) and falls within the range of mineral dust Fe release data compiled from the literature (Table 4). The external precision of the measurements was calculated from repeat analysis of subsamples (Arenal'93 ($n = 2$): $\sim 2\%$ deviation, Sakura-jima'86 ($n = 2$): 44%, Sakura-jima'87 (3 samples): 54% ($\sigma = 47$); Cape Verde dust ($n = 3$): 24% ($\sigma = 7$)). The range in reproducibility most likely primarily results from heterogeneity of the samples (e.g., due to particle size distribution, lithic content). The data from the Fe solubility experiments are presented in Table S2.

[12] Based on the total alkali versus silica diagram in Figure 3, the glass compositions range from andesitic to rhyolitic (SZVA) and from basaltic to andesitic (HSVA). The Fe content of the volcanic glass shards ranges from 1 to 11 wt.%, with significantly lower values for SZVA compared to HSVA samples. The major element data of volcanic glass (expressed as element oxides in wt.%) are presented in Table S3.

[13] The total Fe content of the bulk volcanic ash samples range from 1.2 to 8.0 wt.% and deviates from the Fe content of the glass contained in the same sample (Table 1). The Fe content of the Cape Verde dust sample is 6.5 wt.% (Table 1),

which is in agreement with results from previous studies with the dust samples from Cape Verde (7.6 wt.%) [Desboeufs et al., 2001, 1999].

4. Discussion

4.1. Fe Solubility of Volcanic Ash: Dissolution Rates and Sources of Soluble Fe

[14] The timescale at which the soluble and thus potentially bioavailable Fe that is released from volcanic ash (Figure 2a) is similar to the timescale at which ash particles sink through the photic zone of the surface ocean: few minutes for coarse (2000–500 μm), to 1–2 h for intermediate (250–150 μm), and to 1–2 days for fine (<50 μm) ash particles (based on Stokes' law estimates [Duggen et al., 2007]). Shorter residence times of about 1–2 h may arise for aggregates of ash particles formed during the humid eruption conditions (e.g., ~ 1750 m/d for Pinatubo 1991 ash [Wiesner et al., 1995]). Volcanic ash is a mixture of various particles or components with <2 mm diameter that potentially may release Fe on contact with seawater and on different timescales, such as glass shards (quenched magma fragments), pyrogenic minerals (i.e., silicates and oxides), lithic particles (e.g., eroded rock material from the volcanic conduit of any origin) [Fisher and Schmincke, 1984; Óskarsson, 1981].

[15] The surface of the ash particles are coated by a thin layer of salts in the form of Fe sulfates and Fe halides that are formed through the interaction of ash particles with volcanic gases (S, HCl and HF) and aerosols in the eruption plume [Delmelle et al., 2007; Naughton et al., 1976; Óskarsson, 1980, 1981; Rose, 1977]. Although Fe content of these salts is still unknown, they are likely to be the most soluble components during seawater dissolution of ash particles [Duggen et al., 2007, 2010; Frogner et al., 2001; Jones and Gislason, 2008]. Volcanic glass shards on the other hand usually dominate the bulk composition and can have Fe contents ranging from <1 wt.% to well above 10 wt.% (e.g., Figure 4a; 1–5 wt.% for SZVA and 8–11 wt.% for HSVA). Fe content of pyrogenic minerals ranges from trace to major element level; from basically almost zero (e.g.,

Table 1. Fractional Fe Solubility (%) of Selected Volcanic Ash Samples and Cape Verde Dust^a

Sample Name	Fe Release Into Seawater (nmol/g Sample)	Total (Bulk) Fe Content (wt.%)	$\frac{\%Fe_S^{\text{bulk VA}}}{\%Fe_S^{\text{bulk dust}}}$ or	Glass Fe Content (wt.%)	$\%Fe_S^{\text{VA glass}}$
Sakura-Jima 1986	61	5.1	0.007	2.8	0.01
Sakura-Jima 1987	134	4.8	0.02	4.0	0.02
Sakura-Jima 1999	245	4.8	0.03	4.4	0.03
Sakura-Jima 2007	296	5.2	0.03	3.0	0.05
Arenal 1992	227	5.5	0.02	4.4	0.03
Arenal 1993	307	4.7	0.04	5.0	0.03
Arenal 2004	293	4.3	0.04	2.8	0.06
Popocatepetl 2000-1	230	3.7	0.03	1.6	0.08
Popocatepetl 2000-2	314	4.0	0.04	1.0	0.2
Rabaul 2002-1	278	4.6	0.03	2.8	0.06
Chaiten 2008	239	1.2	0.1	1.0	0.1
Hekla 1947	57	8.0	0.004	11.0	0.003
Cape Verde Dust	25	6.5	0.002	no glass	No glass

^aThe fractional Fe solubilities ($\%Fe_S$) are calculated from the Fe release and total Fe of the bulk samples ($\%Fe_S^{\text{bulk}}$) or volcanic glass shards contained in the ash samples ($\%Fe_S^{\text{VA glass}}$) (see auxiliary material). The calculations are based on the following equation: $\%Fe_S = (DFe/TFe) \times 100$; where DFe is the dissolved Fe ((Fe release nmol/g) \times (55.85 ng Fe/nmol Fe) \times (10^9 g/ng)), and TFe is the total Fe content of bulk ash, dust, and volcanic glass shards (Fe wt./100).

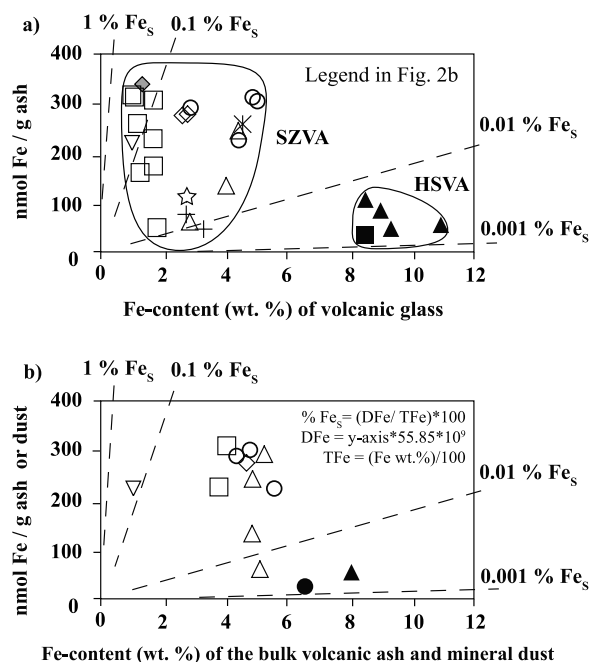


Figure 4. Diagrams display the (a) seawater Fe release of volcanic ash versus the Fe content of volcanic glass shards and (b) seawater Fe release of volcanic and mineral dust versus the total Fe content. Dashed lines show the hypothetical fractional Fe solubilities (%Fe_s) ranging from 0.001% to 1% (%Fe_s = (Dissolved Fe/Total Fe)*100).

plagioclase) through 10–30 wt.% FeO (e.g., clinopyroxene) to up to 50–70 wt.% (e.g., magnetite) [Nakagawa and Ohba, 2003].

[16] The relation between the total iron and the dissolved iron from volcanic ash is shown in Figure 4. As illustrated in Figure 4, no correlation exists between the Fe release (or Fe solubility) and the Fe content of the volcanic glass or bulk ash samples. Ash samples with lower glass Fe content (<6 wt.%) generally release more soluble Fe than the samples with higher Fe content (>8 wt.%) (Figure 4). Although the salt coatings make up less than 1% of the mass of the bulk sample the data, Figure 4a suggests that very rapid (minute-to-hour scale) release of Fe from ash is most likely dominated by swift dissolution of the surface salts rather than the glass shards, which is in accordance with what was argued in previous studies [Duggen *et al.*, 2007; Frogner *et al.*, 2001; Jones and Gislason, 2008]. A recent study with Etna volcanic ash suggests that initial alteration of glass shards and mineral particles may also partly contribute to rapid Fe release [Censi *et al.*, 2010]. On longer timescales (days through weeks to years), alteration of volcanic ash particles deposited as an ash layer at the seafloor is controlled by their bulk chemical composition and may significantly contribute to the surface ocean marine biogeochemical Fe cycle through upwelling.

[17] For the aerosol samples collected over the Pacific Ocean a trend of increasing Fe solubility with decreasing Fe content was reported [Zhuang *et al.*, 1992] similar to what is found for volcanic ash (Figure 4). This trend can be linked to the low Fe contents (or low abundances) of the relatively more dissolvable Fe components. Due to their high Fe con-

tents iron (hydro)-oxides (e.g., hematite, magnetite 60–80 wt.% Fe) are commonly assumed to be the major sources of iron into the surface ocean [Mahowald *et al.*, 2009]. However, it has recently been found that clay minerals are much more soluble although they contain relatively less Fe (<3%–20% Fe) [Journet *et al.*, 2008]. The lack of a correlation between total Fe and the dissolved Fe thus demonstrates that the seawater Fe solubilities of volcanic ash or mineral dust cannot be inferred from the total Fe content but has to be determined directly. Either total iron or the dissolved fraction is not constant rather changing progressively during the long-range transport in the atmosphere. Particle size distribution [Baker and Jickells, 2006], mineral composition (aeolian fractionation [Duggen *et al.*, 2010]), and the particle-surface chemistry (chemical and photochemical atmospheric processes [Duggen *et al.*, 2010; Jickells and Spokes, 2001; Spokes and Jickells, 1996]) may enhance the solubility and bioavailability of Fe in the oceans.

[18] Sample storage is another factor that possibly may affect the Fe mobilization behavior in laboratory experiments. The soluble Fe salts on volcanic ash particles are likely to be unstable and may be affected by storage duration of the sample. Based on the reanalysis of a single ash sample, Jones and Gislason [2008] argued that aging of ash material during storage might reduce the Fe release. As inferred from our new data in Figure 5, ash samples stored for more than 10–20 years tend to release less Fe on contact with seawater than younger samples. Five ash samples from Sakura-jima volcano even display a negative correlation between their age and the amount of Fe mobilized. If considered an aging effect, the Sakura-jima ash samples point to a decrease in rapid Fe release of about 200 nmol Fe/g ash over the course of 25 years. The data therefore suggest that Fe release data inferred from volcanic ash several or more years old are generally minimum estimates and that data from younger samples is more reliable.

[19] From the larger data set available it can now be inferred (by taking into account the possible aging effect and uncertainties indicated by repeat measurements) that volcanic ash samples generally release between 35 and 340 nmol Fe/g ash, with a mean of about 200 ± 50 nmol Fe/g for SZVA and possibly around 70 nmol Fe/g for HSVA (Figures 2 and 5) during dry deposition into the surface ocean. The percental (or fractional) Fe solubilities (as commonly used for mineral dust) are calculated in order to allow comparison with the previous aerosol Fe solubility studies. The calculations are based on the Fe release data and the total Fe content of the samples as follows: %Fe_s = (Dissolved Fe/Total Fe)*100 (Table 1). Accordingly, the Fe solubility for volcanic ash (VA) ranges from 0.007% to 0.1% (%Fe_s^{bulk VA}, using the bulk sample data) and from 0.003% to 0.2% ((%Fe_s^{VA glass}, using the glass data) (Table 1). Since the composition of volcanic ash progressively approaches the composition of the glass shards contained during aeolian fractionation (see Duggen *et al.* [2010] for details), the overall %Fe_s^{VA} can be constrained to 0.003% to 0.2% (Table 4). As the SZVA samples stem from different volcanoes worldwide (Figure 1), the 200 ± 50 nmol Fe/g (0.01%–0.02% Fe_s) value is likely to be representative on a global scale (e.g., dry deposition estimate for global models), and, above all, appears to be largely independent of the bulk composition of the ash samples (Figure 4).

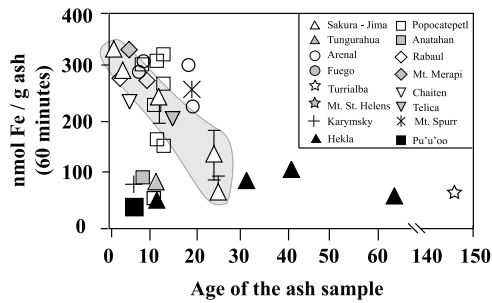


Figure 5. Graph showing the possible influence of storage time on the Fe mobilization behavior of volcanic ash samples. The gray field denotes the correlation between age and Fe release for ash samples from Sakura-jima volcano.

[20] For the Cape Verdian mineral dust sample, the calculated Fe solubility is 0.002% (Table 1). This is in agreement with Fe solubilities reported for other experiments performed at seawater pH (=8) ranging from 0.001% to 0.02% (Table 4) (e.g., 0.001%–0.02% [Guieu and Thomas, 1996] and <0.013% [Spokes and Jickells, 1996]). The strong dependency of Fe solubilities on the experimental setup with different starting materials and different solutions (e.g., aerosol versus soil samples, pH 4 versus pH 8 solutions) is discussed in section 4.4.

4.2. Regional Impact of Major Volcanic Eruptions on Surface Ocean Fe Concentrations

[21] For a case study of the regional impact a single major eruption we chose a well-constructed historical eruption of Barva volcano in the Central American subduction zone (Figure 6). The Barva eruption deposited at least 7.9×10^{16} g of ash that traveled at least 1000 km distance into the eastern

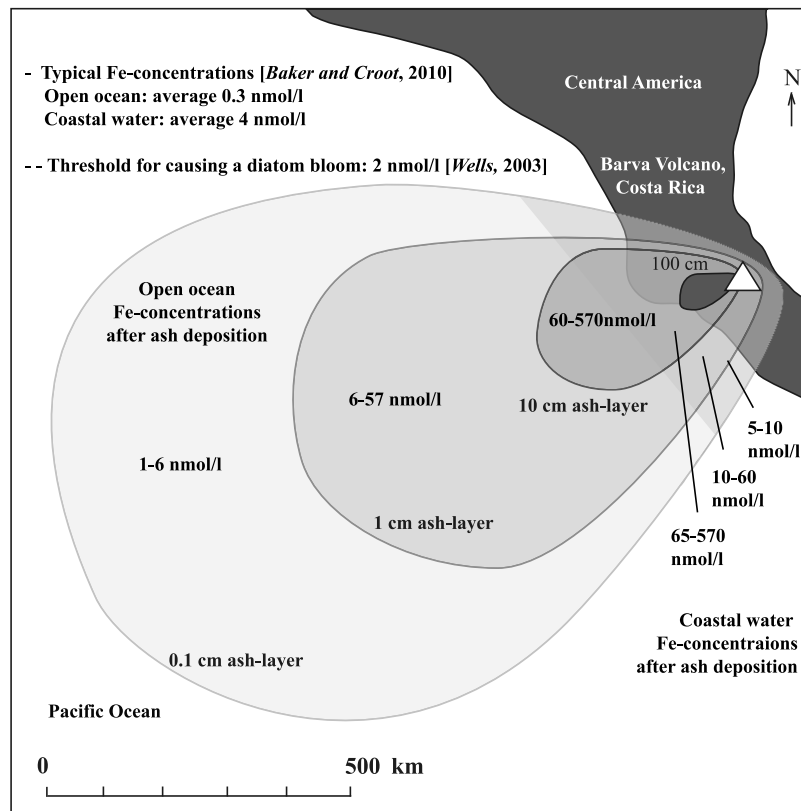


Figure 6. Map showing the extent and particle load in an ash fallout area during a large-scale volcanic eruption, exemplified by the historical Barva eruption (~322,000 years ago) in Costa Rica. Isopachs (ash thickness contours) were mapped on the basis of marine sediment core data [Kutterolf *et al.*, 2008]. Fe concentrations (nmol/L) between the isopachs display the surface ocean Fe levels (100 m mixed layer depth) with ash loads decreasing with increasing distance from the volcano. The Fe levels were inferred from adding the calculated increase in dissolved Fe that is associated with an ash layer of a given thickness (using an average ash density of 2400 kg/m^3 at 30% porosity over 1 dm^2 surface area) to the background seawater Fe levels in coastal waters (typically 4 nmol/L) and the open ocean (typically 0.3 nmol/L) [Baker and Croot, 2010; De Baar and De Jong, 2001; Parekh *et al.*, 2005]. The range of Fe concentrations originates from the variations in Fe release of volcanic ash (35–340 nmol/g ash, Figure 2). As an example, the maximum increase in Fe concentrations in the open ocean during the deposition of 1 mm ash layer was calculated as follows: $[0.3 \text{ nmol/L}] + [((2400 \text{ g/dm}^3 - (2400 \text{ g/dm}^3 \times 0.3)) \times (1 \text{ dm}^2 \times 0.01 \text{ dm}) \times (340 \text{ nmol Fe/g ash}) / (1000 \text{ dm} \times 1 \text{ dm}^2))] = 6 \text{ nmol}$.

equatorial Pacific Ocean [Kutterolf *et al.*, 2008]. Sediment core data allowed the reconstruction of the distribution of the ash layer as well as the thickness that decreases from coast (up to 100 cm thick) to the remote ocean (<1 mm thick) (Figure 6). Assuming an ash density of 2400 kg/m³ at 30% porosity, ash layer thicknesses of 10 cm, 1 cm and 0.1 cm are recalculated to ash loads of ~170 kg/m², ~17 kg/m² ~1.7 kg/m², respectively.

[22] Volcanic ash fallout impact the surface ocean Fe concentrations depending on the initial seawater Fe concentrations prior to ash deposition, the Fe mobilization behavior of volcanic ash, ash load (ash-to-seawater ratio), the mixed layer depth, and the maximum concentration solubility of iron in seawater [Baker and Croot, 2010; Duggen *et al.*, 2010]. In coastal waters, due to higher riverine and continental input, the surface ocean dissolved Fe levels are relatively high and range from 1 to 100 nmol/L with typical concentrations between 8 and 10 nmol/L [Baker and Croot, 2010; Boyd *et al.*, 2007, 2000; Coale *et al.*, 2004; De Baar and De Jong, 2001; Liu and Millero, 2002]. Due to high background levels Fe is generally not limiting phytoplankton growth in coastal waters, although exceptions such as the California upwelling region have been reported [Hutchins and Bruland, 1998]. Assuming an initial Fe concentration of about 4 nmol/L in coastal seawater, deposition of a 0.1 cm, 1 cm and 10 cm ash layer with the range in Fe mobilization (shown in Figure 2; 35–340 nmol Fe/g ash) could raise the dissolved Fe concentrations to about 5–10 nmol/L, 10–60 nmol/L, and 65–570 nmol/L, respectively (Figure 6). The inferred values are in accordance with strongly enhanced Fe levels determined in Mediterranean seawater (~600–700 nmol/L) close to Sicily within the ash fallout area of the 2001 eruption of Etna volcano [Censi *et al.*, 2010].

[23] High particle loadings in the close vicinity of a volcanic source may cause increased Fe scavenging of the particles (as seen in the mineral dust deposition [Baker and Croot, 2010; Guieu *et al.*, 1997; Spokes and Jickells, 1996]) but the distinction of the release versus scavenging is hard to determine. The excess concentrations of dissolved Fe that are above the typical maximum Fe solubility in coastal areas (8–10 nmol/L) would most likely include a large colloidal phase, which is also potentially bioavailable and important to the overall Fe cycling. High Fe levels of several tenths to hundreds nmol/L as observed during the 2001 Etna eruption were argued to be linked to enhanced organic complexation, resulting from lysis of phytoplankton cells during a phytoplankton bloom associated with volcanic ash fallout [Censi *et al.*, 2010]. The short residence time of Fe of about 2–3 months in the surface ocean, however, may limit the biogeochemical impact of volcanic eruptions.

[24] In the surface open ocean, Fe concentrations are extremely low (0.02–0.8 nmol/L) (Figure 7a) thereby limiting phytoplankton growth in HNLC areas [De Baar and De Jong, 2001; Parekh *et al.*, 2005]. Assuming an initial Fe concentration for the upper ocean of about 0.3 nmol/L, deposition of a 0.1 cm, 1 cm and 10 cm ash layer could increase Fe levels to about 1–6 nmol/L (at 1000 km distance from the volcano), 6–57 nmol/L (up to 500 km away), and 60–570 nmol/L (up to 250 km from the volcano), respectively (Figure 6). Mesoscale Fe fertilization experiments show that an increase of Fe levels by only 2 nmol/L can

stimulate massive diatom blooms in Fe-limited oceanic regions [Wells, 2003]. Therefore, even relatively low ash loads corresponding to millimeter-scale ash layers may be sufficient to cause a vigorous MPP response. Based on satellite data a recent study demonstrated a causal connection between the 2008 Kasatochi eruption in the Aleutians and a large scale (~3500 km by 1500 km), about 2–3 months lasting phytoplankton bloom in the subarctic North Pacific [Hamme *et al.*, 2010; Langmann *et al.*, 2010].

4.3. Flux of Volcanic Ash and Mineral Dust Into Pacific Ocean: Millennial-Scale Deposition Rates

[25] The flux of Fe into the Pacific Ocean can be constrained by combining Fe release with geological flux data. Although most of the explosive active volcanoes on Earth are located around the Pacific Ocean that hosts about 70% of the Fe-limited oceanic regions (Figure 7a), an estimate of the airborne volcanic ash input into the Pacific Ocean is so far not available in the literature. Below we therefore constrain the input of airborne volcanic ash into the Pacific, followed by an estimate of the volcanic ash soluble Fe flux, which is then compared with the Fe flux associated with Pacific mineral dust deposition.

[26] The volcanic ash flux into the Pacific Ocean can be considered constant and quasi-continuous over geological timescales, such as the past several 100 ka [Straub and Schmincke, 1998], and millennial mineral dust deposition can be considered largely constant after the last glaciation [Jickells and Spokes, 2001]. A meaningful way to compare the fluxes of volcanic ash and mineral dust, despite the differences in episodicity/seasonality of deposition, is therefore to recalculate mass and hence Fe fluxes to a postglacial millennial base. Being aware of the uncertainties and limitations of such global-scale estimates, the main goal is to constrain the order of magnitude of Fe release from volcanic ash compared to that of mineral dust, which will be useful to further improve our understanding of the potential role of volcanic ash deposition for the surface Pacific Ocean biogeochemical Fe cycle.

4.3.1. Volcanic Ash Flux Into the Pacific Ocean: Millennial-Scale Estimates

[27] Due to their different nature in eruption style two different approaches are advanced for estimating the fluxes of SZVA and HSVA: (1) an arc-length-based approach for subduction zone (SZ) volcanoes and (2) an apron-based approach for hot spot volcanoes (HS). In both cases we first estimate the amount of ash emitted from Pacific volcanoes and then the fraction that was deposited offshore into the Pacific Ocean. The flux estimates are briefly summarized below and outlined in more detail in Tables 2 and 3.

4.3.1.1. Subduction Zone Volcanic Ash Flux: Arc-Length-Based Approach

[28] Large (strato-)volcanoes, which are the sites of intermediate to major explosive volcanic eruptions, are generally found at nearly constant distances of about 60–100 km apart from each other. Therefore, the length of a subduction zone segment (arc) can be considered proportional to its potential volcanic intensity and thus emitted material flux [Sigurdsson *et al.*, 2000]. The inferred ash flux per millennia and kilometer arc length of any active subduction zone can thus, as a first-order approximation, be applied to any other subduction zone segment in the Pacific.

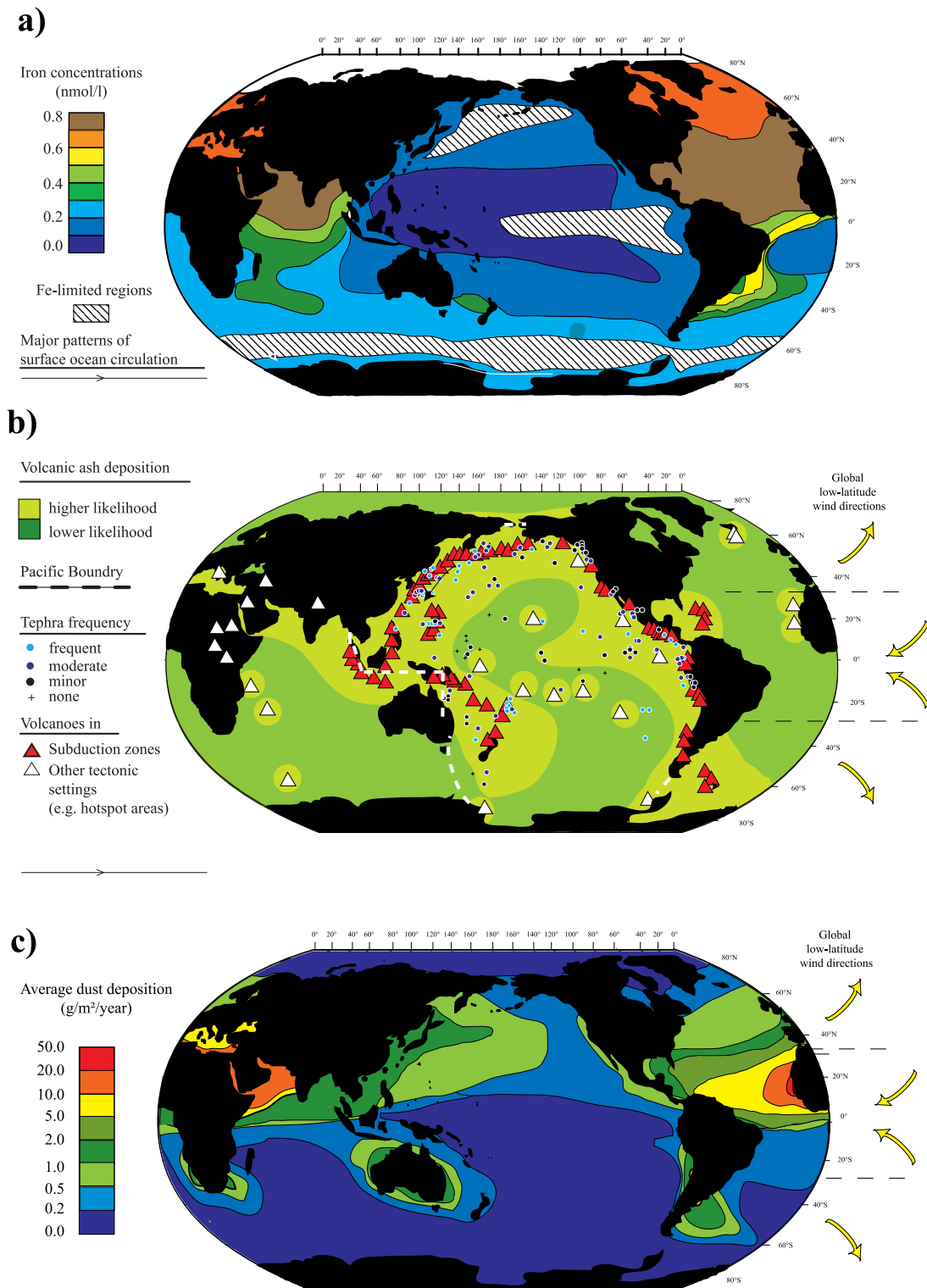


Figure 7. (a) Average surface ocean iron concentrations based on the work of *Parekh et al.* [2005]. High-Nutrient Low-Chlorophyll (HNLC) regions are defined by comparison of the seasonally averaged surface nitrate and silica concentrations [*Watson*, 2001] and annual averaged chlorophyll concentrations (SeaWiFS). (b) Areas of higher versus lower likelihood of volcanic ash deposition, the extent of which are roughly estimated on the basis of the location of historically active volcanoes, low-altitude wind directions, and tephra frequencies in marine sediment drill cores in the Quaternary [*Straub and Schmincke*, 1998]. (c) Averaged annual mineral dust fluxes into the world ocean. Percentage inputs are as follows: North Pacific, 15%; South Pacific, 6%; Southern Ocean, 6%; North Atlantic, 43%; South Atlantic, 4%, and Indian Ocean, 25% [*Jickells et al.*, 2005].

Table 2. Millennial Volcanic Ash Input From Subduction Zone Volcanoes Into the Pacific Ocean

Subduction Zone Volcanic Arcs	Arc Length (km)	Volcanic Ash Emission (10^{15} g/ka) ^a		Offshore Fraction of Emitted Volcanic Ash (%) ^b	Offshore Deposited Volcanic Ash Into the Pacific Ocean (10^{15} g/ka) ^c	
		Min	Max		Min	Max
New Zealand–Tonga–Kermadec	2500	20.0	26.0	85 ± 5	16.0	23.4
Fiji Islands	340	2.7	3.5	85 ± 5	2.2	3.2
New Hebrides	1450	11.6	15.1	85 ± 5	9.3	13.6
Solomon Islands	390	3.1	4.1	85 ± 5	2.5	3.7
New Britain	1000	8.0	10.4	85 ± 5	6.4	9.4
Papua New Guinea	950	7.6	9.9	20 ± 10	0.8	3.0
Indonesia	4700	37.6	48.9	20 ± 10	3.8	14.7
Philippines	1610	12.9	16.8	60 ± 10	6.4	11.7
Ryuku Islands	1210	9.7	12.6	60 ± 10	4.8	8.8
Mariana	1500	12.0	15.6	85 ± 5	9.6	14.1
Izu–Bonin	1100	8.8	11.5	85 ± 5	7.0	10.3
Japan	1400	11.2	14.6	85 ± 5	9.0	13.1
Kuril Islands	1350	10.8	14.1	85 ± 5	8.6	12.6
Kamchatka	1000	8.0	10.4	85 ± 5	6.4	9.4
Aleutians	1900	15.2	19.8	85 ± 5	12.2	17.8
Alaska	800	6.4	8.3	40 ± 10	1.9	4.2
North Canadian Cascades	450	3.6	4.7	20 ± 10	0.4	1.4
High Cascades	1300	10.4	13.5	20 ± 10	1.0	4.1
Mexico	970	7.8	10.1	40 ± 10	2.3	5.0
Central America	1100	8.8 ^d	11.5 ^e	80 ± 10 ^f	6.2	10.3
South America (North)	550	4.4	5.7	80 ± 10	3.1	5.2
South America (Central)	960	7.7	10.0	80 ± 10	5.4	9.0
South America (South)	1300	10.4	13.5	20 ± 10	1.0	4.1
Subduction zone total	29830	239	311	64 ± 8	126	212

^aCalculated by multiplying maximum and minimum ash emissions (see footnotes d and e).

^bEstimated on the basis of the general wind directions and proximity of volcanoes to the ocean (see section 4.3.1.1 for explanation).

^cCalculated by multiplying the result found in footnote a by the estimate from footnote b.

^dMinimum ash emission from Central American Volcanic Arc (CAVA) over the past 191 ka, calculated on the basis of the work of *Kutterolf et al.* [2008]. The minimum rate of volcanic ash emission per kilometer arc corresponds to 8.0×10^{12} g/ka/km.

^eMaximum ash emission from CAVA per millennia, estimated by adding the dispersed ash fraction of 30% [*Scudder et al.*, 2009]. The maximum rate of volcanic ash emission per kilometer arc corresponds to 10.4×10^{12} g/ka/km.

^fEstimated by comparison of proximal and distal ash volumes produced from Central American Arc (see section 4.3.1.1 for explanation).

[29] As a basis for our flux estimates we use the Central American Volcanic Arc (CAVA), which is among the most well-studied subduction zone segments in the Pacific Ring of Fire, with data for offshore deposited ash available for the past 191 ka. Volume estimates of CAVA ash deposits were obtained by fitting straight lines to data on plots of ln isopach thickness versus square root isopach area (e.g., Figure 6) [*Fierstein and Nathenson*, 1992; *Kutterolf et al.*, 2008; *Pyle*, 1989]. It is important to note that the ash volume estimates inferred from discrete ash layers do not account for the dispersed ash, as this fraction is not visible due to mixing with nonvolcanic sediments (e.g., due to bioturbation). The missing dispersed ash fraction corresponds to ~6% to 60% and on average for ~30% of the total erupted mass [*Peters et al.*, 2000; *Rose and Durant*, 2009; *Scudder et al.*, 2009; *Straub and Schmincke*, 1998]. Hence the ash emission rate from CAVA is likely to be underestimated by about 30%.

[30] According to ash thickness contour (isopach) maps inferred from marine drill core data (e.g., Figure 6), about 1139 km^3 of ash was emitted from the 1100 km long CAVA during the past 191 ka (Table S4) [*Kutterolf et al.*, 2008]. By converting volume to mass, this corresponds to about 1680 Pg ($\text{Pg} = \text{petagrams} = 10^{15}$ grams) of ash for the past 191 ka (using dense rock equivalent densities of 1680 kg/m^3 for mafic and 1470 kg/m^3 for felsic tephra [*Kutterolf et al.*,

2008]). The ash emission rate per millennium can then be calculated to 8.8 Pg/ka and to a rate per kilometer arc of 8.0 Tg/ka/km ($\text{Tg} = \text{teragrams} = 10^{12}$ grams) (Table 2). Taking into account the dispersed ash fraction (+30%), we infer an ash emission rate of between 8.0 and 10.4 Tg/ka/km for CAVA (Table 2). Assuming that the millennial ash emission rate (per kilometer arc length) is largely the same for all Pacific subduction zone segments, the total emission of all Pacific arcs can be inferred from multiplying the CAVA ash emission rate (of 8.0– 10.4 Tg/ka/km) with the known lengths of individual arcs (Table 2). The millennial ash emission for Pacific SZ volcanoes is thus estimated to be on the order of 239–311 Pg/ka (Table 2).

[31] Only a part of the emitted ash is deposited over the ocean. In the case of the well-characterized CAVA, proximal and distal sections of ash layers are found both onshore and offshore (e.g., Figure 6) (Table S4). Based on the interception of proximal and distal facies (at ~20–10 cm ash layer thickness [see *Kutterolf et al.*, 2008]) it can be estimated that about 50% (220 Pg) of the proximal and about 90% (1120 Pg) of the distal ash was deposited into the Pacific Ocean over the past 191 ka (Table S4), which corresponds to about $80\% \pm 10\%$ of the ash emitted from the CAVA (6.2– 10.3 Pg/ka). The result is consistent with the location of Central American volcanoes within trade wind

zone and with the frequency of ash layers in marine drill cores offshore Central America (Figure 7b).

[32] For other SZ segments along the Pacific Ring of Fire, the proportion of offshore deposited ash was estimated by taking into account: (1) the general wind directions (e.g., westerlies, trade winds), (2) the overall distance of the volcanoes from the ocean (Figure 7b), and (3) the constraints for onshore and offshore deposition of CAVA ash (Table 1). For example, in the eastern Pacific, ash from SZ volcanoes located in the trade wind area ($\sim 30^{\circ}\text{N}$ to 30°S) is mostly deposited offshore (e.g., $80\% \pm 10\%$ for the northern section of the South American Arc; see Table 2 and Figure 7b), whereas ash from volcanoes situated in the westerlies ($>30^{\circ}\text{N}$ and $>30^{\circ}\text{S}$) is dominantly deposited on land (e.g., only $20\% \pm 10\%$ deposited offshore for the High Cascades; see Table 2 and Figure 7b). The distance of volcanoes from the ocean is generally larger in the eastern Pacific as these are mainly found at continental margins, whereas SZ volcanoes in the western Pacific often form ocean island arcs (Figure 7b). The proportion of the ash deposited offshore thus tends to be higher for island arcs volcanoes, compared to those located at continental margins (e.g., $85\% \pm 5\%$ for Mariana Islands in the western Pacific; see Table 2). We also take into account the boundary of the Pacific Ocean (Figure 7b). The ash from Indonesian volcanoes located in the trade wind zone, for example, is mainly transported into the Indian Ocean rather than into the Pacific Ocean (only $20\% \pm 10\%$ into the Pacific although $80\% \pm 10\%$ is deposited offshore; see Table 2). Together, we infer a SZVA flux into the Pacific Ocean in the range of 126–212 Pg/ka, which takes into account uncertainties arising from the CAVA ash flux estimate, arc lengths and wind directions (Table 2).

4.3.1.2. Hot Spot Oceanic Island Volcanic Ash Flux: Apron-Based Approach

[33] The data basis from scientific ocean drilling is generally insufficient to construct isopach maps of offshore ash layers related to Pacific HS volcanic ocean islands (Figure 7b). In an apron-based approach, two end-member ocean island settings are distinguished: (1) caldera-forming and (2) non-caldera-forming hot spot systems (Table 3). Caldera-forming ocean islands (e.g., Hawaii) potentially create more explosive volcanic eruptions compared to non-caldera-forming ocean islands (e.g., Samoa, Marquesas) [Lipman, 2000] (Figure 7b), for which volcanic apron production rates data are provided by the literature: 230,000 km³ over the past 5.5 my for caldera-forming Hawaii and 10,000 km³ over the past 5.0 my for non-caldera-forming Samoa [Duncan and Clague, 1985; Lonsdale, 1975; Rees et al., 1993; Straub and Schmincke, 1998]. These values suggest apron production rates of 42 km³/ka for caldera-forming and 10 km³/ka for non-caldera-forming ocean islands (Table 3).

[34] Volcanic aprons not only consist of volcanoclastic rocks (e.g., ash, pumice, hyaloclastites) but also of hardrock formed from lava flows etc. [Rees et al., 1993; Schmincke and Sumita, 1998]. The volcanoclastic-to-hardrock ratio is estimated to be about 1:3 (e.g., Hawaii [Wolfe et al., 1994]). Applying this ratio to the apron production rates inferred above and by converting volume to mass using dense rock equivalents of 1680 kg/m³ for mafic tephra (2400 kg/m³ at 30% porosity), the volcanoclastic emission rates of hot spot-

related ocean islands can be calculated to range from 5.7 Pg/ka to 23.7 Pg/ka (Table 3).

[35] Based on the offshore extent and the thickness of ash layers found in Deep Sea Drilling Project (DSDP) cores related to hot spot volcanism [Kelts and McKenzie, 1976; Viereck et al., 1985], the proportion of offshore ash compared to total volcanoclastics is estimated to range from 1% to 5%. The offshore ash deposition rates for individual HS oceanic islands are thus calculated to vary between 0.1 Pg/ka to 2.0 Pg/ka (Table 3). Taking into account whether a hot spot-related ocean island is caldera-forming or non-caldera-forming, the offshore ash deposition rate for Pacific oceanic islands is estimated to be between 2.0 Pg/ka and 9.0 Pg/ka (Table 3), which corresponds to <3% of the apron production rates of HS ocean islands. The HS offshore volcanic ash deposition rate is thus significantly lower than that of SZ volcanoes where in general more large-scale explosive eruptions occur (Table 2).

4.3.1.3. Overall Volcanic Ash Flux Into Pacific Ocean

[36] The Pacific millennial ash input from SZ and HS volcanoes through subaerial eruptions is estimated to range from 128 to 221×10^{15} g/ka (Table 4), more than 90% of which is derived from SZ volcanoes (Tables 2 and 3). Despite the uncertainties involved in such geological flux estimates (e.g., the CAVA ash flux, wind directions, arc lengths etc.) that may easily introduce a factor 2 error we argue that the ash flux estimate provided here serves well as a first-order approximation. For comparison, our millennial flux estimate for the Pacific Ocean is 15–20 times lower than the amount of material ejected from the large Pinatubo eruption (~ 8.1 Pg [Wiesner et al., 1995]). Within a week, a single volcanic eruption can deposit similar amounts ash (e.g., Kasatochi 2008 eruption, at least 650×10^{12} g ash [Langmann et al., 2010]) to the yearly input of volcanic ash into Pacific Ocean ($128\text{--}221 \times 10^{12}$ g/yr based on short-term averaged millennial deposition rates). Therefore, the millennial-scale estimates in Tables 2 and 3 are realistic and rather conservative. The largest uncertainty of our estimate, however, is that it does not consider rare supereruptions that occur with a frequency of $\geq 10,000$ years such as the Toba eruption in Sumatra ~ 74 ka ago that produced about 2000×10^{15} g of ash, much of which was deposited into the ocean [Oppenheimer, 2002].

4.3.2. Mineral Dust Input Into the Pacific Ocean: Millennial-Scale Flux

[37] About half of the global surface ocean dust flux is deposited into the northwest Pacific Ocean and stems from Asian deserts (Figure 7c) [Jickells et al., 2005; Jickells and Spokes, 2001]. Modeling of extrapolated aerosol dust concentrations (from island and coastal collection sites) suggests an annual dust deposition rate of $39\text{--}519 \times 10^{12}$ g/y for the Pacific Ocean [Mahowald et al., 2005]. During the last glaciation the dust input was probably 2–20 times higher than during the more humid (and more vegetated) interglacial periods [Kohfeld and Harrison, 2001; Mahowald et al., 1999; Martin et al., 1990; Winckler et al., 2008]. The post-glacial global pattern of dust deposition most likely did not change significantly [Jickells and Spokes, 2001]. Therefore, assuming a constant annual dust deposition rate in the Holocene, the annual dust deposition rate inferred from modeling [Mahowald et al., 2005] corresponds to a millennial

Table 3. Millennial Volcanic Ash Input From Hot Spot Volcanoes Into the Pacific Ocean

Hot Spot Oceanic Islands	Volcaniclastic Production Rate (10^{15} g/ka) ^a	Offshore Deposited Volcanic Ash Into the Pacific Ocean (10^{15} g/ka) ^b	
		Minimum	Maximum
Hawaii (caldera-forming)	23.7	0.4	2.0
Revillagigedos	5.7	0.1	0.5
Marquesas	5.7	0.1	0.5
Gambier	5.7	0.1	0.5
Society	5.7	0.1	0.5
Austral-Cook	5.7	0.1	0.5
Caroline	5.7	0.1	0.5
Easter hot spot	5.7	0.1	0.5
Galapagos (caldera-forming)	23.7	0.4	2.0
Samoa (non-caldera-forming)	5.7	0.1	0.5
Line Island	5.7	0.1	0.5
Marshall-Gilbert Island	5.7	0.1	0.5
Hot spot total	104	2	9

^aVolcaniclastic emission rates estimated on the basis of apron production rates of Hawaii ($42 \text{ km}^3/\text{ka}$ over 5.5 myr) and Samoa ($10 \text{ km}^3/\text{ka}$ over 5 myr), and applying the ratio between volcaniclastic to the hardrock (1/3) (see section 4.3.1.2 for explanation) [Straub and Schmincke, 1998; Wolfe et al., 1994]. Volumes were converted to masses based on an average mafic ash density of 2400 kg/m^3 at 30% porosity (1680 kg/m^3).

^bFraction of offshore ash compared to emitted volcaniclastics is estimated to range between 1%–5% [Kelts and McKenzie, 1976; Viereck et al., 1985].

dust flux rate of $39\text{--}519 \times 10^{15} \text{ g/ka}$. Based on ocean sediment core data, however, the postglacial dust input is estimated to be 4–5 times lower than the modeling estimates [Rea, 1994], possibly due to a less anthropogenic input before the past 1000 years.

4.4. Significance of Volcanic Ash-Related Fe Input Into the Pacific Ocean: Biogeochemical Implications, Eruption Frequencies, and Spatial Distributions

[38] The millennial flux of airborne volcanic ash into the Pacific Ocean ($128\text{--}221 \times 10^{15} \text{ g/ka}$) is comparable to that of mineral dust ($39\text{--}519 \times 10^{15} \text{ g/ka}$ [Mahowald et al., 2009]) or $50\text{--}115 \times 10^{15} \text{ g/ka}$ if corrected to sediment core observations [Rea, 1994] (see Table 4). From the similarity in both material flux and Fe solubilities in seawater at pH = 8 (Table 4) it follows that the flux of soluble Fe through dry deposition of volcanic ash into the Pacific Ocean is comparable to that of mineral dust ($3\text{--}75 \times 10^9 \text{ mol Fe/ka}$ for volcanic ash and $1\text{--}65 \times 10^9 \text{ mol Fe/ka}$ for mineral dust). These estimates do not consider the effect of wet deposition (by rainwater) that, based on experimental results, would greatly enhance the Fe solubility of both volcanic ash and mineral dust as shown in Table 4 (see discussion in section 4.1) [Baker and Croot, 2010; Duggen et al., 2010; Mahowald et al., 1999]. The ratio of wet to dry deposition may, however, vary from region to region but on a global-scale dry deposition dominates. As outlined by Jickells and Spokes [2001] for the Pacific Ocean, about 70% of the atmospheric particles are derived through dry deposition.

[39] Focusing on the dry deposition process, for mineral dust an overall range of 0.001%–0.02% Fe_S is derived based on the experiments (including this study) providing constraints for the solubility of Fe under seawater conditions (e.g., constant pH of 8) (Table 4). Previously, a value of 0.01% Fe_S was chosen for the dry deposition of Fe into the Saragossa Sea [Jickells, 1999], which is in accordance with the range outlined in Table 4. Results for Fe solubilities inferred from experiments at highly variable pH vary 3–4 orders of magnitude: 0.001%–22% for volcanic ash and 0.001%–80% for mineral dust (Table 4 and, for comparison with the new data, see the dashed lines in Figure 4) [Baker and Croot, 2010; Duggen et al., 2010; Frogner et al., 2001; Jones

Table 4. Summary of the Fe Mobilization Behavior of Volcanic Ash and Mineral Dust in Different Experimental Setups With Variable pH and the Input of Soluble Fe Based on the Millennial Fluxes of Volcanic and Mineral Dust

	Volcanic Ash		Mineral Dust	
	nmol/g Ash	% Fe_S^{VA}	nmol/g Dust	% $\text{Fe}_S^{\text{dust}}$
<i>Fe Release (nmol Fe/g or % Fe_S)</i>				
At seawater pH (8)	35–340 ^a	0.003–0.2 ^a	<10–125 ^{b,c}	0.001–0.02 ^b
In seawater without pH buffer	10–39,000 ^d	0.001–1.8 ^{c,d}	1,600–165,000 ^{c,e}	0.26–26 ^e
in acidic solutions (pH 1–5)	20–200,00 ^f	0.001–22 ^{c,f}	60–500,000 ^{c,g}	0.01–80 ^g
Millennial particle flux into the Pacific Ocean (10^{15} g/ka)	128–221 ^h		39–519 ⁱ	
<i>Soluble Fe Flux Into the Pacific Ocean^j (10^9 mol/ka)</i>				
At seawater pH (8)	3–75		1–65	
In seawater without pH buffer	2–8,600		65–85,000	
In acidic solutions (pH 1–5)	2–44,000		2–260,000	

^aValues as follows: 20–70 nmol/g ash [Duggen et al., 2007]; and 35–340 nmol/g ash (Figures 2a and 2b) (present study (0.003%–0.2% Fe_S^{VA} ; Table 1)).

^bValues as follows: 0.001%–0.02% $\text{Fe}_S^{\text{dust}}$ [Guiou and Thomas, 1996]; <0.013% $\text{Fe}_S^{\text{dust}}$ [Spokes and Jickells, 1996]; and 20–30 nmol/g ash (Figure 2c) (present study (0.002% $\text{Fe}_S^{\text{dust}}$; Table 1)).

^cValues recalculated from Fe release in “nmol Fe/g” to “% Fe_S ” (fractional Fe solubility) and vice versa. Bulk Fe contents are 5% for SZVA, 12% for HSVA, and 3.5% for mineral dust.

^dValues as follows: 10–10,900 nmol/g ash [Jones and Gislason, 2008]; and 39,000 nmol/g ash [Frogner et al., 2001].

^eBuck et al. [2006] and Wu et al. [2007].

^fDuggen et al. [2010, and references therein].

^gBaker and Croot [2010], Mahowald et al. [2009], and references therein.

^hThis study; estimations based on the drill core data (see section 4.3 and Tables 2 and 3).

ⁱDerived from long-term averaged modern deposition rates [Mahowald et al., 2005] (see section 4.3.2 for discussion).

^jCalculated by multiplying the millennial particle fluxes (g/ka) with the Fe release per gram of ash and dust (nmol Fe/g ash or dust).

and Gislason, 2008; Mahowald et al., 2005; Schroth et al., 2009]. Table 4 emphasizes that major uncertainties in estimating Fe flux arise from the strong pH dependency of Fe solubility. Experimental studies demonstrate this with highest Fe solubilities under low pH with minimum Fe solubilities around pH 8 [Desboeufs et al., 1999; Guieu and Thomas, 1996; Spokes and Jickells, 1996]. Since results from experiments with acidic solutions are very likely to overestimate the dissolution of Fe in seawater [Baker et al., 2006], our Fe flux estimates for both volcanic ash and mineral dust were performed with data from experiments at seawater pH of 8.

[40] Volcanic ash and mineral dust particles can serve as cloud condensation nuclei (CCN) [Andreae and Rosenfeld, 2008; Duggen et al., 2010; Jickells and Spokes, 2001; Textor et al., 2006]. Therefore the particles that were transported long distances through the atmosphere may have been affected by interaction with low-pH cloud water prior to dry deposition (soil versus marine aerosol [Zhuang et al., 1992]). The volcanic ash samples used in this study were transported between a few and up to 130 km through the atmosphere (see Table S1), whereas the Cape Verdian loess sample was collected more than 1000 km away from its source. As long-distance atmospheric transportation may enhance Fe solubilities, Fe release data for ash particles sampled in the proximity of volcanic source craters may underestimate actual Fe solubilities in the remote ocean. It is still uncertain to what extent low-pH cloud water cycling of ash and dust particles affects the seawater solubility (hence bioavailability) of Fe. In terms of biogeochemical Fe and C cycles, however, a key parameter is the maximum concentration solubility of Fe that is controlled by various factors (e.g., nature of Fe-binding ligands) and Fe uptake mechanisms by marine photosynthetic organisms which are not completely understood [Baker and Croot, 2010].

[41] Due to differences in temporal and spatial deposition patterns, comparable millennial Fe fluxes into the Pacific Ocean are unlikely to have the similar marine biogeochemical impacts (Figure 7). The episodic deposition nature of mineral dust and volcanic ash (e.g., in the northern Pacific) may be less different than commonly thought. Despite its seasonality the dust input into the Pacific is not uniform throughout the year. About 30%–90% of the annual dust input is derived in the vicinity to the dust source at about 5% of the high deposition days [Mahowald et al., 2009]. Episodic dust storms occur about 20% of the days of a year, and may deposit about half of the yearly input within a 2 week period [Jickells and Spokes, 2001]. In terms of mass flux, the frequency and duration of the storm events is comparable to the moderate level of volcanic eruptions. Low-to-moderate eruptions (volcanic explosivity index of VEI <5 with ejecta volumes <1 km³ and ash plume heights of <10–25 km) are episodic but take place frequently. The relatively frequent volcanic eruptions can be grouped into (1) constant-to-daily gentle eruptions (eruption column height of hundreds of meters, e.g., Hawaiian volcanoes), (2) weekly eruptions (1–3 km ash plume height, e.g., Galeras), and (3) yearly explosive eruptions (3–5 km ash plume height, e.g., Cordón Caulle) (<http://www.volcano.si.edu/>).

[42] Each year at least 25 eruptions of VEI = 2 (<10¹¹ grams ash), about 15 eruptions of VEI = 3 (<10¹⁴ grams ash), and about 1–4 eruptions of VEI = 4 (<10¹⁵ grams ash) occur along the Pacific Ring of Fire (<http://www.volcano.si.edu/>).

Globally, high-magnitude eruptions with ejecta of >10¹⁵ grams (with ash plume heights of 10–25 km) occur every ≥10 years (e.g., Eyjafjallajökull 2010 eruption, VEI = 5). Supereruptions with ejecta of >10¹⁶ grams to >10¹⁹ grams (with ash plume heights of >25 km) are rare and take place every ≥10 to ≥10,000 years, depending on the magnitude (e.g., Pinatubo 1991, VEI = 6; Tambora 1815, VEI = 7; Taupo ~26,500 years ago, VEI = 8). Fe fertilization that may arise from such large-scale eruptions to supereruptions is to date basically unknown but some studies indicate that the effect may have been significant in the Earth's history [Duggen et al., 2010, and references therein].

[43] In terms of biogeochemical response and C cycles, both sources can be expected to have their greatest impact on Fe-limited (HNLC) regions (Figure 7a) [De Baar and De Jong, 2001; Watson, 2001]. While mineral dust deposition is mainly restricted to the northwestern Pacific HNLC region (Figures 7a and 7c), Fe input by volcanic ash is more widespread including the north (subarctic), eastern equatorial and southwestern Pacific (Figure 7b). In the subarctic Pacific, for example, the ash fallout of the intermediate-scale August 2008 eruption of Kasatochi volcano (VEI = 4) was associated with a large-scale phytoplankton bloom in the Fe-limited North Pacific [Hamme et al., 2010; Langmann et al., 2010]. In the Fe-limited eastern equatorial Pacific mineral dust input is relatively rare so that the flux of soluble Fe from ash from Mexican, Central American, and South American volcanoes is likely to dominate the millennial atmospheric input of Fe in these regions (Figure 7). In the Pacific sector of the Southern Ocean mineral dust deposition is very limited too, whereas volcanic ash from active volcanoes in the subduction zones of New Zealand and Tonga-Kermadec can be transported into the Fe-limited Southern Ocean with the westerlies, potentially causing volcanic Fe fertilization (Figure 7b).

5. Conclusions

[44] Airborne volcanic ash from volcanoes in different tectonic settings (subduction zones and hot spots) rapidly mobilizes soluble Fe on contact with natural seawater. Calculations suggest that even low ash loads within the ash fallout area of single volcanic eruptions can raise Fe levels sufficiently to cause massive phytoplankton blooms. Flux estimates suggest that the postglacial millennial input of Fe into the Pacific surface ocean through dry deposition of volcanic ash and mineral dust is comparable. Although the millennial Fe fluxes are found to be similar, the biogeochemical impacts of the two atmospheric sources are distinguished by differences in temporal and spatial deposition patterns in the Pacific surface ocean in general and in Fe-limited (HNLC) regions in particular.

[45] Further research to improve our understanding of the relative importance of volcanic ash and mineral dust for the Pacific surface ocean should include an evaluation of the amount of Fe that is transported into the Pacific through dry versus wet deposition, as Fe release of both volcanic ash and mineral dust particles appears to be strongly pH-dependent, and Fe release is strongly enhanced by interaction with low-pH solutes (e.g., cloud water). Despite the uncertainties typically involved in near-global flux estimates and differences in the biogeochemical impact patterns of volcanic ash

and mineral dust, our results strongly suggests that the role of volcanic ash for the Pacific surface ocean biogeochemical Fe cycle is significant and has so far been underestimated.

[46] **Acknowledgments.** We are grateful to L. Lara, C. Wallace, C. Neal, G. Alvarado-Induni, T. Kobayashi, I. Itikar, M. Iguchi, T. Noal, M. Mc Kinon, A. Gerst, and G. J. Dennis for kindly providing ash samples and to M. Heller for providing the dust sample. We greatly appreciate S. Kutterolf's constructive comments. We are thankful to M. Thoener for technical assistance with the electron microprobe analyses and to Ulrike Westernströer and Sabine Lange for their efforts with the ICP-OES analyses. S.D. was supported by the German Research Foundation, DFG (project Ho1833-16). P.D.'s contribution to this project was supported by a Vice Chancellor's Anniversary Lectureship, University of York. The paper is contribution 174 of the Sonderforschungsbereich (SFB) 574 "Volatiles and Hazards in Subduction Zones." The study was made possible by IFM-GEOMAR through in-house funding of the multidisciplinary research group NOVUM "Nutrients Originating Volcanoes and Their Effects on the Euphotic Zone of the Marine Ecosystem."

References

- Andreae, M. O., and D. Rosenfeld (2008), Aerosol-cloud-precipitation interactions: Part 1. The nature and sources of cloud-active aerosols, *Earth Sci. Rev.*, **89**, 13–41, doi:10.1016/j.earscirev.2008.03.001.
- Baker, A., and P. Croot (2010), Atmospheric and marine controls on aerosol iron solubility in seawater, *Mar. Chem.*, **120**, 4–13, doi:10.1016/j.marchem.2008.09.003.
- Baker, A. R., and T. D. Jickells (2006), Mineral particle size as a control on aerosol iron solubility, *Geophys. Res. Lett.*, **33**, L17608, doi:10.1029/2006GL026557.
- Baker, A., M. French, and K. L. Linge (2006), Trends in aerosol nutrient solubility along a west-east transect of the Saharan dust plume, *Geophys. Res. Lett.*, **33**, L07805, doi:10.1029/2005GL024764.
- Bay, R. C., N. Bramall, and P. B. Price (2004), Bipolar correlation of volcanism with millennial climate change, *Proc. Natl. Acad. Sci. U. S. A.*, **101**, 6341–6345, doi:10.1073/pnas.0400323101.
- Behrenfeld, M. J., A. J. Bale, Z. S. Kolber, J. Aiken, and P. G. Falkowski (1996), Confirmation of iron limitation of phytoplankton photosynthesis in the equatorial Pacific Ocean, *Nature*, **383**, 508–511, doi:10.1038/383508a0.
- Boyd, P. W., et al. (2000), A mesoscale phytoplankton bloom in the polar Southern Ocean stimulated by iron fertilization, *Nature*, **407**, 695–702, doi:10.1038/35037500.
- Boyd, P. W., et al. (2007), Mesoscale iron enrichment experiments 1993–2005: Synthesis and future directions, *Science*, **315**, 612–617, doi:10.1126/science.1131669.
- Buck, S. C., W. M. Landing, J. A. Resing, and G. T. Lebon (2006), Aerosol iron and aluminum solubility in the northwest Pacific Ocean: Results from the 2002 IOC cruise, *Geochem. Geophys. Geosyst.*, **7**, Q04M07, doi:10.1029/2005GC000977.
- Cather, S. M., N. W. Dunbar, F. W. McDowell, W. C. McIntosh, and P. A. Scholle (2009), Climate forcing by iron fertilization from repeated ignimbrite eruptions: The icehouse–silicic large igneous province (SLIP) hypothesis, *Geosphere*, **5**, 315–324, doi:10.1130/GES00188.1.
- Censi, P., L. A. Randazzo, P. Zuddas, F. Saiano, P. Aricò, and S. Andò (2010), Trace element behaviour in seawater during Etna's pyroclastic activity in 2001: Concurrent effects of nutrients and formation of alteration minerals, *J. Volcanol. Geotherm. Res.*, **193**, 106–116, doi:10.1016/j.jvolgeores.2010.03.010.
- Coale, K. H., et al. (1996), A massive phytoplankton bloom induced by an ecosystem-scale iron fertilization experiment in the equatorial Pacific Ocean, *Nature*, **383**, 495–501, doi:10.1038/383495a0.
- Coale, K. H., et al. (2004), Southern Ocean iron enrichment experiment: Carbon cycling in high- and low-Si waters, *Science*, **304**, 408–414, doi:10.1126/science.1089778.
- Cooper, D. J., A. J. Watson, and P. D. Nightingale (1996), Large decrease in ocean-surface CO₂ fugacity in response to in situ iron fertilization, *Nature*, **383**, 511–513, doi:10.1038/383511a0.
- Croot, P., and M. Johansson (2000), Determination of iron speciation by cathodic stripping voltammetry in seawater using the competing ligand 2-(2-Thiazolylazo)-p-creosol (TAC), *Electroanalysis*, **12**, 565–576, doi:10.1002/(SICI)1521-4109(200005)12:8<565::AID-ELAN565>3.0.CO;2-L.
- De Baar, H. J. W., and J. T. M. De Jong (2001), Distributions, sources and sinks of iron in seawater, in *The Biogeochemistry of Iron in Seawater*, edited by D. R. Turner and K. A. Hunter, pp. 212–215, Wiley, Chichester, U. K.
- Delmelle, P., M. Lambert, Y. Dufrene, P. Gerin, and N. Oskarsson (2007), Gas/aerosol–ash interaction in volcanic plumes: New insights from surface analyses of fine ash particles, *Earth Planet. Sci. Lett.*, **259**, 159–170, doi:10.1016/j.epsl.2007.04.052.
- Delmelle, P., C. Maclean, and J. Calkins (2009), Volcanic ash deposition and phytoplankton growth: A plausible connection, poster presented at *SOLAS Open Science Conference*, SCOR, Barcelona, Spain, 16–19 November.
- Desboeufs, K. V., R. Losno, F. Vimeux, and S. Cholbi (1999), The pH-dependent dissolution of wind-transported Saharan dust, *J. Geophys. Res.*, **104**, 21,287–21,299.
- Desboeufs, K. V., R. Losno, and J. L. Colin (2001), Factors influencing aerosol solubility during cloud processes, *Atmos. Environ.*, **35**, 3529–3537, doi:10.1016/S1352-2310(00)00472-6.
- Duggen, S., P. Croot, U. Schacht, and L. Hoffmann (2007), Subduction zone volcanic ash can fertilize the surface ocean and stimulate phytoplankton growth: Evidence from biogeochemical experiments and satellite data, *Geophys. Res. Lett.*, **34**, L01612, doi:10.1029/2006GL027522.
- Duggen, S., N. Olgun, P. Croot, L. Hoffmann, H. Dietze, and C. Teschner (2010), The role of airborne volcanic ash for the surface ocean biogeochemical iron-cycle: A review, *Biogeosciences*, **7**, 827–844, doi:10.5194/bg-7-827-2010.
- Duncan, R. A., and D. A. Clague (Eds.) (1985), *Pacific Plate Motion Recorded by Linear Volcanic Chains*, 89–121 pp., Plenum Press, New York.
- Fierstein, J., and M. Nathenson (1992), Another look at the calculation of fallout tephra volumes, *Bull. Volcanol.*, **54**, 156–167, doi:10.1007/BF00278005.
- Fisher, R. V., and H.-U. Schmincke (1984), *Pyroclastic Rocks*, 472 pp., Springer, Berlin.
- Frogner, P., S. R. Gislason, and N. Óskarsson (2001), Fertilizing potential of volcanic ash in ocean surface water, *Geology*, **29**, 487–490, doi:10.1130/0091-7613(2001)029<0487:FPOVAI>2.0.CO;2.
- Guieu, C., and A. J. Thomas (1996), Saharan aerosols: From the soil to the ocean, in *The Impact of Desert Dust across the Mediterranean*, edited by S. Guerzoni and R. Chester, pp. 207–216, Kluwer, Dordrecht, Netherlands.
- Guieu, C., R. Chester, M. Nimmo, J. M. Martin, S. Guerzoni, E. Nicolas, J. Mateu, and S. Keyse (1997), Atmospheric input of dissolved and particulate metals to the northwestern Mediterranean, *Deep Sea Res., Part II*, **44**, 655–674, doi:10.1016/S0967-0645(97)88508-6.
- Hamme, R. C., et al. (2010), Volcanic ash fuels anomalous plankton bloom in subarctic northeast Pacific, *Geophys. Res. Lett.*, **37**, L19604, doi:10.1029/2010GL044629.
- Heller, M. I., and P. L. Croot (2011), Superoxide decay as a probe for speciation changes during dust dissolution in tropical Atlantic surface waters near Cape Verde, *Mar. Chem.*, in press.
- Hutchins, D. A., and K. A. Bruland (1998), Iron-limited diatom growth and Si:N ratios in a coastal upwelling region, *Nature*, **393**, 561–564, doi:10.1038/31203.
- Jickells, T. D. (1999), The inputs of dust derived elements to the Sargasso Sea; a synthesis, *Mar. Chem.*, **68**, 5–14, doi:10.1016/S0304-4203(99)00061-4.
- Jickells, T. M., and L. J. Spokes (2001), Atmospheric iron inputs to the oceans, in *Biogeochemistry of Iron in Seawater*, edited by D. R. Turner and K. Hunter, pp. 85–121, Wiley, Chichester, U. K.
- Jickells, T. D., Z. S. An, and K. K. Andersen (2005), Global iron connections between desert dust, ocean biogeochemistry, and climate, *Science*, **308**, 67–71, doi:10.1126/science.1105959.
- Johnson, K. S. (2001), Iron supply and demand in the upper ocean: Is extraterrestrial dust a significant source of bioavailable iron?, *Global Biogeochem. Cycles*, **15**, 61–63, doi:10.1029/2000GB001295.
- Jones, M. T., and S. R. Gislason (2008), Rapid releases of metal salts and nutrients following the deposition of volcanic ash into aqueous environments, *Geochim. Cosmochim. Acta*, **72**, 3661–3680, doi:10.1016/j.gca.2008.05.030.
- Journet, E., K. V. Desboeufs, S. Caquineau, and J. L. Colin (2008), Mineralogy as a critical factor of dust iron solubility, *Geophys. Res. Lett.*, **35**, L07805, doi:10.1029/2007GL031589.
- Kelts, K., and J. A. McKenzie (1976), Cretaceous volcanogenic sediments from the Line Island chain: Diagenesis and formation of K-feldspar, DSDP leg 33, site 315 A and site 316, in *Initial Reports of DSDP*, edited by S. O. Schlanger and E. D. Jackson, pp. 789–803, US Govt. Print. Off., Washington, D. C.
- Kohfeld, K. E., and S. P. Harrison (2001), DIRTMAP: The geological record of dust, *Earth Sci. Rev.*, **54**, 81–114, doi:10.1016/S0012-8252(01)00042-3.

- Kutterolf, S., A. Freundt, and W. Perez (2008), Pacific offshore record of plinian arc volcanism in Central America: 2 Tephra volumes and erupted masses, *Geochim. Geophys. Geosyst.*, *9*, Q02S02, doi:10.1029/2007GC001791.
- Langmann, B., K. Zaksek, M. Hort, and S. Duggen (2010), Volcanic ash as fertilizer for the surface ocean, *Atmos. Chem. Phys.*, *10*, 3891–3899, doi:10.5194/acp-10-3891-2010.
- Le Bas, M. J. (1984), Nephelinites and carbonatites, *Geol. Soc. Spec. Publ.*, *30*, 53–83.
- Lipman, P. W. (2000), Calderas, in *Encyclopedia of Volcanoes*, edited by H. Sigurdsson, pp. 645–669, Academic, San Diego, Calif.
- Liu, X. W., and F. J. Millero (2002), The solubility of iron in seawater, *Mar. Chem.*, *77*, 43–54, doi:10.1016/S0304-4203(01)00074-3.
- Lohmann, U., and J. Feichter (2005), Global indirect aerosol effects: A review, *Atmos. Chem. Phys.*, *5*, 715–737, doi:10.5194/acp-5-715-2005.
- Lonsdale, P. (1975), Sedimentation and tectonic modification of Samoan Archipelagic Apron, *Am. Assoc. Pet. Geol.*, *59*, 780–798.
- Mahowald, N., K. Kohfeld, M. Hansson, Y. Balkanski, S. P. Harrison, I. C. Prentice, M. Schluz, and H. Rodhe (1999), Dust sources and deposition during the last glacial maximum and current climate: A comparison of model results with paleodata from ice cores and marine sediments, *J. Geophys. Res.*, *104*(D13), 15,895–15,916, doi:10.1029/1999JD900084.
- Mahowald, N. M., A. R. Baker, G. Bergametti, N. Brooks, R. A. Duce, T. D. Jickells, N. Kubilay, J. M. Prospero, and I. Tegen (2005), Atmospheric global dust cycle and iron inputs to the ocean, *Global Biogeochem. Cycles*, *19*, GB4025, doi:10.1029/2004GB002402.
- Mahowald, N., et al. (2009), Atmospheric iron deposition: Global distribution, variability, and human perturbations, *Annu. Rev. Mar. Sci.*, *1*, 245–278, doi:10.1146/annurev.marine.010908.163727.
- Martin, J. H., and S. E. Fitzwater (1988), Iron deficiency limits phytoplankton growth in the north-east Pacific subarctic, *Nature*, *331*, 341–343, doi:10.1038/331341a0.
- Martin, J. H., R. M. Gordon, and S. E. Fitzwater (1990), Iron in Antarctic waters, *Nature*, *345*, 156–158, doi:10.1038/345156a0.
- Martin, J. H., R. M. Gordon, and S. E. Fitzwater (1991), The case for iron, *Limnol. Oceanogr.*, *36*, 1793–1802, doi:10.4319/lo.1991.36.8.1793.
- Martin, J. H., K. H. Coale, and K. S. Johnson (1994), Testing the iron hypothesis in ecosystems of the equatorial Pacific Ocean, *Nature*, *371*, 123–129, doi:10.1038/371123a0.
- Millero, F. J., and S. Sotolongo (1989), The oxidation of Fe(II) with H₂O₂ in seawater, *Geochim. Cosmochim. Acta*, *53*, 1867–1873, doi:10.1016/0016-7037(89)90307-4.
- Moore, C. M., et al. (2009), Large-scale distribution of Atlantic nitrogen fixation controlled by iron availability, *Nat. Geosci. Lett.*, *2*, 867–871, doi:10.1038/ngeo667.
- Morel, F. M. M., and N. M. Price (2003), The biogeochemical cycles of trace metals in the oceans, *Science*, *300*, 944–947, doi:10.1126/science.1083545.
- Morel, F. M. M., A. J. Milligan, and M. A. Saito (2003), Marine bioinorganic chemistry: The role of trace metals in the oceanic cycles of major nutrients, in *Treatise on Geochemistry*, edited by H. Elderfield, pp. 113–143, Elsevier, Oxford, U. K.
- Nakagawa, M., and T. Ohba (2003), Minerals in volcanic ash I: Primary minerals and volcanic glass, *Global Environ. Res.*, *6*, 41–51.
- Naughton, J. J., V. A. Greenberg, and R. Googuel (1976), Incrustations and fumarolic condensates at Kilauea Volcano, Hawaii: Field, drill-hole, and laboratory observations, *J. Volcanol. Geotherm. Res.*, *1*, 149–165, doi:10.1016/0377-0273(76)90004-4.
- O'Dowd, C. D., M. C. Facchini, F. Cavalli, D. Ceburnis, M. Mircea, S. Decesari, S. Fuzzi, Y. J. Yoon, and J. P. Putaud (2004), Biogenically driven organic contribution to marine aerosol, *Nature*, *431*, 676–680, doi:10.1038/nature02959.
- Oppenheimer, C. (2002), Limited global change due to the largest known Quaternary eruption, Toba ≈ 74 kyr BP?, *Quat. Sci. Rev.*, *21*, 1593–1609.
- Óskarsson, N. (1980), The interaction between volcanic gases and tephra: Fluorine adhering to tephra of the 1970 Hekla eruption, *J. Volcanol. Geotherm. Res.*, *8*, 251–266, doi:10.1016/0377-0273(80)90107-9.
- Óskarsson, N. (1981), The chemistry of Icelandic lava incrustations and the latest stages of degassing, *J. Volcanol. Geotherm. Res.*, *10*, 93–111, doi:10.1016/0377-0273(81)90057-3.
- Parekh, P., M. J. Follows, and E. A. Boyle (2005), Decoupling of iron and phosphate in the global ocean, *Global Biogeochem. Cycles*, *19*, GB2020, doi:10.1029/2004GB002280.
- Peters, J. L., R. W. Murray, J. W. Sparks, and D. S. Coleman (2000), Terrestrial matter and dispersed ash in sediment from the Caribbean Sea; results from Leg 165, *Proc. Ocean Drill. Program, Sci. Results*, *165*, 115–124.
- Pyle, D. M. (1989), The thickness, volume and grain size of tephra fall deposits, *Bull. Volcanol.*, *51*, 1–15, doi:10.1007/BF01086757.
- Rea, D. K. (1994), The paleoclimatic record provided by eolian deposition in the deep sea: The geologic history of wind, *Rev. Geophys.*, *32*, 159–195, doi:10.1029/93RG03257.
- Rees, B., R. Detrick, and B. Coakley (1993), Seismic stratigraphy of the Hawaiian flexural moat, *Mem. Geol. Soc. Am.*, *105*, 189–205, doi:10.1130/0016-7606(1993)105<0189:SSOTHF>2.3.CO;2.
- Rose, W. I. (1977), Scavenging of volcanic aerosol by ash: Atmospheric and volcanologic implications, *Geology*, *5*, 621–624, doi:10.1130/0091-7613(1977)5<621:SOVABA>2.0.CO;2.
- Rose, W. I., and A. J. Durant (2009), Fine ash content of explosive eruptions, *J. Volcanol. Geotherm. Res.*, *186*, 32–39, doi:10.1016/j.jvolgeores.2009.01.010.
- Sarmiento, J. L. (1993), Atmospheric CO₂ stalled, *Nature*, *365*, 697–698, doi:10.1038/365697a0.
- Schmincke, H. U., and M. Sumita (1998), Tephra event stratigraphy and emplacement of volcanoclastic sediments, Mogan and Fataga stratigraphic intervals, ODP leg 157. Part II: Origin and emplacement of volcanoclastic layers, *Weaver PPE*, 267–291.
- Schroth, A. W., J. Crusius, E. R. Sholkovitz, and B. C. Bostick (2009), Iron solubility driven by speciation in dust sources to the ocean, *Nat. Geosci.*, *2*, 337–340, doi:10.1038/ngeo501.
- Scudder, R. P., R. W. Murray, and T. Plank (2009), Dispersed ash in deeply buried sediment from the northwest Pacific Ocean: An example from the Izu–Bonin arc (ODP Site 1149), *Earth Planet. Sci. Lett.*, *284*, 639–648, doi:10.1016/j.epsl.2009.05.037.
- Sedwick, P. N., E. R. Sholkovitz, and T. M. Church (2007), Impact of anthropogenic combustion emissions on the fractional solubility of aerosol iron: Evidence from the Sargasso Sea, *Geochim. Geophys. Geosyst.*, *8*, Q10Q06, doi:10.1029/2007GC001586.
- Sigurdsson, H., B. Houghton, S. R. McNutt, H. Rymer, and J. Stix (Eds.) (2000), *Encyclopedia of Volcanoes*, Academic, San Diego, Calif.
- Spirakis, C. S. (1991), Iron fertilization with volcanic ash, *Eos Trans. AGU*, *72*(47), 525, doi:10.1029/90EO00370.
- Spokes, L. J., and T. D. Jickells (1996), Factors controlling the solubility of aerosol trace metals in the atmosphere and on mixing into seawater, *Aquat. Geochem.*, *1*, 355–374, doi:10.1007/BF00702739.
- Straub, S. M., and H.-U. Schmincke (1998), Evaluating the tephra input into Pacific Ocean sediments: Distribution in space and time, *Geol. Rundsch.*, *87*, 461–476, doi:10.1007/s005310050222.
- Textor, C., H. F. Graf, M. Herzog, J. M. Oberhuber, W. I. Rose, and G. G. J. Ernst (2006), Volcanic particle aggregation in explosive eruption columns. Part I: Parameterization of the microphysics of hydrometeors and ash, *J. Geothermal Res.*, *150*, 359–377, doi:10.1016/j.jvolgeores.2005.09.007.
- Turner, S., N. Arnaud, J. Liu, N. Rogers, C. Hawkesworth, N. Harris, S. Kelley, P. van Calsteren, and W. Deng (1996), Post-collision, Shoshonitic Volcanism on the Tibetan Plateau: Implications for convective thinning of the lithosphere and the source of ocean island basalts, *J. Petrol.*, *37*, 45–71, doi:10.1093/petrology/37.1.45.
- Turner, S. M., M. J. Harvey, C. S. Law, P. D. Nightingale, and P. S. Liss (2004), Iron-induced changes in oceanic sulfur biogeochemistry, *Geophys. Res. Lett.*, *31*, L14307, doi:10.1029/2004GL020296.
- Viereck, L., M. Simon, and H.-U. Schmincke (1985), Primary composition, alteration, and origin of Cretaceous volcanoclastic rocks, East Mariana basin (site 585, leg 89), in *Initial Reports of DSDP*, edited by R. Moberly and S. Schlanger, pp. 529–553, U.S. Govt. Print. Off., Washington, D. C.
- Watson, A. J. (1997), Volcanic Fe, CO₂, ocean productivity and climate, *Nature*, *385*, 587–588, doi:10.1038/385587b0.
- Watson, A. J. (2001), Iron limitation in the oceans, in *The Biogeochemistry of Iron in Seawater*, edited by D. R. Turner and K. A. Hunter, pp. 9–39, John Wiley, West Sussex, U. K.
- Watson, A. J., P. S. Liss, and R. A. Duce (1991), Design of a small scale iron enrichment experiment, *Limnol. Oceanogr.*, *36*, 1960–1965, doi:10.4319/lo.1991.36.8.1960.
- Wells, M. L. (2003), The level of iron enrichment required to initiate diatom blooms in HNLC waters, *Mar. Chem.*, *82*, 101–114, doi:10.1016/S0304-4203(03)00055-0.
- Wiesner, M. G., Y. Wang, and L. Zheng (1995), Fallout of volcanic ash to the deep South China Sea induced by the 1991 eruption of Mount Pinatubo (Philippines), *Geology*, *23*, 885–888, doi:10.1130/0091-7613(1995)023<0885:FOVATT>2.3.CO;2.
- Winckler, G., R. F. Anderson, M. Q. Fleisher, D. McGee, and N. Mahowald (2008), Covariant glacial-interglacial dust fluxes in the equatorial Pacific and Antarctica, *Science*, *320*, 93–96, doi:10.1126/science.1150595.
- Wolfe, C. J., M. K. McNutt, and R. S. Detrick (1994), The Marquesas archipelago apron: Seismic stratigraphy and implications for volcano growth, mass wasting, and crustal underplating, *J. Geophys. Res.*, *99*, 13,591–13,608, doi:10.1029/94JB00686.

Wu, J., R. Rember, and C. Cahill (2007), Dissolution of aerosol iron in the surface waters of the North Pacific and North Atlantic oceans as determined by a semicontinuous flow-through reactor method, *Global Biogeochem. Cycles*, 21, GB4010, doi:10.1029/2006GB002851.

Zhuang, G., Z. Yi, R. A. Duce, and P. R. Brown (1992), Chemistry of iron in marine aerosols, *Global Biogeochem. Cycles*, 6, 161–173, doi:10.1029/92GB00756.

A. Auer, Department of Geology, University of Otago, PO Box 56, Dunedin 9054, New Zealand.

P. L. Croot, Marine Biogeochemistry, Plymouth Marine Laboratory, Prospect Place, Plymouth PL1 3DH, UK.

P. Delmelle, Environment Department, University of York, Heslington, York YO10 5D, UK.

S. Duggen, A. P. Møller Skolen, Upper Secondary School and Sixth Form College of the Danish National Minority in Northern Germany, Fjordallee 1, Schleswig D-24837, Germany.

D. Garbe-Schönberg, Institute of Geosciences, University of Kiel, Olshausenstrasse 40, Kiel D-24118, Germany.

H. Dietze and N. Olgun, Marine Biogeochemistry Division, Leibniz-Institute of Marine Sciences, IFM-GEOMAR, Düsternbrooker Weg 20, Kiel D-24105, Germany. (nolgun@ifm-geomar.de)

N. Óskarsson, Institute of Earth Sciences, University of Iceland, Askja, Sturlugata 7, Reykjavík 101, Iceland.

U. Schacht, CO2CRC, Australian School of Petroleum, University of Adelaide, Gate 6, Frome Road, Adelaide SA 5005, Australia.

C. Siebe, Departamento de Vulcanología, Instituto de Geofísica, Universidad Nacional Autónoma de México, Ciudad Universitaria, 04510 Coyoacán, Mexico.

Supplementary Chapter II**Surface ocean iron fertilization: The role of airborne ash from subduction zone and hotspot volcanoes and related iron fluxes into the Pacific Ocean.**

Nazli Olgun, Svend Duggen, Peter Croot, Pierre Delmelle, Heiner Dietze, Ulrike Schacht, Niels Óskarsson, Claus Siebe, Andreas Auer, Dieter-Garbe Schönberg.

Components: 4 tables

Table S1: Description of the volcanic ash samples.

Table S2: Fe-release of ash from subduction zone and hotspot volcanoes and Saharan dust on contact with natural seawater, determined by means of Cathodic Stripping Voltammetry.

Table S3: Glass composition of subduction zone and hotspot volcanic ash, determined by electron microprobe.

Table S4: Summary of the Central American Volcanic Arc (CAVA) tephra flux over the past 191 ka, based on *Kutterolf et al.*, [2008].

Table S1: Description of the volcanic ash samples.

Volcano	Location	Date	Collection distance and description	Eruption type	
Sakura-Jima '86	Japan	11. June 1986	11 km NW Kagoshima University Campus. Silty	Vulcanian	
Sakura-Jima '87		18. Nov. 1987	At the eastern foot of the volcano. Silty	Vulcanian	
Sakura-Jima '99		6. Dec. 1999	11 km NW Kagoshima University Campus. Silty	Vulcanian	
Sakura-Jima '07		May 2007	3 km NW of the Minamidake Crater. Silty	Vulcanian	
Sakura-Jima '09		2009	At the eastern foot of the volcano. Sandy	Vulcanian	
Arenal '92	Costa Rica	22. July. 1992	At the foot of the volcano, Silty-fine sandy	Strombolian	
Arenal '93		1993	At the foot of the volcano, Silty-fine sandy	Strombolian	
Arenal '03		04. Feb. 2003	At the foot of the volcano, Silty-fine sandy	Pyroclastic flows	
Arenal '04		31. May. 2004	At the foot of the volcano, Silty-fine sandy	Pyroclastic flows	
Turrialba 1864	Costa Rica	1864	Unknown. Sandy	Strombolian	
Mt. Spurr '92	Alaska	18. Aug. 1992	Anchorage. Sandy	Sub-plinian	
Rabaul '02_1	Papua New Guinea	13-14. Nov. 2002	At the foot of the volcano. Fine-sandy	Vulcanian	
Rabaul '02_2		15-23. Nov. 2002	At the foot of the volcano. Fine-sandy	Vulcanian	
Rabaul '08		2008	Unknown. Silty-fine sandy	Vulcanian	
Popocatepetl '98_1	Mexico	19. Nov. 1998	9 km NW from crater. Silty	Vulcanian	
Popocatepetl '98_2		4. Dec. 1998	18.7 km NW from crater. Sandy	Vulcanian	
Popocatepetl '00_1		4. Sep. 2000	18.7 km NW from crater. Silty	Vulcanian	
Popocatepetl '00_2		20. Dec. 2000	4 km NNW from crater. Silty-fine sandy	Vulcanian	
Popocatepetl '00_3		29 -30. Dec. 2000	32 km ENE from crater. Sandy	Vulcanian	
Popocatepetl '01_1		22. Jan. 2001	19 km SE from crater. Sandy	Vulcanian	
Popocatepetl '01_2		5. July. 2001	4 km NNW from crater. Coarse sand	Vulcanian	
Popocatepetl '03		19. July. 2003	65 km NW from Crater. Fine-silty	Vulcanian	
Karymsky '05_1		Kamchatka	10. July. 2005	5 km SE from crater. Coarse sand	Strombolian
Karymsky '05_2			11. July. 2005	5 km SE from crater. Coarse sand	Strombolian
Karymsky '05_3			11. July. 2005	5 km SE from crater. Coarse sand	Strombolian
Karymsky '05_4			12. July. 2005	1.8 km SSE from crater. Coarse sand	Strombolian
Karymsky '05_5			13-14. July. 2005	5 km SE from crater. Coarse sand	Strombolian
Karymsky '05_6			14. July. 2005	5 km SE from crater. Coarse sand	Strombolian
Karymsky '05_7			14. July. 2005	5 km SE from crater. Coarse sand	Strombolian
Karymsky '05_8			14-15. July. 2005	5 km SE from crater. Coarse sand	Strombolian
Karymsky '05_9	15. July. 2005		5 km SE from crater. Coarse sand	Strombolian	
Karymsky '05_10	15. July. 2005	5 km SE from crater. Coarse sand	Strombolian		
Chaiten '08_1	Chile	3. May. 2008	10 km far from summit. Silty	Plinian to sub-plinian	
Chaiten '08_2		6. May. 2008	130 km, El Bolson Argentina. Silty	Plinian to sub-plinian	
Anatahan '03	Mariana Islands		Unknown. Silty-fine sandy	Plinian	
Merapi '06	Central Java	9. June. 2006	Unknown. Silty	Pyroclastic flow	
Mt St Helens '80	Washington USA	18. May. 1980	Unknown. Coarse sand	Plinian	
Fuego '74	Guatemala		Unknown. Coarse sand	Vulcanian	
Telica '00	Nicaragua		Unknown. Silty	Ash explosion	
Tungurahua '00	Equador	22. May 2000	Unknown. Coarse sand	Ash explosion	
Hekla ' 47	Iceland	1947	32 km SSW from the crater. Silty	Plinian to sub-plinian	
Hekla ' 70		1970	45 km NW from the crater. Silty	Plinian to sub-plinian	
Hekla ' 80		1980	12 km N from the crater. Coarse sand	Plinian to sub-plinian	
Pu'u'oo ' 05	Hawaii	17. Sept. 2005	Unknown. Coarse sand	Ash explosions and fissure eruptions	

Table S2: Fe-release of ash from subduction zone and hotspot volcanoes and Saharan dust on contact with natural seawater, determined by means of Cathodic Stripping Voltammetry.**A) Subduction Zone
Volcanic Ash**

Sakura-jima 1986		Sakura-jima 1986, Repeat		Sakura-jima 1987		Sakura-jima 1987, Repeat		Sakura-jima 1987, Repeat	
	nmole Fe per g ash		nmole Fe per g ash		nmole Fe per g ash		nmole Fe per g ash		nmole Fe per g ash
time / min		time / min		time / min		time / min		time / min	
0	0.0	0	0.0	0	0.0	0	0.0	0	0.0
5	18.7	6	35.4	3	25.3	7	28.2	5	23.2
10	28.0	10	47.3	9	48.1	11	36.2	9	31.6
11	28.9	11	56.6	10	52.0	15	43.3	15	38.1
15	32.9	14	57.8	15	65.2	20	55.1	21	46.6
20	38.1	22	71.8	25	83.6	30	68.6	27	52.7
25	40.5	28	77.1	34	103.0	40	79.1	33	58.5
29	46.1	34	88.4	40	137.1	46	89.2	39	72.7
32	47.1	37	90.8	50	144.5	50	92.2	45	68.5
36	50.6	44	99.5	63	179.4	60	118.3	51	75.2
39	51.6	48	101.3			110	134.2	60	83.4
43	54.9	51	104.5						
46	56.1	60	108.3						
50	58.8								
53	63.8								
56	62.8								
60	61.0								
63	69.2								
67	65.0								
70	69.1								
73	70.0								
86	72.8								
Sakura-jima 1999		Sakura-jima 1999, Repeat		Sakura-jima 2007		Sakura-jima 2009		Arenal 1992	
	nmole Fe per g ash		nmole Fe per g ash		nmole Fe per g ash		nmole Fe per g ash		nmole Fe per g ash
time / min		time / min		time / min		time / min		time / min	
0	0.0	0	0.0	0	0.0	0	0.00	0	0.0
3	87.9	6	75.1	5	221.0	5	337.5	4	84.2
8	136.1	8	84.4	10	248.3	10	337.5	8	124.4
10	148.0	14	99.6	13	262.0	15	336.8	10	134.0
14	166.7	21	120.3	20	274.1	20	337.4	12	140.1
21	195.4	30	141.4	27	280.2	25	334.9	18	162.2
30	205.5	40	163.1	30	285.4	30	335.0	27	183.2
40	222.2	47	164.0	50	290.2	35	336.1	35	196.7
50	239.3	50	171.9	53	294.7	45	336.0	45	214.7
60	244.8	60	186.5	60	295.7	50	335.3	51	219.4
65	256.3					55	335.6	60	227.3
						60	336.9		

Arenal 1993		Arenal 1993, Repeat		Arenal 2003		Arenal 2004		Mt. Spurr 1992	
time / min	nmole Fe per g ash	time / min	nmole Fe per g ash	time / min	nmole Fe per g ash	time / min	nmole Fe per g ash	time / min	nmole Fe per g ash
0	0.0	0	0.0	0	0.0	0	0.0	0	0.0
3	61.0	6	83.8	4	206.7	3	213.7	4	77.6
8	106.4	10	104.4	8	292.5	8	283.2	9	119.8
13	144.4	13	122.5	10	306.0	10	292.0	10	127.0
21	193.1	21	162.0	12	312.6	16	292.4	15	154.5
30	229.2	30	186.5	16	317.1	22	291.4	20	182.5
40	252.0	40	214.3	21	318.4	28	290.9	24	198.0
48	267.3	48	238.6	28	318.0	36	290.1	29	207.9
55	273.8	67	284.8	36	316.8	42	290.8	34	218.4
60	286.8	88	286.7	45	317.1	50	286.8	40	241.8
65	290.8			55	316.7	60	293.4	50	246.3
				60	313.8	63	286.6	60	258.5
Turrialba 1864		Rabaul 2002-1		Rabaul 2002-2		Rabaul 2008		Popocatepetl 1998-1	
time / min	nmole Fe per g ash	time / min	nmole Fe per g ash	time / min	nmole Fe per g ash	time / min	nmole Fe per g ash	time / min	nmole Fe per g ash
0	0.0	0	0.0	0	0.0	0	0.0	0	0.0
3	7.5	4	55.2	4	93.2	5	67.3	5	300.6
7	16.4	8	98.7	8	144.1	10	111.2	10	312.0
10	24.0	14	144.4	13	185.3	15	156.7	11	312.3
15	34.5	20	171.9	19	217.9	20	187.2	16	312.7
21	44.2	25	192.3	26	241.7	25	200.8	22	314.3
30	60.8	34	226.2	35	261.1	39	238.0	28	316.8
40	77.1	41	244.8	41	268.3	44	255.9	32	317.9
50	92.9	50	262.0	51	277.0	49	264.6	38	317.8
60	109.6	60	275.8	61	278.0	55	276.0	43	318.9
						60	279.8	50	319.4
								60	318.8
Popocatepetl 1998-2		Popocatepetl 2000-1		Popocatepetl 2000-2		Popocatepetl 2000-3		Popocatepetl 2001-1	
time / min	nmole Fe per g ash	time / min	nmole Fe per g ash	time / min	nmole Fe per g ash	time / min	nmole Fe per g ash	time / min	nmole Fe per g ash
0	0.0	0	0.0	0	0.0	0	0.0	0.00	0.0
10	124.7	8	75.3	7	312.0	6	45.2	7.00	183.1
14	145.4	12	91.8	17	314.6	15	83.0	10.00	169.8
18	164.1	16	113.1	21	312.8	26	92.9	13.00	175.2
24	188.7	23	140.4	26	314.2	30	106.7	18.00	179.4
30	210.3	29	161.3	32	313.2	36	109.6	23.00	178.6
35	221.2	36	178.5	38	314.1	42	122.1	30.00	177.3
40	237.1	43	202.1	44	315.1	48	137.6	40.00	177.3
45	247.7	49	211.9	50	314.6	54	145.9	50.00	176.9
50	251.6	55	230.5			60	162.2	60.00	175.4
60	261.2	60	230.5						

Popocatepetl 2001-2		Popocatepetl 2003		Karymsky 2005-1		Karymsky 2005-2		Karymsky 2005-3	
time / min	nmole Fe per g ash	time / min	nmole Fe per g ash	time / min	nmole Fe per g ash	time / min	nmole Fe per g ash	time / min	nmole Fe per g ash
0	0.0	0	0.0	0	0.0	0	0.0	0	0.0
5	70.6	5	304.9	3	21.3	3	11.1	3	11.1
11	97.4	10	306.7	10	43.0	9	20.6	10	22.9
15	36.4	16	307.0	13	51.4	10	21.5	17	33.9
22	42.5	22	306.0	16	62.9	15	25.7	27	44.1
26	48.8	28	307.5	21	71.4	21	30.4	32	48.0
32	54.6	34	306.7	28	86.5	27	33.5	40	51.9
38	62.3	40	307.7	34	92.2	33	38.6	46	54.7
44	66.5	46	307.1	40	100.9	39	40.6	53	61.2
50	72.2	52	307.9	48	113.0	45	44.5	60	62.8
60	74.6	60	308.0	52	115.9	51	46.9		
				60	116.4	60	50.6		
Karymsky 2005-4		Karymsky 2005-5		Karymsky 2005-6		Karymsky 2005-7		Karymsky 2005-8	
time / min	nmole Fe per g ash	time / min	nmole Fe per g ash	time / min	nmole Fe per g ash	time / min	nmole Fe per g ash	time / min	nmole Fe per g ash
0	0.0	0	0.0	0	0.0	0	0.0	0	0.0
5	18.1	5	38.3	5	14.5	7	13.7	6	12.5
9	23.1	9	45.6	10	17.9	10	17.8	9	17.4
15	33.3	13	54.1	16	22.1	15	23.4	10	18.5
22	43.6	21	64.9	23	25.0	20	24.9	16	23.2
30	51.2	26	61.9	30	27.7	25	28.5	22	29.6
38	58.9	32	64.3	36	30.7	30	31.1	30	34.0
46	64.7	39	70.1	42	30.1	36	33.9	36	37.3
54	72.2	46	75.8	50	34.0	42	35.2	42	40.6
		53	77.6	60	38.3	48	37.6	48	43.7
		60	79.4			55	39.7	55	44.5
						58	41.8	60	46.0
Karymsky 2005-9		Karymsky 2005-10		Chaiten 2008-1		Chaiten 2008-2		Anatahan 2003	
time / min	nmole Fe per g ash	time / min	nmole Fe per g ash	time / min	nmole Fe per g ash	time / min	nmole Fe per g ash	time / min	nmole Fe per g ash
0	0.0	0	0.0	0	0.0	0	0.0	0	0.0
5	15.9	6	19.6	5	56.6	5	39.1	5	22.4
10	24.9	10	26.5	10	84.7	10	62.1	12	31.9
16	30.1	15	30.7	16	111.1	15	85.8	23	46.1
22	31.4	25	38.1	21	130.6	20	100.9	28	52.0
28	35.4	32	39.4	26	152.6	25	119.5	34	56.2
34	36.8	35	42.9	31	166.6	30	136.4	46	66.5
40	39.5	42	45.8	36	181.7	36	160.5	52	73.6
46	42.5	47	50.4	41	195.4	40	173.2	57	76.1
52	46.8	52	49.3	46	208.2	45	186.9		
60	48.8	60	51.9	51	217.5	51	195.1		
				56	225.4	55	209.8		
				60	239.3	60	224.5		
Mount St. Helens 1980		Fuego 1974		Telica 2000		Tungurahua 2000			
time / min	nmole Fe per g ash	time / min	nmole Fe per g ash	time / min	nmole Fe per g ash	time / min	nmole Fe per g ash	time / min	nmole Fe per g ash

0	0.0	0	0.0	0	0	0	0.0
5	27.4	5	110.8	5	109.4848372	5	15.7
12	43.7	10	149.8	10	118.4661604	10	27.4
21	58.3	20	186.5	29	214.5022324	15	34.9
27	66.1	25	213.5	31	205.6416509	21	43.0
33	73.8	33	236.4	37	205.1679721	26	48.8
38	83.7	38	245.8	44	205.6091436	31	55.8
43	91.4	43	261.9	49	217.8922872	36	62.0
60	108.3	49	266.9	54	218.217361	46	69.3
65	109.6	54	275.3	60	218.0362484	51	74.1
		60	279.8			60	81.9

B) Hot spot volcanic ash

Hekla 1947		Hekla 1970		Hekla 1980		Pu'u'oo 2005	
time / min	nmole Fe per g ash	time / min	nmole Fe per g ash	time / min	nmole Fe per g ash	time / min	nmole Fe per g ash
0	0.0	0	0.0	0	0.0	0	0.0
4	10.0	7	40.1	4	13.9	3	7.7
9	17.3	10	37.6	7	27.5	7	12.2
15	22.6	14	45.9	11	33.8	10	13.2
22	29.8	20	54.1	15	40.6	15	19.3
30	35.3	25	72.6	20	48.3	20	20.1
40	42.3	30	64.6	30	62.3	25	24.1
50	49.3	40	73.4	40	70.1	30	24.8
60	56.6	50	94.5	50	79.9	40	29.9
		60	107.4	60	85.5	51	31.6
						60	34.8

C) Cape Verde Dust

Cape Verde Dust Repeat		Cape Verde Dust Repeat		Cape Verde Dust Repeat	
time / min	nmole Fe per g ash	time / min	nmole Fe per g ash	time / min	nmole Fe per g ash
0	0.0	0	0.0	0	0.0
5	8.6	5	13.5	3	4.5
10	10.5	15	15.5	7	5.3
15	12.7	21	18.5	10	8.3
22	14.8	26	19.6	13	9.1
28	16.4	31	23.1	16	10.0
33	18.7	36	24.1	19	7.9
39	19.7	41	25.7	22	8.1
44	21.0	46	28.0	25	11.6
49	23.4	51	27.8	28	12.2
56	24.4	56	27.8	31	12.7
60	27.8	60	29.9	34	13.2

Table S3: Glass composition of subduction zone and hotspot volcanic ash, determined by electron microprobe.

A) Subduction Zone Volcanic Ash	Sakura-Jima '86	Sakura-Jima '87	Sakura-Jima '99	Sakura-Jima '07
Glass composition	Dacite	Dacite	Dacite	Rhyolite
Collection Date	June 11, 1986	November 18, 1987	December 6, 1999	May, 2007
Eruption Type	Vulcanian	Vulcanian	Vulcanian	Vulcanian
Distance from crater	11 km	3 km E	11 km	3 km NW
SiO₂	68.54	66.56	69.58	72.74
TiO₂	0.79	0.80	1.14	0.93
Al₂O₃	14.35	13.91	13.01	13.17
FeO	3.64	5.14	5.64	3.87
MnO	0.08	0.12	0.11	0.06
MgO	0.41	1.21	0.73	0.30
CaO	3.58	3.92	3.30	2.34
Na₂O	4.72	3.95	3.84	3.41
K₂O	2.38	2.50	2.91	3.50
P₂O₅	0.25	0.22	0.30	0.27
Cl	0.05	0.08	0.07	0.04
SO₃	0.01	0.01	0.01	0.01
	Arenal '92	Arenal '93	Arenal '03	Arenal '04
Classification	Dacite	Dacite	Dacite	Rhyolite
Collection Date	July 22, 1992	1993	February 4, 2003	May 31, 2004
Eruption Type	Strombolian	Strombolian	Pyroclastic flows	Pyroclastic flows
Distance from crater	Unknown	Unknown	2 km	Unknown
SiO₂	68.54	67.54	68.28	73.32
TiO₂	0.93	1.03	0.96	1.01
Al₂O₃	12.38	12.23	12.25	11.64
FeO	5.63	6.39	6.19	3.64
MnO	0.14	0.16	0.17	0.09
MgO	0.80	1.10	0.99	0.37
CaO	2.83	3.42	3.11	1.42
Na₂O	4.54	4.27	4.43	4.34
K₂O	2.56	2.42	2.13	3.04
P₂O₅	0.43	0.42	0.33	0.19
Cl	0.10	0.13	0.15	0.08
SO₃	0.00	0.01	0.01	0.01
	Mt. Spurr '92	Turrialba 1864	Rabaul '02-1	Rabaul '02-2
Classification	Andesite	Trachydacite	Trachydacite to Rhyolite	Trachydacite to Rhyolite
Collection Date	August 18, 1992	1864	November 13- 14, 2002	November 15-23, 2002
Eruption Type	Sub-plinian	Strombolian	Vulcanian	Vulcanian
Distance from crater	120 km	Unknown	Unknown	Unknown
SiO₂	62.14	65.75	69.34	68.70
TiO₂	0.90	0.97	0.80	0.82
Al₂O₃	16.85	15.84	13.54	13.67
FeO	5.81	3.53	3.33	3.55
MnO	0.15	0.07	0.10	0.10
MgO	1.78	1.23	0.40	0.36
CaO	5.61	3.37	1.88	1.93
Na₂O	4.91	4.86	4.66	4.91
K₂O	1.58	4.05	4.29	3.96
P₂O₅	0.36	0.22	0.14	0.14
Cl	0.22	0.19	0.24	0.28
SO₃	0.02	0.01	0.01	0.01

	Popocatepetl '98-1	Popocatepetl '98-2	Popocatepetl '00-1	Popocatepetl '00-2
Classification	Rhyolite	Rhyolite	Rhyolite	Rhyolite
Collection Date	November 19, 1998	December 4, 1998	September 4, 2000	December 20, 2000
Eruption Type	Vulcanian	Vulcanian	Vulcanian	Vulcanian
Distance from crater	9 km NW	18.7 km NW	18.7 km NW	4 km NNW
SiO₂	76.75	74.88	75.53	78.44
TiO₂	0.66	0.58	0.72	0.61
Al₂O₃	12.18	13.23	11.68	12.17
FeO	1.24	1.46	2.11	1.34
MnO	0.01	0.03	0.02	0.02
MgO	0.08	0.11	0.26	0.06
CaO	0.81	1.22	0.89	0.93
Na₂O	4.18	4.77	3.88	4.53
K₂O	4.16	3.74	4.48	3.44
P₂O₅	0.07	0.05	0.12	0.07
Cl	0.01	0.01	0.04	0.01
SO₃	0.01	0.01	0.01	0.02
	Popocatepetl '00-3	Popocatepetl '01-1	Popocatepetl '01-2	Popocatepetl '03
Classification	Rhyolite	Rhyolite	Rhyolite	Rhyolite
Collection Date	December 29-30, 2000	January 22, 2001	July 5, 2001	July 19, 2003
Eruption Type	Vulcanian	Vulcanian	Vulcanian	Vulcanian
Distance from crater	32 km ENE	19 km SE	4 km NNW	65 km NW
SiO₂	77.53	75.27	74.84	76.74
TiO₂	0.75	0.67	0.77	0.85
Al₂O₃	12.98	12.42	12.79	11.86
FeO	1.57	2.13	2.27	1.88
MnO	0.02	0.03	0.05	0.01
MgO	0.18	0.30	0.47	0.13
CaO	1.37	1.09	1.17	0.45
Na₂O	3.90	4.16	4.03	3.48
K₂O	2.88	3.86	4.40	5.02
P₂O₅	0.10	0.07	0.12	0.10
Cl	0.01	0.06	0.02	0.03
SO₃	0.04	0.00	0.01	0.01
	Karymsky '05-4	Karymsky '05-8	Chaiten '08-1	Merapi '96
Classification	Rhyolite	Rhyolite	Rhyolite	Rhyolite
Collection Date	July 12, 2005	July 14-15, 2005	3-May-08	9. June. 2006
Eruption Type	Strombolian	Strombolian	Strombolian	Pyroclastic flow
Distance from crater	5 km SE	5 km SE	10 km from the summit	unknown
SiO₂	71.61	72.31	74.64	69.54
TiO₂	0.91	1.01	0.14	0.34
Al₂O₃	13.48	12.70	13.84	14.97
FeO	3.50	4.21	1.32	1.82
MnO	0.07	0.13	0.04	0.07
MgO	0.39	0.54	0.26	0.32
CaO	2.33	2.23	1.40	0.96
Na₂O	4.67	4.12	3.93	4.68
K₂O	2.95	2.79	3.01	5.63
P₂O₅	0.23	0.26	0.05	0.07
Cl	0.09	0.11	0.10	0.07
SO₃	0.01	0.01	0.01	

B) Hot Spot Volcanic Ash

	Hekla '47	Hekla '70	Hekla '80	Pu'u'oo '05
Classification	Dacite	Andesite to Trachyandesite	Andesite	Andesite
Collection Date	1947	1970	1980	September 16, 2005
Eruption Type	Plinian to sub-plinian	Plinian to sub-plinian	Plinian to sub-plinian	Ash explosion
Distance from crater	32 km SSW	45 km NW	12 km N	Unknown
SiO₂	58.71	56.01	56.12	51.35
TiO₂	1.80	1.96	2.18	2.47
Al₂O₃	12.84	14.41	13.88	13.15
FeO	12.34	10.83	11.46	10.61
MnO	0.28	0.32	0.29	0.18
MgO	3.06	2.59	2.71	6.36
CaO	6.71	6.52	6.38	11.14
Na₂O	3.93	4.30	3.98	2.58
K₂O	1.53	1.39	1.63	0.44
P₂O₅	0.77	0.84	0.93	0.21
Cl	0.04	0.04	0.04	0.01
SO₃	0.08	0.07	0.07	0.03

Table S4: Summary of the Central American Volcanic Arc (CAVA) tephra flux over the past 191 ka, based on *Kutterolf et al.*, [2008].

Volcano Complex/Tephra	Source Volcano	Age (ka)	Proximal Tephra volume (km ³)	Distal tephra volume (km ³)	Tephra composition	Total tephra volume	Proximal tephra mass (10 ¹⁶ g)	Distal tephra mass (10 ¹⁶ g)
Terra Blanca Joven	Ilopango Caldera	1.6	32	38.6	felsic	70.6	4.7	5.7
Masaya Tuff/ Ticuantepo Lapilli	Masaya Caldera	1.8	4.8	1.8	mafic	6.6	0.8	0.3
Chiltepe Tephra	Chiltepe complex	1.9	3.9	14	felsic	17.9	0.6	2.1
Masaya Triple Layer/La Concepcio'n Tephra	Masaya Caldera	2.1	0.8	2.6	mafic	3.4	0.1	0.4
San Antonio Tephra	Masaya Caldera	6	0.5	13	mafic	13.5	0.1	2.2
Upper Apoyeque Tephra	Chiltepe complex	12.4	2.2	2.1	felsic	4.3	0.3	0.3
Lower Apoyeque Tephra	Chiltepe complex	17	0.8	3.1	felsic	3.9	0.1	0.5
Upper Ometepe Tephra	Concepcio'n volcano	19	2.9	2.3	felsic	5.2	0.4	0.3
Mafic Cosigu'ina tephra	Cosigu'ina volcano	21-23	1.5	4.5	mafic	6.0	0.3	0.8
Upper Apoyo Tephra	Apoyo Caldera	24.5	7.2	35.7	felsic	42.9	1.1	5.2
Lower Apoyo Tephra	Apoyo Caldera	25	3	3.5	felsic	6.5	0.4	0.5
Pinos Altos Tephra	Ayarza Caldera	23	6.3	1	felsic	7.3	0.9	0.1
Terra Blanca 4 Tephra	Ilopango Caldera	~36	25.9	10.4	felsic	36.3	3.8	1.5
Mixta Tephra	Ayarza Caldera	39	2.9	6.1	felsic	9.0	0.4	0.9
Conacaste Tephra	Coatepeque Caldera	~51	3	1.5	felsic	4.5	0.4	0.2
E-fall Tephra	Amatitla'n Caldera	51	5	40	felsic	45.0	0.7	5.9
Congo Tephra	Coatepeque Caldera	~53	5.5	12.6	felsic	18.1	0.8	1.9
Fontana Tephra	Las Nubes Caldera	60	1.3	1.4	mafic	2.7	0.2	0.2
Twins/A-fall Tephra	Berlin-Pacayal-Volcan group	60	1	9.4	felsic	10.4	0.1	1.4
Arce Tephra	Coatepeque Caldera	75	9.6	6.6	felsic	16.2	1.4	1.0
Blanca Rosa Tephra	Berlin-Pacayal-Volcan group	75	1.9	2.7	felsic	4.6	0.3	0.4
Los Chocoyos Tephra	Atitla'n Caldera	84	128	573	felsic	701.0	18.8	84.2
T-fall Tephra	Amatitla'n Caldera	119	8	9	felsic	17.0	1.2	1.3
W-fall Tephra	Atitla'n Caldera	158	13.6	9.7	felsic	23.3	2.0	1.4
L-fall Tephra	Amatitla'n Caldera	191	18.5	44.7	felsic	63.2	2.7	6.6
Total			290.1	810.7		1139.4	42.8	125.4

*Masses are calculated using average densities of 2100 kg/m³ for felsic and 2400 kg/m³ for mafic tephra.

Chapter III

**Geochemical evidence of oceanic iron fertilization
by the Kasatochi 2008 volcanic eruption and evaluation
of the potential impacts on sockeye salmon population.**

Geochemical evidence of oceanic iron fertilization by the Kasatochi 2008 volcanic eruption and evaluation of the potential impacts on sockeye salmon population.

N. Olgun ^{1,2}, S. Duggen ³, B. Langmann ⁴, M. Hort ⁴, C. F. Waythomas ⁵, L. Hoffmann ⁶ and P. Croot ^{2,7}

¹ Dynamics of the Ocean Floor Division, Leibniz-Institute of Marine Sciences, IFM-GEOMAR, Kiel, Germany.

² Marine Biogeochemistry Division, Leibniz-Institute of Marine Sciences, IFM-GEOMAR, Kiel, Germany.

³ A. P. Møller Skolen, Upper Secondary School and Sixth Form College of the Danish National Minority in Northern Germany, Schleswig, Germany.

⁴ Institute of Geophysics, University of Hamburg, KlimaCampus, Hamburg, Germany.

⁵ U.S. Geological Survey Alaska Volcano Observatory, Anchorage, United States.

⁶ Department of Chemistry, University of Otago, Dunedin, New Zealand.

⁷ Plymouth Marine Laboratory, Plymouth, United Kingdom.

Submitted to Marine Ecology Progress Series

Corresponding author: nolgun@ifm-geomar.de (N. Olgun)

Keywords: Kasatochi volcanic eruption, ashfall, iron limitation, silicate limitation, Gulf of Alaska, sockeye salmon.

Abstract

A century record of 35 million sockeye salmon returned in late summer 2010 to the Fraser River located in the Pacific Coast of Canada, after three years of poor returns of less than 2 million. It was speculated that the Kasatochi volcanic eruption in August 2008 in the North Pacific spurred the salmon boom by first inducing a phytoplankton bloom, which in turn increased the abundance of zooplankton on which the salmon feed. Here we report the first ash leaching experiments with volcanic ash from the Kasatochi 2008 eruption in natural seawater. Our results suggest that the Kasatochi eruption increased the iron concentrations in the surface water column of the Alaskan Gyre by 2.0-2.8 nM, an amount that has been shown to induce diatom bloom in this iron limited region before. The release of macronutrients was insignificant compared to the usual background concentrations in the water, and can therefore not have contributed to the observed phytoplankton bloom. Our study gives evidence that the iron content released from the volcanic ash was indeed sufficient to cause the observed phytoplankton bloom in the eastern North Pacific, which was likely the first of multiple interdependent processes in the oceanic food-web dynamics ending with increased sockeye salmon populations in the Gulf of Alaska and the neighboring rivers.

Introduction

The North Pacific is a high-nutrient and low-chlorophyll (HNLC) ocean region where the phytoplankton growth is known to be limited by iron (Martin & Fitzwater 1988, Boyd et al. 1996, Boyd & Harrison 1999) and sporadically by silicate (Wong & Mearns 1999, Whitney et al. 2005). Episodic increases of aeolian dust input have been observed to increase primary production in the North Pacific (Young et al. 1991). The casual connection between the aeolian iron input and the diatom production over longer time-scales (e.g., Quaternary) has been suggested by the sediment core studies in the region (McDonald & Pedersen 1999).

Oceanic deposition of volcanic ash has recently been considered as an important nutrient source for the surface ocean (Frogner et al. 2001, Duggen et al. 2007, Jones & Gislason 2008, Hamme et al. 2010, Langmann et al. 2010b, Lin et al. 2011, Olgun et al.

2011). Deposition of volcanic ash during explosive eruptions can therefore stimulate the phytoplankton growth by releasing especially iron and other nutrients into the seawater, and eventually affect global carbon-cycle and the marine food-web.

The North Pacific region contains two of the world's most active volcanic belts. More than 150 explosive active volcanoes in the Kurile-Kamchatka and Aleutian arcs typically create at least 10 explosive, ash-producing eruptions in each year (Siebert & Simkin 2002). It has recently shown that atmospheric deposition of volcanic ash is one of the major iron sources in the North Pacific Ocean, due to high flux of ash related to active volcanism in the region (Olgun et al. 2011).

During July-August 2008 three explosive volcanic eruptions occurred in the remote Aleutian Islands of Alaska; on 12 July at Okmok, 21 July at Cleveland, and on 7-8 August at Kasatochi volcano (Waythomas et al. 2008, Larsen et al. 2009, Langmann et al. 2010b). The Kasatochi eruption (Fig. 1) was the largest (volcanic explosivity index of 4) of the three, and produced 10^{15} grams of ash and several ash plumes that reached as high as 18 km above the sea level (Langmann et al. 2010a, Waythomas et al. 2010).

An unusual and extensive phytoplankton bloom in the North Pacific and Gulf of Alaska started a few days after the Kasatochi eruption and has been related to iron-fertilization by Kasatochi ash from the 2008 eruption (Fig. 1) (Hamme et al. 2010, Langmann et al. 2010b). Two years after the Kasatochi eruption, a century record (of 35 million) sockeye salmon returned back to the Fraser River, Canada (Fig. 1) (Larkin 2010). The mystery behind this dramatic number resulted in scientists speculating about possible causes including the effects of the volcanic eruption (Jones 2010, Parsons 2010).

Lack of other nutrient sources (e.g., desert dust from Asia, mesoscale eddies) together with satellite data (Fig. 1) suggest that there is a strong link between the Kasatochi ash fallout and the subsequent phytoplankton bloom in the eastern North Pacific (Hamme et al. 2010, Langmann et al. 2010a, Langmann et al. 2010b). However, this possible link remained speculative as it was unknown if the Kasatochi eruption released sufficient amounts of iron into the seawater. Here we present data from iron and macronutrient dissolution experiments with volcanic ash from the Kasatochi 2008 eruption. We further discuss the potential oceanic food-web dynamics affected by the Kasatochi eruption that indirectly increased the salmon population in 2010 in the Gulf of

Alaska and neighboring rivers in the region.

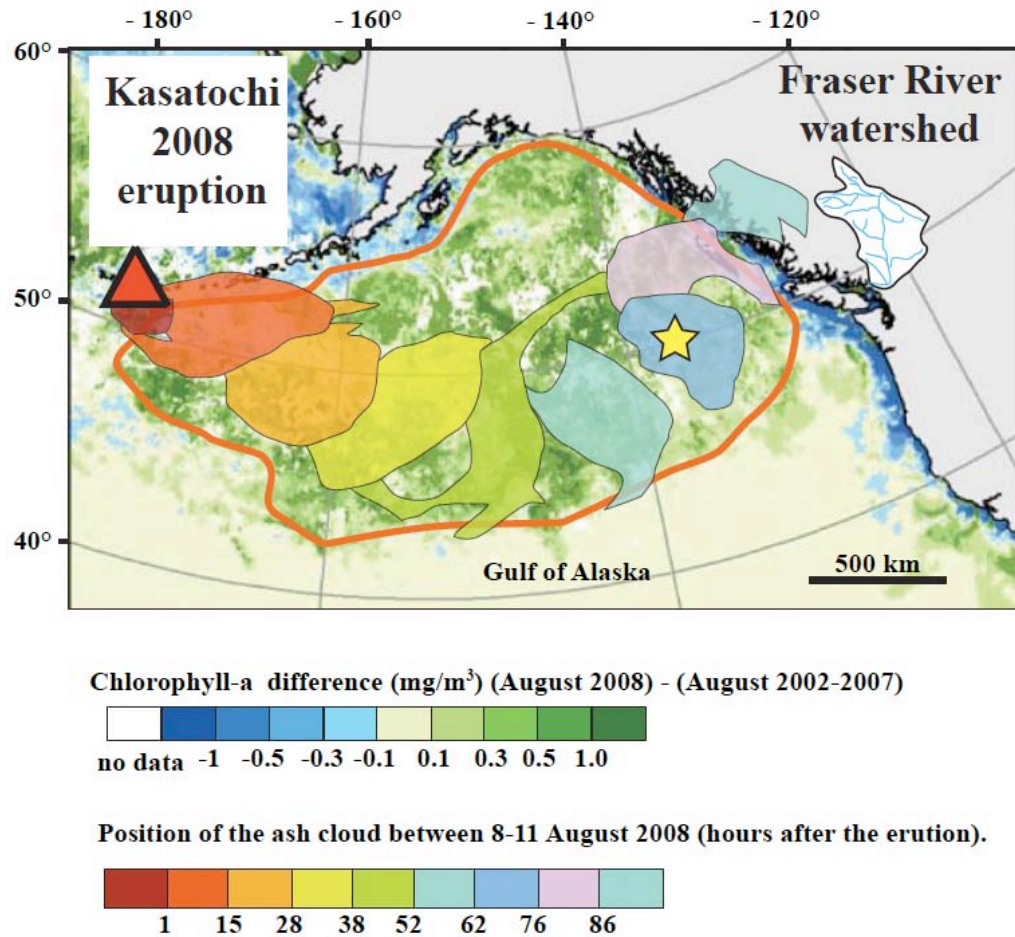


Figure 1: MODIS-Aqua map based on (Langmann et al. 2010b) showing relative increase in chlorophyll-a (mg/m^3) concentrations in August 2008 most likely related to the Kasatochi (red triangle) volcanic eruption on 7th and 8th of August 2008. The position of ash cloud is shown in the colored areas. The bloom area is indicated in a red line. The chlorophyll-a concentrations are the monthly mean August 2008 minus the background monthly mean in the last six years (from August 2002 to August 2007). Also shown are the location of Ocean Station Papa (OSP) (yellow star at 50°N 145°W) and Fraser River watershed area in the Pacific coast of Canada.

Samples and methods

Most of the ash produced by the Kasatochi eruption was deposited in the ocean (Waythomas et al. 2010). The deposits on the Kasatochi and neighboring islands, which are readily available, were however exposed to rain and were wet when sampled (Waythomas et al. 2010). A fishing boat transiting the area about 13 km southwest of the Kasatochi Island during the eruption and received heavy ash fall on 7th of August. Crewmembers on the boat collected dry samples and provided them to the Alaska Volcano Observatory. The sample analyzed in this study came from this fishing boat (Waythomas et al. 2010). The grain-size of the sample was relatively coarse and composed of particles greater than ash-size (ash-size is < 2 mm). We wished to analyze the fine fraction of the tephra deposit and separated the coarser fraction using 2 mm metal-free plastic sieves.

Fe-release experiments were performed with 50 mg portions of the ash sample and 20 mL of natural seawater using an established voltammetric method with competing Fe-binding ligand (Croot & Johansson 2000), largely mimicking the dissolution of volcanic ash through dry deposition in the surface ocean (Duggen et al. 2007, Olgun et al. 2011). Macronutrient-release expressed as total fixed-nitrogen (expressed as NO_3^-), phosphate (PO_4^{3-}) and reactive silica (SiO_2) was examined by means of leaching experiments. Agitation times in low-nutrient seawater of 85 minutes and 20 hours agitation were followed by rapid filtration through a 5 μm mesh PTFE filter (Sartorius). The concentrations of macro-nutrients in the seawater were measured by standard routine photometry.

Results

Repeat measurements suggest the ash particles mobilize ~61-83 nmol of iron per gram of ash within one hour (Fig. 2). The Fe-release range from Kasatochi ash is in the lower third of the range (35-340 nmol/g ash) found for ash from subduction zone volcanoes like Kasatochi (Duggen et al. 2007, Olgun et al. 2011). The results of the macro-nutrient experiments show that within the first hour of contact with seawater

Kasatochi ash releases 374 nmol nitrate (as total fixed-N), 5 nmol phosphate and 170 nmol of silica per gram of ash (Table 1).

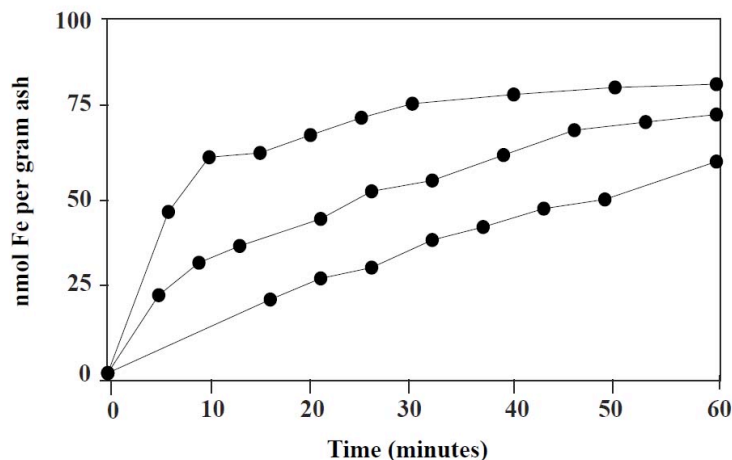


Figure 2: Release of iron from volcanic ash from Kasatochi 2008 eruption in natural seawater, measured by means of Cathodic Stripping Voltammetry.

After the day-scale interaction of ash with natural seawater, 410 nmol nitrate, 6 nmol phosphate, and 585 nmol of silica were released per gram of ash (Table 1). Highest leaching rates were seen for nitrate and silica, while concentration of phosphate stayed constant during 20-hours experiment.

These data likely reflect a minimum limit since the ash sample was coarse and collected near the volcano. Small particle-size and cloud-water interaction may enhance the solubility of surface compounds and hence the nutrient-release of volcanic ash particles in the seawater (Duggen et al. 2010).

Table 1: Estimated new supply of nutrients in the eastern North Pacific Ocean related to the Kasatochi volcanic ash fallout in August 2008, based on the nutrient release from Kasatochi ash.

	Nutrient release by Kasatochi ash in the seawater (nmol/g ash)	Initial nutrient concentrations in the North Pacific Ocean (nM)	New supply by the Kasatochi ash fall (nM) ^c
Iron	61-83	<0.05 ^a	2.0-2.8 ^d
Nitrate (NO ₃ ⁻)	374-410	5,000-10,000 ^b	13-14
Phosphate (PO ₄ ³⁻)	5-6	100-1,000 ^b	<0.2
Silica (SiO ₂)	170-585	5,000-15,000 ^b	6-20

^a (Nishioka et al. 2001).

^b (Levitus et al. 1994, De Baar & De Jong 2001, Tsuda et al. 2003, Boyd et al. 2007).

^c based on the nutrient-release from Kasatochi ash calculated over the fertilized area of 1.5×10^6 km² in the Gulf of Alaska (Fig. 1) and a mixed layer of 20 m (<http://www.pac.dfo-mpo.gc.ca/science/oceans/Argo/Alaska-Argo-eng.htm>).

^d Above the threshold (of 2 nM iron) for stimulating diatom bloom in the iron-limited regions (Wells 2003).

Discussion

Nutrient supply by Kasatochi volcanic ash fallout

The background macro-nutrient concentrations in the eastern North Pacific ranges between 5-10 µM nitrate, 0.1-1 µM phosphate and 5-15 µM silica (Levitus et al. 1994, De Baar & De Jong 2001, Tsuda et al. 2003, Boyd et al. 2007), whereas the dissolved iron concentrations are found to be very low, less than 0.05 nM (Levitus et al. 1994, Nishioka et al. 2001). The input of small amounts of iron can therefore have large impacts on the marine primary production in the Fe-depleted waters of the North Pacific and the Gulf of

Alaska.

The 2008 Kasatochi eruption may have resulted in ash fall-out over a wide area of about 1.5×10^6 km² in the northeast Pacific Ocean (Fig. 1) (Hamme et al. 2010, Langmann et al. 2010a, Langmann et al. 2010b). The phytoplankton bloom started a few days after the eruption and the effect was detectable for over two months until the end of September 2008 (Hamme et al. 2010, Langmann et al. 2010b). The mean chlorophyll-a values in August 2008 were 2-3 times higher than the usual values for this time of the year (Hamme et al. 2010). Ship-board measurements in the southern part of the bloom area showed that the phytoplankton was dominated by large diatoms (Hamme et al. 2010). This is consistent with Fe-enrichment incubation experiments at the Ocean Station Papa (OSP) (Boyd et al. 1996).

The increase of iron-levels in the ash-fertilized region can be inferred from combining our iron-release data (Fig. 2) with constraints for the erupted mass of $\sim 10^{15}$ g ash based on a one dimensional volcanic model (Langmann et al. 2010b), the area of the ash fall region (Fig. 1), and the ocean mixed layer depth of 20 m (<http://www.pac.dfo-mpo.gc.ca/science/oceans/Argo/Alaska-Argo-eng.htm>). The major error rises from the actual volume of the ash deposit, which is unknown since most of the ash was deposited in the ocean. The satellite data indicate ash aloft over a broad area (Hamme et al. 2010, Langmann et al. 2010a, Langmann et al. 2010b), but this does not mean that ash fallout occurred in the same area, and it is likely that the ash fallout was un-uniform over the fertilized area (Langmann et al. 2010a).

Given the uncertainties involved, assuming a homogenous distribution of ash over the 20 m water column, our calculations suggest that the dry deposition of Kasatochi ash might have added 2.0-2.8 nM iron to the ash fall region in the northeast Pacific (Table 1). Mesoscale iron-enrichment experiments demonstrate that a raise of about 2-3 nM of iron is enough to trigger diatom blooms in HNLC regions (Tsuda et al. 2003, Wells 2003), suggesting that iron input from the Kasatochi ash was sufficient to stimulate the evidenced massive phytoplankton bloom in the Gulf of Alaska (Hamme et al. 2010, Langmann et al. 2010a, Langmann et al. 2010b).

Diatoms significantly contribute to the carbon uptake in the global ocean. Based on the pCO₂-decrease (of 25 μ atm) at the Ocean Station Papa (OSP, Fig. 1) in August

2008, the C-drawdown associated with the diatom bloom (extrapolated over the fertilized area) has been previously calculated to be $\sim 6-17 \times 10^{12}$ g C (Hamme et al. 2010). Depending on the phytoplankton species and the seawater iron concentrations, the C:Fe ratio of the phytoplankton may vary widely (from $\sim 10^6$ to $\sim 10^3$) (Sunda & Huntsman 1995).

Given a typical C:Fe ratio of 10^4 for iron uptake under 1-3 nM iron concentrations (Sunda & Huntsman 1995), the C-drawdown based on the new Fe-release data (Fig. 2) is $34-46 \times 10^{12}$ g C, which is about 3-6 times higher than of the actual estimated C-drawdown (Hamme et al. 2010). Considering the uncertainties related to the precipitation and complexation of iron, and utilization of iron by other phytoplankton groups and bacteria, the actual C-drawdown related to the north Pacific bloom could be derived by the Fe-input from Kasatochi ash (Hamme et al. 2010).

The large increase in phytoplankton stock would accompany by strong utilization of macronutrients, to a greater extent in the North Pacific compared to the other HNLC regions (Tsuda et al. 2003). High demand of silica in the fertilized region was indicated by reduced silicic acid concentrations during August 2008 in the eastern North Pacific (Hamme et al. 2010). Based on our data, new supply of macro-nutrients related to the volcanic ashfall in the region are 13-14 nM nitrate, <0.2 nM phosphate and 6-20 nM silica (Table 1). Background concentrations of macro-nutrients (Table 1) are higher compared to the new supply by the ashfall suggesting that the impact of macro-nutrient input from Kasatochi ash for the marine primary production is probably marginal.

Did sockeye salmon population benefit from the 2008 Kasatochi volcanic eruption?

After twenty years of decline in sockeye population, about 35 million sockeye salmon returned in 2010 to the Fraser River in Canada, the largest return since 1913 and seventeen times higher than the average (Larkin 2010). The enigmatic sockeye run in 2010 has been linked to an increase in marine survival rates related to increased food-supply in the ocean in summer 2008 (Parsons 2010).

Typically 95% of the Fraser River sockeye (*Orcorhyncus nerka*) has four-year life cycle spending 2 years in the ocean before returning to nursery rivers to spawn and die (Foerster 1968, Cass & Wood 1994). Unlike other salmon species, young sockeye are not

often seen inshore waters once they reach the ocean (Miller & Brannon 1982), and sockeye travel most notably towards the northern Alaskan and Arctic waters (Hartt 1980, Brannon 1982). On average only about 10% (from 2% to 13%) of the seaward sockeye migrants return back to the nursery rivers (Thorne & Ames 1987, Quinn 2004).

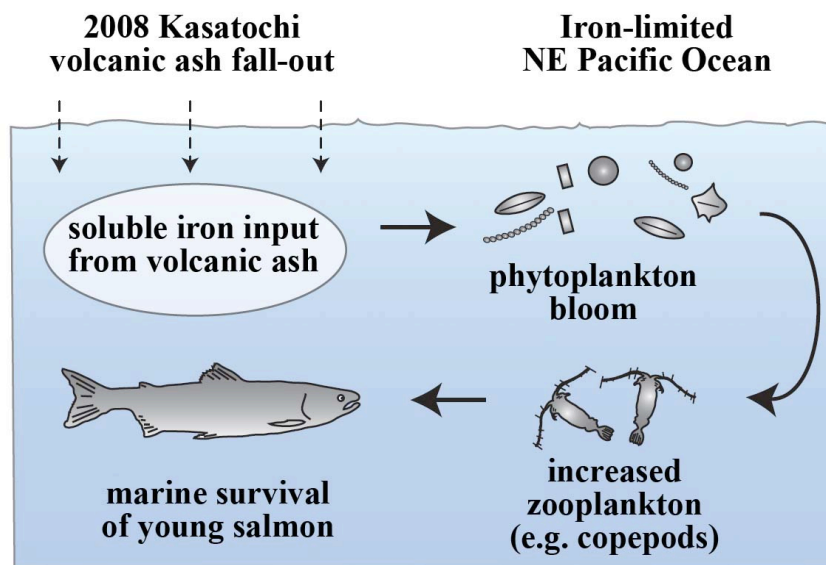


Figure 3: The simple sketch illustrates the casual chain within the marine food-web after the 2008 Kasatochi volcanic eruption. The processes range from volcanic ash-induced surface ocean iron-fertilization, through phytoplankton and zooplankton bloom to sockeye salmon feeding and marine survival of young sockeye in the ocean.

The most critical life-stage of the young sockeye is the early marine stage. About 90% of the sockeye mortality in the ocean occurs between July and October, during the first four-months in the ocean (Hartt 1980, Furnell & Brett 1986). In August-September 2008, there was an unusual increase in mesozooplankton abundance near the OSP located in the bloom area (Fig. 1) dominated by large copepods, compared to the same months in 2000-2007 and 2009 (Hamme et al. 2010). Increased abundance of larger copepods has been related to the feeding closer to the surface ocean due to the diatom bloom (Hamme et al. 2010).

Juvenile sockeye salmon feed extensively on zooplankton, preferentially larger zooplankton (Foerster 1968), which were abundant in the bloom region in the North

Pacific (Hamme et al. 2010). Since the timing of the zooplankton bloom in late summer 2008 matches with the critical life stage of the sockeye salmon, it is therefore, very plausible that the diatom bloom related to the Kasatochi eruption stimulated the ocean food-web and provided a food-source for zooplankton, and thus making the link to the sockeye salmon survival (Fig. 3).

Young salmon released into the zooplankton bloom survives better compared to poor zooplankton conditions (Cooney et al. 1995, Cross et al. 2008). Calm food conditions increase the body-growth rate of salmon so that the salmon builds up stronger bodies, which affects the overall marine survival (Beauchamp et al. 2007, Duff 2009). The in-direct link between the marine survival of sockeye and algal biomass was also previously indicated in the reports of the Pacific Salmon Commission by a strong positive correlation of these parameters ($r^2=0.87$) (Peterman et al. 2010).

Massive sockeye returns in 2010 in Fraser River were four-year old fish (Commission July 22, 2011 2011). In 2011, low numbers sockeye returned to Fraser River (~1.8 million), however, with a large proportion of five-year old fish (Commission July 22, 2011) supporting the hypothesis of increased marine survival rates in 2008 that is likely associated to the diatom bloom in North Pacific in summer 2008 (Fig. 3).

Volcanic eruptions and ecosystem response in the North Pacific Ocean

Volcanic eruptions may have influenced the marine food-web in the North Pacific and neighboring regions in the past (Duggen et al. 2010). The fertilizing potential of volcanic eruptions have been evidenced in North Pacific Ocean (e.g., Miyake-Jima 2000, Anatahan 2003) (Uematsu et al. 2004, Lin et al. 2011), and the neighboring rivers and lakes (e.g., Mt St. Helens 1980) (Smith & White 1985). Interestingly, one of the largest salmon runs in 1958 (Groot & Quinn 1987) followed the large eruption of Benzymjanny volcano in Kamchatka that started on mid November 1955 (Gorshkov 1959).

Ash fallout from 1912 Katmai-Novarupta eruption in Alaska has been suggested to fertilize the nearby lakes (by ash-derived phosphorus) (Eicher & Rousefell 1957). However, the direct impact of the extreme ash load from Katmai-Novarupta eruption was the initial mortality of pre-smolts in the local rivers due to damage of the gills of the salmon (Eicher & Rousefell 1957, Duggen et al. 2010). Despite the smaller number of

spawning fish in the rivers and lakes after the Katmai-Novarupta eruption, numbers of sockeye returned in the following four years were as large as the pre-eruption, indicating a rapid recovery possibly associated with the favorable ocean conditions (Eicher & Rousefell 1957).

Conclusions

The role of volcanic eruptions in the oceanic biogeochemical cycles is still not fully understood but there is increasing evidence of their significant impact on marine primary production. Our study shows that the iron release from the Kasatochi volcanic ash is sufficient to induce large-scale phytoplankton blooms with potentially significant implications for higher trophic levels as in this case the sockeye salmon population. However, potential varying ecologic impacts of volcanic ash in fresh waters, in coastal regions and in the open ocean require more scientific attention in order to evaluate the importance for oceanic food web dynamics.

References

- Beauchamp DA, Cross AD, Armstrong JL, Myers KW, Moss JH, Boldt JL, Haldorson LJ (2007) Bioenergetic responses by Pacific salmon to climate and ecosystem variation. *North Pacific Anadromous Fish Commission Bulletin* 4:257–269
- Boyd P, Harrison PJ (1999) Phytoplankton dynamics in the NE subarctic Pacific. *Deep Sea Research II* 46:2405-2432
- Boyd PW, Jickells T, Law CS, Blain S, Boyle EA, Buesseler KO, Coale KH, Cullen JJ, de Baar HJW, Follows M, Harvey M, Lancelot C, Levasseur M, Owens NPJ, Pollard R, Rivkin RB, Sarmiento J, Schoemann V, Smetacek V, Takeda S, Tsuda A, Turner S, Watson AJ (2007) Mesoscale Iron Enrichment Experiments 1993–2005: Synthesis and Future Directions. *Science* 315:612-617
- Boyd PW, Muggli DL, Varela DE, Goldblatt RH, Chretien R, Orians KJ, Harrison PJ (1996) In vitro iron enrichment experiments in the NE subarctic Pacific. *Marine Ecology Progress Series* 136:179–193
- Brannon EL (1982) Orientation mechanisms of homing salmonids. In: Brannon EL, Salo EO (eds) *Proceedings of the salmon and trout migratory behavior symposium*. University of Washington Press, Seattle, p 219-227

- Cass AJ, Wood CC (1994) Evaluation of the depensatory fishing hypothesis as an explanation for population cycles in Fraser River sockeye salmon (*Oncorhynchus nerka*). *Canadian Journal of Fisheries and Aquatic Sciences* 51:1839-1854
- Commission PS (July 22, 2011) News Release
www.gulftrollers.com/news/PSC_July_22.pdf
- Cooney RT, Willette TM, Sharr S, Sharp D, Olsen J (1995) The effect of climate on North Pacific pink salmon (*Oncorhynchus gorbuscha*) production: examining some details of a natural experiment. *Canadian Special Publication of Fisheries and Aquatic Sciences* 121:475–482
- Croot P, Johansson M (2000) Determination of iron speciation by cathodic stripping voltammetry in seawater using the competing ligand 2-(2-Thiazolylazo)-*p*-creosol (TAC). *Electroanalysis* 12:565-576
- Cross AD, Beauchamp DA, Myers KW, Moss JH (2008) Early marine growth of pink salmon in Prince William Sound and the coastal Gulf of Alaska during years of low and high Survival. *Transactions of the American Fisheries Society* 137:927-939
- De Baar HJW, De Jong JTM (2001) Distributions, sources and sinks of iron in seawater. In: Turner DR, Hunter KA (eds) *The Biogeochemistry of Iron in Seawater*. Wiley, Chichester, UK, p 212-215
- del Moral R (2010) The Importance of Long-Term Studies of Ecosystem Reassembly after the Eruption of the Kasatochi Island Volcano. *Arctic, Antarctic, and Alpine Research* 42:335-341
- Drew GS, Dragoo GS, Renner M, Piatt JF (2010) At-sea observations of marine birds and their habitats before and after the 2008 eruption of Kasatochi Volcano, Alaska. *Arctic, Antarctic, and Alpine Research* 42:325-334
- Duff E (2009) Factors during early marine life that affect smolt-to-adult survival of ocean-type Puget Sound Chinook salmon (*Oncorhynchus tshawytscha*). University of Washington
- Duggen S, Croot P, Schacht U, Hoffmann L (2007) Subduction zone volcanic ash can fertilize the surface ocean and stimulate phytoplankton growth: Evidence from biogeochemical experiments and satellite data. *Geophysical Research Letters* 34

- Duggen S, Olgun N, Croot P, Hoffmann L, Dietze H, Teschner C (2010) The role of airborne volcanic ash for the surface ocean biogeochemical iron-cycle: a review. *Biogeosciences* 7
- Eicher GJ, Rousefell GA (1957) Effects of lake fertilization by volcanic activity on abundance of salmon. *Advancing the Science of Limnology and Oceanography* 2:70-76
- Foerster RE (1968) The sockeye salmon, *Oncorhynchus nerka*. *Bulletin of Fisheries Research Board of Canada* 162:422 pp
- Frogner P, Gislason SR, Óskarsson N (2001) Fertilizing potential of volcanic ash in ocean surface water. *Geology* 29:487-490
- Furnell DJ, Brett JR (1986) Model of monthly marine growth and natural mortality for Babine Lake sockeye salmon (*Oncorhynchus nerka*). *Can J Fish Aquat Sci* 43:999-1004
- Gorshkov GS (1959) Gigantic eruption of the volcano Bezymianny. *Bulletin of Volcanology* 20,:77-109
- Groot C, Quinn TP (1987) Homing migration of sockeye salmon, *Oncorhynchus nerka*, to the Fraser River. *Fishery Bulletin* 85:455-469
- Hamme RC, Webley PW, Crawford WR, Whitney FA, DeGrandpre MD, Emerson SR, Eriksen CC, Giesbrecht KE, Gower JFR, Kavanaugh MT, Angelica PM, Sabine CL, Batten SD, Coogan LA, Grundle DS, Lockwood D (2010) Volcanic ash fuels anomalous plankton bloom in subarctic northeast Pacific. *Geophysical Research Letters* 37
- Hartt AC (1980) Juvenile salmonids in the oceanic ecosystem: the critical first summer. In: McNeil WJ, Himsworth DC (eds) *Symposium on salmonid ecosystems of the North Pacific*. Oregon State University Press, Corvallis, p 25-57
- Jones MT, Gislason SR (2008) Rapid releases of metal salts and nutrients following the deposition of volcanic ash into aqueous environments. *Geochimica et Cosmochimica Acta* 72:3661-3680
- Jones N (2010) Sparks fly over theory that volcano caused salmon boom. *Nature News*

- Langmann B, Zakšek K, Hort M (2010a) Atmospheric distribution and removal of volcanic ash after the eruption of Kasatochi volcano: A regional model study. *Journal of Geophysical Research* 115
- Langmann B, Zakšek K, Hort M, Duggen S (2010b) Volcanic ash as fertiliser for the surface ocean. *Atmospheric Chemistry and Physics* 10:3891–3899
- Larkin K (2010) Canada sees shock salmon glut. *Nature*
- Larsen J, Neal C, Webley P, Freymueller J, Haney M, Mc-Nutt S, Schneider D, Prejean S, Schaefer J, Wessels R, Rabitti S (2009) Eruption of Alaska volcano breaks historic pattern. *EOS* 90:173–174
- Levitus S, Burgett R, Boyer T (1994) Nutrients NOAA Atlas NESDIS, Vol 3. US Department of Commerce, Washington, DC.
- Lin II, Hu C, Li YH, Ho TY, Fischer TP, Wong GTF, Wu J, Huang CW, Chu DA, Ko DS, Chen JP (2011) Fertilization potential of volcanic dust in the low-nutrient low-chlorophyll western North Pacific subtropical gyre: Satellite evidence and laboratory study. *Global Biogeochemical Cycles* 25
- Martin JH, Fitzwater SE (1988) Iron deficiency limits phytoplankton growth in the northeast Pacific subarctic. *Nature* 331:341-343
- McDonald D, Pedersen TF (1999) Multiple late Quaternary episodes of exceptional diatom production in the Gulf of Alaska. *Deep-Sea Research II* 46:2993-3017
- Miller RJ, Brannon EL (1982) The origin and development of life history patterns in Pacific salmonids. In: Brannon EL, Salo EO (eds) *Proceedings of the salmon and trout migratory behavior symposium*. University of Washington Press, Seattle, p 296-309
- Nishioka J, Takeda S, Wong C, Johnson WK (2001) Size-fractionated iron concentrations in the northeast Pacific Ocean: Distribution of soluble and small colloidal iron. *Marine Chemistry* 74:157-179
- Olgun N, Duggen S, Croot PL, Delmelle P, Dietze H, Schacht U, Óskarsson N, Siebe C, Auer A (2011) Surface ocean iron fertilization: The role of airborne volcanic ash from subduction zone and hotspot volcanoes and related iron-fluxes into the Pacific Ocean. *Global Biogeochemical Cycles* 25
- Parsons TR (2010). In: Bay B (ed) *Cohen Commission Public Submission #0264*

- Peterman RM, Marmorek D, Beckman B, Bradford M, Lapointe M, Mantua N, Riddell BE, Scheuerell M, Staley M, Wieckowski K, Winton JR, Wood CC (2010) Synthesis of evidence from a workshop on the decline of Fraser River sockeye., Pacific Salmon Commission, Vancouver, B.C.
- Quinn TP (2004) The behavior and ecology of Pacific salmon and trout., Vol. University of Washington Press, Seattle, Washington
- Siebert L, Simkin T (2002) Volcanoes of the world: An illustrated catalog of Holocene Volcanoes and their Eruptions. Smithsonian Institution. Global Volcanism Program Digital Information Series, GVP-3
- Smith MA, White M (1985) Observations on lakes near Mount St. Helens: Phytoplankton. *Journal Arch Hydrobiology* 104:345-363
- Sunda WG, Huntsman SA (1995) Iron uptake and growth limitation in oceanic and coastal phytoplankton. *Marine Chemistry* 50:189-206
- Thorne RE, Ames JJ (1987) A note on variability of marine survival of sockeye salmon (*Oncorhynchus nerka*) and effects of flooding on spawning success. *Canadian Journal of Fisheries and Aquatic Sciences* 44:1791-1795
- Tsuda A, Takeda S, Saito H, Nishioka J, Nojiri Y, Kudo I, Kiyosawa H, Shiimoto A, Imai K, Ono T, Shimamoto A, Tsumune D, Yoshimura T, Aono T, Hinuma A, Kinugasa M, Suzuki K, Sohrin Y, Noiri Y, Tani H, Deguchi Y, Tsurushima N, Ogawa H, Fukami K, Kuma K, Saino T (2003) A Mesoscale Iron Enrichment in the Western Subarctic Pacific Induces a Large Centric Diatom Bloom. *Science* 300: 958-960
- Uematsu M, Toratani M, M. K, Narita Y, Senga Y, Kimoto T (2004) Enhancement of primary productivity in the western North Pacific caused by the eruption of the Miyake-jima volcano. *Geophysical Research Letters* 31:1-4
- Waythomas CF, Schneider DJ, Prejean SG (2008) The 2008 eruption of Kasatochi volcano, Central Aleutian Islands: Reconnaissance observations and preliminary physical volcanology. *Eos Transactions AGU Fall Meeting*
- Waythomas CF, Scott WE, Prejean SG, Schneider DJ, Izbekov P, Nye CJ (2010) The August 7-8 eruption of Kasatochi volcano, central Aleutian Islands, Alaska. *Journal of Geophysical Research* 115:23 PP

- Wells ML (2003) The level of iron enrichment required to initiate diatom blooms in HNLC waters. *Marine Chemistry* 82:101-114
- Whitney FA, Crawford DW, Yoshimura T (2005) The uptake and export of Si and N in HNLC waters of the NE Pacific. *Deep-Sea Research II* 52:1055-1067
- Williams JC, Drummond BA, Buxton RT (2010) Initial effects of the August 2008 volcanic eruption on breeding birds and marine mammals at Kasatochi Island, Alaska. *Arctic, Antarctic, and Alpine Research* 42:306–314
- Wong CS, Matear RJ (1999) Sporadic silicate limitation of phytoplankton productivity in the subarctic NE Pacific. *Deep-Sea Research II* 46:2539–2555
- Young RW, Carder KL, Betzer PR, Costello DK, Duce RA, DiTuiro GR, Tindale NW, Laws EA, Uematsu M, Merrill JT, Feely RA (1991) Atmospheric iron inputs and primary productivity: phytoplankton responses in the North Pacific. *Global Biogeochemical Cycles* 5:119-134

Chapter IV

**Possible impacts of volcanic ash emissions of
Mount Etna on the oligotrophic Mediterranean Sea:
Results from the nutrient-release experiments
in seawater.**

Possible impacts of volcanic ash emissions of Mount Etna on the oligotrophic Mediterranean Sea: Results from the nutrient-release experiments in seawater.

Nazlı Olgun^{1,2}, Svend Duggen^{1,3}, Daniele Andronico⁴, Steffen Kutterolf¹, Peter Leslie Croot^{2,5}, Salvatore Giammanco⁴, Paolo Censi⁶, Loredana Randazzo⁶

¹ Dynamics of the Ocean Floor Division, Helmholtz-Center for Ocean Research, GEOMAR, Kiel, Germany.

² Marine Biogeochemistry Division, Helmholtz-Center for Ocean Research, GEOMAR, Kiel, Germany.

³ A. P. Møller Skolen Upper Secondary School and Sixth Form College of the Danish national minority in Germany, Schleswig, Germany.

⁴ Istituto Nazionale di Geofisica e Vulcanologia, Sezione di Catania, Osservatorio Etneo, Piazza Roma 2, Catania, 95123, Italy.

⁵ Plymouth Marine Laboratory, Plymouth, United Kingdom.

⁶ Dipartimento di Scienze della Terra e del Mare (DiSTeM), Università di Palermo, Via Archirafi, 36 90123 Palermo, Italy.

Submitted to Marine Chemistry

Corresponding author: nolgun@geomar.de (N. Olgun)

Keywords: Mount Etna, volcanic ash, nutrient release, Mediterranean Sea, oligotrophy, fertilization, phosphate, iron.

Abstract

Atmospheric deposition of volcanic ash has recently been recognized as a nutrient source into the surface ocean. Mount Etna, in Sicily (Italy), one of the world's most active volcanoes, is located in the oligotrophic Mediterranean Sea (MedSea). Despite the active volcanism on Mount Etna, biogeochemical impact of volcanic ash fallouts in the MedSea remains largely unknown. Here we present the results of seawater nutrient release experiments with Etna ash samples collected during different eruptive episodes between 2001 and 2007. Our results show that volcanic ash from Mount Etna releases significant amounts of fixed-nitrogen (60-970 nmol/g), phosphate (7-970 nmol/g), silica (3-2060 nmol/g), iron (10-130 nmol/g) and zinc (0-21 nmol/g). By using the general relation between the thicknesses of the ash deposits and the depositional areas, we further estimated an example representative of ash fluxes emitted during an ash emission event of Etna based on the case-study focussing on 4-5 November 2002 activity, during the 2002-03 eruption. Etna explosive eruptions can transport volcanic ash as far as 800 km, with ash emissions exceeding the particle flux during dust storm events (of 10 g/m² input) as far as 400 km downwind from the volcano. Our results emphasize that the Etna ash can supply dissolved phosphate in amounts (> 3 nM) sufficient to relieve phosphate limitation in the oligotrophic MedSea. Input of dissolved iron input together with phosphate may enhance nitrogen-fixation rates within the ash fallout region in MedSea, and may further favour the enhancement of the marine primary production, particularly in the central MedSea.

1. Introduction

Atmospheric deposition of nutrients into the ocean can affect the marine primary production (MPP) (Falkowski, 2004; Falkowski et al., 1998; Morel and Price, 2003). Volcanic ash ejected from explosive eruptions has recently recognized as an important nutrient source to the surface ocean (Censi et al., 2010; Duggen et al., 2007; Frogner et al., 2001; Hamme et al., 2010; Hoffmann et al., submitted; Jones and Gislason, 2008; Langmann et al., 2010; Lin et al., 2011; Olgun et al., 2011). Recent geochemical and bio-incubation experiments, in fact, have shown that volcanic ash from various subduction

zone and hotspot volcanic eruptions rapidly mobilizes significant amounts of biologically relevant elements (e.g., fixed-N, P, Si, Fe) into the seawater (Censi et al., 2010; Duggen et al., 2007; Frogner et al., 2001; Jones and Gislason, 2008; Olgun et al., 2011) that are utilized by the phytoplankton for reproduction (Duggen et al., 2007; Hoffmann et al.). Iron-fertilization by volcanic ash has been evidenced by massive phytoplankton blooms in the ash fallout areas in the high-nutrient low-chlorophyll (HNLC) oceanic regions, such as the North Pacific (Hamme et al., 2010; Langmann et al., 2010; Lin et al., 2011). However, impacts of volcanic ash fallout in low-nutrient, low-chlorophyll regions remain has not been very well constrained.

The Mediterranean Sea (MedSea), although a nearly-enclosed basin, is a low-nutrient, low-chlorophyll (LNLC) region (Dugdale, 1976; Moutin and Raimbault, 2002) characterized by strong seasonality with very low nutrient levels (like the open ocean gyres) during the stratification period in summer and autumn (Bergametti et al., 1992; Bethoux et al., 1998; Bethoux et al., 1992; Bonnet et al., 2005; Estrada, 1996; Moutin and Raimbault, 2002). Phytoplankton growth in the MedSea is known to be limited by phosphorus (Bonnet et al., 2005; Guerzoni et al., 1999; Krom et al., 1991; Thingstad and Rassoulzadegan, 1995; Thingstad et al., 1998). However, depending on the time of the year (or the region), nutrient limitation may shift from phosphorus to nitrogen (Guerzoni et al., 1999; Herut et al., 2005) (Krom et al., 1991) or to another macro-nutrient such as silica associated particularly to diatom production (Leblanc et al., 2005). MedSea is at the same time one of the regions that is close the copper-toxicity during more than half a year (Paytan et al., 2009).

The oligotrophy of the MedSea has been related to a variety of hydrographical conditions such as the input of low-nutrient surface Atlantic waters through Strait of Gibraltar (Fig. 6), absence of significant upwelling regions, and relatively local and seasonal riverine input (Azov, 1991; Estrada, 1996). It has also been suggested that high input desert dust into the MedSea may act as a sink of phosphate through scavenging onto the dust particles (Krom et al., 1991). The atmosphere therefore plays an important role in the external supply of nutrients to this region (Guerzoni et al., 1999; Guieu et al., 1997; Guieu et al., 1991; Kocak et al., 2005; Krom et al., 1991; Markaki et al., 2003; Martin et al., 1989). Large amounts of desert dust, originating from the adjacent arid

regions in North Africa and Middle East, are deposited into the MedSea (Guerzoni et al., 1999; Guieu et al., 2002). There is also significant input of anthropogenic aerosols derived from industrial and domestic activities in the populated areas around the region such as the Europe (Chester et al., 1996; Guieu et al., 2005; Guieu et al., 1997; Migon et al., 2001).

Mount Etna, located on the island of Sicily in the central MedSea, is the biggest volcano in Europe and one of the most active world-wide (Figure 1). Over the last decades, due to a gradual transition of the magma source (Branca and Del Carlo, 2005; Schiano et al., 2001), there has been a dramatic increase in the frequency of explosive eruptions of Etna (Andronico et al., 2005; Behncke and Neri, 2003a; Branca and Del Carlo, 2005). It is noteworthy, in fact, that between 1995 and 2011 Etna produced more than 150 paroxysmal episodes lasting tens of minutes to several hours, most of which generating tephra-loaded, buoyantly driven eruption plumes (e.g., (Andronico et al., 2009b)). One of the most powerful eruptions in the last three hundred years occurred on 5 January 1990 ejecting an ash plume as high as 15 km above sea level (a.s.l.) (Calvari et al., 1991; Carveni et al., 1994). Explosive eruptions of Etna can deposit significant amounts of volcanic ash into MedSea (Fig. 1). During the 2002-03 eruption, the amount of ash ejected into the atmosphere was about $38\text{-}50 \times 10^{12}$ g (Andronico et al., 2008b), as high as the annual dust input in the MedSea of 40×10^{12} g dust (Guerzoni et al., 1999).

A number of ash plumes generated by Etna were transported by the wind blowing at high altitude hundreds of kilometers over the MedSea reaching as far as Greece and Libya (Figs. 1 and 6) (Andronico et al., 2008b; Dellino and Kyriakopoulos, 2003; Kelepertsis et al., 2003). Rapid dissolution of Etna ash in the photic zone of the water column may affect the nutrient budget, and hence the MPP in the MedSea. During the July-August 2001 eruption (e.g., (INGV-Staff, 2001), (Coltelli et al., 2007)), seawater analyses in the Ionian coast have shown increased chlorophyll-a and trace-metal concentrations (e.g., Fe, Cu) (Censi et al., 2010). Despite increasing explosivity and the large input of volcanic ash from Mount Etna, the biogeochemical impacts of this ash on the nutrient-starved MedSea remains largely unknown.

In this study, we performed nutrient-release experiments in seawater with volcanic ash samples from Etna and a loess sample consisting of dust originated from

Sahara desert. We analyzed release of fixed-nitrogen species (NO_3^- , NH_4^+ , NO_2^-), phosphate (PO_4^{3-}), silica (SiO_2), and trace metals iron, zinc and copper. As a case-study, we further constrained the downwind ash-flux in the MedSea during the explosive activity of Etna occurred on 4 November 2002 (Andronico et al., 2008b). Finally, our analysis/research allowed us to evaluate the possible nutrient supply and the biological impact within the Etna ash fallout areas in the MedSea during explosive eruptions of Etna.

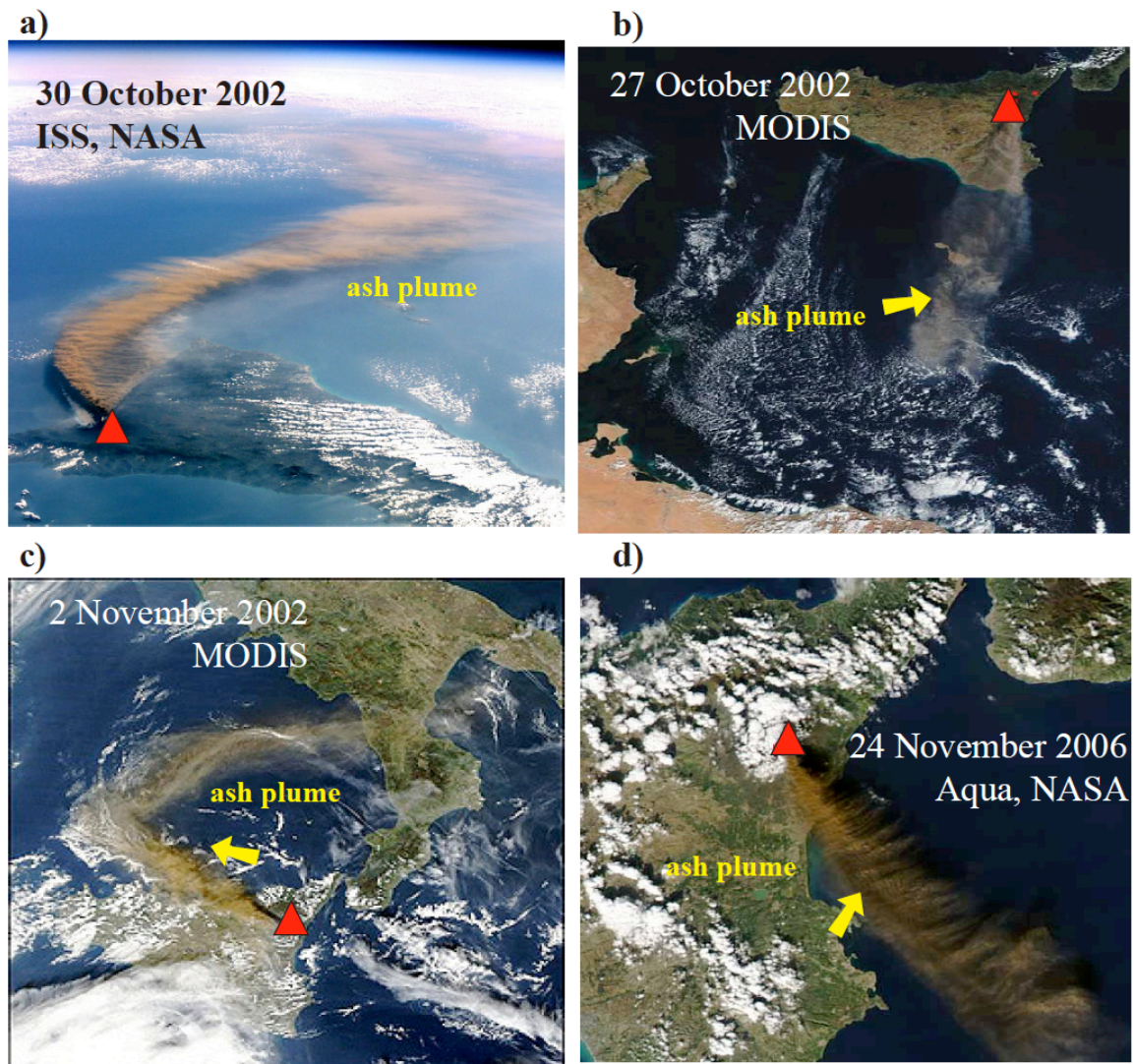


Figure 1: Ash plumes erupted from Mount Etna (red triangle) being carried by the wind across the MedSea, a) 30 October 2002 International Space Station (ISS), NASA, the photo is looking to southeast, b) 27 October 2002, Moderate Resolution Imaging Spectroradiometer (MODIS), NASA, ashfall was reported as far away as Libya travelling over 600 kilometers (Andronico et al., 2005), c) 2 November 2002, (MODIS), NASA, the ash plume is transported north-western towards the Tyrrhenian Sea in the western MedSea, d) 24 November 2006, Aqua, NASA, the ash plume from a strombolian eruption is transported south-southeast over the Ionian Sea.

2. Samples and Methods

We have analyzed the seawater-nutrient release of thirteen Etna ash samples and one loess sample. The ash samples were freshly collected after the eruptions and archived in the Istituto Nazionale di Geofisica e Vulcanologia (INGV), Sezione di Catania, Osservatorio Etneo. The ash samples were selected from eruptions covering a range in the years 2001, 2002, 2004, 2005, 2006 and 2007. A synthetic description of the samples is shown in Table 1. We have chosen the samples whose eruption plume directed towards Ionian Sea, i.e. mostly to the E, SE and NE directions (Table 1). The ash samples used were composed of dry ash that had not been in contact with water after deposition or metal containing equipment (e.g., sieves) after collection.

Table 1: Description of the Etna ash samples.

Sample name	Eruption date	Plume direction	Eruption Style (and duration)
Et-2001a	28 June 2001	SE	Strong strombolian (<3 hours)
Et-2001b	22 July 2001	E to SE	Phreatomagmatic ash emission (days)
Et-2001c	03 August 2001	E to SE	Discontinuous ash emission (days)
Et-2002a	29 October 2002	SSE	Continuous ash emission (days)
Et-2002b	30 October 2002	SSE	Continuous ash emission (days)
Et-2002c	3 November 2002	SE	Continuous ash emission (days)
Et-2002d	2 December 2002	S	Continuous ash emission (days)
Et-2004	17 November 2004	S	Episodic ash emission (tens of minutes)
Et-2005	8 January 2005	SW	Episodic ash emission (3< x <6 hours)
Et-2006a	29 October 2006	S	Episodic ash emission (minutes)
Et-2006b	21 November 2006	E	Strong strombolian (3< x <6 hours)
Et-2007a	11 April 2007	SE	Lava fountain (<3 hours)
Et-2007b	23 November 2007	NE	Lava fountain (6<x<10 hours)

The loess sample from Cape Verde Island simulates a Saharan aerosol. The same loess sample was used in other recent studies (Olgun et al., 2011) and (Heller and Croot, 2011). In brief, this sample was collected from loess deposits from the northeastern

corner of the island of Sao Vicente (16.9°N, 24.9°W) in the Cape Verdean archipelago that are composed of aerosols transported from North African deserts (80-95% Saharan origin). The loess sample was collected from ground and sieved through 100 µm plastic filters.

The release of NO_3^- , NH_4^+ , NO_2^- , PO_4^{3-} and SiO_2 were examined by means of leaching experiments. One gram of samples was mixed with 50 ml low-nutrient Atlantic seawater in 60 ml Nalgene polypropylene (PP) plastic bottles and shaken gently for about twenty minutes. After agitation of one hour and twenty hours (for selected samples), the solutions were filtered through a 5 µm mesh PTFE filter (Sartorius). Seawater concentrations of macro-nutrients were measured by standard routine photometry at IFM-GEOMAR. Measurements with the dust sample were made using the same methodology applied to the volcanic ash for direct comparison (Table 2). The measured concentrations of dissolved macro-nutrients were converted to nanomoles per gram of ash and dust (nmol/g ash, nmol/g dust).

Trace-metal release experiments (Fe, Zn and Cu) were performed by voltammetry using a hanging mercury drop electrode (a Metrohm VA757) *in situ* in natural surface ocean seawater collected from the eastern equatorial Atlantic and buffered at pH 8.0 (by using 200 µl EPPS pH-buffer). The pH chosen for our experiments directly mimics the dissolution of nutrients in the seawater through dry deposition process. Strict dry deposition is a highly effective mechanism of dust deposition in MedSea, e.g., up to 56% in the eastern MedSea increasing up to 93% in summer (Bonnet and Guieu, 2004; Kubilay et al., 2000).

Fe-release measurements were performed using Cathodic Stripping Voltammetry with the same method used previously by (Duggen et al., 2007; Olgun et al., 2011). An artificial Fe-binding organic ligand (20 µl of TAC) was added in the seawater before the Fe-solubility measurements (Croot and Johansson, 2000). Dissolution of Zn and Cu were measured by means of Anodic Stripping Voltammetry (Duggen et al., 2007). A known quantity of ash (~50 mg) was added to the prepared 20 ml seawater and an ash/seawater ratio of ~1/400 was obtained, which mimics the deposition of a 0.1 m-thick ash layer onto the sea surface (Duggen et al., 2007; Olgun et al., 2011). The precision of the voltametric measurements was calculated from replicates. The deviation in the

measurements, probably resulting from particle-size heterogeneity in the sub-samples, ranges between 8-20% for Fe-and <1-7% for Zn-measurements (Et-2001b n=3; Et-2002c n=2; Et-2005 n=2).

Six Etna ash samples were selected (Table 3) for the major elemental compositions of glass shards and matrix glass that were determined by electron microprobe analysis (JEOL-JXA-8200). For the measurements, a fraction of the ash samples (~10 mg) were separated and sieved with de-ionised water to the size fraction 32-125 µm using de-ionized water. The ash particles were mounted on a tray with resin and analyzed with a beam current of 6 nA and a beam size of 5 µm. The average glass composition was inferred from ~25 individual measurements.

Bulk (total) Fe-contents of the six selected Etna ash samples and the loess sample were determined by inductively coupled plasma spectrometry at the Institute of Geosciences, CAU University of Kiel. Approximately 100 mg of ash and the dust sample(s) were weighed into perfluoralkoxy (PFA) vials and digested using a multi-step table-top procedure with hydrofluoric acid, aqua regia, and perchloric acid. Fe-content (in wt.%) was determined by inductively coupled plasma-optical emission spectrometry (ICP-OES) using a Spectro Ciros SOP instrument. SiO₂ content of the Saharan loess sample was referred from the lithium tetraborate fusion analyses (digestion with 0.5% tartaric acid and 4% nitric acid) in ITS Testing Services (UK). Concentrations were measured by ICP-OES analyses.

Zn and Cu contents (in ppm) of the digest solutions were performed by ICP-mass spectrometry (ICP-MS) using an Agilent 7500cs instrument. Analytical quality routines involved the preparation and analysis of procedural blanks, sample duplicates, and international certified reference materials BHVO-2, JR-1, BR measured as unknowns. Analytical error as estimated from replicate measurements was better than 2% RSD for Zn, Cu, and below 1% RSD for Fe. Details of analytical procedures can be found in (Garbe-Schönberg, 1993).

Volcanic activity producing the analysed samples

In the last 15 years, Etna proved to be a volcano showing not only what are commonly called Strombolian explosions or lava fountains, but different explosive styles (Andronico et al., 2008a; Andronico et al., 2008b; Andronico et al., 2009b; Andronico et

al., 2009c). In this section we shortly describe the analysed samples by characterising the eruption activity and the associated deposit. It is noteworthy that the grain-size of the collected ash is usually strongly depending on the distance of sampling, but some eruption types can produce coarser tephra fallout than others. Further, the erupted ash can be composed of different components, whose relative percentage usually is strictly linked to the eruptive styles: sideromelane, corresponding to glass, light to brown particles related to the fresh, erupting magma; tachylite, dark, blocky fragments reflecting portions of magma more crystallised and cool; lithics, differently-coloured particles derived by old, solidified and pre-existing material (lavas, tephra or sedimentary rocks); crystals (felsic or mafic).

For the purposes of this paper we subdivide the eruptions into a) episodic, during which the explosive activity lasted from a few minutes to several hours, and b) long-lasting, when we observe a continuous ash emission lasting several days, as occurred during the 2001 and 2002-03 eruptions. All the episodic eruptions/ash emissions occurred from the Southeast Crater, the most active summit crater at Etna. Again, samples from long-lasting activity obviously represent some hours of activity within that eruption.

Samples Et-2001a (28 June 2001) and Et-2006b (21 November 2006) were erupted during episodic explosive eruptions, characterised by strong Strombolian activity which for periods of few minutes can produce continuous lava ejection or lava fountains (Andronico et al., 2009b). Samples Et-2007a (11 April 2007) and Et-2007b (23 November 2007) are related to typical episodes of lava fountains, that's continuous magma jets for tens of minutes to hours (Alparone et al., 2003; Andronico et al., 2008a). Both strong Strombolian activity and lava fountains produced significant eruption plumes above the volcano, but different tephra deposits, being the former fine-grained and composed of different components, while the latter are usually coarser and almost totally composed of sideromelane. The 2001 eruption (INGV-Staff, 2001) was characterised by the opening of an eruptive fissure at about 2550 m where explosive activity lasted about 3 weeks. We analysed a sample (Et-2001b) related to the first eruption days, during which observations of hydration-cracks under Scanning Electron Microscope allowed to suppose magma-water interaction and define the eruption style as phreatomagmatic

(Taddeucci et al., 2002). Sample Et-2001c, on the contrary, is related to the final phase of the eruption, characterised by pulsing explosions emitting tachylite-rich ash.

Samples Et-2002a, b, c, d were collected in 2002 on 29 October, 30 October, 4 November and 2 December, respectively. The 2002-03 eruption was characterised by a particular explosive activity defined *ash-rich jets and plumes* by (Andronico et al., 2009a), producing fine tephra deposits with abundant crystal-rich tachylite clasts. Sample Et-2004 was produced during an explosive activity lasting 1-2 minutes, whose deposit was fine, lithic-rich and sideromelane-poor. Sample Et-2005 is related to prolonged ash emission lasting several hours, characterised by scarce explosivity, which produced a lithic-rich, poor deposit. Finally, sample Et-2006a was erupted during a short-lasting explosion (Cristaldi and Scollo, 2006) which occurred on 29 October erupting a poor deposit composed of abundant lithics and tachylite fragments.

3. Results

3.1 Etna Ash

The Etna ash samples released variable amounts of fixed nitrogen (N), along with PO_4^{3-} (P) and SiO_2 (Si) (Table 2, Fig. 2). Fixed-N mobilized from volcanic ash (and Cape Verde loess) was primarily as nitrate (>75%) (Table 2). Within the one hour of contact with seawater, Etna ash samples released 60-880 nmol/g of total fixed-N (expressed as nitrate), 7-140 nmol/g of P, and 3-790 nmol/g of Si (Fig. 2). At the end of twenty hours agitation, the four-selected ash samples released about 250-970 nmol/g of total fixed-N, 10-970 nmol/g of P, and 90-2060 nmol/g of Si. Each g of ash liberated 10-130 nmol/g of Fe, and 0-30 nmol/g of Zn within the 60 minutes contact with seawater (Fig 2). Etna ash samples did not mobilize detectable amounts of Cu. Time dependent trace-metal release showed similar trends in with relatively higher mobilization within 20 minutes (Fig. 3).

Mobilization of P and Si from Etna ash was relatively higher compared to the volcanic ash from subduction zone volcanoes (10-100 nmol/g of P, and 50-200 nmol/g of Si; (Duggen et al., 2007). Release of fixed-N, Fe, and Zn are within the range found in the previous voltametric measurements at pH 8 (~ 250-1150 nmol/g of N, 35-340 nmol/g of Fe, 2-27 nmol/g of Zn; (Duggen et al., 2010; Olgun et al., 2011). Unlike some of the subduction zone volcanic ash samples (releasing up to 50 nmol/g of Cu (Duggen et al., 2007)), Etna ash released no Cu into the seawater.

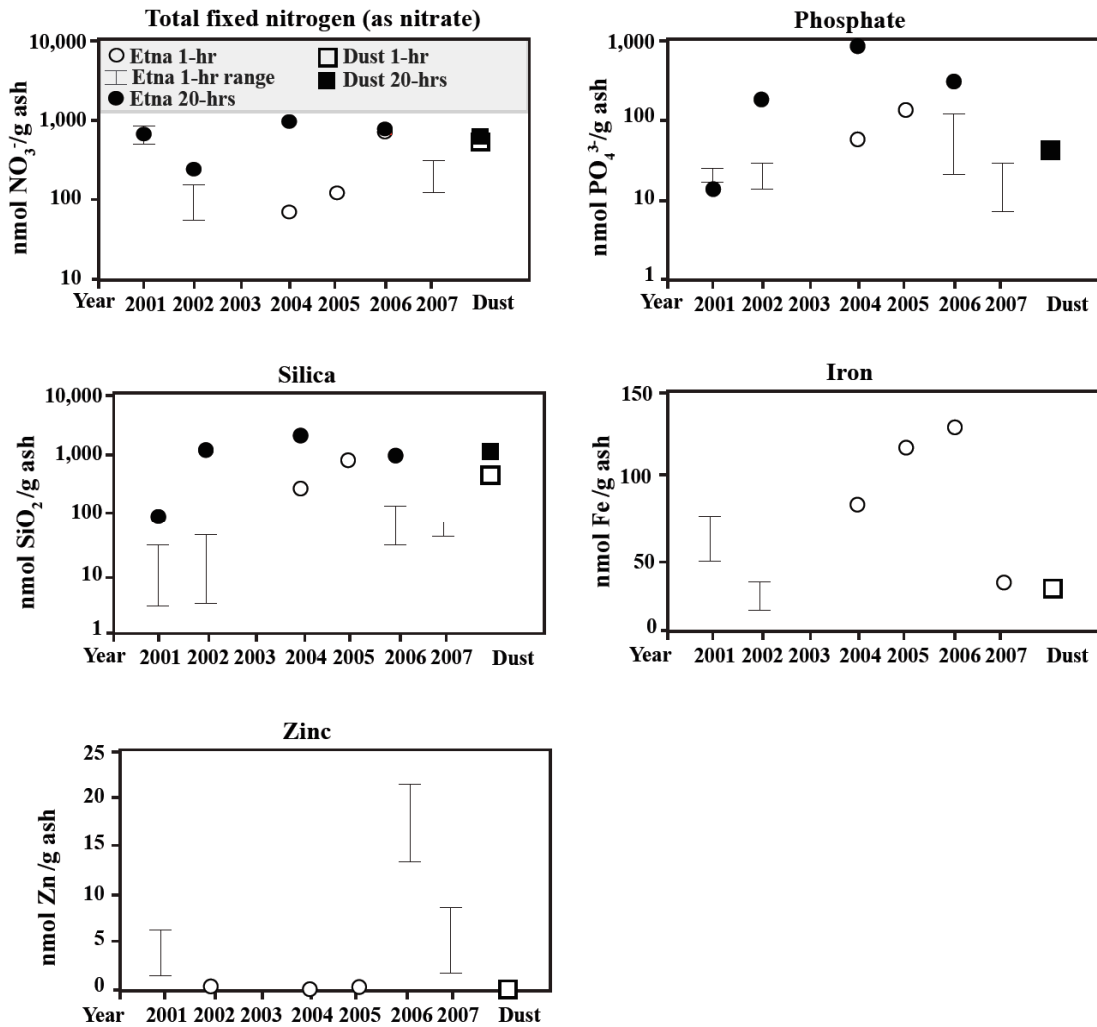


Figure 2: Nutrient-release from Etna volcanic ash (circles) and Cape Verde loess sample (rectangles) into the seawater. The years on the x-axis indicate the corresponding ejection and sampling of the Etna volcanic ash (Table 1). White symbols show the one-hour experiments and black symbols show the twenty-hours experiments in seawater. Error bars indicate the range in repeat measurements.

The major and trace element contents (except for N) of the bulk ash and the volcanic glass are shown in Table 3. Bulk phosphorus contents, re-calculated from P_2O_5 , are 0.1-0.2 wt.%, with similar phosphorus contents found for volcanic glasses 0.2-0.3 wt.%. SiO_2 -contents of the volcanic glasses do not vary much ranging from 49 to 50 wt.%. Fe-contents of Etna ash are 7-8 wt.%, re-calculated from oxide forms Fe_2O_3 for bulk and FeO for volcanic glass. Variation of Fe-content of the bulk ash and the volcanic glass is relatively small ($< 1\%$ Fe), indicating the glass compositions likely dominate the total Fe-content of the samples (Table 3). Zn and Cu content of the bulk ash samples ranges between 100-110 ppm, and 110-160 ppm, respectively.

Based on the dissolved concentrations and the elements contents (except for nitrogen), the percent soluble fractions of P, Si, Fe, and Zn were calculated by the equation $\%X_S = (\text{Dissolved X}/\text{Total X}) * 100$ (Fig. 4). $\%P_S$ (fraction of soluble phosphate) of Etna ash ranges from 0.003% to 0.4% (Fig. 4a). Highest $\%P_S$ for Etna ash were measured during twenty hours agitation experiments. $\%Si_S$ (fraction of soluble silica) ranges from 0.0001% to 0.05% for Etna ash, from 0.006% to 0.014% for the Cape Verde loess sample (Fig. 4b). Higher $\%Si_S$ values were found for the twenty hours agitation experiments for Etna ash (and the loess sample).

$\%Fe_S$ (fraction of soluble iron) ranges between from 0.001% to 0.01% for Etna ash, 0.002% for Cape Verde loess sample (Fig. 4c). $\%Fe_S$ of Etna ash is in the lower most limit obtained by voltametric experiments (at pH 8) by volcanic ash from subduction zone volcanoes (0.003-0.2% Fe_S) (Olgun et al., 2011). Leaching experiments of volcanic ash with acidic solutions may show a wide variety of $\%Fe_S$ from 0.001% to values as high as 22% (see references in (Duggen et al., 2010)), which is likely linked to strong pH-dependency on the Fe solubility (see discussion in (Duggen et al., 2010)). $\%Zn_S$ for Etna ash range is 0.0-0.6%, while Etna ash mobilized no copper.

a) Iron release

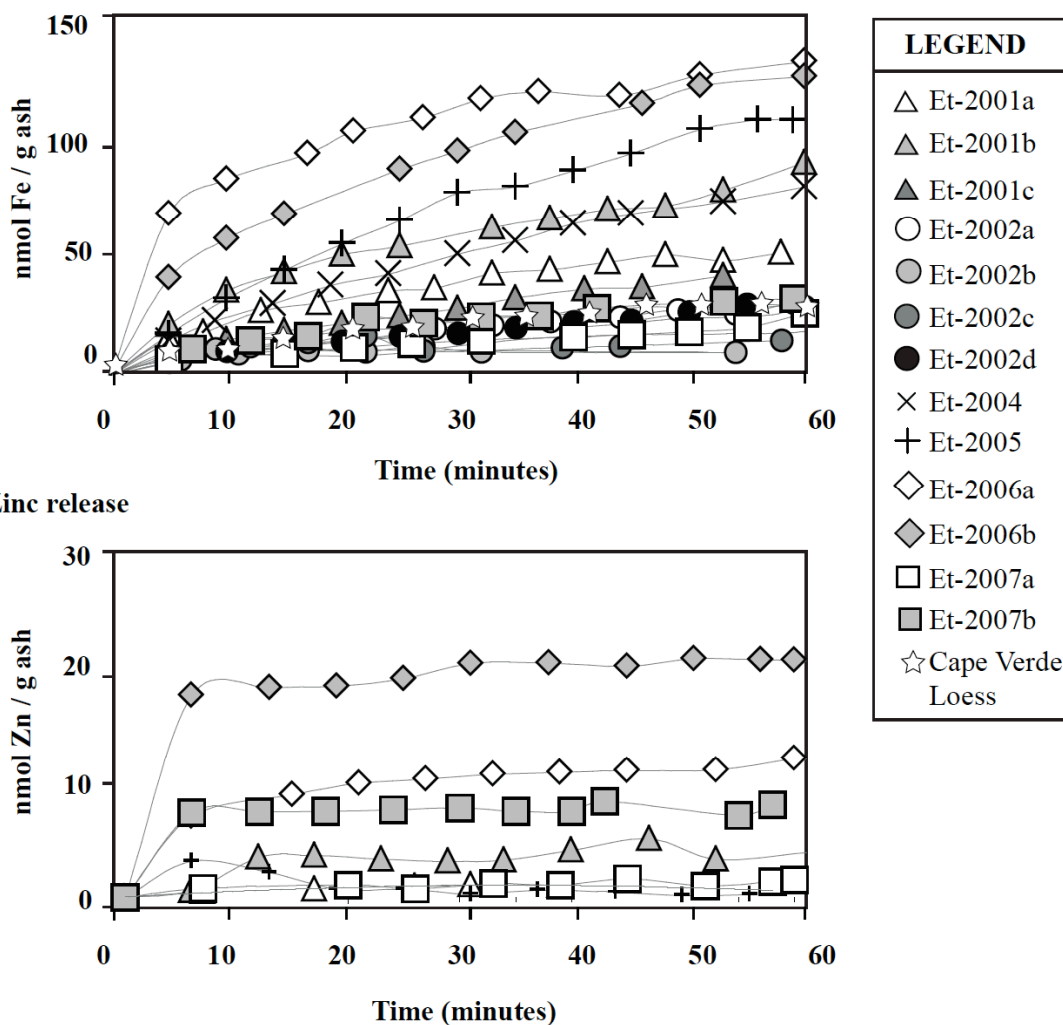


Figure 3: Time-dependent release of a) iron and b) zinc from Etna volcanic ash samples and the Cape Verde loess sample during 60 minutes contact with seawater. The measurements were conducted by mixing of 50 mg of sample and 20 ml of seawater, in-situ by means of a) Cathodic- and b) Anodic Stripping Voltammeter. The results are presented in nanomoles per gram of ash or dust (nmol/g).

Table 2: Nutrient-release from the Etna volcanic ash samples and the Cape Verde loess sample. Release of N, P and Si were measured by standard photometry by mixing 1 g of volcanic ash with 50 ml of low-nutrient seawater with agitation times of one hour and twenty hours. Fe and Zn release data were measured in-situ by stripping Voltammetry by mixing 50 mg of volcanic ash with 20 ml natural Atlantic seawater buffered at pH 8. The results are expressed as nutrient release in nmoles per gram of ash or dust.

	Sample name	Total fixed-N (as NO ₃ ⁻)*	NO ₃ ⁻ (nmol /g)	NH ₄ ⁺ (nmol/g)	NO ₂ ⁻ (nmol/g)	PO ₄ ³⁻ (nmol/g)	SiO ₂ (nmol/g)	Fe (nmol/g)	Zn (nmol/g)
One hour data	Etna Samples								
	Et-2001a	538	419	50	1	25	26	51	1.0
	Et-2001b	601	387	90	1	18	19	69	6.0
	Et-2001c	883	835	20	1	18	3	41	4.0
	Et-2002a	168	149	7	2	13	4	30	0.0
	Et-2002b	89	86	1	1	17	3	11	0.0
	Et-2002c	153	144	3	2	21	20	23	0.4
	Et-2002d	62	37	9	3	28	37	28	0.7
	Et-2004	73	7	27	2	59	266	78	0.0
	Et-2005	126	19	45	2	137	793	114	0.2
	Et-2006a	703	570	55	3	125	127	130	12.9
	Et-2006b	725	324	169	1	20	27	124	21.2
	Et-2007a	340	136	86	1	26	69	26	1.6
	Et-2007b	141	44	41	1	7	39	32	8.2
Twenty hours	Et-2001a	255	255	0	0	14	89		
	Et-2002b	248	90	53	27	186	1173		
	Et-2004	971	82	303	136	970	2058		
	Et-2006b	786	277	174	76	310	949		
Loess									
	One hour	Loess	536	312	92	5	43	450	20-30
Twenty hours	Loess	630	385	99	8	43	1110		

*Total fixed nitrogen is expressed as nitrate, where ammonia and nitrite values are converted by using molecular weights (NO₃⁻=76.01g/mol, NH₄⁺=32.01g/mol, NO₂⁻=60.01 g/mol).

Table 3: Major-element and trace-element contents of the bulk ash and the loess sample(s) and the volcanic glass shards. Bulk element concentrations of were analyzed by ICP-OES for major elements, and by ICP-MS for trace elements. Bulk SiO₂-concentration of the volcanic ash samples were referred from the volcanic glass composition measured by electron microprobe analyses.

Element oxides (wt. %)		Et-2001b	Et-2002c	Et-2004	Et-2005	Et-2006b	Et-2007b	Loess
SiO ₂		50.2	50.7	49.8	50.1	50.5	49.2	21.8
Al ₂ O ₃	bulk	17.6	17.1	16.8	16.8	17.1	17.5	6.6
	glass	16.6	16.5	16.8	16.6	16.3	16.2	-
Fe ₂ O ₃	bulk (Fe ₂ O ₃)	9.8	11.2	10.5	10.7	10.4	10.5	9.3
	glass (FeO)	10.6	10.4	10.6	10.2	10.5	10.6	-
Fe*	bulk	6.9	7.8	7.4	7.5	7.3	7.4	6.5
	glass	8.2	8.1	8.2	7.9	8.2	8.2	-
P ₂ O ₅	bulk	0.7	0.7	0.7	0.6	0.8	0.8	0.5
	glass	0.9	0.9	0.8	0.8	0.8	0.7	-
P*	bulk	0.15	0.14	0.16	0.14	0.17	0.17	0.10
	glass	0.30	0.29	0.27	0.27	0.26	0.24	-
MnO	bulk	0.2	0.2	0.2	0.2	0.2	0.2	0.1
	glass	0.2	0.2	0.2	0.2	0.2	0.2	-
MgO	bulk	4.4	5.3	4.3	4.7	4.5	4.1	7.4
	glass	3.1	3.0	3.3	3.1	3.2	3.6	-
CaO	bulk	9.1	10.2	9.2	9.6	9.3	9.0	25.1
	glass	7.6	7.2	7.1	6.8	7.4	8.6	-
Na ₂ O	bulk	3.9	3.3	3.4	3.5	3.9	4.0	1.3
	glass	5.2	5.2	4.6	5.3	4.8	4.7	-
K ₂ O	bulk	2.0	1.9	3.0	2.2	2.3	2.3	0.5
	glass	3.5	3.8	3.4	4.4	3.6	2.9	-
TiO ₂	bulk	1.5	1.7	1.7	1.7	1.6	1.7	2.4
	glass	2.0	2.0	2.0	2.0	2.1	2.1	-
Trace elements (ppm)								
Zn	bulk	101	99	94	104	108	110	87
Cu	bulk	112	155	164	136	158	150	45

* re-calculated from oxide-forms.

3.2 Cape Verde loess

The Cape Verde loess sample released 536 nmol/g of total fixed-N (expressed as nitrate), 43 nmol/g of P, 450 nmol/g of Si within one hour contact with seawater. After twenty hours agitation in seawater, loess sample released 630 nmol/g of total fixed-N, 43 nmol/g of P, 1110 nmol/g of Si (Fig. 2). P-release from Cape Verdean loess did not increase during twenty hours agitation experiment, while other nutrients showed higher mobilization. Fe-release of the loess sample is 20-30 nmol/g of Fe referred from (Olgun et al., 2011) (Fig 2), where no release of Zn and Cu were detected.

Based on the major and trace element contents, Cape Verde loess sample consists of 0.1 wt.% phosphorus (re-calculated from P_2O_5), 22 wt.% SiO_2 , 6.5 wt.% Fe (re-calculated from Fe_2O_3), 87 ppm Zn, and 45 ppm Cu (Table 3). The phosphorus content of Cape Verde loess sample is consistent with the Saharan soils from southern Algeria (Mills et al., 2004; Ridame and Guieu, 2002). Fe-content of the loess sample (6.5 wt.%) was similar to those found for other Cape Verdian loess samples (7.6% Fe; (Desboeufs et al., 2001)).

Fractional solubilities of Cape Verde loess were calculated in the same way for volcanic ash (Fig. 4). % P_s of Cape Verde loess is 0.003% during one hour agitation, and stayed constant for over the twenty hours agitation (Fig. 4). % Fe_s of the loess sample was 0.002%, consistent with the experiments with Saharan soils in seawater at pH 8 (e.g., 0.001-0.02%; (Guieu and Thomas, 1996)).

Higher nutrient mobilizations from dust samples have been reported in earlier experiments which employed different experimental set-ups (Bonnet et al., 2005; Bonnet and Guieu, 2004; Pulido-Villena et al., 2010; Ridame and Guieu, 2002) to that used in the present study. The main reason for this discrepancy probably arises from acidification of sample solutions (dust + seawater) to pH 2 with HCl, which may significantly affect the nutrient leaching from dust or volcanic ash. For example, by mixing 1.2 mg/l dust, 0.5-1.2 μ M nitrate (Bonnet et al., 2005) and 5 nM phosphate (Pulido-Villena et al., 2010) was mobilized from Saharan dust samples. On the other hand, in some cases, nutrient concentrations before and after the dust addition stayed below detection limits (Bonnet et al., 2005).

$\%P_s$ for Saharan soils are found between 0.5% up to 21%, with lowest P-solubilities found for the high particle concentrations between 500-8,000 mg/l (Ridame and Guieu, 2002). Based on the mixing ratio in our experiments (50 mg, 20 ml), particle concentration is about 2,500 mg/l, which is representative for high intensity dust events (Ridame and Guieu, 2002), and likely underestimates the solubility of low particle concentrations. $\%Fe_s$ in our experiments is also much lower compared to experiments with acidified solutions (e.g., $\%Fe_s$: 0.23-6.1%; (Bonnet and Guieu, 2004), probably due to high pH dependency of Fe-solubility (Baker and Croot, 2010).

As shown in Fig. 2, nutrient-mobilization from the Cape Verde loess sample is within the range found for Etna ash. However, as we used only one type of dust sample, it is difficult then to assess the natural variability in the dust samples, thus making comparison with the wide range of observed values for the nutrient-release from Etna ash complicated. In terms of methodology, our study shows the first data for macro-nutrient release from dust by means of voltametric measurements at seawater pH 8, therefore, provide a basis for comparison with volcanic ash.

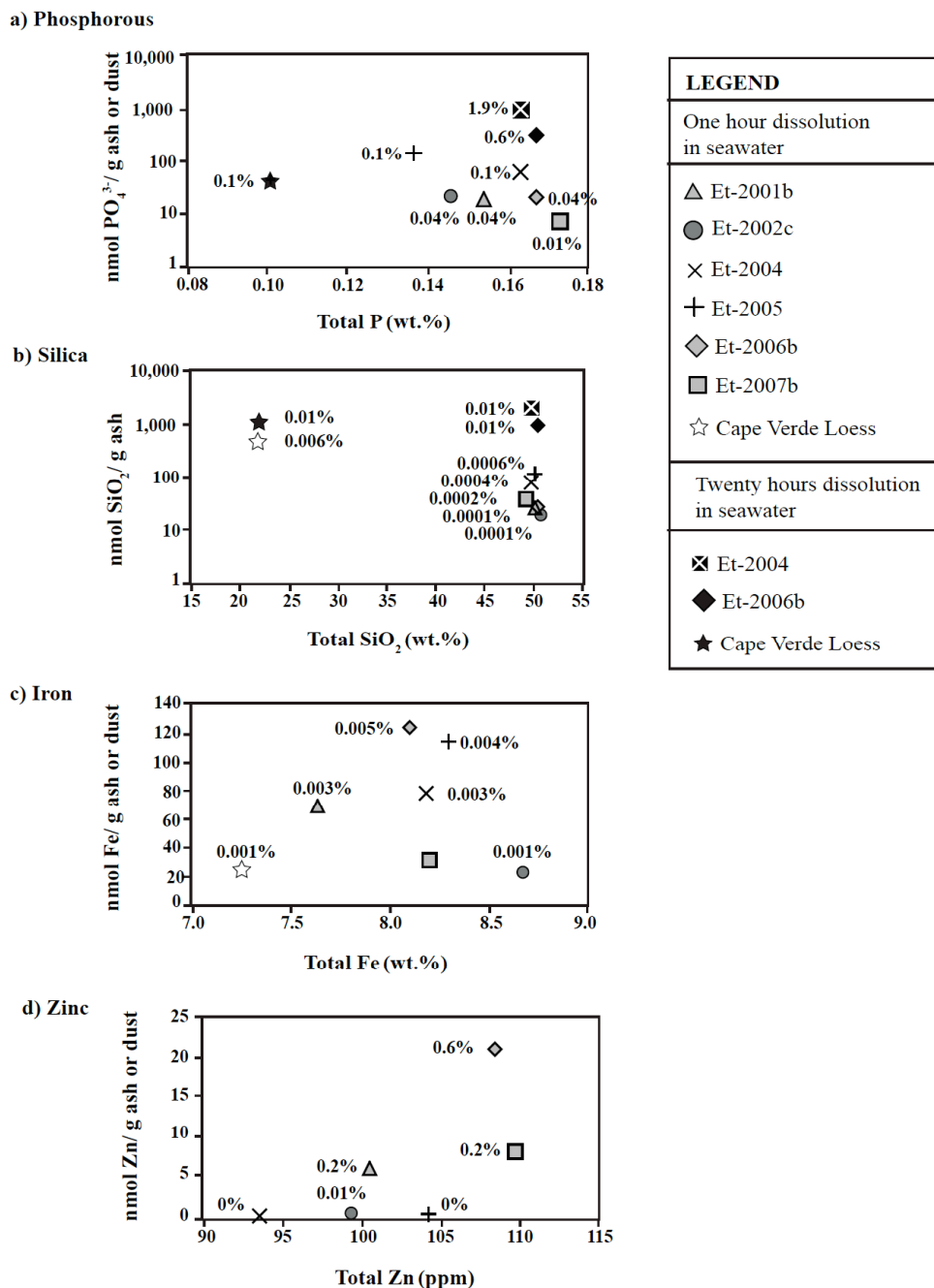


Figure 4: Total phosphorous, silica, iron and zinc contents of volcanic ash and dust sample(s) versus the leached amounts into the seawater (Fig. 2). Total element contents are referred from the bulk compositions, except for the silica in volcanic ash (Table 3). Also indicated are the fractional solubilities calculated by using the formula $\%X_{\text{soluble}} = (\text{Dissolved } X / \text{Total } X) * 100$. Total phosphorous and iron contents (wt.%) are re-calculated from the oxide forms of P_2O_5 and Fe_2O_3 of the bulk compositions (Table 3).

4. Discussion

4.1 Volcanic ash input from Etna: On a decadal time-scale

The results of the geochemical experiments show that, upon a short contact with seawater volcanic ash from Etna volcano readily dissolves macro-nutrients and trace metals that can be bioavailable for the phytoplankton in the nutrient-starved MedSea. MedSea is one of the highest dust input regions in the global ocean ($20\text{-}50 \times 10^{12}$ g/y), with dust input of $3\text{-}7 \times 10^{12}$ g/y in the western, $4\text{-}11 \times 10^{12}$ g/y in the central, and $13\text{-}32 \times 10^{12}$ g/y in the eastern MedSea (Guerzoni et al., 1999). The region that is frequently affected by the Etna ash fallout is the central MedSea including largely the Ionian and the Tyrrhenian Sea (Figs. 1 and 6). Focusing exclusively on the ash producing events, the explosive eruptions of Etna can be considered as episodic. However, increased explosive activity periods can last several months (e.g., 2002-2003 eruption, (Andronico et al., 2008a)) and frequent episodes can occur during a single day (e.g., lava fountains occurred up to 3-times within a single day in February 2000 (Alparone et al., 2003)).

The total amount of tephra ejected from Etna during ten years period between 1998 and 2008 is about $45\text{-}79 \times 10^{12}$ g (Table 4). Based on the isopach maps in the Central American Volcanic arc (Kutterolf et al., 2008), it has been suggested that about 60-80% of the ejected tephra during explosive eruptions is deposited offshore (Olgun et al., 2011). Assuming a similar offshore deposition (60-80%), the annual averaged offshore Etna ash flux would correspond to $3\text{-}5 \times 10^{12}$ g/y, most of which have been likely to be deposited into the central MedSea (Table 4). On a decadal basis (Table 4), Etna ash input corresponds to about 45-75% of the dust input in the central MedSea, and likely to contribute to about one third of the marine sediments in the Ionian seafloor and may provide additional nutrients through upwelling during mixed winter conditions. The offshore ash input from Mount Etna can reach values up to 2.5×10^{12} g during episodic explosive eruptions (e.g., 22 July 1998; Table 4), in amounts as high as the yearly dust input in the central MedSea region, showing that volcanic ash fallout during explosive activities of Mount Etna can be an important nutrient supply in the central MedSea.

Table 4: Summary of ejected tephra during explosive eruptions of Mount Etna within 10 years period between 1998-2008. Volcanic ash flux in the Mediterranean Sea is calculated by assuming 60-80 % of ejected tephra is deposited offshore (based on Olgun et al., 2011). Tephra volumes are converted to mass by using ash density of 2600 kg/m³.

Year	Period	Description	Ejected Tephra
1998	11 June 1998 - 4 Feb. 1999	> 22 paroxysms, alternating magnitude of eruptions on the Voragine Crater. Plumes reached 12 km (a.s.l.) on 22 July 1998. ~ 38 days of ash-emissions, and during ~8 days ash reached to the sea.	0.8-3 x10 ¹² g ^(a, b) on 22 July 1998 (in 12 minutes)
2000	26 Jan.-24 June 28-29 Aug.	Paroxysm events reached up to 3 times per day on some days in February, 64 lava fountain episodes within less than six months. Plumes reach a maximum height of 6 km a.s.l. ~ 35 days of ash-emissions, and during ~12 days ash reached to the sea.	5.2-7.8 x10 ¹² g ^(c)
2001	17 July-9 Aug.	Flank eruptions in the SE crater. The most explosive phases 20-24 July and 31 July-5 August. Plumes reached 5 km a.s.l. Closure of Catania airport for several days. ~ 26 days of ash-emissions, and during ~9 days ash reached to the sea.	18x10 ¹² g ^(d) 1-2.3 x10 ¹² g ^(e)
2002- 2003	27 Oct. 2002- 9 Jan. 2003	Phreatomagmatic intense activity in the SE crater. Plumes rose 4-6 km high a.s.l., reached Greece and Libya (Dellino and Kyriakopoulos, 2003; Kelepertsis et al., 2003). The plume tracked over 1,000 km into the North Africa. ~58 days of ash emission, and during ~30 days ash reached to the sea.	38-50x10 ¹² g ^(f, g, h) (the entire period)
2006	14-31 July and 31 Aug.- 15 Dec.	Alternating eruptive intensity with light to moderate ash fallout lasting several hours to 2-4 days intervals. ~70 days of ash emissions, and during ~9 days ash reached to the sea.	> 0.4x10 ¹² g ^(i, j, k) (total of some daily records)
2007	11-29 Apr., 15-21 Aug. 4-5 Sept., 1 Oct-24 Nov.	Long-lasting powerful lava fountain episodes started at the SE crater. Plumes reached 5 km a.s.l. ~40 days of ash-emission, and during ~9 days ash reached to the Sea	3.1-4.5x10 ⁶ g ^(l) (4-5 September)
		Total tephra flux 1998-2008	45-79 x 10 ¹² g/decade
		Offshore ash flux into the MedSea (assuming 60-80 % of the ejected material is deposited offshore)	27-48 x 10 ¹² g/decade (3-5 x 10 ¹² g/year)

a) (Folch et al., 2009), b) (Andronico et al., 1999), c) (Alparone et al., 2003), d) (Behncke and Neri, 2003b), e) (Scollo et al., 2007), f) (Andronico et al., 2008b), g) (Andronico et al., 2005), h) (Carn, 2005), i) (Andronico et al., 2009b), j) (Andronico et al., 2009c), k) (Corradini et al., 2008), l) (Andronico et al., 2008a).

4.2 Volcanic ash flux during explosive eruptions of Etna

The phytoplankton response to episodic volcanic ash inputs may see an initial response in a couple of days followed by blooms lasting several weeks (e.g., bloom related to Kasatochi eruption lasted 5-6 weeks (Hamme et al., 2010; Langmann et al., 2010). Therefore, in order to evaluate the biogeochemical impacts of Etna ash fall, the ash flux during single eruptions have to be considered. The new supply of nutrients from volcanic ash fall during an explosive Etna eruption can be constrained by combining the ash fluxes (g/m^2) and the nutrient release from Etna volcanic ash upon contact with seawater (nmol/g ash).

Based on the ash samples collected on land, coastal ash fallouts were demonstrated by the isomass maps (contours in g/m^2) (e.g., Fig 5). Etna eruptions can deposit $>1,000 \text{ g/m}^2$ of ash in the coastal regions (Andronico et al., 2008b). The ash flux and therefore the ash-load on the ground gradually decrease from the source (Fig. 5). Although for most of the explosive Etna eruptions a larger fraction of ash is deposited into the MedSea, the ash fallouts in the open sea is not documented. Offshore deposited volcanic ash layers are usually/typically/normally preserved in the marine sediments. However, drill cores studies soon after the eruptions are very rare world-wide, except in the case of 1991 Pinatubo eruption in Philippines, for which the ash layers in the South China Sea were documented shortly after the eruption (Wiesner et al., 1995).

In the absence of marine sediment core data, an alternative way to estimate ash flux in the open MedSea is to combine the available proximal data with the distal ash fallout records (e.g., Greece, Libya) (see Fig. 6). The ash flux in remote regions in the MedSea can be constrained by using the universal relation between the thickness of the ash layers and the depositional areas (Fierstein and Nathenson, 1992; Pyle, 1989).

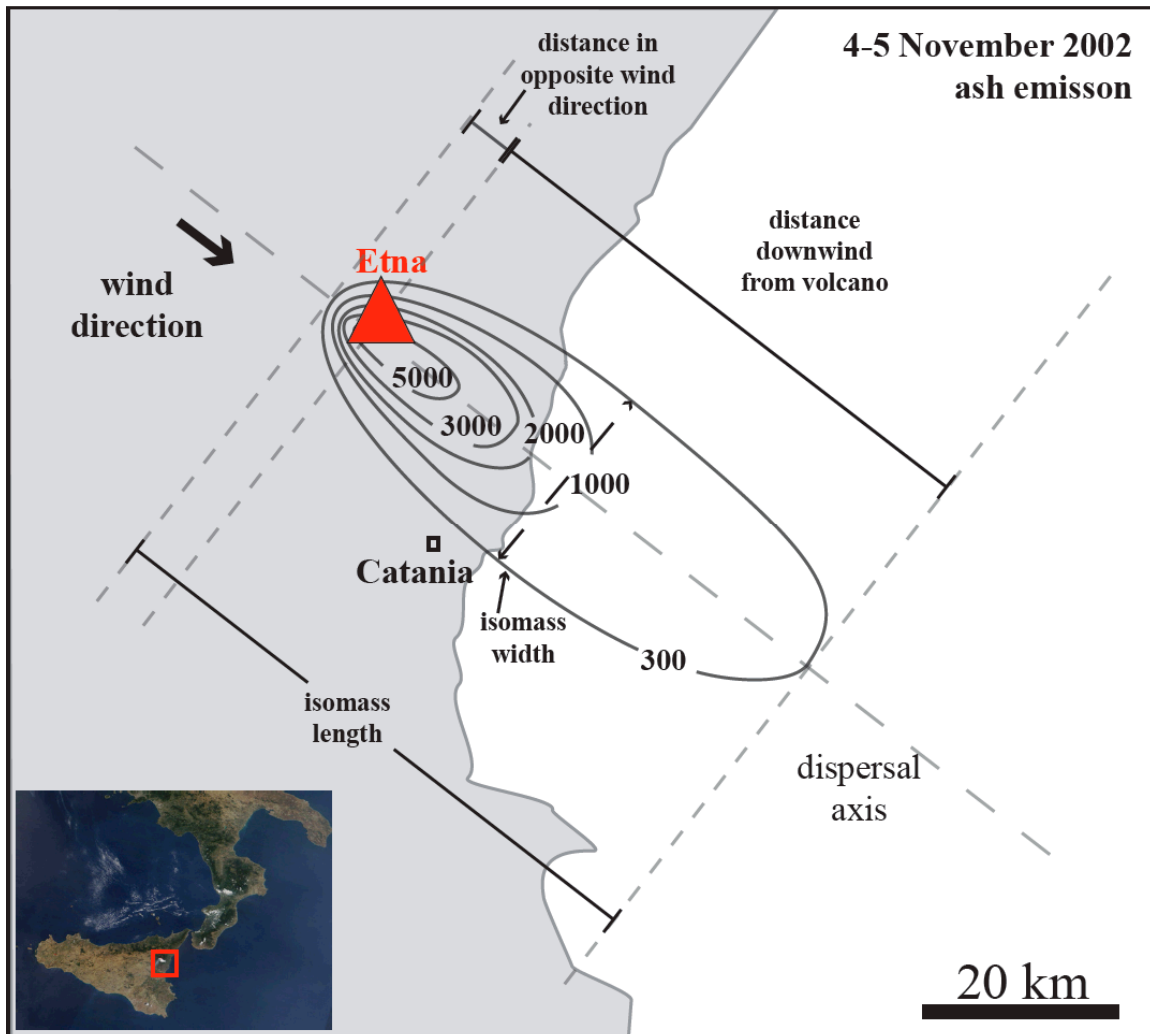


Figure 5: Isomass map showing the ash-fall deposition (in g/m^2) of the 4-5 November 2002 ash emission activity of Etna, based on (Andronico et al., 2008b). Also shown are the parameters mentioned in the text (e.g. isomass width, isomass length, the dispersal axis and the distance downwind).

4.2.1 A case study: 4-5 November 2002 ash emission

In this section, we estimated the ash felt on 4-5 November 2002 activity as a function of distance downwind in the MedSea. Intense explosive activity here considered lasted about eighteen hours, generating ash plumes up to ~6 km above the sea level (a.s.l.) and depositing about 1.4×10^{12} g of tephra (Andronico et al., 2005). Based on the isomass maps, coastal ash flux during 4 November 2002 eruption was $>1,000 \text{ g/m}^2$ (Fig. 5) (Andronico et al., 2008b). Notably, higher-level eruptions could have deposited ash in larger distances in the MedSea (e.g., 22 July 1998 eruption with plume height of 12 km a.s.l. (Table 4) (Andronico et al., 1999; Folch et al., 2009). However, due to scarcity of data, the ash flux over the MedSea could only be constructed for the 4 November 2002 eruption, which is used as a case study to show the marine biogeochemical impact of volcanic ash during single explosive eruptions.

Etna ash was recorded twice in Athens on 5 and 6 November 2002, twice also on the Greek Island of Kefalonia on 27 October and 5 November 2002, and once in Libya on 27 October 2002 (Andronico et al., 2005; Dellino and Kyriakopoulos, 2003; Kelepertsis et al., 2003). Among all these records, the amount of ash fallout was reported only in Athens (Kelepertsis et al., 2003). On 5 November 2002, 20 mg of ash was deposited in Athens, sampled over 706 cm^2 collectors (Dikaiakos et al., 1990; Kelepertsis et al., 2003), corresponding to an ash deposition of 0.3 g/m^2 . Based on the backward wind trajectories (Kelepertsis et al., 2003), the eruption started on 4 November 2002 transported the ash plume first in south-east and later in north-east, and arrived Athens from south-west direction (see Fig. 6).

In order to estimate the ash flux between Etna and Athens (0.3 g/m^2), we used the relation between the thickness of ash deposits and the depositional areas. Fallout deposits thin exponentially from the source. Therefore the relation between the \ln [thickness] and the square root [area] is quasi-linear, which is mainly used for estimating the total volume of the erupted deposit (Fierstein and Nathenson, 1992; Pyle, 1989). Based on the slopes provided in \ln [thickness] and sqrt [area], it is possible to calculate the ash-layer thicknesses for given isopach areas (Fig. 7).

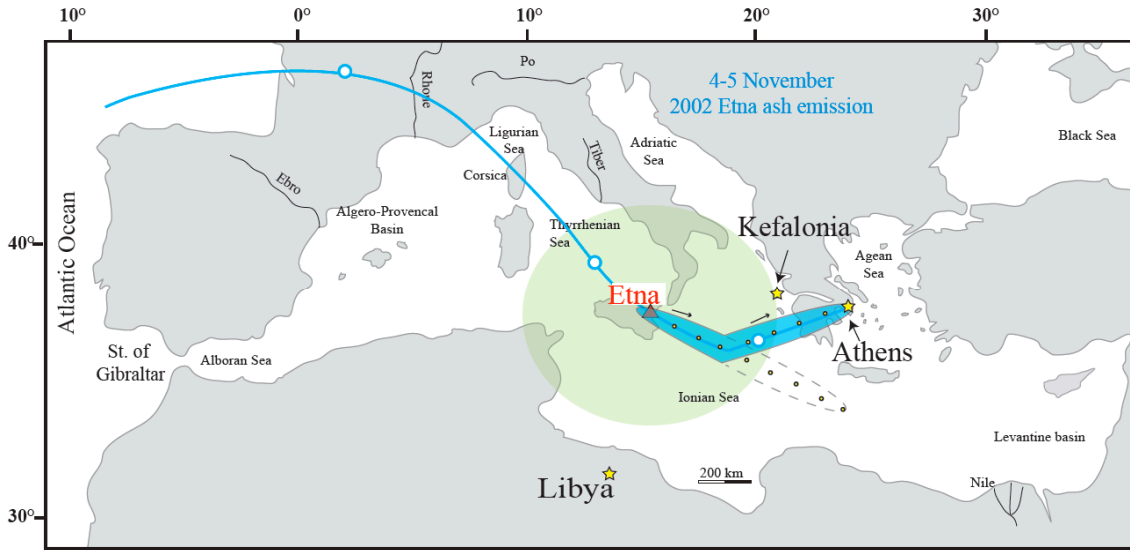


Figure 6: Map showing the arbitrary shape of the ash-plume produced by the 4-5 November 2002 explosive activity from Etna, which is used for ash-flux estimations as a case-study. The blue line is the 3-days backwards wind trajectory ending at 10:00 UTC on 5 November 2002 based on (Kelepertsis et al., 2003). Elliptical blue area shows the 0.3 g/m^2 isomass for the 4-5 November 2002 ash emission, based on ash fall in Athens (Kelepertsis et al., 2003). Yellow circles indicate downwind distance from volcano in 100 km intervals. The circular green areas show the region where Etna ash fallout is likely to impact MPP based on the nutrient supply from Etna ash indicated in Fig. 9. Yellow stars indicate the distal ash fallout records mentioned in the main text; Athens on 5-6 November 2002 (Kelepertsis et al., 2003), Kefalonia on 27 October 2002 and 5 November 2002 (Dellino and Kyriakopoulos, 2003; Kelepertsis et al., 2003), Libya on 27 October 2002 (Andronico et al., 2005; Carn, 2005).

The plots of \ln [thickness] and square root [area] show in most cases two straight-line segments for the proximal and distal isomass data, respectively (Fig. 7) (Fierstein and Nathenson, 1992; Pyle, 1989). In order to estimate the distal ash flux in the open sea, the necessary slope is the distal slope since, for this size of Etna eruptions, such fallout deposits at similar distances are considered distal; therefore the proximal slope likely to underestimate the actual dispersal of ash particles (see the steeper slope in Fig. 7). In the case of 4-5 November 2002 activity, we combined two data points for the distal slope which are the 0.3 g/m^2 of Athens data (Kelepertsis et al., 2003) and the 300 g/m^2 isomass of (Andronico et al., 2008b) (Fig 5).

Based on the wind trajectories, we estimated a curve-shape for the distal isomass with about 800 km downwind from the volcano (Fig. 6). Isomass length and width are calculated based on the last two proximal data (Table 5), assuming constant enlargement. The length that is deposited in the opposite direction increases about 0.05 km per km isopach length and the width increases about 0.2 per km increase in isopach length. Accordingly, the dimensions of the 0.3 g/m^2 isomass drawn in Athens is estimated to be 848 km long and 186 km wide (Table 5). For simplicity in calculations we assumed elliptical isopach areas ($\text{Area}=\pi*(\text{width}/2)*(\text{length}/2)$), which is also the closest shape in the proximal isomass map of the 4 November 2002 activity (Fig. 5). By using the distal equation, the ash layer thicknesses were calculated for downwind distances up to 800 km. The data for 848 km elliptical isomass is projected to the curve-shape isomass for the actual location of the corresponding ash-flux, as described in Fig. 6.

Table 5: Ash-flux estimations for the case-study on 4-5 November 2002 Etna ash emission by using the relation between the natural logarithm of the ash-thickness and the depositional area (Fierstein and Nathenson, 1992; Pyle, 1989). Based on the plots of \ln [thickness] versus square root [area] (see Fig. 7), three distal equations were calculated for three different isomass dimensions; a) moderate (extrapolated based on proximal data), b) narrower and c) wider plume.

Table 5a: Moderate plume (distal equation: $y=(-0.0216x)+2.0289$, see Fig. 7)

Ash-flux (g/m^2)	Downwind distance (km)	Isomass Length (km)	Isomass width (km)	Area (km^2)	Area ^{-1/2} (km)	Ln thickness (mm)	Thickness (mm)
5000	11	13	5	44	7	4.15	63
3000	17	21	9	138	12	3.64	38
2000	21	25	12	193	14	3.23	25
1000	31	36	15	382	20	2.54	13
300	55	61	20	1029	32	1.34	4
231	100	109	30	2571	51	0.9	2.5
91	200	215	52	8840	94	0.0	1.0
36	300	320	74	18713	137	-0.9	0.4
14	400	426	97	32378	180	-1.9	0.156
5.6	500	531	119	49577	223	-2.8	0.062
2.2	600	637	141	70639	266	-3.7	0.024
0.9	700	743	164	95416	309	-4.6	0.010
0.3	800	848	186	123622	352	-5.6	0.004

Table 5b: Narrower plume (distal equation: $y=(-0.0308x)+2.3234$, see Fig 7)

Ash-flux (g/m^2)	Downwind distance (km)	Isomass Length (km)	Isomass width (km)	Area (km^2)	Area ^{-1/2} (km)	Ln thickness (mm)	Thickness (mm)
5000	11	13	5	44	7	4.15	63
3000	17	21	9	138	12	3.64	38
2000	21	25	12	193	14	3.23	25
1000	31	36	15	382	20	2.54	13
300	55	61	20	1029	32	1.34	4
225	100	109	25	2120	46	0.9	2.5
86	200	215	35	5972	77	-0.1	0.9
34	300	320	46	11528	107	-1.0	0.4
13	400	426	56	18893	137	-1.9	0.148
5.4	500	531	67	27928	167	-2.8	0.059
2.1	600	637	78	38806	197	-3.7	0.024
0.9	700	743	88	51450	227	-4.7	0.009
0.3	800	848	99	65714	256	-5.6	0.004

Table 5c: Wider plume (distal equation: $y=(-0.01816x+1.9172)$, see Fig. 7)

Ash-flux (g/m ²)	Downwind distance (km)	Isomass Length (km)	Isomass width (km)	Area (km ²)	Area ^{-1/2} (km)	Ln thickness (mm)	Thickness (mm)
5000	11	13	5	44	7	4.15	63
3000	17	21	9	138	12	3.64	38
2000	21	25	12	193	14	3.23	25
1000	31	36	15	382	20	2.54	13
300	55	61	20	1029	32	1.34	4
232	100	109	34	2936	54	0.9	2.6
91	200	215	66	11162	106	0.0	1.0
36	300	320	98	24530	157	-0.9	0.4
14	400	426	129	43295	208	-1.8	0.157
5.7	500	531	161	67103	259	-2.8	0.063
2.2	600	637	193	96407	310	-3.7	0.025
0.9	700	743	225	131007	362	-4.6	0.010
0.3	800	848	256	170500	413	-5.6	0.004

Proximal mass-fluxes in g/m² were converted to thicknesses in millimeters (isopachs) by using the average ash density of 2600 kg/m³ (Carn, 2005), porosity (30 %) and interparticle pore space (50% proximal, 30% distal) of the ash deposits (Kutterolf et al., 2008). The equivalent volumes for the proximal and distal layers are 3.3 m³ and 2.9 m³, respectively. Deposition of one g of ash per square meter area corresponds to ash layer thicknesses of 0.0127 mm for the proximal and 0.011 mm for the distal ash layers, with corrected bulk densities of 789 kg/m³ and 910 kg/m³, respectively.

Error related to the ash flux estimates for 4-5 November 2002 ash emission case

The method of ln [thickness] and square root [area] is valid for any shape of isomass (Fierstein and Nathenson, 1992). Due to cloudy conditions during the eruption phase (<http://www.fvalk.com/etna.htm>), the actual isomass area is unknown and the dimensions of the plume subject to some error. Different isopach areas give different distal equations so that the ash-load variation can be estimated (Fig. 7). To test the magnitude of the variation, the error was estimated by using a range of isopach widths for given isopach lengths. Based on the last two proximal data, the width (w) of the isomass expands with a rate of 0.2 per km increase in isopach length (l), referred here as w:l ratio. Alternative width dimensions were calculated for narrower and wider isopachs with w:l ratios of 0.1 (Scenario 1), 0.2 (Scenario 2) and 0.3 (Scenario 3), respectively (Fig. 7). The calculated width of 0.3 g/m² isomass ranges from 99 km to 256 km, giving a wide range

of isomass area between 65,714 km² - 170,500 km², which enables us to calculate the variation in the ash-flux in the two end-member scenarios for isomass area.

4.2.2 Ash fallout during the 4-5 November 2002 ash emission of Etna

As shown in Table 5, the variation in the ash-load decreases downwind from the volcano. The maximum error found at 100 km distance from the volcanic source is about ± 3 g ranging from 225 g to 232 g. The variation in the ash-load decreases down to less than 0.1 g ash in 800 km downwind from the volcanic source (Table 5). It is important to note that the flux estimated for the 4-5 November 2002 can be an order of magnitude lower compared to the large eruptions, like the Pinatubo 1991 eruption, during which the ash fallout was 20-30 g/m² as far 585 km west of the volcano (Fig. 8) (Wiesner et al., 1995).

In terms of nutrient supply, since the nutrient solubility of Etna ash samples is highly variable, the error associated with the ash flux is negligible in the open sea. The downwind ash-flux can also be used for comparisons with desert dust flux in the MedSea (Fig. 8). Extreme dust events can deposit as high as 29 g/m² in the MedSea (probably once every year) (Guieu et al., 2010; TERNON et al., 2010), average dust storm event deposit 10 g/m² dust (Guieu et al., 2010), and low-intensity dust events deposit about 0.05 g/m² (occurred 27 times at the DYAFAMED-site during four year period) (TERNON et al., 2010). Based on the estimates for 4 November 2002 eruption (Fig. 8), in the coastal region, the particle flux during eruptions can be 10-50 times higher than the extreme dust events. Ash flux simulates an extreme dust event about 300 km and resembles an average dust storm event about 400-450 km downwind. In distances as far 800 km, ash flux is above a low-level desert input (Fig. 8).

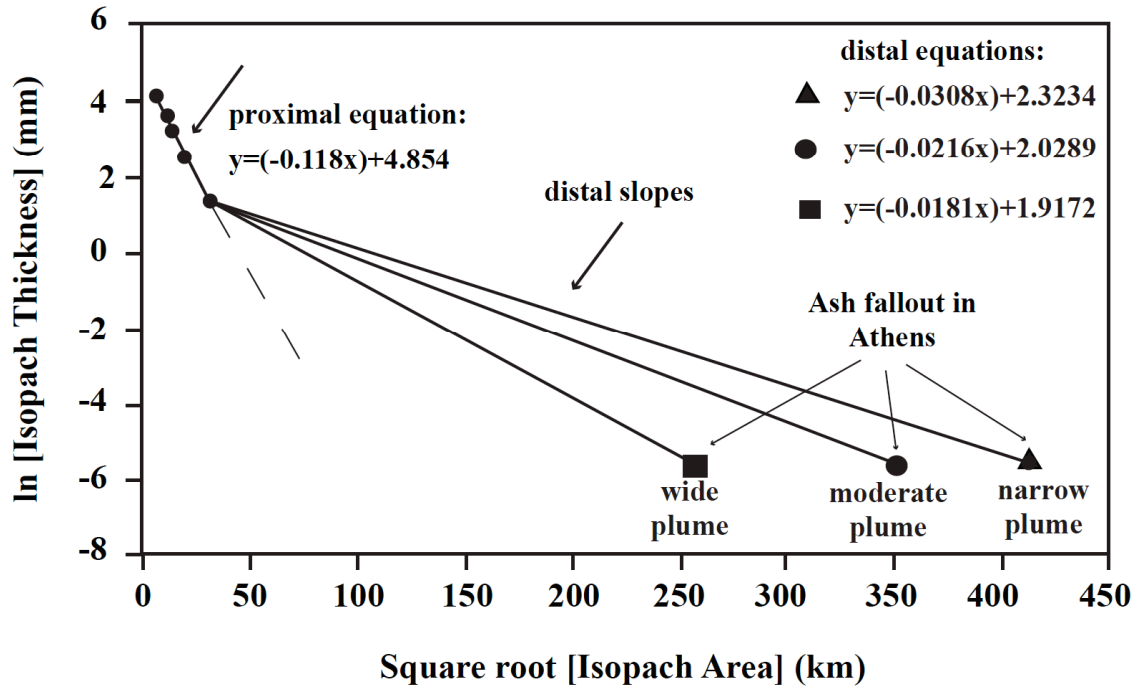


Figure 7: Plots of natural logarithm of the thickness of the ash layer and the square root of the ash depositional area. The equations provided by the distal slope are used for estimating the ash-fall as a function of distance from the volcano (shown in Table 5). The three different isopach areas were calculated based on the varying plume width for a wide, moderate and narrow isopach area. See section 4.2.1 for discussion.

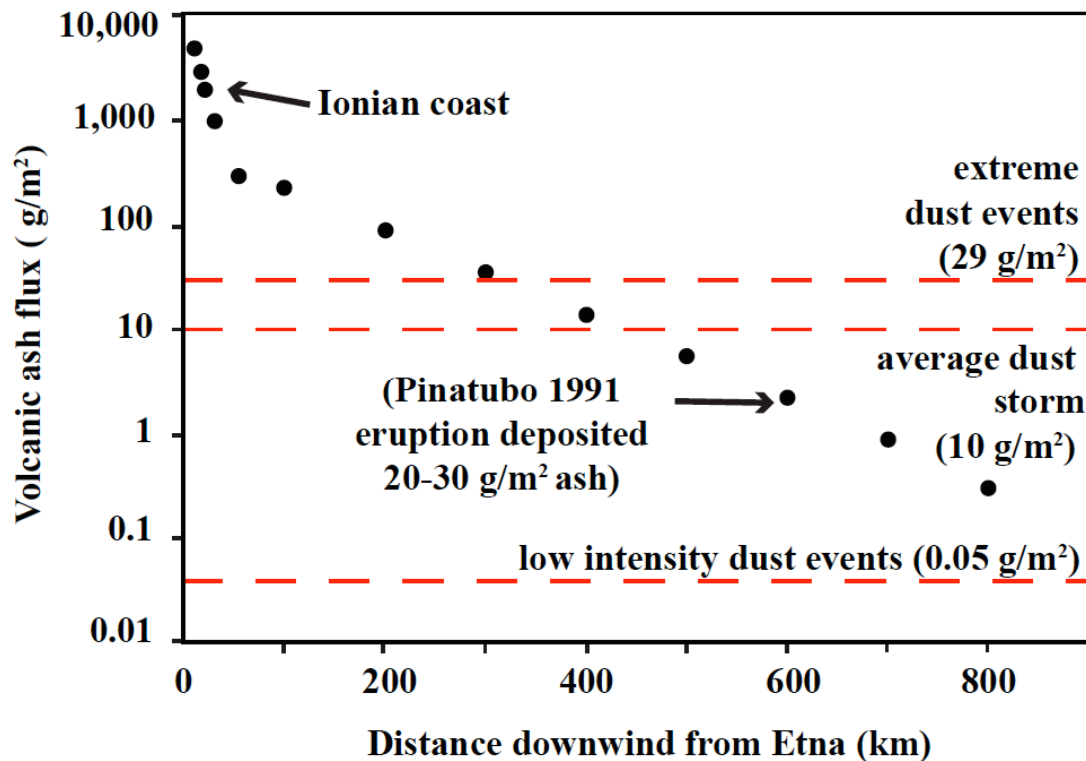


Figure 8: Estimated volcanic ash-flux in the MedSea for the case-study based on the 4-5 November 2002 ash emission of Etna. Ash-flux is plotted as a function of distance (km) from the Etna volcano. Error related to the ash-flux estimates is smaller than the symbols (maximum error is ± 3 g in the 100 km, < 0.1 g in 800 km) (see Table 5). The dashed lines indicate the dust flux during extreme events (29 g/m^2) (Guieu et al., 2010; Ternon et al., 2010), average storm events (10 g/m^2) (Guieu et al., 2010), and low intensity dust events (0.05 g/m^2) (Ternon et al., 2010). Also indicated is the ash-flux during Pinatubo 1991 eruption based on the marine sediment core data, corresponding to $20\text{-}30 \text{ g/m}^2$ as far 585 km from the volcano (Wiesner et al., 1995).

4.3 Biogeochemical implications of nutrient supply during an Etna eruption

Fertilizing potential of Etna ash fallout has been evidenced during July 2001 by the increased chlorophyll-a concentrations in the Ionian Sea ash fallout region (Censi et al., 2010). However, the mechanisms that stimulated the MPP remained uncertain. Here we predicted the input of dissolved nutrient in the surface water by using ash flux and nutrient-release from Etna ash. We assumed a homogenous distribution of particles over top meter of the column.

4.3.1 Phosphate fertilization by Etna ash fallout

The main limiting factor for MPP in the MedSea is likely P (Krom et al., 1991; Thingstad et al., 1998). The N:P ratio of the seawater is commonly used to establish the limiting nutrient. The N:P ratio of MedSea surface waters is 20-27, higher compared to normal oceanic N:P ratio (of 16:1), and has been suggested to reflect P-limitation in the MedSea (Bonnet et al., 2005; Guerzoni et al., 1999; Socal et al., 1999). Dissolved P-concentrations in the MedSea are generally less than standard detection limits (of 20 nM) (Bonnet et al., 2005). Based on a recent one-year-time-series study in the western MedSea, the highest P-concentrations are found during winter mixed period reaching values of 200-350 nM (Fig. 9), and decreases to 30 nM in April, after the spring bloom (Pulido-Villena et al., 2010). Throughout the stratified period, between May to December, surface P-concentrations (in upper 8-20 km) are found to be as low as <1-6 nM in the western MedSea (Fig. 9) (Pulido-Villena et al., 2010), similar to measured concentrations in the eastern MedSea with P-concentrations of <2-4 nM (Krom et al., 2005). P-concentrations <1 nM are sufficiently low to result in P control on the MPP (Wu et al., 2000).

P-fertilizing effects of dust deposition in the MedSea has previously suggested by microcosm (Bonnet et al., 2005; Herut et al., 2005; Lekunberri et al., 2010) and mesocosm experiments (Laghdass et al., 2011; Pulido-Villena et al., 2010). However, the threshold concentrations of P to stimulate the MPP in the MedSea remain poorly understood. By measurements of P-uptake, the concentration of bioavailable P was estimated to be 3nM (Moutin et al., 2002).

During a large-scale mesocosm experiment (54 m³, 15 m depth) in the western MedSea, dust addition (mimicking 10 g/m² dust deposition) increased the dissolved P-concentrations in the upper 40 cm in the surface by about 12 nM (Pulido-Villena et al., 2010). However, no significant P increase was observed at 5 m and 10 m depths, probably because most of the particles stay in the surface during the first hours of deposition, and lead a transient increase in the surface P-concentrations (Pulido-Villena et al., 2010). Based on the P-release per gram of Cape Verdean loess in our study (43 nmol/g; Fig. 2), the input of P in the surface water through dry deposition of dust would be 15 nM for deposition of 10 g/m² dust, which is consistent with the mesocosm experiments in the western MedSea (Pulido-Villena et al., 2010). If we assume a homogenous distribution of particles and constant dissolution in the upper 1 m water column, the supply of P from dust would be 6 nM, lower compared to the calculations for the upper 40 cm. P-input during extreme events (29 g/m²) would be as high 42 nM in the upper 40 cm and 17 nM in the upper 1 m. Input of P during low intensity events (0.05 g/m²) would be as low as 0.07 nM in the upper 40 cm and 0.03 nM at 1 m depth. These variations in our estimates highlight the importance vertical distribution and dissolution rates of the particles during the settlement in the ocean.

The maximum P-input during Etna eruptions would be in the first 100 km downwind from the volcano, ranging from 1,940 nM to 220 nM (calculated for 1 m depth), above the highest P-concentrations during winter period (Fig. 9). The minimum P-input based on the geochemical data, ranges between 14 nM and 2 nM in the first 100 km (Fig. 9). A fraction of the dissolved P may be scavenged by adsorption on the ash particle surface, similar to what has been suggested for dust particles (Krom et al., 1991; Ridame et al., 2003). However, scavenging of nutrients to the volcanic ash surface has not been evaluated yet. In the open ocean, assuming a threshold of 3 nM of P for biological response (Fig. 9) (Moutin et al., 2002), the minimum impact on the P fertilization is at least 100-150 km downwind. Depending the P-release potential of the erupted ash (Fig. 2), the maximum distance for P-fertilization can extend as far as 600 km in the MedSea (Fig. 9). Therefore, following the deposition of volcanic ash into the sea surface, ash plumes ejected from Etna may have significant effect on the MPP through supplying P, the ultimate limiting nutrient in the surface MedSea.

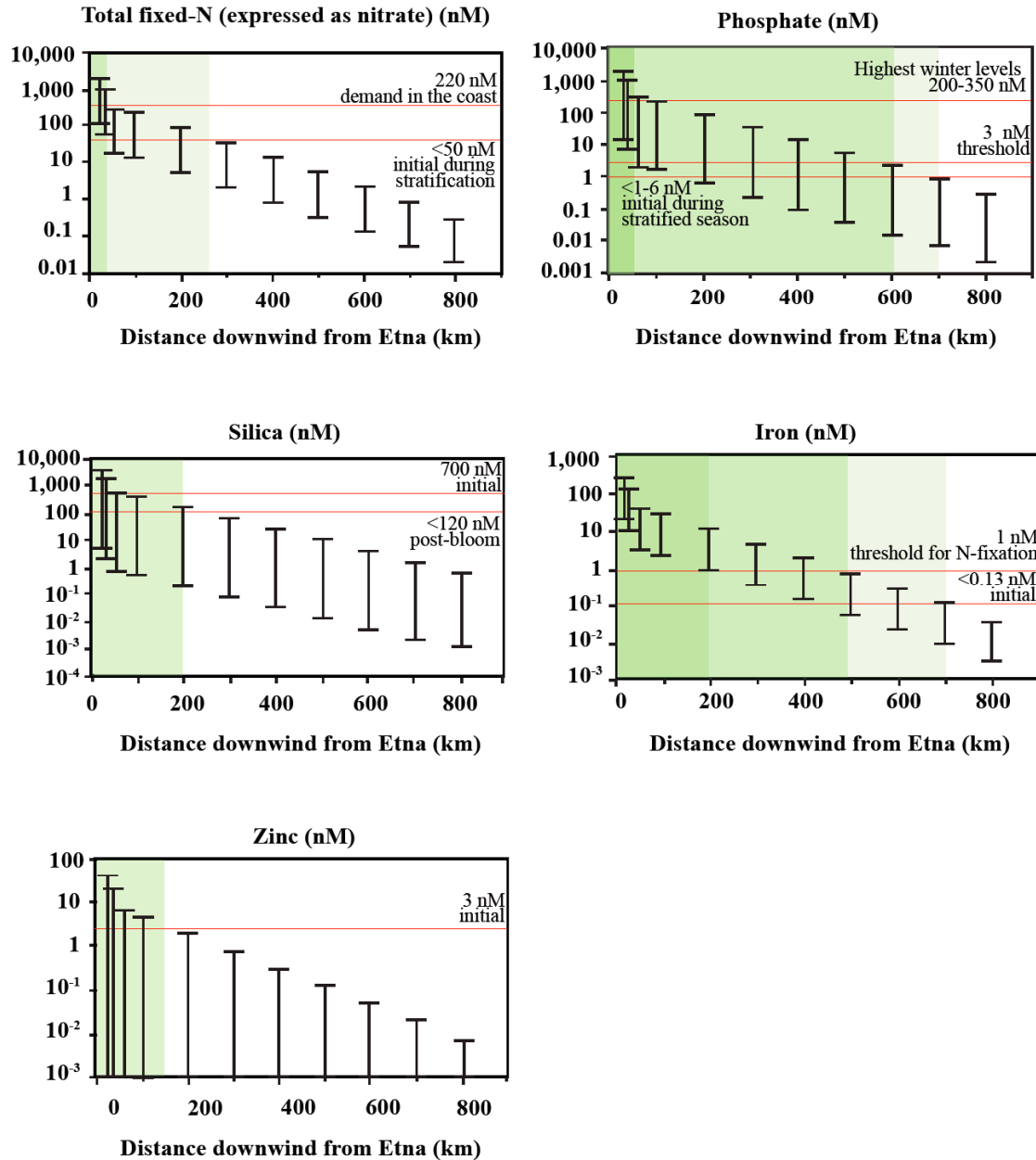


Figure 9: Supply of nutrients related to an Etna ash fall integrated to top meter of water depth, based on the 4-5 November 2002 ash emissions (Fig. 8) and the nutrient release data (Fig. 2). Concentrations in nM show the range indicated by the minimum and the maximum release of nutrients by Etna ash samples (Fig. 2). The initial and threshold seawater concentrations are indicated as red lines (see section 4.3 for discussion). The green areas indicate the regions where Etna ash fall would likely to affect marine primary productivity (dark green regions with higher likelihood). The corresponding distances downwind from Etna is shown in the MedSea map in Fig. 6.

4.3.2 Iron and nitrogen fixation

Addition of P alone in the MedSea may not enhance MPP since the limitation may immediately shift to nitrogen (Herut et al., 2005), as the concentrations N during the stratified season are as low as P (less than detection limits of 50 nM) (Fig 9) (Bonnet et al., 2005; Mihalopoulos et al., 1997). Indeed, N-limitation after ash deposition is very likely to occur due to low N:P ratio of the ash leachates. Most of the Etna samples showed N:P ratios less than 16, which are lower if compared to the typical N:P ratio of MedSea (20-27).

The input of total fixed N related to an Etna ash fallout is 120-1940 nM in the coast, 14-225 nM in the first 100 km, decreasing <1-14 nM at distances 400 km downwind from the volcano (Fig. 9). The concentrations of fixed N sufficient to maintain plankton demand in the coast is found be high (220 nM), in the coastal zone of Gulf of Lion (Fig 9) (Diaz and Raimbault, 2000). The maximum estimates of nitrate input from ash would be significant up to 200 km downwind from the volcano (>220 nM), while the minimum estimates are slightly lower than limit to sustain N demand for new production (e.g., 300-150 nM, in the 30 km coastal zone) (Fig 9). The requirement of fixed-N is probably lower in the open sea, and N-fixation may additionally increase the N-concentrations in the surface MedSea.

Nitrogen fixation is co-limited by P and Fe, and is an important source of dissolved nitrogen in the MedSea (Bonnet et al., 2005; Mills et al., 2004). Like the eastern tropical Atlantic Ocean (Mills et al., 2004), there is growing evidence supporting the importance of N₂-fixation on the phytoplankton community (and the diazotrophs) in the Mediterranean waters (Bonnet et al., 2005; Herut et al., 2005; Lenton and Watson, 2000). In fact, the high N:P ratio found in the MedSea has been related to elevated N-fixation rates associated to high Fe-input through desert dust, shifting the system towards P-limitation (Lenton and Watson, 2000; Wu et al., 2000). Since Etna ash provides P along with Fe, ash fallout from Etna can therefore impact the surface N-concentrations by directly through particle dissolution, and indirectly through N-fixation by addition of P and Fe.

Fe-concentrations in MedSea are around 1-3 nM in the coast (e.g., (Censi et al., 2010)), while very low concentrations of <0.13 nM were found in the open MedSea (Fig. 9) (Sarhou and Jeandel, 2001), despite the high input of desert dust. Microcosm experiments in the MedSea showed that addition of Fe together with P stimulates MPP more effectively compared to addition of Fe alone or P alone, which has been linked to increased N-fixation (Bonnet et al., 2005). In a bioassay experiment in the eastern tropical Atlantic Ocean, addition of ~3-11 nM of P together with 1-4 nM of Fe swiftly doubled the N-fixation rates (Mills et al., 2004).

Based on the Fe-release data, dry deposition of Etna ash can supply 22-260 nM of Fe in the coast, and 10-130 nM of Fe about 30 km from the coast, 1-12 nM within 300 km distance, decreasing down to 0.1 nM to 2 nM in the distances 400 km downwind from the volcano (Fig. 9). If we assume 3 nM P and 1 nM Fe as threshold for N-fixation (Mills et al., 2004), ash fallout would have strong impacts on the N-fixation extending as far as 500 km distances downwind from the volcano with strongest potential in the first 100 km (based on minimum release) (Fig. 6 and Fig. 9)

In the high-nutrient, low-chlorophyll (HNLC) ocean regions, Fe is the major limiting nutrient, where 2 nM increase in the Fe-concentrations is found to be sufficient to trigger phytoplankton blooms (Wells, 2003). However, the role of Fe for the MPP in the LNLC ocean regions is still not entirely understood. It has been suggested that the deposition of reduced Fe to surface waters of MedSea has the potential to induce phytoplankton blooms (Saydam, 1996). For example, wet deposition of Saharan dust on July 1988 in the central MedSea off the coast of Libya was associated to an *Emiliania huxleyi* bloom (evidenced by the Meteosat scenes) (Dulac et al., 1996). Fe-concentrations in the surface MedSea during this dust event were increased by 6 nM (Dulac et al., 1996). In contrast, a recent mesocosm study in the western MedSea showed that, large dust deposition events might act as sink of Fe (rather than a source), through scavenging of Fe on to the dust particles (by 0.4 ± 0.1 nmol Fe/mg dust) (Wagener et al., 2010). Our data for Cape Verde loess suggest low amounts of Fe-input by <1 nM even for extreme dust events of 29 g/m² dust flux.

Dissolved Fe concentrations in the Ionian coast within the Etna ash fallout region on 21 July 2001 were by 640-690 nM (Censi et al., 2010), significantly higher compared

to our estimates based on the geochemical data (highest by 260 nM) (Fig. 9). The high concentrations of dissolved Fe in the ash fallout region has been previously linked to increased lysis of phytoplankton (by grazing), which may in turn increase the complexation of the Fe released from Etna ash (i.e. higher organic ligand concentrations) (Censi et al., 2010). Another possibility would be a decay of the soluble Fe-compounds (e.g., Fe-bearing salts) on our ash samples through storage time of the ash samples, which may underestimate the actual Fe-mobilization from volcanic ash (Jones and Gislason, 2008; Olgun et al., 2011).

4.3.3 Silica

New production in the MedSea is characterized by dominance of diatoms (Socal et al., 1999). Silica is an ultimate nutrient required by the phytoplankton to build up the silica shells. Si-concentrations during stratified season are relatively high (700 nM) (Fig. 9) (Bonnet et al., 2005; Schink and Kingston, 1967). By contrast, severe Si-limitation of the diatom spring bloom has been observed at least for one coastal zone (in the Gulf of Lion) (Leblanc et al., 2005). Elevated demand of Si by the diatom blooms can reduce the Si concentrations to 120 nM (Fig. 9), indicating the significance of Si after the bloom period at the end of April. Si-supply based on the data from Cape Verde loess samples would range between 13 nM to 32 nM calculated for the extreme dust events of 29 g/m² dust flux.

Based on the lowest Si-release by Etna ash into the seawater, the minimum supply of Si is insignificant (below 5 nM), while the maximum input based on highest mobilization would be about 4.1 μM in the coast, 2 μM in the 30 km in the coast, and >120 nM in the 200 km downwind from the volcano, indicating eruptions can impact on Si-budget in the surface MedSea waters, however very dependent on the Si-mobilization behavior of the ash (Fig. 9). Recent biological experiments have shown that, when grown in ash-fertilized seawater, diatoms (e.g., *Thalassiosira pseudonana*) benefit more from volcanic ash compared to coccolithopores (e.g., *Emiliania huxleyi*) (Hoffmann et al., submitted to Marine Chemistry). It is therefore very likely that ash fallout from Etna may change the composition of phytoplankton assemblage in the ash fallout regions towards domination of diatoms in the surface water, and further increase demand of Si in the surface waters.

4.3.4 Zinc

Zinc is a bioactive trace metal required by the phytoplankton and a co-factor in alkaline phosphatase, an enzyme that allows phytoplankton to utilize phosphate from organic compounds (Morel and Price, 2003). Typical Zn-levels are around 3 nM in the MedSea (Ruiz-Pino et al., 1991), with highest Zn concentrations of 10 nM found in the Alboran Sea (Sherrell and Boyle, 1988). In the North Atlantic Ocean, the lessening of P-limitation of N-fixers was linked to Zn that is possibly introduced by the dust particles (Mills et al., 2004). However, the Cape Verde loess sample did not show any Zn-release. Together, not all the Etna samples released Zn during the first hour contact with seawater (Fig. 9). Highest input of Zn related to the ash fallout would be 42 nM in the coast, and above 3 nM in distances about 150 km downwind from Etna (Fig. 9). Addition of Zn together with P by the ashfall may increase the up-take of P and relieve the P-limitation in the MedSea.

4.3.5 Copper-toxicity

The MedSea, especially the central and eastern part, were inferred to be close to the Cu-toxicity during large part of the year (Paytan et al., 2009). Our voltammetric experiments showed that during the first hour of interaction with seawater, Etna ash releases no detectable amounts of Cu into the seawater. Long-term ash-dissolution experiments also showed that the dissolved Cu concentrations remain below 1 nM until the end of the first week (Censi et al., 2010). Therefore, in terms of Cu, eruptions of Etna are unlikely to increase the Cu-toxicity in the MedSea. Atmospheric input Cu and Zn therefore is likely dominated by the anthropogenic particles, since most of the trace metals are more mobile from pollution derived aerosols (Boyle et al., 1985; Guerzoni et al., 1999; Guieu et al., 1997).

Conclusive Remarks

- Volcanic ash ejected during Etna eruptions release fixed-nitrogen, phosphate, silica, iron and zinc into seawater, and provide an atmospheric source of nutrients in the oligotrophic surface waters of MedSea.
- Ash flux estimates based on the 4-5 November 2002 Etna ash emission event showed that during explosive eruptions of Etna, volcanic ash flux in the central

MedSea exceeds the particle flux during dust storm events. Volcanic ash flux of $>10 \text{ g/m}^2$, similar to average dust storms, can be deposited as far as 400 km downwind from Etna.

- Based on the ash flux during an Etna eruption and the nutrient release from Etna ash, the highest impact of Etna ash fallout would be relieving the phosphate limitation in the LNLC MedSea by providing a good source of dissolved phosphate in the surface water column.
- Delivery of significant amounts of iron together phosphate is very likely to increase nitrogen-fixation rates in the Etna ash fallout regions in the MedSea.
- Input of iron and silica by the Etna ash would be more pronounced during post-bloom periods due to strong utilization by diatoms, compared to winter mixed season.
- Compared to the more widespread inputs of desert dust that affects the entire MedSea, the impact of Etna ash is more episodic and affects mainly the central MedSea region. However, increased explosivity of the Etna over the last decades, suggests that the biogeochemical impact of Etna ash fallout on the nutrient-starved LNLC MedSea is likely to increase in the near future.

Acknowledgements

We thank to Frank Malien for helping during the photometric measurements. We also thank M. Thoener for technical assistance with the electron microprobe analyses. We thank Antonio Cristaldi and Simona Scollo; INGV- Sezione di Catania for their help in the ash sample collection, and Deborah Lo Castro (INGV-Sezione di Catania) for assisting in the sample selection. This study was supported by IFM-GEOMAR through the multidisciplinary research group NOVUM “Nutrients originating volcanoes and their effects on the euphotic zone of the marine ecosystem”. This study is contribution number 174 of the Sonderforschungsbereich (SFB) 574 “Volatiles and Hazards in Subduction Zones”.

References

- Alparone, S., Andronico, D., Lodato, L. and SgROI, T., 2003. Relationship between tremor and volcanic activity during the Southeast Crater eruption on Mount Etna in early 2000. *Journal of Geophysical Research*, 108.
- Andronico, D. et al., 2005. A multi-disciplinary study of the 2002–03 Etna eruption: insights for a complex plumbing system. *Bulletin of Volcanology*.
- Andronico, D., Cristaldi, A., P., D.C. and Taddeucci, J., 2009a. Shifting styles of basaltic explosive activity during the 2002-03 eruption of Mt Etna, Italy. *Journal of Volcanology and Geothermal Research*, 180(2-4): 110-122.
- Andronico, D., Cristaldi, A. and Scollo, S., 2008a. The 4–5 September 2007 lava fountain at South-East Crater of Mt Etna, Italy. *Journal of Volcanology and Geothermal Research*, 173: 325–328.
- Andronico, D., Del Carlo, P. and Coltelli, M., 1999. The 22 July 1998 fire fountain episode at Voragine Crater (Mt. Etna, Italy), *Proceedings of the Volcanic and Magmatic Studies Group - Annual Meeting, Birmingham*.
- Andronico, D., Scollo, S., Caruso, S. and Cristaldi, A., 2008b. The 2002–03 Etna explosive activity: Tephra dispersal and features of the deposits. *Journal of Geophysical Research*, 113.
- Andronico, D., Scollo, S., Cristaldi, A. and Ferrari, F., 2009b. Monitoring ash emission episodes at Mt. Etna: The 16 November 2006 case study. *Journal of Volcanology and Geothermal Research*, 180: 123-134.
- Andronico, D., Spinetti, C., Cristaldi, A. and Buongiorno, M.F., 2009c. Observations of Mt. Etna volcanic ash plumes in 2006: An integrated approach from ground-based and polar satellite NOAA–AVHRR monitoring system. *Journal of Volcanology and Geothermal Research*, 180: 135-147.
- Azov, Y., 1991. Eastern Mediterranean-a Marine Desert? *Marine Pollution Bulletin*, 23: 225-232.

- Baker, A. and Croot, P., 2010. Atmospheric and marine controls on aerosol iron solubility in seawater. *Marine Chemistry*, 120: 4-13.
- Behncke, B. and Neri, M., 2003a. Cycles and trends in the recent eruptive behaviour of Mount Etna (Italy). *Canadian Journal of Earth Sciences*, 40: 1405-1411.
- Behncke, B. and Neri, M., 2003b. The July–August 2001 eruption of Mt. Etna (Sicily). *Bulletin of Volcanology*, 65: 461-476.
- Bergametti, G. et al., 1992. Source, transport and deposition of atmospheric phosphorus over the northwestern Mediterranean. *Journal of Atmospheric Chemistry*, 14: 501-513.
- Bethoux, J.P. et al., 1998. Nutrients in the Mediterranean Sea, mass balance and statistical analysis of concentrations with respect to environmental change. *Marine Chemistry*, 63: 155–169.
- Bethoux, J.P., Morin, P., Madec, C. and Gentili, B., 1992. Phosphorus and nitrogen behaviour in the Mediterranean Sea. *Deep-Sea Research*, 39: 1641 - 1654.
- Bonnet, S., Guie, C., Chiaverini, J., Ras, J. and Stock, A., 2005. Effect of atmospheric nutrients on the autotrophic communities in a low Nutrient, low chlorophyll system. *Limnology and Oceanography*, 50: 1810-1819.
- Bonnet, S. and Guieu, C., 2004. Dissolution of atmospheric iron in seawater. *Geophysical Research Letters*, 31.
- Boyle, E.A., Chapnick, S.D., Bai, X.X. and Spivack, A., 1985. Trace metal enrichments in the Mediterranean Sea. *Earth and Planetary Science Letters*, 74: 405-419.
- Branca, S. and Del Carlo, P., 2005. Types of eruptions of Etna volcano AD 1670–2003: implications for short-term eruptive behaviour. *Bulletin of Volcanology*, 67: 732-742.
- Calvari, S., Coltelli, M., Pompilio, M. and Scribano, V., 1991. The eruptive activity between October 1989 and December 1990. *Acta Vulcanologica*(1): 257–260.
- Carn, S.A., 2005. Quantifying tropospheric volcanic emissions with AIRS: The 2002 eruption of Mt. Etna (Italy). *Geophysical Research Letters*, 32.
- Carveni, P., Romano, R., Caltabiano, T., Grasso, M.F. and Gresta, S., 1994. The exceptional explosive activity of 5 January 1990 at the SE-Crater of Mt. Etna Volcano (Sicily). *Boll. Soc. Geol. It.* , 113: 613–631.

- Censi, P. et al., 2010. Trace element behaviour in seawater during Etna's pyroclastic activity in 2001: Concurrent effects of nutrients and formation of alteration minerals. *Journal of Volcanology and Geothermal Research*, 193: 106-116.
- Chester, R., Nimmo, M. and Keyse, S., 1996. The influence of Saharan and Middle Eastern desert derived dust on the trace metal composition of Mediterranean aerosols and rainwater: An overview. In: S. Guerzoni and R. Chester (Editors), *The Impact of Desert Dust Across the Mediterranean*. Springer, New York, pp. 253– 273.
- Coltelli, M. et al., 2007. Analysis of the 2001 lava flow eruption of Mt. Etna from three-dimensional mapping. *Journal of Geophysical Research*, 112.
- Corradini, S. et al., 2008. Mt. Etna tropospheric ash retrieval and sensitivity analysis using Moderate Resolution Imaging Spectroradiometer measurements. *Journal of Applied Remote Sensing*, 2.
- Cristaldi, A. and Scollo, S., 2006. Rapporto sull'emissione di cenere all'Etna nei giorni 29 e 31 ottobre 2006.
- Croot, P. and Johansson, M., 2000. Determination of iron speciation by cathodic stripping voltammetry in seawater using the competing ligand 2-(2-Thiazolylazo)-*p*-creosol (TAC). *Electroanalysis*, 12(8): 565-576.
- Dellino, P. and Kyriakopoulos, K., 2003. Phreatomagmatic ash from the ongoing eruption of Etna reaching the Greek island of Cefalonia. *Journal of Volcanology and Geothermal Research*, 126: 341-345.
- Desboeufs, K.V., Losno, R. and Colin, J.L., 2001. Factors influencing aerosol solubility during cloud processes. *Atmospheric Environment* 35: 3529-3537.
- Diaz, F. and Raimbault, P., 2000. Nitrogen regeneration and DON release during 15N experiments during spring in a north-western Mediterranean coastal zone (Gulf of Lions): Implications on the estimations of f ratio and new production. *Marine Ecology Progress Series*, 197: 53-66.
- Dikaiakos, J.G., Tsitouris, C.G., Siskos, P.A., Melissos, D.A. and Nastos, P., 1990. Rainwater composition in Athens, Greece. *Atmospheric Environment*, 24B: 171-176.

- Dugdale, R.C., 1976. Nutrient cycles. In: D.H. Cushing (Editor), *The ecology of the sea*. Blackwell.
- Duggen, S., Croot, P., Schacht, U. and Hoffmann, L., 2007. Subduction zone volcanic ash can fertilize the surface ocean and stimulate phytoplankton growth: Evidence from biogeochemical experiments and satellite data. *Geophysical Research Letters*, 34.
- Duggen, S. et al., 2010. The role of airborne volcanic ash for the surface ocean biogeochemical iron-cycle: a review. *Biogeosciences*, 7(Iron biogeochemistry across marine systems at changing times).
- Dulac, F. et al., 1996. Quantitative remote sensing of African dust transport to the Mediterranean. In: S. Guerzoni and R. Chester (Editors), *The impact of desert dust across the Mediterranean*. Kluwer Academic Publishers, pp. 25–49.
- Estrada, M., 1996. Primary production in the northwestern Mediterranean. *Scientia Marina*, 60: 55-64.
- Falkowski, P.G., 2004. Biogeochemistry of primary production in the sea. In: W.H. Schlesinger (Editor), *Biogeochemistry. Treatise on Geochemistry*. Elsevier Pergamon, Amsterdam-Boston-Heidelberg-London-New York-Oxford-Paris-San Diego-San Francisco-Singapore-Sydney-Tokyo, pp. 185-213.
- Falkowski, P.G., Barber, R.T. and Smetacek, V., 1998. Biogeochemical controls and feedbacks on ocean primary production. *Science*, 281.
- Fierstein, J. and Nathenson, M., 1992. Another look at the calculation of fallout tephra volumes. *Bulletin of Volcanology*, 54: 156-167.
- Folch, A., Costa, A. and Macedonio, G., 2009. FALL3D: A computational model for transport and deposition of volcanic ash. *Computers & Geosciences*, 35: 1334–1342.
- Frogner, P., Gislason, S.R. and Óskarsson, N., 2001. Fertilizing potential of volcanic ash in ocean surface water. *Geology*, 29: 487–490.
- Garbe-Schönberg, C.D., 1993. Simultaneous determination of thirty-seven trace elements in twenty-eight international rock standards by ICP-MS. *Geostandard Newsletters*, 17(1): 81-97.

- Guerzoni, S. et al., 1999. The role of atmospheric deposition in the biogeochemistry of the Mediterranean Sea. *Progress in Oceanography*, 44: 147–190.
- Guieu, C., Bonnet, S. and Wagener, T., 2005. Biomass burning as a source of dissolved iron to the open ocean? *Geophysical Research Letters*, 32.
- Guieu, C. et al., 2002. Impact of high Saharan dust inputs on dissolved iron concentrations in the Mediterranean Sea. *Geophysical Research Letters*, 29.
- Guieu, C. et al., 1997. Atmospheric input of dissolved and particulate metals to the Northwestern Mediterranean. *Deep-Sea Research II*, 44: 644-674.
- Guieu, C., Loÿe-Pilot, M.-D., Benyahya, L. and Dufour, A., 2010. Spatial variability of atmospheric fluxes of metals (Al, Fe, Cd, Zn and Pb) and phosphorus over the whole Mediterranean from a one-year monitoring experiment: Biogeochemical implications. *Marine Chemistry*, 120: 164–178.
- Guieu, C., Martin, J.M., Thomas, A.J. and Elbaz-Poulichet, F., 1991. Atmospheric versus river inputs of metals to the Gulf of Lions. *Marine Pollution Bulletin*, 22(4): 176–183.
- Guieu, C. and Thomas, A.J., 1996. Saharan aerosols: from the soil to the ocean. In: S. Guerzoni and R. Chester (Editors), *The Impact of Desert Dust across the Mediterranean*. Kluwer, Dordrecht, pp. 207-216.
- Hamme, R.C. et al., 2010. Volcanic ash fuels anomalous plankton bloom in subarctic northeast Pacific. *Geophysical Research Letters*, 37.
- Heller, M.I. and Croot, P.L., 2011. Superoxide decay as a probe for speciation changes during dust dissolution in Tropical Atlantic surface waters near Cape Verde. *Marine Chemistry*, 126(1-4): 37-55.
- Herut, B. et al., 2005. Response of east Mediterranean surface water to Saharan dust: on-board microcosm experiment and field observations. *Deep Sea Research II*, 52: 3024-3040.
- Hoffmann, L. et al., submitted to *Marine Chemistry*. Influence of volcanic ash and pumice on phytoplankton growth and Cu ligand production of *Thalassiosira pseudonana* and *Emiliana huxleyi*.
- INGV-Staff, S.d.C., 2001. Multidisciplinary approach yields insight into Mt. Etna 2001 eruption. *EOS Transactions AGU* 82(52): 653–656.

- Jones, M.T. and Gislason, S.R., 2008. Rapid releases of metal salts and nutrients following the deposition of volcanic ash into aqueous environments. *Geochimica et Cosmochimica Acta*, 72: 3661–3680.
- Kelepertsis, A.E., Alexakis, D.E., Nastos, P.T. and Kanellopoulou, E.A., 2003. The presence of volcanic ash in the western Greece and its association with the eruption of the Etna volcano, Italy. Consequences on the environment, 8th International Conference on Environmental Science and Technology, Lemnos island, Greece, pp. 408-415.
- Kocak, M., Kubilay, N., Herut, B. and Nimmo, M., 2005. Dry atmospheric fluxes of trace metals (Al, Fe, Mn, Pb, Cd, Zn, Cu) over the Levantine Basin: A refined assessment. *Atmospheric Environment*, 39: 7330–7341.
- Krom, M.D., Kress, N., Brenner, S. and Gordon, L.I., 1991. Phosphorus limitation of primary productivity in the eastern Mediterranean Sea. *Limnology and Oceanography*, 36: 424-432.
- Krom, M.D. et al., 2005. Nutrient cycling in the south east Levantine basin of the eastern Mediterranean: Results from a phosphorus starved system. *Deep Sea Research II*, 52: 2879-2896.
- Kubilay, N., Nickovic, S., Moulin, C. and Dulac, F., 2000. An illustration of the transport and deposition of mineral dust onto the eastern Mediterranean. *Atmospheric Environment*, 34: 1293-1303.
- Kutterolf, S., Freundt, A. and Perez, W., 2008. Pacific offshore record of plinian arc volcanism in Central America: 2 Tephra volumes and erupted masses. *Geochemistry Geophysics Geosystems*, 9: 1-19.
- Laghdass, M. et al., 2011. Effects of Saharan dust on the microbial community during a large in situ mesocosm experiment in the NW Mediterranean Sea. *Aquatic Microbial Ecology*, 62: 201–213.
- Langmann, B., Zaksek, K., Hort, M. and Duggen, S., 2010. Volcanic ash as fertiliser for the surface ocean. *Atmospheric Chemistry and Physics*, 10: 3891–3899.
- Leblanc, K., Qu'éguiner, B., Raimbault, P. and Garcia, N., 2005. Efficiency of the silicate pump at a coastal oligotrophic site in the Mediterranean Sea. *Biogeosciences Discussions*, 2: 551–580.

- Lekunberri, I. et al., 2010. Effects of a dust deposition event on coastal marine microbial abundance and activity, bacterial community structure and ecosystem function. *Journal of Plankton Research*, 32: 381-396.
- Lenton, T.M. and Watson, A.J., 2000. Redfield revisited 1. Regulation of nitrate, phosphate, and oxygen in the ocean. *Global Biogeochemical Cycles*, 14: 225-248.
- Lin, I.I. et al., 2011. Fertilization potential of volcanic dust in the low-nutrient low-chlorophyll western North Pacific subtropical gyre: Satellite evidence and laboratory study. *Global Biogeochemical Cycles*, 25.
- Markaki, Z. et al., 2003. Atmospheric deposition of inorganic phosphorus in the Levantine Basin, eastern Mediterranean: spatial and temporal variability and its role in seawater productivity. *Limnology and Oceanography*, 48: 1557–1568.
- Martin, J.-M., Elbaz-Poulichet, F., Guieu, C., Loye-Pilot, M.-D. and Han, G., 1989. River versus atmospheric input of material to the Mediterranean Sea: an overview. *Marine Chemistry*, 28: 159-182.
- Migon, C., Sandroni, V. and Be'thoux, J.-P., 2001. Atmospheric input of anthropogenic phosphorus to the northwest Mediterranean under oligotrophic conditions. *Marine Environmental Research*, 52: 413–426.
- Mihalopoulos, N., Stephanou, E., Kanakidou, M., Pilitsidis, S. and Bousquet, P., 1997. Tropospheric aerosol ionic composition in the Eastern Mediterranean region. *Tellus*, 49B: 314–326.
- Mills, M.M., Ridame, C., Davey, M., La Roche, J. and Geider, R., 2004. Iron and phosphorus co-limit nitrogen fixation in the eastern tropical North Atlantic. *Nature*, 429: 292-294.
- Morel, F.M.M. and Price, N.M., 2003. The biogeochemical cycles of trace metals in the oceans. *Science*, 300(5621): 944-947.
- Moutin, T. and Raimbault, P., 2002. Primary production, carbon export and nutrients availability in western and eastern Mediterranean Sea in early summer 1996 (MINOS cruise). *Journal of Marine Systems*, 33-34: 273-288.
- Moutin, T. et al., 2002. Does competition for nanomolar phosphate supply explain the predominance of the cyanobacterium *Synechococcus*? *Limnology and Oceanography*, 47: 1582-1567.

- Olgun, N. et al., 2011. Surface ocean iron fertilization: The role of airborne volcanic ash from subduction zone and hotspot volcanoes and related iron-fluxes into the Pacific Ocean. *Global Biogeochemical Cycles*, 25.
- Paytan, A. et al., 2009. Toxicity of atmospheric aerosols on marine phytoplankton. *Proceedings of the National Academy of Sciences*, 106: 4601-4605.
- Pulido-Villena, E., Rerolle, V. and Guieu, C., 2010. Transient fertilizing effect of dust in P-deficient LNLC surface ocean. *Geophysical Research Letters*, 37.
- Pyle, D.M., 1989. The thickness, volume and grain size of tephra fall deposits. *Bulletin of Volcanology*, 51: 1-15.
- Ridame, C. and Guieu, C., 2002. Saharan input of phosphate to the oligotrophic water of the open western Mediterranean Sea. *Limnology and Oceanography*, 47: 856–869.
- Ridame, C., Moutin, T. and Guieu, C., 2003. Does phosphate adsorption onto Saharan dust explain the unusual N/P ratio in the Mediterranean Sea? *Oceanologica Acta*, 26: 629–634.
- Ruiz-Pino, D.P., Nicolas, E., Bethoux, J.P. and Lambert, C.E., 1991. Zinc budget in the Mediterranean Sea: a hypothesis for non-steady-state behavior. *Marine Chemistry*, 33: 145-169.
- Sarthou, G. and Jeandel, C., 2001. Seasonal variations of iron concentrations in the Ligurian Sea and iron budget in the Western Mediterranean Sea. *Marine Chemistry*, 74: 115–129.
- Saydam, A.C., 1996. Can we predict harmful algae blooms. *Harmful Algae News*, 15: 5–6.
- Schiano, P., Clocchiatti, R., Ottolini, L. and Busa, T., 2001. Transition of Mount Etna lavas from a mantle-plume to an island-arc magmatic source. *Nature* 412: 900-904.
- Schink, D.R. and Kingston, R.I., 1967. Budget for dissolved silica in the Mediterranean Sea. *Geochimica et Cosmochimica Acta*, 31: 987-999.
- Scollo, S., Carlo, P.D. and Coltelli, M., 2007. Tephra fallout of 2001 Etna flank eruption: Analysis of the deposit and plume dispersion. *Journal of Volcanology and Geothermal Research*, 160: 147-164.

- Sherrell, R.M. and Boyle, E.A., 1988. Zinc, chromium, vanadium and iron in the Mediterranean Sea. *Deep-Sea Research*, 35: 1319-1334.
- Socal, G. et al., 1999. Nutrient, particulate matter and phytoplankton variability in the photic layer of the Otranto strait. *Journal of Marine Systems*, 20: 381– 398.
- Taddeucci, J., Pompilio, M. and Scarlato, P., 2002. Monitoring the explosive activity of the July–August 2001 eruption of Mt. Etna (Italy) by ash characterization. *Geophysical Research Letters*, 29.
- Ternon, E. et al., 2010. The impact of Saharan dust on the particulate export in the water column of the North Western Mediterranean Sea. *Biogeosciences*, 7: 809-826.
- Thingstad, T.F. and Rassoulzadegan, F., 1995. Nutrient limitations, microbial food webs, and 'biological C-pumps: suggested interactions in a P-limited Mediterranean. *Marine Ecology Progress Series*, 117: 299-306.
- Thingstad, T.F., Zweifel, U.L. and Rassoulzadegan, F., 1998. P limitation of heterotrophic bacteria and phytoplankton in the northwest Mediterranean. *Limnology and Oceanography*, 43: 88-94.
- Wagener, T., Guieu, C. and Leblond, N., 2010. Effects of dust deposition on iron cycle in the surface Mediterranean Sea: results from a mesocosm seeding experiment. *Biogeosciences*, 7: 2799–2830.
- Wells, M.L., 2003. The level of iron enrichment required to initiate diatom blooms in HNLC waters. *Marine Chemistry*, 82: 101-114.
- Wiesner, M.G., Wang, Y. and Zheng, L., 1995. Fallout of volcanic ash to the deep South China Sea induced by the 1991 eruption of Mount Pinatubo (Philippines). *Geology*, 23(10): 885-888.
- Wu, J., Sunda, W., Boyle, E.A. and Karl, D.M., 2000. Phosphate depletion in the western North Atlantic Ocean. *Science*, 289: 759–762.

Chapter V

Influence of trace metal release from volcanic ash on growth of *Thalassiosira pseudonana* and *Emiliana huxleyi*

Influence of trace metal release from volcanic ash on growth of *Thalassiosira pseudonana* and *Emiliana huxleyi*.

L. J. Hoffmann^{a,1}, E. Breitbarth^{b,1}, M. V. Ardelan^c, S. Duggen^{d,2}, N. Olgun^d, M. Hasselhöf^b, S.-Å. Wängberg^a

^aDepartment of Plant and Environmental Sciences, University of Gothenburg, Gothenburg, Sweden

^bDepartment of Chemistry, University of Gothenburg, Analytical and Marine Chemistry, Gothenburg, Sweden,

^cDepartment of Chemistry, Norwegian University of Science and Technology, Trondheim, Norway,

^dLeibniz-Institute of Marine Sciences, Kiel, Germany

¹present address: Department of Chemistry, University of Otago, Dunedin, New Zealand

²present address: A. P. Møller Skolen, Upper Secondary School and Sixth Form College of the Danish National Minority in Northern Germany, Schleswig, Germany.

Submitted to Marine Chemistry

Corresponding author: lhoffmann@chemistry.otago.ac.nz (Dr. L. J. Hoffmann)

Key words: *Thalassiosira pseudonana*, *Emiliana huxleyi*, volcanic ash, pumice, fertilization, toxicity

Abstract

Recent studies demonstrate that volcanic ash has the potential to increase phytoplankton biomass in the open ocean. However, besides fertilizing trace metals such as Fe, volcanic ash contains a variety of potentially toxic metals such as Cd, Cu, Pb, and Zn. Especially in coastal regions closer to the volcanic eruption, where ash depositions can be very high, toxic effects are possible. Here we present the first results of laboratory experiments, showing that trace metal release from different volcanic materials can have both fertilizing and toxic effects on marine phytoplankton in natural coastal seawater. The diatom *Thalassiosira pseudonana* generally showed higher growth rates in seawater that was in short contact with volcanic ash compared to the controls without ash addition. In contrast to that, the addition of volcanic ash had either no effect or significantly decreased the growth rate of the coccolithophoride *Emiliana huxleyi*. It was not possible to attribute the effects to single trace metals, however, our results suggest that Mn plays an important role in regulating the antagonistic and synergistic effects of the different trace metals. This study shows that volcanic ash can lead to changes in the phytoplankton species composition in the high fall-out area of the surface ocean.

1. Introduction

Large volcanic eruptions can eject enormous amounts of ash and pumice far into the open ocean (Olgun, et al. 2011, and references therein). The importance of volcanic ash as a source of nutrients and trace metals in the ocean, however, has been largely overlooked compared to the much better studied effects of desert dust inputs (Jickells, et al. 2005). This is mainly because of the unpredictability of volcanic eruptions and the difficulties associated with sampling of uncontaminated and unhydrated volcanic ash material. Therefore, direct measurements of the effect of volcanic ash on marine phytoplankton in the field are very rare. The first trace metal analysis within the ash fall-out area of a volcanic eruption (Etna, Sicily, 2001) demonstrates both strongly elevated trace metal concentrations (e.g., over 600 nM Fe in surface waters) and higher chlorophyll values compared to previous years (Censi, et al. 2010). Also, there is growing evidence from satellite data that phytoplankton productivity is increased with volcanic ash deposition in the open ocean (Duggen, et al. 2007, Hamme, et al. 2010, Langmann, et

al. 2010, Lin, et al. 2011). A main factor suggested for this is fertilization with iron (Duggen, et al. 2010), which limits phytoplankton productivity in large regions of the world's ocean.

Besides iron, volcanic ash releases macronutrients such as NH_4^+ , NO_3^- , PO_4^{3-} , and SiO_2 ; volatile compounds such as Br^- , Cl^- , F^- , SO_4^{2-} ; and a variety of trace metals such as Al, Cd, Co, Cu, Mn, Ni, Pb, and Zn (Duggen, et al. 2007, Frogner Kockum, et al. 2006, Frogner, et al. 2001, Jones and Gislason 2008, Witham, et al. 2005). Some of these trace metals, especially Cd, Cu, Pb, and Zn, have potentially toxic effects on marine phytoplankton in higher concentrations (Brand, et al. 1986, Sunda 1988). Toxic effects of Cu from desert dust have recently been shown in incubation experiments (Paytan, et al. 2009), however, the degree of Cu toxicity from this source in the open ocean remains questionable (Sholkovitz, et al. 2010). Since the amount of volcanic ash deposition into seawater is strongly dependent on the distance from the volcano, coastal areas will receive higher trace metal inputs with so far unpredicted effects for their phytoplankton community structure. Most studies addressing the combined effects of different trace metals for marine phytoplankton have been performed in laboratory experiments using trace metal chelators such as EDTA to control free trace metal concentrations (e.g., Sunda and Huntsman 1996, Sunda and Huntsman 1983, Sunda and Huntsman 2000, Sunda and Huntsman 1998b, Tortell and Price 1996). Further, the main focus of these studies was to mimic low trace metal availability as in open ocean regions. Therefore, our understanding of antagonistic and synergistic effects of trace metals in coastal regions is still very limited today.

In this study we investigate the trace metal release of four volcanic ashes and one pumice sample from different regions of the Pacific Ring of Fire and their effect on the growth rate and Cu ligand production of the diatom *Thalassiosira pseudonana* and the coccolithophoride *Emiliana huxleyi* in natural coastal seawater.

2. Material and Methods

Throughout the experiment trace metal clean techniques were used to prevent trace metal contamination. All materials that came in contact with the ash, the cultures, or

the media were acid cleaned before use. Sample and culture handling took place inside a class 100 clean bench.

2.1. Volcanic ash and pumice samples

All volcanic ashes were sampled as clean as possible shortly after explosive eruptions and never had contact with rain or seawater before the experiments. The location and time of the eruptions, as well as the collection sites are described in Table 1. The ash and crushed pumice were stored double bagged in zip lock bags in a dry environment. The samples are unsieved and had no contact with metal-containing materials.

Table 1: Origin of the volcanic ash, year of eruption, and description of sampling site.

Volcano, location	Eruption year	Collection distance	Description
Arenal, Costa Rica	1993	At the foot of the volcano	Silty-fine sandy
Popocatepetl, Mexico	2000	18.7 km NW from crater	Silty
Rabaul-Tavurvur, Papua New Guinea	2002	At the foot of the volcano	Fine-sandy
Sakura-jima, Japan	2007	3 km NW of the Minamidake crater	Silty

2.2 Cultures

Axenic cultures of *Thalassiosira pseudonana* and *Emiliana huxleyi* were obtained from the Provasoli-Guillard Center for Culture of Marine Phytoplankton, Bigelow Laboratories. The cultures were grown at 18 °C and 100 $\mu\text{mol quanta m}^{-2} \text{s}^{-1}$ at a light : dark cycle of 16 : 8 hours. Before the experiments, both cultures were grown for at least 8 generations in natural coastal seawater enriched with nitrate, phosphate, silicate and vitamins in f/2 concentrations (*T. pseudonana*) and in f/20 concentrations without silicate additions (*E. huxleyi*). The f/2 trace metal mix was prepared without EDTA and added 1/500 times more diluted compared to the original recipe. To ensure that no EDTA was left in the media, the cultures were transferred into fresh, EDTA free media several times until EDTA concentrations were diluted to values below 1 pM.

For both, the growth and the ligand experiments, the growth medium was prepared as described above using the same coastal seawater but only the macronutrients and no trace metals were added. All experiments were incubated in triplicates for 9 days.

2.3. Growth experiments

For every experiment, 2 g ash were added to 750 ml natural seawater and gently shaken for 10 minutes by hand, followed by a 5 minutes settling time. This ash concentration corresponds to a ~ 6.6 cm thick sediment ash layer as calculated by Duggen et al. (2007), which is realistic for coastal regions (Cao, et al. 1995, Olgun, et al. 2011). Afterwards the ash was removed through in-line sterile filtration using 0.22 μm , Millipore, Sterivex units. This water was mixed in different ratios with sterile filtered natural seawater to gain four concentrations corresponding to contact with 0.53, 1.07, 1.6, and 2.67 g ash l^{-1} . The controls were grown in natural seawater without ash addition. No or only a low decrease in pH of maximum 0.1 units was observed after the ash addition. Afterwards, the cultures were added at cell densities of about 200 cells ml^{-1} for *T. pseudonana* and 300 cells ml^{-1} for *E. huxleyi* and incubated for 9 days. Samples for cell numbers were taken every third day and immediately measured without addition of preservatives using a Flow Cytometer (Becton Dickinson FACSCalibur). Specific growth rates (μd^{-1}) were calculated from the least-squares regression of cell counts versus time during exponential growth. For statistical analyses Students t-tests were used. Differences found are reported as significant in the text if $p < 0.05$.

2.4. Ligand experiment

In a second experiment, we tested the effect of addition of Sakura-jima ash and pumice addition on the Cu ligand production of *Thalassiosira pseudonana* and *Emiliania huxleyi*. The cultures were grown in the same seawater as for the growth experiment. Since we only measured cell densities at day one and 9 in this experiment we did not calculate growth rates. The copper complexing ligand concentrations were determined using cathodic stripping voltammetry after Campos and van den Berg (1994). Seawater samples were filtered through in-line sterile filtration using 0.22 μm , Millipore, Sterivex units and stored frozen until analysis. The samples were slowly thawed in a fridge and

aliquots of 10 ml each were given in Teflon voltammetric cells. 50 μ l borate buffer and 20 μ l SA (0.01 M) as well as copper standard at increasing concentration from 0 – 180 nM were added to each sample. The solutions were equilibrated over night.

2.5. Trace metal concentrations

The trace metal concentration of the seawater before and after 15 minutes of contact with the volcanic material was measured in direct determination after 10 times dilution in MilliQ using a HR-ICP-MS (Thermo Finnigan Element) as described in Ardalan et al. (2009). All samples (10 ml) were filtered through a 0.22 μ m syringe top filter (Millipore Sterivex) and acidified with 20 μ l HNO₃ (FLUKA, trace select).

3. Results

3.1. Trace metal release

Volcanic ash samples generally mobilized significant amounts of trace metals after short (15 minutes) contact with seawater. However, the trace metal release of the four ash samples and the pumice showed significant variations. From all the four ashes tested, Al, Mn, and Zn were released in very high concentrations between 17.4 nM and 1749.7 nM (Table 2). Cu and Fe were released at concentrations of 10.2 nM and 2.1 nM and 10.8 nM and 5.7 nM from the Arenal and the Rabaul-Tavurvur volcanoes, respectively. For the ashes from the Popocatepetl and the Sakura-jima volcanoes, Fe release exceeded Cu release with 7.0 nM and 83.2 nM compared to 4.4 nM and 5.6 nM. Cd, Co, Ni, and Pb were released in concentrations \leq 1.5 nM from the Arenal, Popocatepetl, and the Rabaul-Tavurvur ashes. The ash from the Sakura-jima volcano generally released the highest trace metal concentrations of the four ashes tested except for Al, Cu, and Zn. The concentrations for Cd, Co, and Mn released from this ash were about 20 to 45 times higher compared to the other ashes while Fe and Ni were about 10 times higher compared to the other ashes.

In contrast, the pumice material released relatively low concentrations of trace metals within 15 minutes contact time. No release of the metals Cd, Pb and Zn was detected. Fe and Mn were the trace metals released in the highest concentrations with 3.9 nM and 5.9 nM, respectively.

Table 2: Trace metal concentrations (in nM) of the coastal seawater used as growth medium and the concentrations released by 1 g (calculated from the 2g added to 750 ml) of the different ashes and the pumice material after 15 minutes of contact with seawater for the growth experiment (upper 5 lines) and the ligand experiments (bottom 3 lines). Note that due to the different ash concentrations used in this study the final concentrations released in the incubations were 0.53, 1.07, 1.6, and 2.67 times the values given in this table.

	Al	Cd	Co	Cu	Fe	Mn	Ni	Pb	Zn
seawater	44.5	0.5	0.5	6.3	15.1	3.1	8.5	0.2	279.4
Arenal	1749.7	0.0	0.1	10.2	2.1	17.4	0.5	0.0	77.5
Popocatepetl	77.6	0.2	0.4	4.4	7.0	29.5	1.5	0.1	119.7
Rabaul-Tavurvur	330.9	0.1	1.0	10.8	5.7	69.5	1.3	0.0	58.0
Sakura-jima	1377.6	4.2	33.0	5.6	83.2	1298.6	13.9	0.8	34.0
seawater	78.3	0.6	0.1	6.4	22.6	1.7	8.4	0.01	158.9
pumice	1.5	0.0	0.2	1.3	3.9	5.9	1.2	0.0	0.0
Sakura-jima	1105.0	3.8	31.4	9.0	50.6	1237.3	9.9	0.6	39.1

3. 2. Phytoplankton growth

In most cases the addition of volcanic ash significantly changed the growth rate of *T. pseudonana* and *E. huxleyi*. Interestingly, the ashes tested had an opposite effect on both species (Fig. 1). *T. pseudonana* had a growth rate between 0.37 and 0.5 in the controls. The addition of medium ash concentrations between 0.53 and 1.6 g l⁻¹ significantly increased the growth rate to values between 0.53 and 0.65 (p values between 0.004 and 0.04) for the ashes Popocatepetl, Rabaul-Tavurvur, and Sakura-jima. In contrast, the ash of the Arenal volcano significantly (p values between 0.002 and 0.007) decreased the growth rate of this species at medium ash concentrations. Here, the growth rates were 0.17, 0.23, and 0.15, respectively. At the highest ash concentrations added (2.67 g l⁻¹) the growth rate of *T. pseudonana* was significantly higher compared to the controls for the three ashes Arenal ($\mu=1.15$; $p=0.03$), Popocatepetl ($\mu=0.75$, $p=0.007$), and Sakura-jima ($\mu=1.0$, $p=0.001$). Only the incubation with the ash from the Rabaul-

Tavurvur volcano did not show a significant difference at the highest ash concentration compared to the control.

The growth rates in the controls without ash addition were between 0.64 and 0.96 for *E. huxleyi*. The incubations with different ash concentrations from the Arenal, Popocatepetl, and Rabaul-Tavurvur eruptions did not show any significant difference compared to the respective controls. However, the Sakura-jima ash significantly decreased the growth rate of this species at every concentration tested. Here growth rates decreased from 0.76 in the controls down to 0.07 at the highest ash concentration (p values between 0.03 and 0.002).

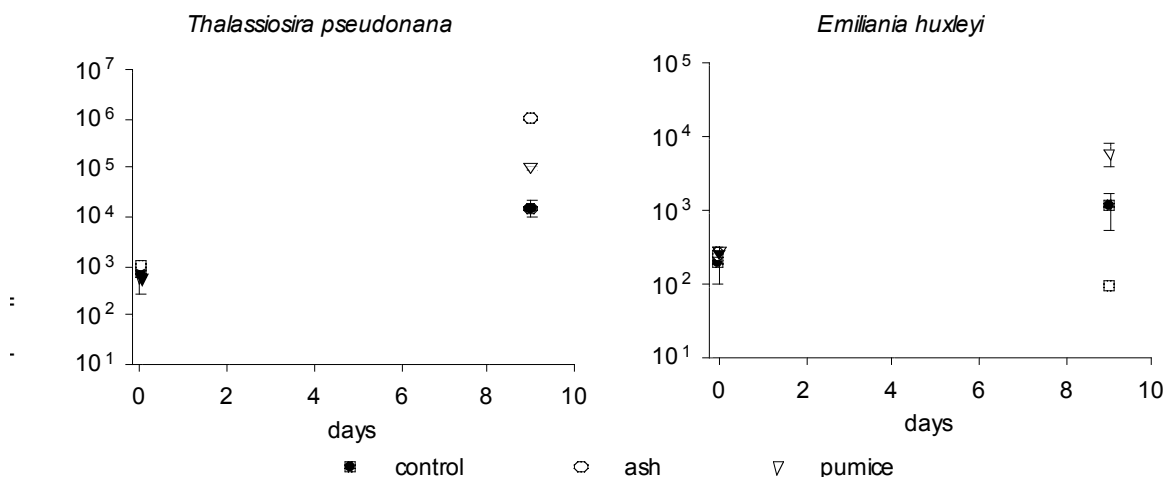


Figure 1: Growth rate of *T. pseudonana* and *E. huxleyi* grown at different concentrations of the four ashes. All measurements are done in triplicates, error bars denote standard deviation. If not visible, error bars are smaller than symbols.

3. 3. Ligand experiment

Compared to the control, *T. pseudonana* again showed a much higher growth with addition of the Sakura-jima ash (Fig. 2). After 9 days of incubation the cell numbers were 67.5 times higher in the ash treatment. Addition of pumice material still increased the growth rate of this species and final cell numbers were 6.8 times higher compared to the control.

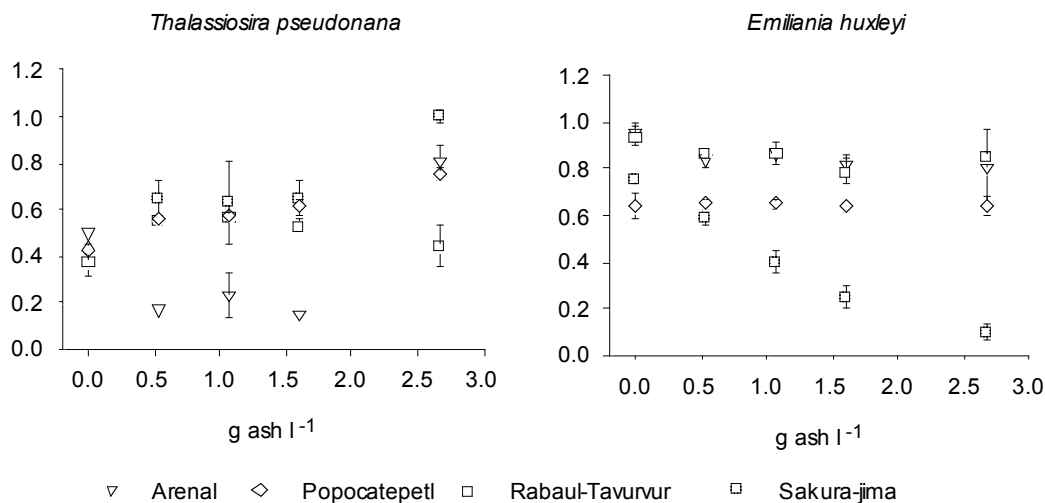


Figure 2: Cell numbers of *T. pseudonana* and *E. huxleyi* in the controls, with addition of Sakura-jima ash, and with addition of pumice material over nine days. All measurements are done in triplicates, error bars denote standard deviation. If not visible, error bars are smaller than symbols.

Like in the first experiment, ash from the Sakura-jima eruption decreased the growth of *E. huxleyi*, which did not grow at all in the ash treatment of this experiment. However, addition of pumice material increased the growth of *E. huxleyi* with final cell numbers being 5.5 times higher compared to the controls.

The copper ligand concentration in the medium before the incubation was 3.5 ± 1.1 nM. Right after the addition of volcanic ash or pumice material to the seawater, the ligand titrations became very noisy and the concentration measured varied between 2.5 and 22.1 nM. Most likely surface complexation of colloids leaching from the volcanic materials interfered with the measurements. These colloids may be nanoparticles disaggregating from the ash on contact with the water, or it may be colloidal secondary phases precipitating either before or after filtration, e.g., iron oxyhydroxides. Similar problems have been observed in glacial meltwaters in Iceland containing large concentrations of volcanic ash (M. Bau pers. comm.). These very variable ligand concentrations in the beginning of the experiment make it difficult to determine any changes during the course of the incubations (Fig. 3) and we did not find a production of Cu binding ligands in any of the incubations with the Sakura-jima ash. However, our data

show a strong production of about 60 nM of Cu binding ligands by *T. pseudonana* in the incubations with pumice material (Fig. 3).

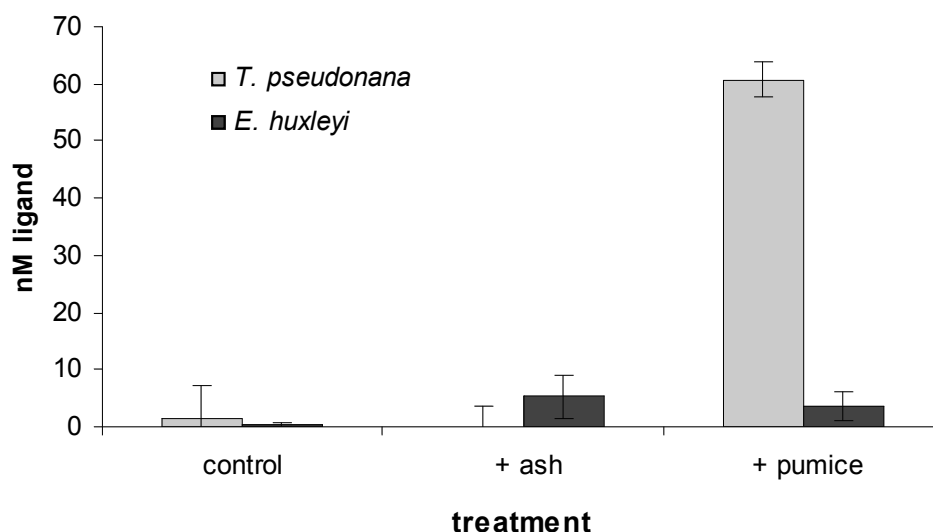


Figure 3: Changes in Cu ligand concentration after the 9 days of incubation compared to the start.

4. Discussion

The Cd, Co, Cu, Fe, Ni, Pb, and Zn concentrations in the coastal seawater used as culture media were close to those reported for other coastal regions (Kozelka and Bruland 1998, Kuma, et al. 1998, Lares, et al. 2009, Öztürk, et al. 2002, Wells, et al. 1998). Since trace metal concentrations in coastal regions are much higher compared to the open ocean, trace metal additions would usually not be expected to have significant effects here. However, Öztürk et al. (2002) show that phytoplankton growth can also be limited by iron in coastal regions. The bioavailability of iron in natural systems is dependent on the chemical form of iron rather than on the total concentration. In coastal systems a large fraction of iron is colloidal Fe, which releases bioavailable iron much slower compared to dissolved labile Fe(III) organic complexes (Kuma, et al. 1995). Moreover, high concentrations of organic matter can also reduce Fe bioavailability in coastal waters (Breitbarth, et al. 2009). Therefore, addition of iron could possibly have beneficial effects even in high-metal coastal systems.

Further, addition of trace metals can in some cases alter toxicity effects of other metals as in the case of Mn. Since Cd, Cu, Zn and Mn compete for the same uptake systems in *T. pseudonana*, high Mn concentrations inhibit the uptake of these trace metals and prevent toxicity (Sunda, et al. 1981, Sunda and Huntsman 1996, Sunda and Huntsman 1998a, Sunda and Huntsman 1998b, Sunda and Huntsman 1998c). Rather than the absolute free Cd, Cu, and Zn concentration, it is the ratio of Mn to these metals that determines their toxicity. In other words, input of Mn to polluted, high Cd, Cu, and Zn waters could quench toxic effects of these metals for phytoplankton and increase growth.

4. 1. Fertilizing effects of volcanic material for *T. pseudonana*

In our study, *T. pseudonana* had a growth rate between 0.37 and 0.5 in the controls, which is clearly below the maximum growth rate of this species reported for artificial media (about 1.7 (e.g., Ellwood and Hunter 2000, Price, et al. 1987, Sunda and Huntsman 1992)). This indicates that the coastal seawater either did not supply this species with efficient nutrients or that the concentration of toxic metals was high enough to depress growth of this species. Since we added the macronutrients nitrate, phosphate, and silicate to the incubations, this species can not have suffered macronutrient limitation. It is possible though that the high Zn and Cu concentrations in the controls (279.4 and 6.3 nM, Table 2) suppressed growth of this species since the Mn concentrations were relatively low (3,1 nM, Table 2). In laboratory experiments, *T. pseudonana* only showed a distinct reduction in growth rate to about 40 % of the maximum growth rate at much higher free Cu concentrations of 10 μ M (Brand, et al. 1986). However, in Brand et al.'s experiment (1986) all other trace metals, including Mn, were buffered to levels ideal for phytoplankton growth, excluding the possibility of antagonistic and/or synergistic effects of different trace metals. Toxic effects of Cu for *T. pseudonana* can be reached at much lower concentrations when Mn concentrations are suboptimal (Sunda and Huntsman 1983). Another possibility could be that the growth of *T. pseudonana* in the controls is limited by the relatively low Co concentrations (0.5 nM Table 2). Other than *E. huxleyi*, *T. pseudonana* is known to have Co requirements which can not be met by Zn (Sunda and Huntsman 1995, Whitfield 2001).

The general increase in growth rate of the diatom *T. pseudonana* with addition of the volcanic ash could be caused by a combination of Mn, Fe, and Co fertilization. It is noticeable that the ash with the highest concentration of Mn, Fe, and Co (Sakura-jima) had the strongest effect on the growth rate of *T. pseudonana* (Fig. 1). The input of potentially toxic trace metals such as Cd and Cu did not seem to have a significant effect on this species, most likely because they are buffered by the high input of Mn from the ash. Since the Mn release from the volcanic materials tested here was always higher compared to the combined Cu and Cd release (Table 2) it is likely that this would quench Cd, Cu, and Zn toxicity for diatoms in the field in general. A recent evidence of volcanic ash fertilization in coastal waters was shown in the Ionian coast during the 2001 eruption of Mount Etna (Censi, et al. 2010). Here, similar effects could be responsible for the reported increase in chlorophyll as in particular the dissolved concentrations of Mn, Fe, and Co increased more compared to other metals (Censi, et al. 2010).

4. 2. Toxic effects for *E. huxleyi*

The maximum growth rate for *E. huxleyi* reported in the literature is about 1.1 (Zondervan 2007) which is close to the maximum growth rate we observed in the controls without ash addition (0.96 ± 0.04 , Fig. 1). Since *E. huxleyi* can meet its Co requirements partly by replacing it with Zn (Sunda and Huntsman 1995, Whitfield 2001) it is possible that the high Zn concentrations in the controls are beneficial for this species. Also, *E. huxleyi* showed to be very tolerant to Cu toxicity and only reduced its growth rate to about 80% at free Cu concentrations of 20 μM in EDTA buffered media (Brand, et al. 1986) and above 48 nM in culture experiments without addition of EDTA (Leal, et al. 1999), which is much higher than the Cu concentrations in the controls and in any of our ash addition treatments.

In contrast to *T. pseudonana*, addition of volcanic material did not have any significant effect (Arenal, Popocatepetl and Rabaul-Tavurvur ash, Fig.1) or resulted in a significant decrease of the growth rate of *E. huxleyi* (Sakura-jima ash, Fig. 1). The only volcanic material that increased the growth of this species compared to the controls was the pumice, which released trace metals in much lower concentration compared to the

other ashes tested (Table 2). In both incubations with the Sakura-jima ash we observed a strong toxic effect for *E. huxleyi* despite the high Fe and Mn concentrations released from the ash (Figs. 1 and 2). We can only speculate what caused this effect but direct toxic effects of Cu, Cd, Pb, or Zn seem implausible for the following reasons:

E. huxleyi is known to produce Cu binding ligands when grown under Cu stress (Leal, et al. 1999) but we did not find any production of Cu binding ligands by *E. huxleyi* above the high variance when incubated with the Sakura-jima ash (Fig. 3). Further, the Cu and Zn concentrations released from the Sakura-jima ash are lower compared to the other ashes and *E. huxleyi* has a high Cu tolerance (Brand, et al. 1986, Leal, et al. 1999). Cd and Pb are released in higher concentrations from the Sakura-jima ash compared to the others, however, similar to Cu, *E. huxleyi* showed to be very tolerant to Cd compared to other species tested (including *T. pseudonana*) and only reduced its growth rates by 50 % at free Cd concentrations of 580 nM in the NTA buffered media used (Payne and Price 1999), and at 1 μ M free Cd in EDTA buffered media, respectively (Brand, et al. 1986). Further, Pb and Cd additions of up to 25 nM each to coastal seawater without the addition of EDTA only showed a low toxic effect on *E. huxleyi* and reduced its growth rate by about 13% (Vasconcelos and Leal 2001).

Other than for *T. pseudonana*, the extremely high Mn concentrations released by the Sakura-jima ash might have negative effects for the growth of *E. huxleyi*. It is known that metal uptake in *E. huxleyi* is regulated by different uptake systems than in diatoms and Mn does not seem to play the same role in preventing uptake of toxic metals as in diatoms (Sunda and Huntsman 2000). It is therefore possible that the very high Mn concentrations released from the Sakura-jima ash might interfere with the uptake of essential metals rather than that of toxic ones as for diatoms. This theory is supported by the observation that the addition of pumice, which released the lowest Mn concentration of all volcanic materials tested, was the only one that significantly increased the growth of *E. huxleyi* (Fig. 2).

4. 3. Conclusions

Our experiment shows that the same volcanic ash can both, increase and decrease growth rates of different phytoplankton species, which will ultimately lead to changes in species composition with implications for community productivity and export of the affected ocean regions. Other than suggested for open ocean regions, however, it seems that the inputs of Fe and Cu through volcanic eruptions are not the main factors influencing phytoplankton growth and species composition in coastal, high trace metal regions. Rather, the complex interactions of antagonistic and synergistic effects between different trace metals and especially the Mn concentration seem to control phytoplankton growth in our experiments. If similar effects could also apply for the open ocean are difficult to predict. However, it is likely that the overall effects of volcanic eruptions for the marine ecosystem are much more complex than only the previously suggested Fe fertilization and a possible Cu toxicity.

Despite the enormous amount of work in this field, most studies investigating combined effects of different trace metals for marine phytoplankton have been performed in EDTA buffered media using mainly the diatom species *T. oceanica*, *T. weissflogii*, and *T. pseudonana*, and the coccolithophoride *E. huxleyi*. We know very little about combined trace metal interactions and their effects for other marine phytoplankton species in natural seawater. To be able to better understand implications of combined natural trace metal inputs such as volcanic eruptions or also desert dust storms for natural phytoplankton communities and their effects for ecosystem productivity we urgently need more detailed studies addressing synergistic and antagonistic effects of trace metals under more natural culture conditions without the addition of metal chelators in both coastal and open ocean regions.

Acknowledgements

This research was funded by the German Academic Exchange Service (DAAD). L. J. H. and E. B. acknowledge current funding by the German Research Foundation (DFG grants HO 4217 and BR 3794). S. D. and N. O. were supported by the multidisciplinary research group NOVUM at the IFM-GEOMAR, Kiel, Germany.

References

- Ardelan, M.V., E. Steinnes, S. Lierhagen, S.O. Linde, 2009. Effects of experimental CO₂ leakage on solubility and transport of seven trace metals in seawater and sediment. *Sci. Total Environ.* 407, 6255-6266.
- Brand, L.E., W.G. Sunda, R.R.L. Guillard, 1986. Reduction of marine phytoplankton reproduction rates by copper and cadmium. *J. Exp. Mar. Bio. Ecol.* 96, 225-250.
- Breitbarth, E., J. Gelting, J. Walve, L.J. Hoffmann, D.R. Turner, M. Hassellöv, J. Ingri, 2009. Dissolved iron (II) in the Baltic Sea surface water and implications for cyanobacterial bloom development. *Biogeosci.* 6, 2397-2420.
- Campos, M.L.A.M., C.M.G. van den Berg, 1994. Determination of copper complexation in sea water by cathodic stripping voltammetry and ligand competition with salicylaldoxime. *Anal. Chim. Acta.* 284, 481-496.
- Cao, L.-Q., R.J. Arculus, B.C. McKelvey, Geochemistry and petrology of volcanic ashes recovered from Sites 881 through 884: A temporal record of Kamchatka and Kurile volcanism., in: D.K. Rea, D.W. Scholl, J.F. Allan, (Eds), *Proceedings of the Ocean Drilling Program 145, Scientific Results*, 1995, pp. 345-381.
- Censi, P., L.A. Randazzo, P. Zuddas, F. Saiano, P. Aricò, S. Andò, 2010. Trace element behaviour in seawater during Etna's pyroclastic activity in 2001: Concurrent effects of nutrients and formation of alteration minerals. *J. Volcanol. Geotherm. Res.* 193, 106-116.
- Duggen, S., P. Croot, U. Schacht, L. Hoffmann, 2007. Subduction zone volcanic ash can fertilize the surface ocean and stimulate phytoplankton growth: Evidence from biogeochemical experiments and satellite data. *Geophys. Res. Lett.* 34, L01612.
- Duggen, S., N. Olgun, P.L. Croot, L. Hoffmann, H. Dietze, C. Teschner, 2010. The role of airborne volcanic ash for the surface ocean biogeochemical iron-cycle: a review. *Biogeosci.* 7, 827-844.
- Ellwood, M.J., K.A. Hunter, 2000. The incorporation of zinc and iron into the frustule of the marine diatom *Thalassiosira pseudonana*. *Limnol. Oceanogr.* 45, 1517-1524.
- Frogner Kockum, P.C., R.B. Herbert, S.R. Gislason, 2006. A diverse ecosystem response to volcanic aerosols. *Chem. Geol.* 231, 57-66.

- Frogner, P., S.R. Gíslason, N. Óskarsson, 2001. Fertilizing potential of volcanic ash in ocean surface water. *Geol. Soc. Am.* 29, 487-490.
- Hamme, R.C., P.W. Webley, W.R. Crawford, F.A. Whitney, M.D. DeGrandpre, S.R. Emerson, C.C. Eriksen, K.E. Giesbrecht, J.F.R. Gower, M.T. Kavanaugh, M.A. Peña, C.L. Sabine, S.D. Batten, L.A. Coogan, D.S. Grundle, D. Lockwood, 2010. Volcanic ash fuels anomalous plankton bloom in subarctic northeast Pacific. *Geophys. Res. Lett.* 37, L19604.
- Jickells, T.D., Z.S. An, K.K. Andersen, A.R. Baker, G. Bergametti, N. Brooks, J.J. Cao, P.W. Boyd, R.A. Duce, K.A. Hunter, H. Kawahata, N. Kubilay, J. laRoche, P.S. Liss, N. Mahowald, J.M. Prospero, A.J. Ridgwell, I. Tegen, R. Torres, 2005. Global iron connections between desert dust, ocean biogeochemistry, and climate. *Science* 308, 67-71.
- Jones, M.T., S.R. Gíslason, 2008. Rapid releases of metal salts and nutrients following the deposition of volcanic ash into aqueous environments. *Geochim. Cosmochim. Acta* 72, 3661-3680.
- Kozelka, P.B., K.W. Bruland, 1998. Chemical speciation of dissolved Cu, Zn, Cd, Pb in Narragansett Bay, Rhode Island. *Mar. Chem.* 60, 267-282.
- Kuma, K., A. Katsumoto, J. Nishioka, K. Matsunaga, 1998. Size-fractionated iron concentrations and Fe(III) hydroxide solubilities in various coastal waters. *Estuar. Coast. Shelf Sci.* 47, 275-283.
- Kuma, K., S. Nakabayashi, K. Matsunaga, 1995. Photoreduction of Fe(III) by hydroxycarboxylic acids in seawater. *Water Res.* 29, 1559-1569.
- Langmann, B., K. Zakšek, M. Hort, S. Duggen, 2010. Volcanic ash as fertiliser for the surface ocean. *Atmos. Chem. Phys.* 10, 3891-3899.
- Lares, M.L., S.G. Marinone, I. Rivera-Duarte, A. Beck, S. Sanudo-Wilhelmy, 2009. Spatial Variability of Trace Metals and Inorganic Nutrients in Surface Waters of Todos Santos Bay, Mexico in the Summer of 2005 During a Red Tide Algal Bloom. *Arch. Environ. Contam. Toxicol.* 56, 707-716.
- Leal, M.F.C., M.T.S.D. Vasconcelos, C.M.G. van den Berg, 1999. Copper-induced release of complexing ligands similar to thiols by *Emiliania huxleyi* in seawater cultures. *Limnol. Oceanogr.* 44.

- Lin, I.-I., C. Hu, Y.-H. Li, T.-Y. Ho, T.P. Fischer, G.T.F. Wong, J. Wu, C.-W. Huang, D.A. Chu, D.S. Ko, J.-P. Chen, 2011. Fertilization potential of volcanic dust in the low-nutrient low-chlorophyll western North Pacific subtropical gyre: Satellite evidence and laboratory study. *Global Biogeochem. Cy.* 25, GB1006, doi:10.1029/2009GB003758.
- Olgun, N., S. Duggen, P.L. Croot, P. Delmelle, H. Dietze, U. Schacht, N. Óskarsson, C. Siebe, A. Auer, 2011. Surface ocean iron fertilization: The role of airborne volcanic ash from subduction zone and hotspot volcanoes and related iron-fluxes into the Pacific Ocean. *Global Biogeochem. Cy.* 25, GB4001, doi:10.1029/2009GB003761.
- Öztürk, M., E. Steinnes, E. Sakshaug, 2002. Iron speciation in the Trondheim Fjord from the perspective of iron limitation for phytoplankton. *Estuar. Coast. Shelf Sci.* 55.
- Payne, C.D., N.M. Price, 1999. Effects of cadmium toxicity on growth and elemental composition of marine phytoplankton. *J. Phycol.* 35, 293-302.
- Paytan, A., K.R.M. Mackey, Y. Chen, I.D. Lima, S.C. Doney, N. Mahowald, R. Labiosa, A.F. Post, 2009. Toxicity of atmospheric aerosols on marine phytoplankton. *Proc. Nat. Acad. Sci.* 106, 4601-4605.
- Price, N.M., P.A. Thompson, P.J. Harrison, 1987. Selenium: An essential element for growth of the coastal marine diatom *Thalassiosira pseudonana* (Bacillariophyceae). *J. Phycol.* 23, 1-9.
- Sholkovitz, E.R., P.N. Sedwick, T.M. Church, 2010. On the fractional solubility of copper in marine aerosols: Toxicity of aeolian copper revisited. *Geophys. Res. Lett.* 37, 4.
- Sunda, W.G., 1988. Trace metal interactions with marine phytoplankton. *Biol. Oceanogr.* 6, 411-442.
- Sunda, W.G., R.T. Barber, S.A. Huntsman, 1981. Phytoplankton growth in nutrient rich seawater: importance of copper-manganese cellular interactions. *J. Mar. Res.* 39, 567-586.
- Sunda, W.G., S.A. Huntsman, 1996. Antagonisms between cadmium and zinc toxicity and manganese limitation in a coastal diatom. *Limnol. Oceanogr.* 41, 373-387.

- Sunda, W.G., S.A. Huntsman, 1995. Cobalt and zinc interreplacement in marine phytoplankton: Biological and geochemical implications. *Limnol. Oceanogr.* 40, 1404-1417.
- Sunda, W.G., S.A. Huntsman, 1998a. Control of Cd concentrations in a coastal diatom by interactions among free ionic Cd, Zn, and Mn in seawater. *Environ. Sci. Technol.* 32, 2961-2968.
- Sunda, W.G., S.A. Huntsman, 1983. Effect of competitive interactions between manganese and copper on cellular manganese and growth in estuarine and oceanic species of the diatom *Thalassiosira*. *Limnol. Oceanogr.* 28, 924-934.
- Sunda, W.G., S.A. Huntsman, 2000. Effect of Zn, Mn, and Fe on Cd accumulation in phytoplankton: Implications for oceanic Cd cycling. *Limnol. Oceanogr.* 45, 1501-1516.
- Sunda, W.G., S.A. Huntsman, 1992. Feedback interactions between zinc and phytoplankton in seawater. *Limnol. Oceanogr.* 37, 25-40.
- Sunda, W.G., S.A. Huntsman, 1998b. Interactions among Cu^{2+} , Zn^{2+} , and Mn^{2+} in controlling cellular Mn, Zn, and growth rate in the coastal algae *Chlamydomonas*. *Limnol. Oceanogr.* 43, 1055-1064.
- Sunda, W.G., S.A. Huntsman, 1998c. Interactive effects of external manganese, the toxic metals copper and zinc, and light in controlling cellular manganese and growth in a coastal diatom. *Limnol. Oceanogr.* 43, 1467-1475.
- Tortell, P.D., N.M. Price, 1996. Cadmium toxicity and zinc limitation in centric diatoms of the genus *Thalassiosira*. *Mar. Ecol. Prog. Ser.* 138, 245-254.
- Vasconcelos, M.T.S.D., M.F.C. Leal, 2001. Antagonistic interactions of Pb and Cd on Cu uptake, growth inhibition and chelator release in the marine algae *Emiliania huxleyi*. *Mar. Chem.* 75, 123-139.
- Wells, M.L., P.B. Kozelka, K.W. Bruland, 1998. The complexation of 'dissolved' Cu, Zn, Cd and Pb by soluble and colloidal organic matter in Narragansett Bay, RI. *Mar. Chem.* 62, 203-217.
- Whitfield, M., 2001. Interactions between phytoplankton and trace metals in the ocean. *Adv. Mar. Biol.* 41, 3-128.

- Witham, C.S., C. Oppenheimer, C.J. Horwell, 2005. Volcanic ash-leachates: a review and recommendations for sampling methods. *J. Volc. Geotherm. Res.* 141, 299-326.
- Zondervan, I., 2007. The effect of light, macronutrient, trace metals and CO₂ on the production of calcium carbonate and organic carbon in coccolithophores-A review. *Deep Sea Res. II* 54, 521-537.

CONCLUSIONS

&

FUTURE PERSPECTIVES

CONCLUSIONS AND FUTURE PERSPECTIVES

The present study shows that volcanic ash deposition is an important source of macro-nutrients and trace metals for the surface ocean. The influence of volcanic eruptions can be striking in the iron-limited ocean regions during single major eruptions. The iron release data based on the ash samples from volcanoes world-wide (of 200 ± 50 nmol Fe/g ash) can be used as a representative value in the global models (e.g., dry deposition of volcanic ash). Similarly, atmospheric deposition rate of volcanic ash estimated for the Pacific Ocean ($128\text{-}221 \times 10^{15}$ g/ka) shows that volcanic ash deposition is an important nutrient source over geological time-scales, and the results provide a basis for the flux estimates for other trace-metals and macro-nutrients into a large basin like the Pacific Ocean.

Macro-nutrients and trace-metals released from volcanic into the seawater can have strong impacts on the MPP in the low-nutrient, low-chlorophyll ocean regions too. Flux estimates of volcanic ash and the related nutrient input downwind an eruption (based on the 4-5 November 2002 Etna eruption) serves a good basis for future experimental studies in the oceans.

Another the key conclusion of this study is that the different phytoplankton may respond in different ways to volcanic ash deposition, which can alter the composition of the phytoplankton assemblage in the ash fallout regions. And above all, it appears that the volcanic ash can not only stimulate MPP but also may affect the higher trophic levels including the zooplankton and the fish populations in the oceans and the neighboring rivers and lakes.

A number of problems, however, still remains in order to fully understand the solubility and the bioavailability of nutrients released by volcanic ash. The possible fertilizing or toxic effects of volcanic ash should be investigated by more biological experiments. Several processes in the eruption plume (e.g., HF, HCl reactions) and in the atmosphere (e.g., low pH cloud cycling) can control the surface chemistry of volcanic ash, most of which remained poorly understood. Below, I wanted to mention some of the unpublished data that can provide initial ideas for the future work.

- Particles size effect in iron dissolution of volcanic ash (unpublished data)

The effect of ash particle size on iron dissolution is an important factor that remains unanswered. Finer volcanic ash travelling long-distances can release more iron into the seawater (Duggen et al., 2010). In the iron-release experiments, I observed that the finer ash samples released higher amounts of iron into the seawater compared to the coarse ash samples, which is consistent with previous hypothesis (Chapter II). To test the particle size effect, I sieved (using plastic sieves) four ash samples into five different size fractions (samples from Hekla 2000 (coarse sample), Merapi 1996 (fine) and Sakura-Jima 2007 (fine) were sub-divided into size fractions of >1mm, only for coarse Hekla ash, 1mm-500 μ m, 500-250 μ m, 250-100 μ m and <100 μ m). With the method I used (voltammetry of 20 ml sample) I did not find differences between the size fractions of a sample that were larger than the internal precision of the experiment. Long-term traveled ash can release more iron, however, I suggest that sieving the samples may still underestimate the actual iron-release in the remote ocean.

- Scavenging of nutrients from ash ?

It has been suggested that the mineral dust particles can scavenge nutrients from the water column through adsorption on the particle surfaces (e.g., phosphate and iron (Krom et al., 1991; Wagener et al., 2010)). The net effect of nutrient dissolution from particles likely to depend on the relative rates of “release” versus “scavenging”. For volcanic ash, in the case of iron, the net effect was “release”. In another set of experiments, I tested the release of zinc and copper from twenty subduction volcanic ash samples. Most of the ash samples released zinc (up to 90 nmol Zn/g ash) and copper (up to 110 nmol Cu/g ash) (Olgun et al., 2008). Interestingly, some volcanic ash samples did not show a net release of zinc and copper but instead a net decrease in experiments with Zn-Cu-doped seawater, pointing to a scavenging potential of volcanic ash (up to 10 \pm 5 nM ash) (Olgun et al., 2008). Scavenging of nutrients can be another important issue during major eruptions that may affect the trace metal composition of biologically relevant metals in affected areas. This process is so far completely unexplored and it is therefore not possible to estimate its importance for the marine ecosystem.

FUTURE PERSPECTIVES

I suggest the following research priorities for the future studies to improve our understanding on the impacts of volcanic eruptions in the marine environments: (i) large-scale experiments with volcanic ash, (ii) palaeo indications from the marine drill cores, (iii) *in-situ* observations during volcanic eruptions.

(i) Large scale experiments - mesocosms

A considerable number of studies focus on the mineral dust and its marine biogeochemical impacts. The knowledge provided in these studies can easily be applied for volcanic ash. Large mesocosms suited in the sea (down to 15 m depth in the water column, of 53 m³ volume) have been used recently to investigate the effects of mineral dust, for example in the western Mediterranean Sea in the frame of the DUNE-project (a Dust experiment in low Nutrient low chlorophyll Ecosystem) in Laboratoire d'Océanographie de Villefranche/Mer, CNRS-INSU in France. Volcanic ash fertilization experiments can be done in the Mediterranean Sea by using the same mesocosm method used for the mineral dust studies (described in detail in (Guieu et al., 2010a)). Ash from Etna volcano would be the most suitable samples for such a study in the Mediterranean (see Chapter IV). The key parameters that can be measured in the ash fertilization mesocosm experiments are the dissolved nutrients, concentrations of chlorophyll-a and bacteria, nitrogen and carbon in the particulate matter and isotope mass balance for rate of N₂-fixation. Additionally, in order to mimic different deposition process, ash samples can be treated in different ways prior to experiments. For example, samples can be diluted in acidic solutions or ultra-pure water to resemble deposition by rain (wet deposition) to be able to see the influence of low pH in iron dissolution in seawater. Effect of particle size and possible scavenging of nutrients on the ash particles can also be tested more adequately in the mesocosm seeding experiments compared to small-scale laboratory experiments. Realistic volcanic ash addition can be referred from the estimated downwind ash flux typical for explosive eruptions of Etna volcano (Olgun et al., submitted to Marine Chemistry). Ash fluxes of >100 g/m², >10 g/m² and >1 g/m² can be

representative for flux in the coast, in 400 km downwind from the volcano, and in 600 km downwind from the volcano, respectively (Olgun et al., submitted to Marine Chemistry). The results of the ash fertilization mesocosm experiments would be helpful also for comparison with the phytoplankton response to mineral dust addition.

(ii) Palaeo indications: Marine drill core studies

Volcanic ash layers are commonly found in the marine drill cores but often ignored in terms of interpretation of the plankton composition of the core. Possible correlations of volcanic ash layers with the overlying episodic plankton-rich (or plankton-poor) layers can provide evidence for casual link between the volcanic eruptions and the marine primary productivity. Study regions can be selected based on the ash deposition pattern in the global ocean that has been presented in Olgun et. al. (2011). Or, particular attention can be given to deposits of specific eruptions like the Pinatubo eruption in 1991 (Philippines), which has been speculated to iron-fertilize the Southern Ocean. Abundances of biogenic silica (opal-contents), CaCO_3 , organic carbon and biogenic barium can be used as proxies of palaeo-productivity. Besides the marine phytoplankton, the shells of planktonic zooplankton can also be useful to investigate the environmental impacts of volcanic ash fallouts. A careful examination of marine drill cores can clearly provide several new insights for further developments.

(iii) In-situ atmospheric and marine observations during volcanic eruptions

Atmospheric sampling of volcanic ash can provide valuable information to assess the nutrient solubility of the long-transported fine ash, and also can be used for more precise ash flux estimations. More than thirty atmospheric sampling stations are located in the coasts or in the oceans (see (Jickells and Spokes, 2001)), some of which are sited downwind of the active and explosive volcanoes, like the Ocean Station Papa in the north Pacific is in downwind of Alaskan volcanoes, or the Mace Head station in the north Pacific is in downwind of Icelandic volcanoes. These stations can be used for volcanic ash sampling during explosive events. Importantly, Fe/Al ratio of aerosols, which is a traditional tracer for mineral dust, may not be reliable for distinguishing every volcanic ash, since Fe/Al ratio of volcanic ash (0.15 to 0.88 for ash, unpublished data) can be very

similar to that of mineral dust (0.63 for dust; (Guieu et al., 2010b)). Instead, calcium content of the aerosol samples may be a better tracer since volcanic ash samples in this study showed lower calcium contents (1-10 wt.%) compared to mineral dust sample (25 wt.%).

A significant challenge lies in the *in situ* marine observations during major volcanic eruptions. Geochemical, biological and satellite investigations in the volcanic ash fallout regions will be helpful to understand the natural processes occurring in the oceans. However, this approach is very challenging due to the episodic nature of volcanic eruptions. Selecting the right study sites can reduce the difficulties related to the logistics and scientific collaborations. Here in Table 1, I would suggest the following ten priority locations for *in-situ* observations. Increased scientific awareness on the importance of volcanic eruptions for the marine ecosystems may hopefully increase the number of investigations in the near future.

Table 1: Priority locations that could be suitable for future *in situ* observations during explosive volcanic eruptions.

	Location	Volcano	Ocean regions affected by the ash fallout, based on (Olgun et al., 2011)
1	Italy	Etna	Central Mediterranean
2	Iceland	Grimsvötn	North Atlantic
3	USA	Cleveland	North Pacific
4	Chile	Puyehue	South Atlantic (and potentially Southern Ocean)
5	Costa Rica	Arenal	Eastern equatorial Pacific
6	Ecuador	Tungurahua	Eastern equatorial Pacific
7	Russia	Shilevuch	Northwest Pacific
8	Japan	Sakura-jima	Northwest Pacific
9	Indonesia	Merapi	Indian Ocean (and potentially Southern Ocean)
10	Philippines	Mayon	Indian Ocean (and potentially Southern Ocean)

REFERENCES

- Duggen, S. et al., 2010. The role of airborne volcanic ash for the surface ocean biogeochemical iron-cycle: a review. *Biogeosciences*, 7(Iron biogeochemistry across marine systems at changing times).
- Guieu, C. et al., 2010a. Large clean mesocosms and simulated dust deposition: a new methodology to investigate responses of marine oligotrophic ecosystems to atmospheric inputs. *Biogeosciences*, 7: 2681–2738.
- Guieu, C., Loÿe-Pilot, M.-D., Benyahya, L. and Dufour, A., 2010b. Spatial variability of atmospheric fluxes of metals (Al, Fe, Cd, Zn and Pb) and phosphorus over the whole Mediterranean from a one-year monitoring experiment: Biogeochemical implications. *Marine Chemistry*, 120: 164–178.
- Jickells, T.M. and Spokes, L.J., 2001. Atmospheric iron inputs to the oceans. In: D.R. Turner and K. Hunter (Editors), *Biogeochemistry of Iron in Seawater*. Wiley, Chichester, UK, pp. 85-121.
- Krom, M.D., Kress, N., Brenner, S. and Gordon, L.I., 1991. Phosphorus limitation of primary productivity in the eastern Mediterranean Sea. *Limnology and Oceanography*, 36: 424-432.
- Olgun, N. et al., submitted to *Marine Chemistry*. Possible impacts of volcanic ash emissions of Mount Etna on the oligotrophic Mediterranean Sea: Results from the nutrient-release experiments in seawater.
- Olgun, N., Duggen, S., Croot, P. and Hoffmann, L., 2008. Fertilizing and/or toxic effects of volcanic ash on marine primary production by trace metal release to the surface ocean International Association of Volcanology and Chemistry of Earth's Interior (IAVCEI) Meeting, Reykjavik, Iceland.
- Olgun, N. et al., 2011. Surface ocean iron fertilization: The role of airborne volcanic ash from subduction zone and hotspot volcanoes and related iron-fluxes into the Pacific Ocean. *Global Biogeochemical Cycles*, 25.
- Wagener, T., Guieu, C. and Leblond, N., 2010. Effects of dust deposition on iron cycle in the surface Mediterranean Sea: results from a mesocosm seeding experiment. *Biogeosciences*, 7: 2799–2830.